CLINICAL AND MOLECULAR ANALYSES OF INTESTINAL GOBLET CELL ACIDOMUCINS AND CYSTEINE METABOLISM

BY

JENNIFER ANN CROIX

DISSERTATION

Submitted in partial fulfillment of the requirements
for the degree of Doctor of Philosophy in Nutritional Sciences
in the Graduate College of the
University of Illinois at Urbana-Champaign, 2010

Urbana, Illinois

Doctoral Committee:

Professor Sharon M. Donovan, Chair
Professor H. Rex Gaskins, Director of Research
Professor Kelly A. Tappenden
Associate Professor Richard I. Tapping

ABSTRACT

Goblet cells are key contributors to intestinal mucosal barrier function through their role in production of mucins and other important secretory products, which include trefoil factor 3 (TFF3) and resistin like molecule β (RETNLB). Goblet cell mucins show great structural heterogeneity but can be broadly classified into neutral and acidic subtypes (chemotypes), which can be further classified into sulfomucins or sialomucins based on the presence of terminal sulfate or sialic acid groups on the oligosaccharide chains. Sulfomucins and sialomucins vary regionally throughout the gastrointestinal tract and changes in their expression have been observed in diseases such as inflammatory bowel disease and colorectal cancer. It is likely that there is variation in these chemotypes among individuals and that both regional and interindividual variation in sulfo- and sialomucins may influence microbial colonization. However, quantitative data and a description of interindividual variation in sulfo- and sialomucin content in the human colon are lacking. There is an absence of data describing the relationship between microbial species and these mucin chemotypes in the human colon. In Chapter 2, we begin to fill these gaps in the literature via a pilot study examining sulfo- and sialomucins in the healthy human colon and their relationship with sulfate reducing bacteria (SRB). Quantitative differences in mucin abundance among specific regions of the colon and individuals are described. In addition, we observe that the relationship between these mucin chemotypes and SRB is not influenced by location in the colon, but rather by the host. In Chapter 3, we begin to identify factors that may contribute to changes in sulfomucin in disease and possibly interindividual variation, using human adenocarcinoma-derived LS174T cells, which have a goblet cell-like phenotype and produce both sulfo- and sialomucins. We specifically focused on the effects of bacterial flagellin, IL-13, and TNFα on the expression of genes encoding the major

secretory mucin, *MUC2*, and Golgi sulfotransfereases, *CHST5* and *GAL3ST2*. In addition, expression of sulfomucin and Sulfo Le^a antigen, which is synthesized in part by GAL3ST2, was examined. Overall, the results indicated that both host and microbial factors influence sulfomucin expression, possibly via modulation of *CHST5* and *GAL3ST2* expression.

Because goblet cells synthesize and secrete cysteine-rich products, including mucins, TFF3, and RETNLB, they may have a high cysteine requirement. Furthermore, they may require additional cysteine, which can be catabolized to sulfate, for mucin sulfation. Cysteine is also used in the production of other proteins as well as essential molecules including glutathione, taurine, and pyruvate. However, high cysteine levels are cytotoxic. Mammals regulate cysteine metabolism to maintain levels within a range that is sufficient for synthesis of essential molecules but below the level of cytotoxicity through the use of cysteine dioxygenase (CDO), which catalyzes the first step in cysteine catabolism. In Chapter 4, CDO expression and localization in mouse small and large intestine is examined using immunohistochemical and immunofluorescence staining techniques. We observed that CDO is expressed in goblet cells as well as Paneth and enteroendocrine cells, which are also members of the secretory lineage, while expression was absent in absorptive enterocytes. We postulate that this striking difference in CDO expression between the absorptive and secretory cell lineages is due to higher cysteine catabolism requirements in goblet, Paneth, and enteroendocrine cells relative to absorptive epithelial cells, either to synthesize additional taurine and sulfate or to metabolize excess cysteine when cells are not actively synthesizing cysteine-rich secretory products. In Chapter 5, we examine the possibility that goblet cells are using CDO to synthesize taurine and determine whether inflammatory stimuli alter taurine biosynthesis, using the LS174T cell line as a model. There are two pathways for taurine synthesis. One pathway involves the oxidation of cysteine via

CDO to cysteinesulfinate, which is decarboxylated by cysteinesulfinic acid decarboxylase (CSAD) to hypotaurine. The other pathway involves the conversion of cysteine to Coenzyme A, which releases cysteamine during turnover. Cysteamine is then oxidized to hypotaurine via cysteamine dioxygenase (ADO). In both pathways, hypotaurine is then oxidized to taurine. We confirm that LS174T cells synthesize taurine via the ADO pathway and possibly the CDO/CSAD pathway. We also demonstrate that certain inflammatory triggers can enhance taurine biosynthesis and/or export, which may provide taurine for other cell types in an in vivo setting. The anti-inflammatory effects of taurine in the intestine have been described, so these results may represent a novel mechanism by which goblet cells attenuate inflammation. Overall, the findings described in this dissertation provide novel information regarding the role of intestinal goblet cells in mucosal barrier function.

To My Mother and Husband

ACKNOWLEDGEMENTS

This work would not have been possible without the support of many people. I would first like to thank my adviser, H. Rex Gaskins, for giving me the opportunity to complete this work in his lab and for supporting and guiding me during the process. I am also thankful to my committee members, Sharon Donovan, Kelly Tappenden, and Richard Tapping for their support and guidance. I would like to thank Gerardo Nava for his assistance with the analysis in Chapter 2 and for being a good friend in the lab. I am also thankful to all the other former and current members of the Gaskins' lab that I have had the chance to work with, but would particularly like to thank Tarannum Khan, Vladimir Kolossov, Ann Benefiel, Matias Attene-Ramos, Mark Russell, and Grace Maloney. Thanks to Mayandi Sivaguru for teaching me to use the microscopy equipment in the IGB Core Facilities. I would like to thank Martha Stipanuk for her assistance and guidance with the CDO work. I would also like to thank Dr. Eugene Greenberg for his assistance in collecting samples for the study described in Chapter 2 and for furthering my clinical knowledge. Finally, and most importantly, thanks to my husband (Alex Jerez), mom (Tina Croix), brother (Michael Croix), grandmas (Claudine Stein and Dolores Croix), pets (Precious, Don Nube, Jam Master J, BunBun, Minnie, and Lexie), and numerous friends and other family members for their love and support.

TABLE OF CONTENTS

Chapter 1

LITRATURE REVIEW

INTRODUCTION

Goblet cells are specialized columnar epithelial cells, which secrete mucins and other products that provide critical barrier function for the host and contribute to intestinal microhabitats that are colonized by mutualistic microbes [1]. The secreted mucus gel layer is an integral structural component of the gut mucosal surface, acting as a medium for protection, lubrication, and transport between luminal contents and the epithelial lining of the intestine. Without this protective cover, the single-celled layer of epithelium is at constant risk of injury from exposure to luminal insults, including chemical irritants, digested food products, toxins, resident microbiota, and intestinal pathogens and their products [1].

The intestinal epithelium also acts as a barrier limiting interaction between the intestinal microbes and immune cells contained in the lamina propria and lymphoid aggregates. The small intestinal epithelium consists of absorptive enterocytes and secretory cells, which include the mucin-secreting goblet cells, peptide hormone-secreting enteroendocrine cells, and microbicide-secreting Paneth cells [2]. Goblet cells can be identified by their unique mucus filled theca. They are normally found in the crypts of both the small intestine and colon and scattered between the absorptive enterocytes in the villi of the small intestine and colonocytes on the surface of the colonic cuffs. Goblet cell density in the small intestine increases from duodenum to ileum, but enterocytes remain the predominant epithelial cell type, reflecting the largely absorptive function of the small intestine [3]. The simple columnar epithelium of the colon also contains absorptive cells (colonocytes), goblet cells, and enteroendocrine cells, but Paneth cells are noticeably

absent. Goblet cells and colonocytes comprise the majority of the epithelial cell content in the colon with goblet cells primarily occupying the colonic crypts and colonocytes making up the surface of the colonic cuffs. Goblet cells are found in much greater numbers within the colon and their density increases in a proximal to distal manner from the cecum to the rectum [3]. This may reflect the increased importance of goblet cells and the secreted mucus layer for host protection in more distal regions of the colon.

GOBLET CELL DIFFERENTIATION

The intestinal epithelial cell lineages are thought to arise by mitosis of multipotent stem cells that are maintained near the base of the crypts in the small intestine and at the base of the crypts in the colon [2]. As the stem cells migrate from crypt to villus in the small intestine and from crypt to the surface of the colonic cuffs in the large intestine, they are believed to differentiate into progenitor cells, which then further differentiate into the specific epithelial lineages. In the small intestine, most differentiation occurs from near the base of the crypt up until the crypt-villus junction. At this important junction, goblet cells, enterocytes, and enteroendocrine cells continue to migrate up the villi, while Paneth cells migrate down to the base of the crypts. Since Paneth cells are not found in the colon, all migration and differentiation in this region occurs in the direction from crypt base to lumen. In the case of the human goblet cell, migration is completed from small intestinal crypt to villus tip within 4 to 5 days and from colonic crypt to the surface of colonic cuffs in approximately 6 days [1]. Upon reaching the lumen, the cells may undergo apoptosis and/or be sloughed off into the lumen.

A considerable amount of progress has been made in elucidating signaling pathways involved in intestinal goblet cell differentiation. The Wnt/β-catenin signaling pathway appears to

be essential for maintenance of undifferentiated stem/progenitor cells in intestinal crypts and for switching from a proliferating progenitor phenotype to a differentiated epithelial cell [2]. Wnt target gene expression indicates that the Wnt pathway is active in a gradient with greatest activity at the crypt base [4], which is consistent with its reported importance in Paneth cell maturation [5].

The canonical Notch signaling pathway, which regulates cell fate in a number of systems through close range cell-cell interactions, plays a key role in epithelial cell lineage determination in the intestine by maintaining the proliferative progenitor state of stem cells and limiting the fate of cells of the secretory lineage. Disturbance of the Notch pathway results in loss or overabundance of goblet cells [6-9]. Inhibition of the pathway in the intestine through removal of the transcription factor CSL/RBP-J or use of gamma-secretase inhibitors led to massive conversion of proliferative cells into goblet cells in the small intestine and a similar increase in goblet cells in the colon [8]. A complementary gain-of-function approach produced the opposite phenotype, which exhibited reduced abundance of secretory cells and an expansion of immature progenitor cells [9]. *HesI*, a direct target gene of Notch, represses transcription of the transcription factor MathI, which is required for commitment toward the secretory lineage [6]. Consequently, $Hes1^{-/-}$ mice show increases in goblet, enteroendocrine, and Paneth cells, while $MathI^{-/-}$ mice show depletion of goblet, enteroendocrine, and Paneth cells without affecting enterocytes [6, 10]. *Gfi1*, a zinc-finger transcriptional repressor that appears to function downstream of MathI, is involved in the selection of the goblet/Paneth cell lineage over the enteroendocrine lineage [11]. The Wnt pathway may also influence cell lineage via effects on MathI. Impairment of Wnt signaling decreases MathI-positive precursor cells in the crypt, leading to loss of the secretory lineage [12].

Bone morphogenetic protein (Bmp) signaling, which was previously identified as a key mediator in crypt and villus morphogenesis as well as maintenance of intestinal stem cells, was shown recently to also be necessary for terminal differentiation of the secretory lineage [13]. Disruption of the Bmp signaling pathway results in smaller, but not fewer, goblet cells with immature appearing granules and decreased expression of secretory lineage–specific genes, indicating loss of goblet cell terminal differentiation and maturity. These effects may have been mediated by decreased expression of the zinc-finger transcription factor, Krüppel-like factor 4 (Klf4), which was previously identified as being required for terminal goblet cell differentiation in the colon [14]. Recently, *Klf4* expression was also found to be inhibited by Notch signaling. When Notch signaling was inhibited, Klf4 expression and goblet cell numbers increased [15].

CDX2, a member of the caudal-related homeobox gene family, has anti-proliferative effects on intestinal epithelial cells and regulates transcription of both enterocyte and goblet cell specific genes [16-21]. In the case of goblet cells, CDX2 transactivates the promoters of genes encoding goblet cell secretory products, including mucin 2 (*MUC2*), resistin-like molecule beta (*RETNLB* or RELMβ), and trefoil factor 3 (*TFF3*) [19, 21, 22]. CDX2 was also reported to activate expression of KLF4 and modulate the notch signaling pathway, indicating that CDX2 has an important role in mature goblet cell development and function on multiple levels [23, 24].

GOBLET CELL SECRETORY PRODUCTS

Mature goblet cells are unique in their synthesis and secretion of a number of products including specific mucins, TFF3, and RELMβ. These products are important in the maintenance of intestinal barrier function. The most recognized contribution of goblet cell secretory products

is the formation of the mucus gel layer that overlays the intestinal epithelium and forms a selective barrier between the host and the luminal contents.

MUCINS

Mucus is a heterogeneous mixture of secretions comprised of approximately 95% water and containing electrolytes (Na^+, K^+, Mg^{2+}, and Ca^{2+}), carbohydrates, proteins, amino acids, and lipids [25]. The viscoelastic, polymer-like properties of mucus are derived from the major gel-forming glycoprotein components called mucins [1]. Mucins consist of a peptide backbone containing alternating glycosylated and nonglycosylated domains, with glycosylated regions comprising 50 to 90% of the polymer. The peptide backbones of mucins are encoded by the *MUC* family of genes [26, 27]. Mucins can be categorized as secreted or membrane-bound. Membrane associated mucins are bound to cells by an integral transmembrane domain found in their carboxy terminus and appear to be important in signal transduction. Secreted mucins are released from cells and are further classified into gel-forming (MUC2, MUC5AC, MUC5B, MUC6) and non-gel-forming mucins (MUC7). The gel-forming mucins contain cysteine-rich motifs in their C- and N-terminal domains necessary for oligomerization and formation of a protective mucus gel [28].

MUC2, which is secreted exclusively by goblet cells, is the major secretory mucin of the small intestine and colon [29]. Structurally it consists of two central tandem repeat domains rich in serine, threonine, and proline that serve as potential *O*-glycosylation sites and multiple cysteine-rich domains that are not glycosylated. The cysteine-rich domains include four von-Willebrand-factor (VWF) D-like domains, a VWF-C-like domain, a C terminal domain with similar topology to a cystine knot motif, and two cysteine-rich domains that flank the first

tandem repeat domain [26, 29]. Oligosaccharide side chains are linked to the mucin peptide core by *O*-glycosidic bonds between threonine or serine on the peptide core and N-acetylgalactosamine (GalNAc) on the sugar chains [30]. The oligosaccharide chains typically occur in clusters along the polypeptide with the amino and carboxyl terminal ends being less glycosylated [31]. The clusters of O-linked oligosaccharide chains provide the mucins with regions that are protease resistant and highly hydrated, which is important in protecting the mucins from degradation and for lubricating the epithelium [31].

The composition of the mucin oligosaccharide chains is highly variable, contributing to the heterogeneity of mucins and thus the mucus layer. The structure of an oligosaccharide chain can be described according to the core sequence directly linked to the peptide, the backbone (not always present), and the peripheral region, which is made up of sialic acid, blood group antigens, or ester sulfate substitutions [31]. There can be a number of variations in each of these components including sugar type, chain length, and degree of branching. Termination of mucin oligosaccharide chains with sialic acid or sulfate groups accounts for the polyanionic nature of mucins at a neutral pH [1, 30]. These variations likely alter the biological and physiological properties of the mucins and affect which bacteria are able to colonize the mucus layer. Carbohydrates and terminal groups on mucin oligosaccharide chains can serve both as binding sites and as a potential source of nutrients for microbes. A number of interactions between microbes and mucins have been demonstrated in the colon and other mucosal regions of the body [32, 33]. However, there are likely many more that remain to be characterized.

MUCIN BIOSYNTHESIS

The biosynthesis of a secreted mucin is a complex process that requires a number of steps including translation of the *MUC* gene, folding and dimerization of the peptide, *O*-glycosylation, polymerization and storage [34]. In line with the central dogma, *MUC* genes are first transcribed in the nucleus to produce MUC transcripts, which are translated into MUC proteins on endoplasmic reticulum (ER)-associated ribosomes. Post-translationally, mucins are folded, *N*-glycosylated and form disulfide-linked dimers in the ER before being modified by one or several glycosyltransferases in the Golgi [28, 34]. Most *O*-glycosylation occurs in the *cis*-Golgi beginning with the transfer of GalNAc from UDP-GalNac by an *N*-acetylgalactosaminyl peptidyltransferase to a serine or threonine in the tandem repeat domains. The addition of GalNac to a serine or threonine on a nascent mucin peptide forms what is known as the Tn antigen. Elongation of each *O*-glycan is accomplished by the stepwise addition of galactose (Gal), *N*-acetylglucosamine (GlcNAc), fucose, or sialic acid from nucleotide sugar donors by specific glycosyltransferases in the Golgi [28, 31].

Eight different core structures linked to the mucin peptide have been identified, but cores 1-4 are found most commonly in mucins throughout the gastrointestinal tract (**Table 1.1**) [31]. The core 1 subtype is formed by the addition of Gal in a β1-3 linkage to GalNac. Subsequent glycosyltransferases can elongate the core 1 structure or convert it into the core 2 subtype by the addition GalNac. The core 3 subtype, which is predominant in normal colonic tissue, is generated by adding GlcNA to GalNAc and can be branched with the addition of GlcNac to form core 4. The core structures can be elongated by Gal and GlcNAc transferases to form Galβ1,3/4GlcNAc units. *O*-glycan synthesis is terminated by the addition of fucose, Gal, GalNac, and sialic acid via an α-glycosidic linkage, which prevents further elongation and gives

rise to the ABH and Lewis blood group antigens. Sialic acid moieties and sulfates are transferred to Gal or GlcNAc moieties and impart negative charges to mucins. To add another dimension of heterogeneity, sialic acid residues may be mono- or poly-O-acetylated [34, 35]. Mature, fully glycosylated, mucins are sorted and packaged into secretory granules where they are stored until regulatory signals trigger granule exocytosis [1].

Sulfation occurs within the *trans*-Golgi as a late step in glycoprotein synthesis when specific sulfotransferases transfer sulfate from 3′-phosphoadenosine 5′-phosphosulfate (PAPS) to mucin *O*-glycans at the C-3 position of galactose residues or the C-6 position of *N*-acetylglucosamine [36, 37]. Of the four galactose 3-*O*-sulfotransferase (*GAL3ST*) genes that have been described, GAL3ST2 appears to be the sulfotransferase responsible for sulfate addition to the C-3 position of Gal in human colonic mucins [38]. GAL3ST2 expression is downregulated in non-mucicnous adenocarcinomas, which corresponds with the lower expression of sulfomucin seen in this type of colonic adenocarcinomas [38]. Of the known *N*-acetylglucosamine-6-*O* sulfotransferases, CHST5 (GlcNac6ST-3) is the only one that shows specificity for the intestine and is the most abundant of the *N*-acetylglucosamine-6-*O* sulfotransferases in the human colon and small intestine [39, 40]. In addition, CHST5 shows a preference for sulfating O-linked chains of the mucin-type [39], suggesting that it is involved in transfer of sulfate to the C-6 position of *N*-acetylglucosamine in sulfomucins. Furthermore, like GAL3ST2, CHST5 expression is downregulated in colonic adenocarcinomas [38].

Sialic acid can be obtained from the diet or can be synthesized endogenously from glucose or other products of glycolysis [41, 42]. Synthesis of sialic acid occurs in the cytosol, but it is transferred to the nucleus to be converted to its active form, cytidine monophosphate-N-acetylneuraminic acid (CMP-Neu5Ac), by CMP-NeuAc synthetase (CMAS) [42, 43]. Sialic acid

is transferred from CMP-Neu5Ac to mucin *O*-glycans in the Golgi by sialyltransferases. However, unlike the sulfotransferases, sialyltransferases acting on *O*-glycans can be found distributed from *cis*-Golgi to *trans*-Golgi [44]. This is important because sialyltransferases can compete with enzymes involved in core structure formation for certain substrates and addition of sialic acid can prevent further elongation of an *O*-glycan. Thus, if a sialyltransferase is localized in an earlier compartment of the Golgi, it may prevent synthesis of core structures, resulting in short, sialylated *O*-glycans [36, 44]. In most oligosaccharides, the sialic acids occur as peripheral residues in alpha-2-3 and alpha-2-6 linkages [34]. The sialyltransferases that appear to be particularly important for colonic mucins are ST6 beta-galactosamide alpha-2,6-sialyltranferase 1 (ST6GAL1) and ST3 beta-galactoside alpha-2,3-sialyltransferase 4 (ST3GAL4) [45]. Sialic acids in colonic mucins are commonly *O*-acetylated at positions C4, 7, 8, or 9 [34]. This occurs by transfer of an *O*-acetyl group from acetyl-CoA by action of an *O*-acetyltransferase [36]. *O*-acetylation of sialomucins changes their physical properties and appears to confer resistance against bacterial degradation.

GOBLET CELL MUCINS IN NORMAL HUMAN SMALL INTESTINE AND COLON

Goblet cell mucin *O*-glycans can be analyzed using various methods, including histochemisty [35, 46], lectin histochemistry [47], immunohistochemistry [48], metabolic labeling [49], chromatographic methods, mass spectrometry [37, 50], and NMR [37]. While chromatographic and spectroscopic methods can provide much more structural detail, they lack the ability to provide information about localization that can be achieved with histochemical and immunohistochemical techniques. Conventional histochemical methods can be used to classify mucins as neutral or acidic mucins, which can be further classified into sialomucin or sulfomucin

[35]. The periodic acid Schiff (PAS)/Alcian blue (AB) pH 2.5 stain can be used to distinguish neutral and acidic mucins depending on whether they stain the PAS-positive magenta (neutral), AB-positive blue (acidic), or PAS- and AB-positive purple (mixed acidic and neutral mucins). The high iron diamine (HID) Alcian blue (AB) pH 2.5 stain can be used to distinguish sialomucins (blue) and sulfated mucins (brown/black).

Regional and spatial differences in intestinal goblet cell mucins based on histochemical staining have been previously described. A summary of typical patterns observed for neutral, sialo-, and sulfomucins in the small intestine and colon is shown in **Figure 1.1**. Goblet cells in the normal small intestine primarily synthesize and secrete neutral mucins and sialomucins, but few sulfated mucins are found in the ileum near the ileocecal junction [35, 51]. The distribution of neutral and sialomucins varies from crypt to villus with goblet cells located in the crypts predominantly producing neutral mucins and those along the villi producing sialomucins [51, 52]. This distribution also appears to correlate with goblet cell differentiation and development, indicating that more mature goblet cells in the small intestine express sialomucin [52, 53]. Regulation of mucin composition by pathways involved in goblet cell differentiation, however, remain to be examined. *O*-acetylated derivatives of sialic acid become more apparent in moving from the duodenum to ileum, and the ratio of sialic acid to fucose increases. This observation along with the appearance of sulfomucins in the distal ileum suggests a gradual transition from small intestine to colon, which contains more *O*-acetylated sialomucin and sulfomucins. Robbe et al (2004) also demonstrated that a number of gradients exist in moving from the ileum to the rectum and provided additional insight into the composition of ileal mucins using a combination of NMR spectroscopy, gas chromatography, and MALDI-MS. They reported that mucins in the ileum contain the largest oligosaccharides and these are predominantly neutral and highly

fucosylated [37]. In an earlier study, they also reported a decreasing gradient of fucose and ABH blood group expression from ileum to rectum [50]. An increasing acidic gradient was observed in associated with an increase in both 3-*O*-sulfated Gal and sialic acid. This observed gradient correlates with histochemical data obtained for the normal colon.

Normal colonic goblet cell mucins contain neutral mucins, sialomucins, and sulfomucins with sulfomucins predominating. Both *N*- and *O*-acetylated sialic acids are present and these may include derivatives which are mono-, di, or tri-acetylated. The mucin pattern varies both regionally and along the crypt-surface axis, again paralleling cellular differentiation. Decreased PAS-reactivity is found moving from cecum to rectum indicating a proximal to distal decrease in neutral mucins. Neutral mucins may be found in moderate amounts in the upper crypts and to a lesser extent in the lower crypt. In the cecum and ascending (or right) colon, sialomucins are found in goblet cells in the lower third of the crypt and a few along the surface epithelium while sulfated goblet cells predominate in the upper crypt region [35]. A different pattern is observed in the left colon where goblet cells containing sulfated mucins are found in the lower half of the crypt and a variable number of sulfomucin and sialomucin containing goblet cells are contained in the upper half of the crypt [35]. In the rectum, a greater portion of the upper crypt appears to contain sialomucins and a number of goblet cells containing a mixture of both sulfated and sialic acid containing mucins are found [35, 54]. Thus, both the sialomucin content and heterogeneity of mucins appears to increase in moving from the left colon to the rectum. While these general patterns in mucin chemotype expression have been reported, few studies have examined interindividual variation in mucin composition.

MUCINS AND INFLAMMATORY BOWEL DISEASE

It has been known for many years that alterations in mucins and the mucus layer occur in a range of gastrointestinal diseases, including adenocarcinomas and inflammatory bowel disease (IBD). In the case of IBD, changes in the thickness of the mucus gel layer, goblet cell number and intracellular mucin content, and mucin glycosylation have all been reported [55-58]. Defects in mucins may contribute to the chronic inflammation seen in Crohn's disease and ulcerative colitis by facilitating a breach of the epithelial barrier or altering mucosal-bacterial interactions [55]. Another possibility is immunological or bacterial factors that are altered in response to initial or ongoing inflammation affect mucin production, which then leads to perpetuation of the inflammation.

The thickness of the mucus layer appears to be a distinguishing feature between CD and UC. Pullan et al. (1994) described a decrease in the thickness of the mucus layer of UC patients and an increased thickness in the mucus layer covering the rectum in CD patients compared with the rectum of normal subjects [59]. A reduction in the area of epithelium covered by mucus in the sigmoid colon of UC patients compared to normal sigmoid colon was also described by Swidniski [58]. Recently, the thickness and continuity of the adherent mucus layer of the rectum were assessed in patients with rectal CD and different grades of UC [57]. Significant differences were not seen in the thickness of the mucus layer between normal subjects and subjects with inactive, mild or moderate UC, but a significant difference was observed between healthy subjects and subjects with severe UC. The percentage of the mucus layer that was discontinuous was significantly increased in active UC, and this discontinuity appeared to increase with severity of UC. The decrease in mucus thickness and continuity may have been the result of reduced goblet cell density, which was found to be especially apparent in severe UC [57]. In the

case of CD patients, the thickness and continuity of the mucus layer and goblet cell number were unaltered when compared with controls. This is in contrast to the results of Pullan and coworkers (1994) and may reflect the stage and type of CD, differences in the preservation of the adherent versus the loose layer of mucus, or the small number of specimens examined.

Alterations in mucin glycosylation that have been described in IBD include decreased length of the mucin oligosaccharide chain, decreased sulfation and *O*-acetylation of sialic acid, increased sialylation, and increased expression of the TF and sialyl-Tn antigens [55, 56, 60]. Both metabolic labeling and HID/AB staining have demonstrated a significant loss of mucin sulfation in UC [61, 62], which appeared to correlate with severity of disease. Van Klinken et al. provided further insight into this phenomenon and reported that while MUC2 is undersulfated, sulfated MUC2 is selectively secreted [49]. Furthermore, the decrease in secreted MUC2 is likely due to decreased MUC2 production rather than just a decreased in secretion since the percent secreted did not change. Intriguingly, upon remission the number and appearance of the goblet cells return to normal, indicating that the goblet cell changes are observed only during active inflammation. This suggests that the observed mucin changes are not a cause of the inflammation but a consequence. However, a study comparing mucin sulfation in European and South Asian patients with UC suggests the role of a genetically determined abnormality in glycosylation [63]. Staining of rectal biopsies from South Asian colitics revealed a high degree of sulfation, resembling normal human rectal tissue, irrespective of disease activity. On the other hand, biopsies from European colitics, showed decreased sulfation and increased sialylation with increased disease activity. These findings are particularly interesting given that South Asians have a reduced risk of severe colitis and colorectal cancer [63].

The loss of sulfation and increased appearance of sialomucin that is observed in UC is not considered to be a feature of CD. However, both Ehsanullah and Allen described an abnormal predominance of sialomucins in the majority of rectal biopsies collected from CD subjects [64, 65]. Attempts were not made in these studies to score disease severity in CD patients. There is also some evidence using metabolic labeling that sulfation is decreased in rectal biopsies from CD patients [62]. The observed reduction did not reach statistical significance, but this may have been due in part to the small sample size (n=6 for CD and n = 16 for controls).

Expression of the TF antigen, which is a reflection of abnormal glycosylation, occurs in a portion of UC and CD subjects [60]. The presence of this antigen was examined in monozygotic UC and CD twins and unaffected monozygotic twins of UC and CD patients. Positive staining for the antigen using peanut lectin histochemistry was found among all 22 affected monozygotic twins with IBD and nearly all (15/16) unaffected twin siblings of IBD patients. Staining was localized in the supranuclear region plus a variable degree in the glycocalyx and secreted mucus layer. About ¼ of the control subjects also showed positive staining, but staining only localized to the supranuclear region. A strong correlation was seen between PNA positivity and NFκB activation, indicating a relationship to inflammation. Overall, the study indicates that the changes in glycosylation may be the result of a genetically predisposed individual being exposed to an environmental trigger [60].

MICROBIAL AND HOST MODULATION OF MUCIN COMPOSITION

Although decreased sulfation of mucins has been associated with active inflammation in human IBD, the underlying causes and the relationship to disease pathology remain undefined.

Both animal and *in vitro* studies demonstrate that mucin chemotype may be altered by changes in the normal microbiota and inflammation [33, 66-69]. The evidence for microbial modulation of mucin chemotypes comes from developmental studies and those comparing conventionally-raised and germfree rodents. In mice, for example, the temporal development of sialo- and sulfomucin chemotypes in the colon appears to parallel the establishment of microbial communities and is not observed in germfree mice, in which crypt mucins remain predominantly sulfated [33, 70]. Specific microbial components or products may be responsible for the observed effects of the microbiota on mucin chemotypes. A number of bioactive microbial factors have been shown to induce mucin synthesis, secretion, and degradation, but few studies have examined the role of these in determining mucin composition [33]. There is, however, some evidence for the ability of certain microbial components to mediate mucin chemotypes [33, 71, 72]. For example, administration of lipopolysaccharide (LPS) from a commensal strain of *E. coli* to germfree rats increased colonic neutral mucin [71]. In addition, LPS from *H. pylori* inhibited mucin glycosylation and sulfation when applied to rat gastric mucosal segments [72]. Whether the effects of the microbiota and specific microbial components on mucin chemotypes occur via direct recognition by intestinal goblet cells or by a microbe-induced inflammatory response to which goblet cells respond remains to be determined. In addition, because there are very distinct interspecies differences in mucin chemotype patterns [51], it is important to keep in mind that changes in sialo- and sulfomucin observed in animal models may not translate exactly to humans. For example, differences in sialomucin and sulfomucin patterns between normal rodents and humans are shown in **Figure 1.2**.

Similar to microbial components, a number of host inflammatory signals have been demonstrated to alter mucin synthesis and secretion, but only a few studies have examined

effects on mucin composition [33]. TNFα, IL-1β, and IL-6, which are all proinflammatory cytokines considered to be involved in the pathogenesis of CD [73], were found to induce the release of less glycosylated mucins with altered carbohydrate composition from the mucin secreting intestinal cancer cell line LS180 [69]. In another study, TNFα increased the expression of α-2,3-sialyltransferase expression in HT29 cells [74], a finding that could possibly explain the increased sialomucin seen in active IBD. Likewise, TNFα increased α-2,3-sialyltransferase expression and mucin sialylation in a human respiratory glandular cell line [75]. However, TNFα may also contribute to mucin sulfation as evidenced by a mouse model of salmonellosis where TNFα was determined to be involved in an observed increase in sulfomucins in villus goblet cells [66]. A study using human bronchial mucosa indicated that IL-6 and IL-8 can increase expression of sialyltransferases and sulfotransferases, paralleling an increase in sialyl-Lewis^x and 6-sulfo-sialyl-Lewis^x epitopes on bronchial proteins, including MUC4 [67]. Thus, proinflammatory cytokines, especially TNFα, may have an important role in mucin glycosyation, sulfation, and sialylation that remains to be fully understood.

Increased sialomucins and sulfomucins, altered terminal sugar chains, and increased gene expression of sulfotransferases have been observed in rodent models of intestinal nematode infections [76-78]. While the Th2 cytokines, IL-4 and IL-13, are considered to be mucogenic cytokines and important mediators of a number of other goblet cell responses to intestinal nematode infections, little is known regarding the ability of these cytokines to alter mucin composition in the human colon [79, 80]. IL-4 treatment of the human goblet-cell like line, LS174T, resulted in enhanced gene expression of specific *N*–acetylgalactosaminyltransferases and attached more *N*-acetylgalactosamine into a tandem repeat domain of the MUC2 [81]. In the rat intestinal epithelial cell line, IEC-6, both IL-4 and IL-13 increased gene expression of

sialyltransferase 4C (ST3GalIV), considered to be the major sialyltransferase expressed in the intestine following nematode infection [82]. Therefore, there is some indication that IL-4 and IL-13 may be able to alter mucin composition via effects on specific glycosyltransferases, sulfotransferases, and sialyltranferases involved in mucin biosynthesis.

TFF3 and RELMβ

Rapid repair of mucosal epithelial damage is critical to the maintenance of epithelial barrier function and the prevention of prolonged inflammation. Trefoil factors (TFFs) are a family of small, cysteine-rich mucin-associated peptides secreted by mucus-producing cells that are involved in the protection and healing of mucosal epithelium [83]. The name of the family refers to the presence of one or more trefoil domains, which have a characteristic three-looped structure stabilized by three disulfide bonds formed by 6 conserved cysteine residues. Of the three members that have been characterized in this family, only TFF2 contains two trefoil domains whereas TFF1 and TFF3 contain a single domain. However, both TFF1 and TFF3 contain a seventh cysteine, which allows for the formation of homodimers. The human trefoil genes are clustered on chromosome 21 at 21q22.3 in a head to tail manner [84].

Trefoil factors have region-specific expression within the gastrointestinal tract and have been shown to co-localize with mucins, suggesting an interaction between mucin and trefoil factors in gut protection. TFF1 is expressed in superficial cells in the fundus and antrum of the stomach and co-localizes specifically with MUC5AC. Direct interaction between TFF1 and MUC5AC has been demonstrated. TFF2 is expressed in the foveolar pits in the antrum of the stomach and duodenal Brunner’s glands and appears to co-localize with MUC6. TFF3 is expressed almost exclusively by goblet cells throughout the small and large intestine and co-

localizes specifically with MUC2 [85]. *In situ* hybridization performed in the small intestine demonstrated hTFF3 localization within goblet cell theca and in the mucus layers. The greatest expression of TFF3 appears in the distal portions of the ileum and colon [86].

TFF3 has been reported to be involved in a number of important biological functions, including protection of intestinal epithelium, promotion of wound healing, and promotion of epithelial cell migration. It has been shown to protect the mucosa from injury by noxious agents *in vivo* [79, 87, 88] and stimulate epithelial cell migration and restitution after monolayer wounding *in vitro* [89]. Targeted disruption of the TFF3 gene in mice was associated with increased susceptibility to dextran sodium sulfate (DSS)-induced colitis, which could be healed by luminal repletion of TFF3. TFF3 was also shown *in vitro* to be important to intestinal barrier function by decreasing paracellular transport through effects on claudin expression [90].

RELMβ belongs to the family of resistin like molecules/found in inflammatory zone (RELM/FIZZ). The RELMs are a family of secreted peptides, which share unique cysteine-rich C termini homologous to that found in the adipocyte hormone resistin. Three RELMs, excluding resistin, have been discovered to date: RELMα, RELMβ, and RELMγ. Of the identified RELMs, only RELMγ has not been described in humans. The RELM protein has three principal domains: (*i*) an N-terminal signal sequence, (*ii*) a variable middle portion, and (*iii*) a highly conserved C-terminal signature sequence C-X_{11}-C-X_8-C-X-C-X_3-C-X_{10}-C-X-C-X-C-X_9-CC-$X_{3–6}$-END. Only RELMβ and resistin share a conserved 11^{th}cysteine found in the N-terminus. This extra cysteine appears to enable homodimer formation under non-reducing conditions by both resistin and RELMβ [91]. Similar to the TFF and MUC proteins, the RELMs are expressed in a region-specific manner. RELMα is most abundant in white adipose tissue but has also been detected in mammary tissue, heart, lung, and tongue [92]. RELMβ expression appears to be restricted to

goblet cells. RELMγ has been detected in bone marrow, spleen, lung, and in peripheral blood granulocytes [92].

RELMβ mRNA and protein expression in mouse is greatest in large intestine and cecum with limited expression in the small intestine. Analysis by *in situ* hybridization revealed that mRELMβ mRNA expression is most abundant in the lower one-half to one-third of the colonic crypts, coinciding with the proliferative region of the colonic epithelium, and weakened near the surface of the epithelium [92, 93]. Similarly, mRELMβ mRNA expression in the small intestine appears to be more abundant in the crypts than in the villi [93]. In min mice, which develop tumors akin to humans familial adenomatous polyposis due to a mutation in the *Apc* gene, RELMβ expression was greatly increased in adjacent tumors compared to normal tissues, further indicating a preference for RELMβ mRNA expression in cells with an enhanced rate of proliferation [92]. Murine RELMβ mRNA appears to have segmental pattern expression along the length of the colon. *In situ* hybridization in mouse showed alternating contiguous segments (~2cm long) positive for RELMβ with comparably long segments negative for RELMβ mRNA [93]. The significance of this pattern is not understood. Immunohistochemical analysis of protein expression in the colon indicated the presence of RELMβ in goblet cells in the upper crypt and colonic surface epithelium. Although mRNA expression was not found in upper crypts, this can be explained by the migration of goblet cells expressing RELMβ mRNA in the lower crypts towards the surface of the colonic epithelium. Immunohistochemistry also indicated that RELMβ was released apically rather than basally. This was confirmed by the isolation of RELMβ (as a homodimer) from mouse stool and detection of RELMβ in human stool [92, 93].

RELMβ appears to play a role in host protection against pathogens, interaction with the commensal bacteria, cell proliferation, inflammation, and even insulin resistance. In a study

comparing conventional and germfree mice, RELMβ mRNA and protein expression were reduced in a segmental manner in germfree mice compared to conventional mice. Conventionalization of germfree mice led to strong expression of RELMβ. Differences were not observed in the magnitude of RELMβ expression or timing for conventionalization of germfree BALB/c mice compared to germfree CB17SCID mice, suggesting that bacterial RELMβ induction occurs independent of the adaptive immune system [94].

It has been suggested that RELMβ may be a novel Th2 cytokine-induced immune-effector molecule in resistance to GI nematode infection [94]. Expression and secretion of RELMβ is induced by intestinal nematode infection, and RELMβ binds to components of the nematode chemosensory apparatus and thereby inhibits its chemotaxic function [80, 94]. Further analysis in mice and human goblet cell lines revealed that Th1- and Th2-associated cytokines may play a direct role in regulating *RELMβ* expression in goblet cells. More specifically, RELMβ mRNA expression is induced by IL-4 and IL-13 and inhibited by IFNγ [94].

Recent studies, which have focused on RELMβ in mouse models of IBD, support the immune effector role of RELMβ and suggest that RELMβ may be involved in the initiation and perpetuation of inflammation. Hogan et al demonstrated that RELMβ$^{-/-}$ mice have increased transepithelial permeability and are more susceptible to TNBS-induced colitis but more protected from DSS-induced colitis [95]. The finding that RELMβ$^{-/-}$ mice are more protected from DSS-induced colitis was confirmed by McVay et al [96]. In SAMP1/Fc mice, a model of spontaneous ileitis sharing many features with human Crohn's disease, RELMβ was greatly increased in the ileum coincident with the onset of ileal inflammation [97]. Interestingly, the induction of RELMβ in early inflammation appeared to be independent of microbial colonization and specific Th1 (TNFα and IFNγ) and Th2 (IL-4 and IL-13) cytokines, raising the possibility that induction

and expression of RELMβ may promote inflammation and/or mucosal injury under appropriate pathological circumstances. Consistent with this possibility, recombinant RELMβ is able to induce macrophage activation and secretion of TNFα and IL-6, cytokines previously identified as playing a role in the pathogenesis of CD [96]. Thus, delivery of RELMβ from the lumen to the lamina propria through a disrupted epithelial barrier may promote inflammation by activating immune cells to produce inflammatory mediators [96]. Despite these interesting findings in the mouse, currently published studies have not examined expression or localization of RELMβ in CD or UC.

CYSTEINE AND CYSTEINE DIOXYGENASE

The cysteine-rich nature of goblet cell secretory products and the requirement for sulfate in sulfomucin production suggests that cysteine metabolism may be of central importance for intestinal goblet cells. In addition, cysteine is essential for a number of other cellular products including other proteins, glutathione, coenzyme A, and taurine (**Figure 1.3**). Provision of a cocktail containing L-cysteine along with L-threonine, L-serine, and L-proline to DSS-treated mice increased Muc2-positive goblet cell numbers in the surface epithelium of ulcerated regions and stimulated mucin synthesis while protein turnover was unaltered [98]. L-cysteine supplementation alone also improved colon histology and reduced DSS-induced weight loss and intestinal permeability, as well as local chemokine expression and neutrophil influx in a porcine model of colitis [99]. However, there was no mention of effects on goblet cells or mucins. Sulfur amino acid deficiency in neonatal pigs reduced villus and crypt goblet cell numbers in the jejunum but not in the ileum or colon [100]. Thus, regional differences in cysteine utilization may exist for intestinal goblet cells.

Cysteine for the intestine is likely derived from both dietary methionine and cysteine. In piglets, 20% of the dietary methionine intake was found to be metabolized by the gastrointestinal tract and primarily converted to homocysteine and cysteine via transmethylation and trans-sulfuration, respectively [101]. Studies in rat also indicate that the small intestine possesses the full set of trans-sulfuration enzymes necessary to convert methionine to cysteine [102, 103]. In the case of dietary cysteine, less than 100% of dietary cysteine was recovered in the portal blood in pig studies [104, 105], indicating cysteine utilization by the intestine.

The first step in cysteine catabolism is the oxidation of cysteine to cysteinesulfinate via cysteine dioxygenase (CDO, EC 1.13.11.20) [106, 107]. Cysteinesulfinate is then further metabolized to yield products, including hypotaurine/taurine, pyruvate and sulfate. Rodent and human CDO gene expression has been reported in a number of tissues [108-112], indicating the importance of CDO in whole body cysteine homeostasis. However, the highest mRNA levels of CDO were present in the liver of rats, mice, and humans. CDO mRNA was detected in whole tissue homogenates of murine small intestine, but the level of expression was quite low and appeared to be undetected at the protein level [108]. A recently published paper, though, demonstrated low but detectable CDO expression at the protein level in both mouse duodenum and colon [113]. Published studies examining CDO expression in rat or human small intestine or colon at the mRNA level could not be found, although an earlier study reported that rat enterocytes could metabolize cysteine to cysteinesulfinate via CDO [114]. However, a recent report described the localization of CDO specifically to goblet cells in the rat small intestine [115]. To our knowledge, there have been no published descriptions of CDO localization in the colon. Possible reasons for CDO expression in intestinal goblet cells include a mechanism for regulating cysteine levels when cells are not actively synthesizing cysteine-rich secretory

products and production of sulfate and/or taurine. Indeed, taurine was demonstrated to localize to mucus granules in goblet cells in mouse intestine [116].

TAURINE

Taurine (2-aminoethanesulfonate) is one of the most abundant free amino acids present in the body and was reported to be the second most abundant free amino acid in human colonic mucosa [117-119]. Taurine is well known for its role as a conjugation substrate for bile acids, helping to increase polarity and aqueous solubility [118]. Taurine also has a number of cytoprotective properties in various tissues, including antioxidant, anti-inflammatory, osmoregulatory, and membrane-stabilizing effects [117, 118]. The direct precursor of taurine, hypotaurine, can also serve as an antioxidant [118].

In the intestine, recent studies have revealed taurine supplementation to be beneficial in rodent models of inflammatory bowel disease due to its anti-inflammatory and antioxidant properties. Taurine supplementation was demonstrated to ameliorate inflammatory parameters in trinitrobenzene sulfonic acid (TNBS)-induced inflammatory bowel disease in rats, possibly by decreasing inflammatory reactions, oxidative damage, and apoptosis [120, 121]. Likewise, taurine supplementation diminished disease severity and inflammatory response in DSS-induced colitis in mice [122, 123]. Use of 5-aminosalicyltaurine as a colon-specific prodrug of 5-aminosalicylic acid (5-ASA), which is cleaved into taurine and 5-ASA in cecal contents [124], showed enhanced anti-inflammatory effects compared to 5-ASA alone in TNBS-induced colitis in rats [125], again suggesting an anti-inflammatory role for taurine in the colon. Taurine can react with hypochlorous acid, produced by myeloperoxidase in activated neutrophils to form taurine chloramines [126]. Taurine chloramine exhibits strong anti-inflammatory activity by

downregulating nuclear factor-κb (NF-κB) activity and proinflammatory products including prostaglandins, nitric oxide, and cytokines, and is considered to be the major mechanism by which taurine potentiates the effect of 5-ASA in TNBS-induced colitis [127-129]. *In vitro* studies using human intestinal epithelial Caco-2 cells showed that taurine could inhibit TNFα-induced IL-8 secretion and mRNA expression [123]. Since Caco-2 cells do not express myeloperoxidase, this indicates that taurine alone also has anti-inflammatory effects. Taurine is absorbed across the apical membrane in the intestine by two transporters, TauT and PAT1 [130]. IL-1β and TNFα were found to increase taurine uptake by Caco-2 cells, which was associated with an increase in TauT mRNA levels and affinity [131]. Thus, the current evidence indicates that taurine is beneficial in its effects on inflammation and that intestinal epithelial cells can increase taurine uptake in response to inflammatory signals. However, the ability of intestinal epithelial cells to synthesize taurine under normal conditions and in response to inflammation remains unknown.

In mammals, there are two pathways for taurine synthesis (**Figure 1.3**). One is via the oxidation of cysteine to cysteinesulfinate (CSA) by CDO, followed by decarboxylation of CSA to hypotaurine by cysteinesulfinic acid decarboxylase (CSAD; EC4.1.1.29), and finally the oxidation of hypotaurine to taurine by a poorly understood mechanism [132]. The other pathway begins with the incorporation of cysteine into Coenzyme A (CoA), followed by the release of cysteamine during CoA degradation, the oxidation of cysteamine to hypotaurine by cysteamine dioxygenase (ADO), and finally the oxidation of hypotaurine to taurine [133]. While CDO is expressed in both a tissue- and cell-specific manner and is especially abundant in the liver, ADO expression appears to be more ubiquitous [108, 113, 133, 134]. CSAD expression tends to be high in tissues expressing high levels of CDO [113]. There have been no published descriptions of ADO expression within the small intestine or colon. CSAD was also shown to be expressed in

mouse colon at the protein level but was not detected in mouse duodenum [113]. The inability to detect CSAD in mouse duodenum, however, might have been due to the use of whole tissue homogenates, of which goblet cells would comprise a small portion. The observed expression of CDO and taurine in intestinal goblet cells suggests that goblet cells may also utilize cysteine to synthesize taurine. Should goblet cells be capable of synthesizing taurine this might be yet another means by which these cells contribute to host mucosal protection.

REFERENCES

1. Moncada, D. and K. Chadee, *Production, structure, and biologic relevance of gastrointestinal mucins*, in *Infections of the Gastrointestinal Tract*, S.P.D. Blaser M. J., Ravdin J. I., Greenberg H. B., Guerrant R. L., Editor. 2002, Lippincott Williams & Wilkins: Philadelphia. p. 57-79.

2. Blanpain, C., V. Horsley, and E. Fuchs, *Epithelial stem cells: turning over new leaves.* Cell, 2007. **128**(3): p. 445-58.

3. Specian, R.D. and M.G. Oliver, *Functional biology of intestinal goblet cells.* Am J Physiol, 1991. **260**(2 Pt 1): p. C183-93.

4. van der Flier, L.G. and H. Clevers, *Stem cells, self-renewal, and differentiation in the intestinal epithelium.* Annu Rev Physiol, 2009. **71**: p. 241-60.

5. van Es, J.H., et al., *Wnt signalling induces maturation of Paneth cells in intestinal crypts.* Nat Cell Biol, 2005. **7**(4): p. 381-6.

6. Jensen, J., et al., *Control of endodermal endocrine development by Hes-1.* Nat Genet, 2000. **24**(1): p. 36-44.

7. Suzuki, K., et al., *Hes1-deficient mice show precocious differentiation of Paneth cells in the small intestine.* Biochem Biophys Res Commun, 2005. **328**(1): p. 348-52.

8. van Es, J.H., et al., *Notch/gamma-secretase inhibition turns proliferative cells in intestinal crypts and adenomas into goblet cells.* Nature, 2005. **435**(7044): p. 959-63.

9. Fre, S., et al., *Notch signals control the fate of immature progenitor cells in the intestine.* Nature, 2005. **435**(7044): p. 964-8.

10. Yang, Q., et al., *Requirement of Math1 for secretory cell lineage commitment in the mouse intestine.* Science, 2001. **294**(5549): p. 2155-8.

11. Shroyer, N.F., et al., *Gfi1 functions downstream of Math1 to control intestinal secretory cell subtype allocation and differentiation.* Genes Dev, 2005. **19**(20): p. 2412-7.

12. Pinto, D., et al., *Canonical Wnt signals are essential for homeostasis of the intestinal epithelium.* Genes Dev, 2003. **17**(14): p. 1709-13.

13. Auclair, B.A., et al., *Bone morphogenetic protein signaling is essential for terminal differentiation of the intestinal secretory cell lineage.* Gastroenterology, 2007. **133**(3): p. 887-96.

14. Katz, J.P., et al., *The zinc-finger transcription factor Klf4 is required for terminal differentiation of goblet cells in the colon.* Development, 2002. **129**(11): p. 2619-28.

15. Ghaleb, A.M., et al., *Notch inhibits expression of the Kruppel-like factor 4 tumor suppressor in the intestinal epithelium.* Mol Cancer Res, 2008. **6**(12): p. 1920-7.

16. Lorentz, O., et al., *Key role of the Cdx2 homeobox gene in extracellular matrix-mediated intestinal cell differentiation.* J Cell Biol, 1997. **139**(6): p. 1553-65.

17. Mallo, G.V., et al., *Expression of the Cdx1 and Cdx2 homeotic genes leads to reduced malignancy in colon cancer-derived cells.* J Biol Chem, 1998. **273**(22): p. 14030-6.

18. Shimada, T., et al., *Regulation of TFF3 expression by homeodomain protein CDX2.* Regul Pept, 2007. **140**(1-2): p. 81-7.

19. Silberg, D.G., et al., *Cdx1 and cdx2 expression during intestinal development.* Gastroenterology, 2000. **119**(4): p. 961-71.

20. Suh, E., et al., *A homeodomain protein related to caudal regulates intestine-specific gene transcription.* Mol Cell Biol, 1994. **14**(11): p. 7340-51.

21. Yamamoto, H., Y.Q. Bai, and Y. Yuasa, *Homeodomain protein CDX2 regulates goblet-specific MUC2 gene expression.* Biochem Biophys Res Commun, 2003. **300**(4): p. 813-8.

22. Wang, M.L., et al., *Regulation of RELM/FIZZ isoform expression by Cdx2 in response to innate and adaptive immune stimulation in the intestine.* Am J Physiol Gastrointest Liver Physiol, 2005. **288**(5): p. G1074-83.

23. Dang, D.T., et al., *Expression of the gut-enriched Kruppel-like factor (Kruppel-like factor 4) gene in the human colon cancer cell line RKO is dependent on CDX2.* Oncogene, 2001. **20**(35): p. 4884-90.

24. Mutoh, H., et al., *The intestine-specific homeobox gene Cdx2 induces expression of the basic helix-loop-helix transcription factor Math1.* Differentiation, 2006. **74**(6): p. 313-21.

25. Verdugo, P., *Goblet cells secretion and mucogenesis.* Annu Rev Physiol, 1990. **52**: p. 157-76.

26. Dekker, J., et al., *The MUC family: an obituary.* Trends Biochem Sci, 2002. **27**(3): p. 126-31.

27. Gendler, S.J. and A.P. Spicer, *Epithelial mucin genes.* Annu Rev Physiol, 1995. **57**: p. 607-34.

28. Rose, M.C. and J.A. Voynow, *Respiratory tract mucin genes and mucin glycoproteins in health and disease.* Physiol Rev, 2006. **86**(1): p. 245-78.

29. Allen, A., D.A. Hutton, and J.P. Pearson, *The MUC2 gene product: a human intestinal mucin.* Int J Biochem Cell Biol, 1998. **30**(7): p. 797-801.

30. Neutra MR, F.J., *Gastrointestinal mucus: synthesis, secretion, and function*, in *Physiology of the Gastrointestial Tract*, L. Johnson, Editor. 1987, Raven Press: New York. p. 975.

31. Byrd, J.C. and R.S. Bresalier, *Mucins and mucin binding proteins in colorectal cancer.* Cancer Metastasis Rev, 2004. **23**(1-2): p. 77-99.

32. Linden, S.K., et al., *Mucins in the mucosal barrier to infection.* Mucosal Immunol, 2008. **1**(3): p. 183-97.

33. Deplancke, B. and H.R. Gaskins, *Microbial modulation of innate defense: goblet cells and the intestinal mucus layer.* Am J Clin Nutr, 2001. **73**(6): p. 1131S-1141S.

34. Corfield, A.P., et al., *Mucins in the gastrointestinal tract in health and disease.* Front Biosci, 2001. **6**: p. D1321-57.

35. Filipe, M.I., *Mucins in the human gastrointestinal epithelium: a review.* Invest Cell Pathol, 1979. **2**(3): p. 195-216.

36. Brockhausen, I., *Pathways of O-glycan biosynthesis in cancer cells.* Biochim Biophys Acta, 1999. **1473**(1): p. 67-95.

37. Robbe, C., et al., *Structural diversity and specific distribution of O-glycans in normal human mucins along the intestinal tract.* Biochem J, 2004. **384**(Pt 2): p. 307-16.

38. Seko, A., et al., *Down-regulation of Gal 3-O-sulfotransferase-2 (Gal3ST-2) expression in human colonic non-mucinous adenocarcinoma.* Jpn J Cancer Res, 2002. **93**(5): p. 507-15.

39. Lee, J.K., et al., *Activities and expression pattern of the carbohydrate sulfotransferase GlcNAc6ST-3 (I-GlcNAc6ST): functional implications.* Glycobiology, 2003. **13**(4): p. 245-54.

40. Nishimura, M. and S. Naito, *Tissue-specific mRNA expression profiles of human carbohydrate sulfotransferase and tyrosylprotein sulfotransferase.* Biol Pharm Bull, 2007. **30**(4): p. 821-5.

41. Tanner, M.E., *The enzymes of sialic acid biosynthesis.* Bioorg Chem, 2005. **33**(3): p. 216-28.

42. Wang, B., *Sialic acid is an essential nutrient for brain development and cognition.* Annu Rev Nutr, 2009. **29**: p. 177-222.

43. Kean, E.L., *Sialic acid activation.* Glycobiology, 1991. **1**(5): p. 441-7.

44. Brockhausen, I., *Mucin-type O-glycans in human colon and breast cancer: glycodynamics and functions.* EMBO Rep, 2006. **7**(6): p. 599-604.

45. Kemmner, W., et al., *Glycosyltransferase expression in human colonic tissue examined by oligonucleotide arrays.* Biochim Biophys Acta, 2003. **1621**(3): p. 272-9.

46. Spicer, S.S. and B.A. Schulte, *Diversity of cell glycoconjugates shown histochemically: a perspective.* J Histochem Cytochem, 1992. **40**(1): p. 1-38.

47. McMahon, R.F., M.J. Panesar, and R.W. Stoddart, *Glycoconjugates of the normal human colorectum: a lectin histochemical study.* Histochem J, 1994. **26**(6): p. 504-18.

48. Irimura, T., et al., *Human colonic sulfomucin identified by a specific monoclonal antibody*. Cancer Res, 1991. **51**(20): p. 5728-35.

49. Van Klinken, B.J., et al., *Sulphation and secretion of the predominant secretory human colonic mucin MUC2 in ulcerative colitis.* Gut, 1999. **44**(3): p. 387-93.

50. Robbe, C., et al., *Evidence of regio-specific glycosylation in human intestinal mucins: presence of an acidic gradient along the intestinal tract.* J Biol Chem, 2003. **278**(47): p. 46337-48.

51. Sheahan, D.G. and H.R. Jervis, *Comparative histochemistry of gastrointestinal mucosubstances.* Am J Anat, 1976. **146**(2): p. 103-31.

52. Filipe, M.I. and C. Fenger, *Histochemical characteristics of mucins in the small intestine. A comparative study of normal mucosa, benign epithelial tumours and carcinoma.* Histochem J, 1979. **11**(3): p. 277-87.

53. Lev, R., H.I. Siegel, and J. Bartman, *Histochemical studies of developing human fetal small intestine.* Histochemie, 1972. **29**(2): p. 103-19.

54. Matsuo, K., et al., *Histochemistry of the surface mucous gel layer of the human colon.* Gut, 1997. **40**(6): p. 782-9.

55. Campbell, B.J., L.G. Yu, and J.M. Rhodes, *Altered glycosylation in inflammatory bowel disease: a possible role in cancer development.* Glycoconj J, 2001. **18**(11-12): p. 851-8.

56. Shirazi, T., et al., *Mucins and inflammatory bowel disease.* Postgrad Med J, 2000. **76**(898): p. 473-8.

57. Strugala, V., P.W. Dettmar, and J.P. Pearson, *Thickness and continuity of the adherent colonic mucus barrier in active and quiescent ulcerative colitis and Crohn's disease.* Int J Clin Pract, 2008. **62**(5): p. 762-9.

58. Swidsinski, A., et al., *Comparative study of the intestinal mucus barrier in normal and inflamed colon.* Gut, 2007. **56**(3): p. 343-50.

59. Pullan, R.D., et al., *Thickness of adherent mucus gel on colonic mucosa in humans and its relevance to colitis.* Gut, 1994. **35**(3): p. 353-9.

60. Bodger, K., et al., *Altered colonic glycoprotein expression in unaffected monozygotic twins of inflammatory bowel disease patients.* Gut, 2006. **55**(7): p. 973-7.

61. Corfield, A.P., et al., *Colonic mucins in ulcerative colitis: evidence for loss of sulfation.* Glycoconj J, 1996. **13**(5): p. 809-22.

62. Raouf, A.H., et al., *Sulphation of colonic and rectal mucin in inflammatory bowel disease: reduced sulphation of rectal mucus in ulcerative colitis.* Clin Sci (Lond), 1992. **83**(5): p. 623-6.

63. Probert, C.S., et al., *South Asian and European colitics show characteristic differences in colonic mucus glycoprotein type and turnover.* Gut, 1995. **36**(5): p. 696-702.

64. Allen, D.C., N.S. Connolly, and J.D. Biggart, *Mucin profiles in ulcerative colitis with dysplasia and carcinoma.* Histopathology, 1988. **13**(4): p. 413-24.

65. Ehsanullah, M., M.I. Filipe, and B. Gazzard, *Mucin secretion in inflammatory bowel disease: correlation with disease activity and dysplasia.* Gut, 1982. **23**(6): p. 485-9.

66. Arnold, J.W., G.R. Klimpel, and D.W. Niesel, *Tumor necrosis factor (TNF alpha) regulates intestinal mucus production during salmonellosis.* Cell Immunol, 1993. **151**(2): p. 336-44.

67. Groux-Degroote, S., et al., *IL-6 and IL-8 increase the expression of glycosyltransferases and sulfotransferases involved in the biosynthesis of sialylated and/or sulfated Lewisx epitopes in the human bronchial mucosa.* Biochem J, 2008. **410**(1): p. 213-23.

68. Conour, J.E., et al., *Acidomucin goblet cell expansion induced by parenteral nutrition in the small intestine of piglets.* Am J Physiol Gastrointest Liver Physiol, 2002. **283**(5): p. G1185-96.

69. Enss, M.L., et al., *Proinflammatory cytokines trigger MUC gene expression and mucin release in the intestinal cancer cell line LS180.* Inflamm Res, 2000. **49**(4): p. 162-9.

70. Hill, R.R., H.M. Cowley, and A. Andremont, *Influence of colonizing micro-flora on the mucin histochemistry of the neonatal mouse colon.* Histochem J, 1990. **22**(2): p. 102-5.

71. Enss, M.L., et al., *Effects of perorally applied endotoxin on colonic mucins of germfree rats.* Scand J Gastroenterol, 1996. **31**(9): p. 868-74.

72. Liau, Y.H., et al., *Helicobacter pylori lipopolysaccharide effect on the synthesis and secretion of gastric sulfomucin.* Biochem Biophys Res Commun, 1992. **184**(3): p. 1411-7.

73. Baumgart, D.C. and S.R. Carding, *Inflammatory bowel disease: cause and immunobiology.* Lancet, 2007. **369**(9573): p. 1627-40.

74. Majuri, M.L., et al., *Expression and function of alpha 2,3-sialyl- and alpha 1,3/1,4-fucosyltransferases in colon adenocarcinoma cell lines: role in synthesis of E-selectin counter-receptors.* Int J Cancer, 1995. **63**(4): p. 551-9.

75. Delmotte, P., et al., *Influence of TNFalpha on the sialylation of mucins produced by a transformed cell line MM-39 derived from human tracheal gland cells.* Glycoconj J, 2001. **18**(6): p. 487-97.

76. Karlsson, N.G., et al., *Identification of transient glycosylation alterations of sialylated mucin oligosaccharides during infection by the rat intestinal parasite Nippostrongylus brasiliensis.* Biochem J, 2000. **350 Pt 3**: p. 805-14.

77. Ishikawa, N., Y. Horii, and Y. Nawa, *Immune-mediated alteration of the terminal sugars of goblet cell mucins in the small intestine of Nippostrongylus brasiliensis-infected rats.* Immunology, 1993. **78**(2): p. 303-7.

78. Soga, K., et al., *Alteration of the expression profiles of acidic mucin, sialytransferase, and sulfotransferases in the intestinal epithelium of rats infected with the nematode Nippostrongylus brasiliensis.* Parasitol Res, 2008. **103**(6): p. 1427-34.

79. Blanchard, C., et al., *IL-4 and IL-13 up-regulate intestinal trefoil factor expression: requirement for STAT6 and de novo protein synthesis.* J Immunol, 2004. **172**(6): p. 3775-83.

80. Artis, D., et al., *RELMbeta/FIZZ2 is a goblet cell-specific immune-effector molecule in the gastrointestinal tract.* Proc Natl Acad Sci U S A, 2004. **101**(37): p. 13596-600.

81. Kanoh, A., et al., *Interleukin-4 induces specific pp-GalNAc-T expression and alterations in mucin O-glycosylation in colonic epithelial cells.* Biochim Biophys Acta, 2008. **1780**(3): p. 577-84.

82. Takeda, K., et al., *Direct effects of IL-4/IL-13 and the nematode Nippostrongylus brasiliensis on intestinal epithelial cells in vitro.* Parasite Immunol. **32**(6): p. 420-9.

83. Taupin, D. and D.K. Podolsky, *Trefoil factors: initiators of mucosal healing.* Nat Rev Mol Cell Biol, 2003. **4**(9): p. 721-32.

84. Thim, L. and F.E. May, *Structure of mammalian trefoil factors and functional insights.* Cell Mol Life Sci, 2005. **62**(24): p. 2956-73.

85. Wright, N.A., *Interaction of trefoil family factors with mucins: clues to their mechanism of action?* Gut, 2001. **48**(3): p. 293-4.

86. Matsuoka, Y., J.C. Pascall, and K.D. Brown, *Quantitative analysis reveals differential expression of mucin (MUC2) and intestinal trefoil factor mRNAs along the longitudinal axis of rat intestine.* Biochim Biophys Acta, 1999. **1489**(2-3): p. 336-44.

87. Playford, R.J., et al., *Human spasmolytic polypeptide is a cytoprotective agent that stimulates cell migration.* Gastroenterology, 1995. **108**(1): p. 108-16.

88. Playford, R.J., et al., *Transgenic mice that overexpress the human trefoil peptide pS2 have an increased resistance to intestinal damage.* Proc Natl Acad Sci U S A, 1996. **93**(5): p. 2137-42.

89. Cook, G.A., et al., *Oral human spasmolytic polypeptide protects against aspirin-induced gastric injury in rats.* J Gastroenterol Hepatol, 1998. **13**(4): p. 363-70.

90. Meyer zum Buschenfelde, D., R. Tauber, and O. Huber, *TFF3-peptide increases transepithelial resistance in epithelial cells by modulating claudin-1 and -2 expression.* Peptides, 2006. **27**(12): p. 3383-90.

91. Banerjee, R.R. and M.A. Lazar, *Dimerization of resistin and resistin-like molecules is determined by a single cysteine.* J Biol Chem, 2001. **276**(28): p. 25970-3.

92. Steppan, C.M., et al., *A family of tissue-specific resistin-like molecules.* Proc Natl Acad Sci U S A, 2001. **98**(2): p. 502-6.

93. Holcomb, I.N., et al., *FIZZ1, a novel cysteine-rich secreted protein associated with pulmonary inflammation, defines a new gene family.* Embo J, 2000. **19**(15): p. 4046-55.

94. He, W., et al., *Bacterial colonization leads to the colonic secretion of RELMbeta/FIZZ2, a novel goblet cell-specific protein.* Gastroenterology, 2003. **125**(5): p. 1388-97.

95. Hogan, S.P., et al., *Resistin-like molecule beta regulates innate colonic function: barrier integrity and inflammation susceptibility.* J Allergy Clin Immunol, 2006. **118**(1): p. 257-68.

96. McVay, L.D., et al., *Absence of bacterially induced RELMbeta reduces injury in the dextran sodium sulfate model of colitis.* J Clin Invest, 2006. **116**(11): p. 2914-23.

97. Barnes, S.L., et al., *Resistin-like molecule beta (RELMbeta/FIZZ2) is highly expressed in the ileum of SAMP1/YitFc mice and is associated with initiation of ileitis.* J Immunol, 2007. **179**(10): p. 7012-20.

98. Faure, M., et al., *Specific amino acids increase mucin synthesis and microbiota in dextran sulfate sodium-treated rats.* J Nutr, 2006. **136**(6): p. 1558-64.

99. Kim, C.J., et al., *L-cysteine supplementation attenuates local inflammation and restores gut homeostasis in a porcine model of colitis.* Biochim Biophys Acta, 2009. **1790**(10): p. 1161-9.

100. Bauchart-Thevret, C., et al., *Sulfur amino acid deficiency upregulates intestinal methionine cycle activity and suppresses epithelial growth in neonatal pigs.* Am J Physiol Endocrinol Metab, 2009. **296**(6): p. E1239-50.

101. Riedijk, M.A., et al., *Methionine transmethylation and transsulfuration in the piglet gastrointestinal tract.* Proc Natl Acad Sci U S A, 2007. **104**(9): p. 3408-13.

102. Finkelstein, J.D., *Methionine metabolism in mammals.* J Nutr Biochem, 1990. **1**(5): p. 228-37.

103. Finkelstein, J.D., *The metabolism of homocysteine: pathways and regulation.* Eur J Pediatr, 1998. **157 Suppl 2**: p. S40-4.

104. Stoll, B., et al., *Catabolism dominates the first-pass intestinal metabolism of dietary essential amino acids in milk protein-fed piglets.* J Nutr, 1998. **128**(3): p. 606-14.

105. Bos, C., et al., *Intestinal lysine metabolism is driven by the enteral availability of dietary lysine in piglets fed a bolus meal.* Am J Physiol Endocrinol Metab, 2003. **285**(6): p. E1246-57.

106. Stipanuk, M.H., et al., *Mammalian cysteine metabolism: new insights into regulation of cysteine metabolism.* J Nutr, 2006. **136**(6 Suppl): p. 1652S-1659S.

107. Joseph, C.A. and M.J. Maroney, *Cysteine dioxygenase: structure and mechanism.* Chem Commun (Camb), 2007(32): p. 3338-49.

108. Hirschberger, L.L., et al., *Murine cysteine dioxygenase gene: structural organization, tissue-specific expression and promoter identification.* Gene, 2001. **277**(1-2): p. 153-61.

109. Tsuboyama, N., et al., *Structural organization and tissue-specific expression of the gene encoding rat cysteine dioxygenase.* Gene, 1996. **181**(1-2): p. 161-5.

110. Tsuboyama-Kasaoka, N., et al., *Human cysteine dioxygenase gene: structural organization, tissue-specific expression and downregulation by phorbol 12-myristate 13-acetate.* Biosci Biotechnol Biochem, 1999. **63**(6): p. 1017-24.

111. Ueki, I. and M.H. Stipanuk, *Enzymes of the taurine biosynthetic pathway are expressed in rat mammary gland.* J Nutr, 2007. **137**(8): p. 1887-94.

112. Shimada, M., et al., *Expression and localization of cysteine dioxygenase mRNA in the liver, lung, and kidney of the rat.* Amino Acids, 1998. **15**(1-2): p. 143-50.

113. Stipanuk, M.H. and I. Ueki, *Dealing with methionine/homocysteine sulfur: cysteine metabolism to taurine and inorganic sulfur.* J Inherit Metab Dis.

114. Coloso, R.M. and M.H. Stipanuk, *Metabolism of cyst(e)ine in rat enterocytes.* J Nutr, 1989. **119**(12): p. 1914-24.

115. Stipanuk, M.H., et al., *Cysteine dioxygenase: a robust system for regulation of cellular cysteine levels.* Amino Acids, 2009. **37**(1): p. 55-63.

116. Terauchi, A., et al., *Immunohistochemical localization of taurine in various tissues of the mouse.* Amino Acids, 1998. **15**(1-2): p. 151-60.

117. Sturman, J.A., *Taurine in development.* Physiol Rev, 1993. **73**(1): p. 119-47.

118. Huxtable, R.J., *Physiological actions of taurine.* Physiol Rev, 1992. **72**(1): p. 101-63.

119. Ahlman, B., et al., *Free amino acids in biopsy specimens from the human colonic mucosa.* J Surg Res, 1993. **55**(6): p. 647-53.

120. Son, M.W., et al., *Protective effect of taurine on TNBS-induced inflammatory bowel disease in rats.* Arch Pharm Res, 1998. **21**(5): p. 531-6.

121. Giris, M., et al., *Effect of taurine on oxidative stress and apoptosis-related protein expression in trinitrobenzene sulphonic acid-induced colitis.* Clin Exp Immunol, 2008. **152**(1): p. 102-10.

122. Shimizu, M., et al., *Dietary taurine attenuates dextran sulfate sodium (DSS)-induced experimental colitis in mice.* Adv Exp Med Biol, 2009. **643**: p. 265-71.

123. Zhao, Z., et al., *Attenuation by dietary taurine of dextran sulfate sodium-induced colitis in mice and of THP-1-induced damage to intestinal Caco-2 cell monolayers.* Amino Acids, 2008. **35**(1): p. 217-24.

124. Jung, Y.J., et al., *Synthesis and properties of 5-aminosalicyl-taurine as a colon-specific prodrug of 5-aminosalicylic acid.* Arch Pharm Res, 2003. **26**(4): p. 264-9.

125. Jung, Y., et al., *Evaluation of 5-aminosalicyltaurine as a colon-specific prodrug of 5-aminosalicylic acid for treatment of experimental colitis.* Eur J Pharm Sci, 2006. **28**(1-2): p. 26-33.

126. Schuller-Levis, G., et al., *Taurine protects against oxidant-induced lung injury: possible mechanism(s) of action.* Adv Exp Med Biol, 1994. **359**: p. 31-9.

127. Barua, M., Y. Liu, and M.R. Quinn, *Taurine chloramine inhibits inducible nitric oxide synthase and TNF-alpha gene expression in activated alveolar macrophages: decreased NF-kappaB activation and IkappaB kinase activity.* J Immunol, 2001. **167**(4): p. 2275-81.

128. Schuller-Levis, G.B. and E. Park, *Taurine and its chloramine: modulators of immunity.* Neurochem Res, 2004. **29**(1): p. 117-26.

129. Kim, H., et al., *A molecular mechanism for the anti-inflammatory effect of taurine-conjugated 5-aminosalicylic acid in inflamed colon.* Mol Pharmacol, 2006. **69**(4): p. 1405-12.

130. Anderson, C.M., et al., *Taurine uptake across the human intestinal brush-border membrane is via two transporters: H+-coupled PAT1 (SLC36A1) and Na+- and Cl(-)-dependent TauT (SLC6A6).* J Physiol, 2009. **587**(Pt 4): p. 731-44.

131. Mochizuki, T., H. Satsu, and M. Shimizu, *Tumor necrosis factor alpha stimulates taurine uptake and transporter gene expression in human intestinal Caco-2 cells.* FEBS Lett, 2002. **517**(1-3): p. 92-6.

132. Stipanuk, M.H., *Sulfur amino acid metabolism: pathways for production and removal of homocysteine and cysteine.* Annu Rev Nutr, 2004. **24**: p. 539-77.

133. Coloso, R.M., et al., *Cysteamine dioxygenase: evidence for the physiological conversion of cysteamine to hypotaurine in rat and mouse tissues.* Adv Exp Med Biol, 2006. **583**: p. 25-36.

134. Dominy, J.E., Jr., et al., *Discovery and characterization of a second mammalian thiol dioxygenase, cysteamine dioxygenase.* J Biol Chem, 2007. **282**(35): p. 25189-98.

FIGURES AND TABLES

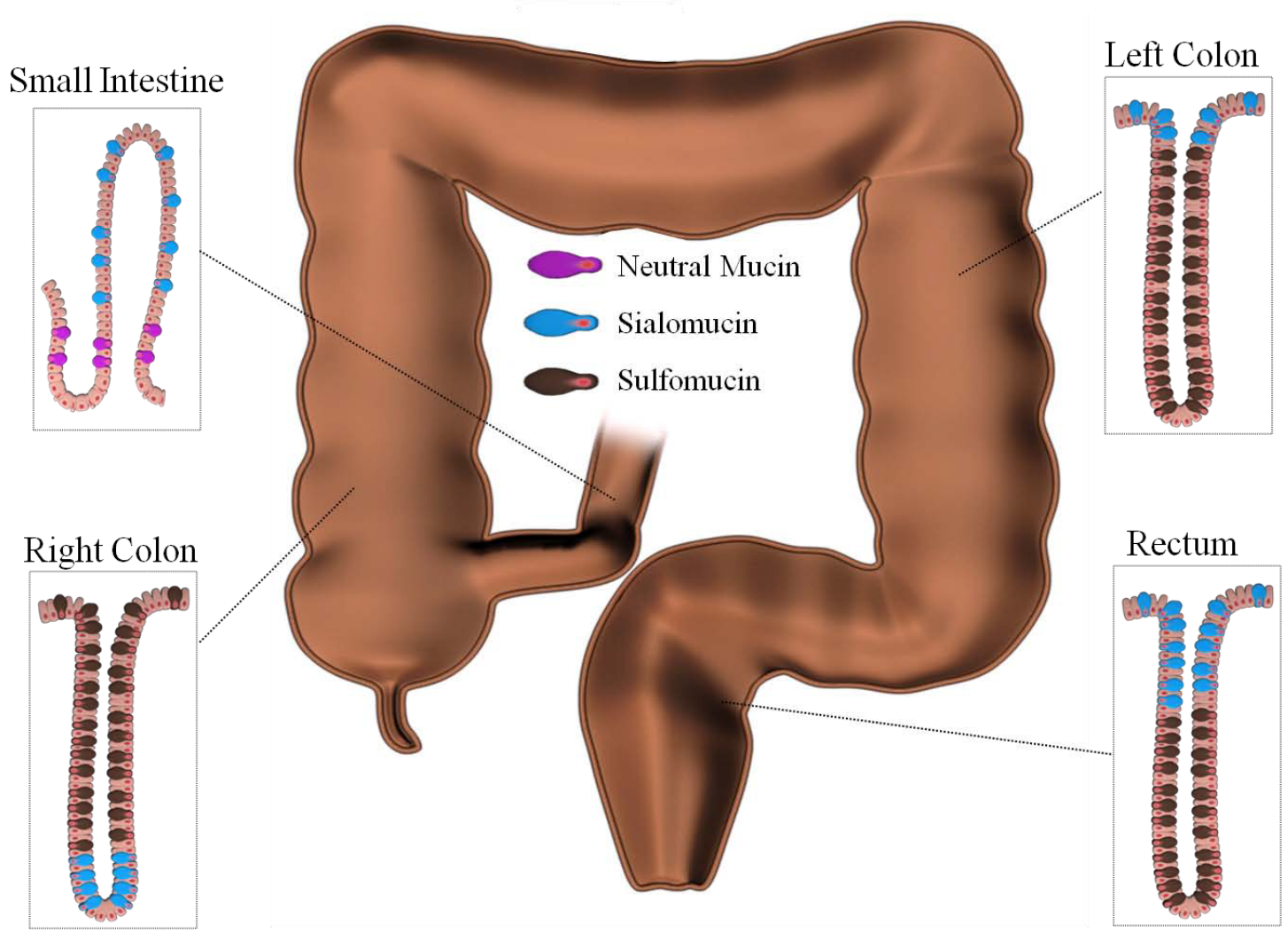

Figure 1.1: Schematic showing previously described regional and spatial distribution of neutral mucin, sialomucin, and sulfomucin in the human small intestine and colon.

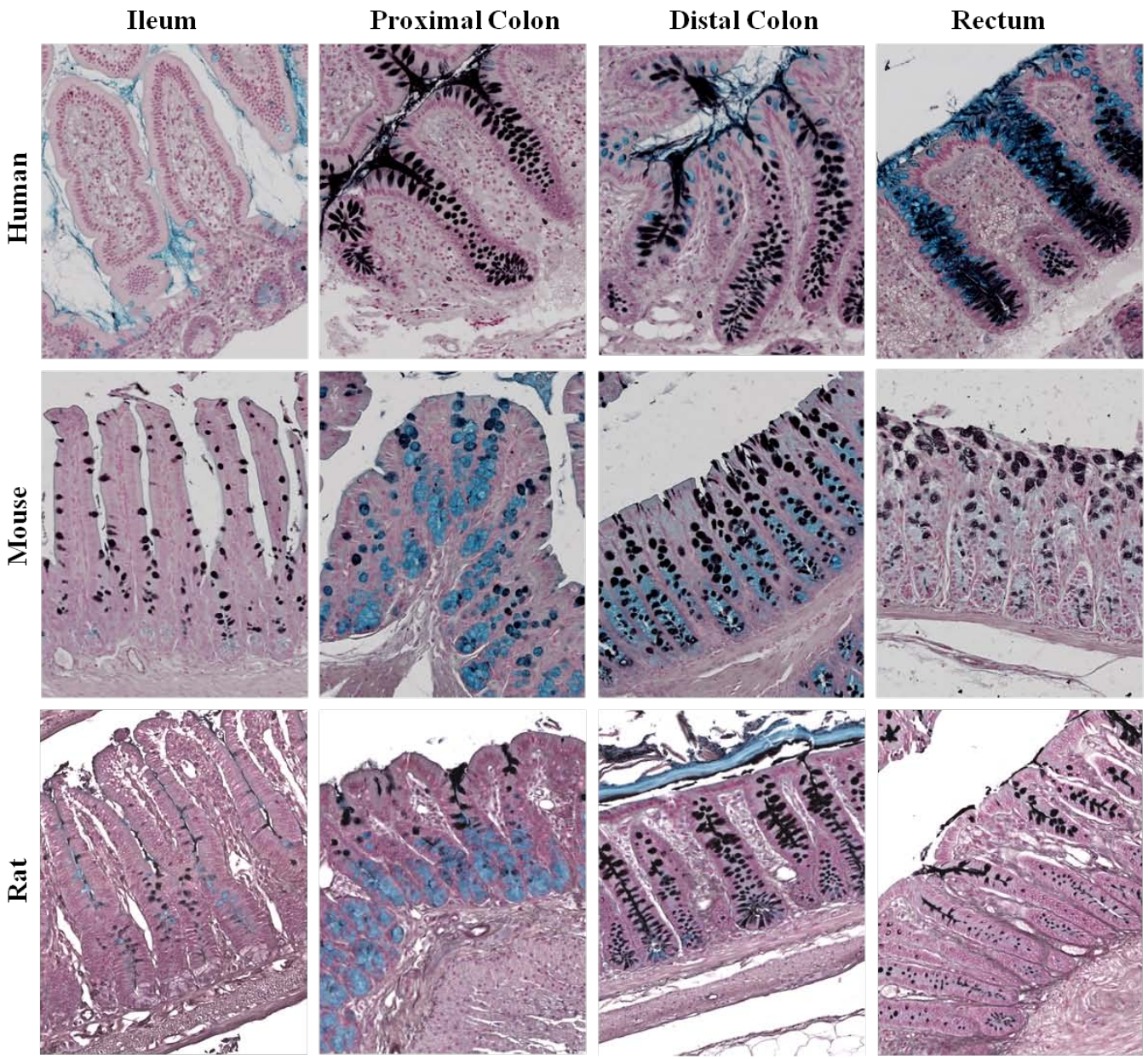

Figure 1.2: High iron diamine and acian blue, pH 2.5 staining of human, mouse, and rat small intestine, colon, and rectum showing differences in sialomucin (blue) and sulfomucin (brown/black) staining between species.

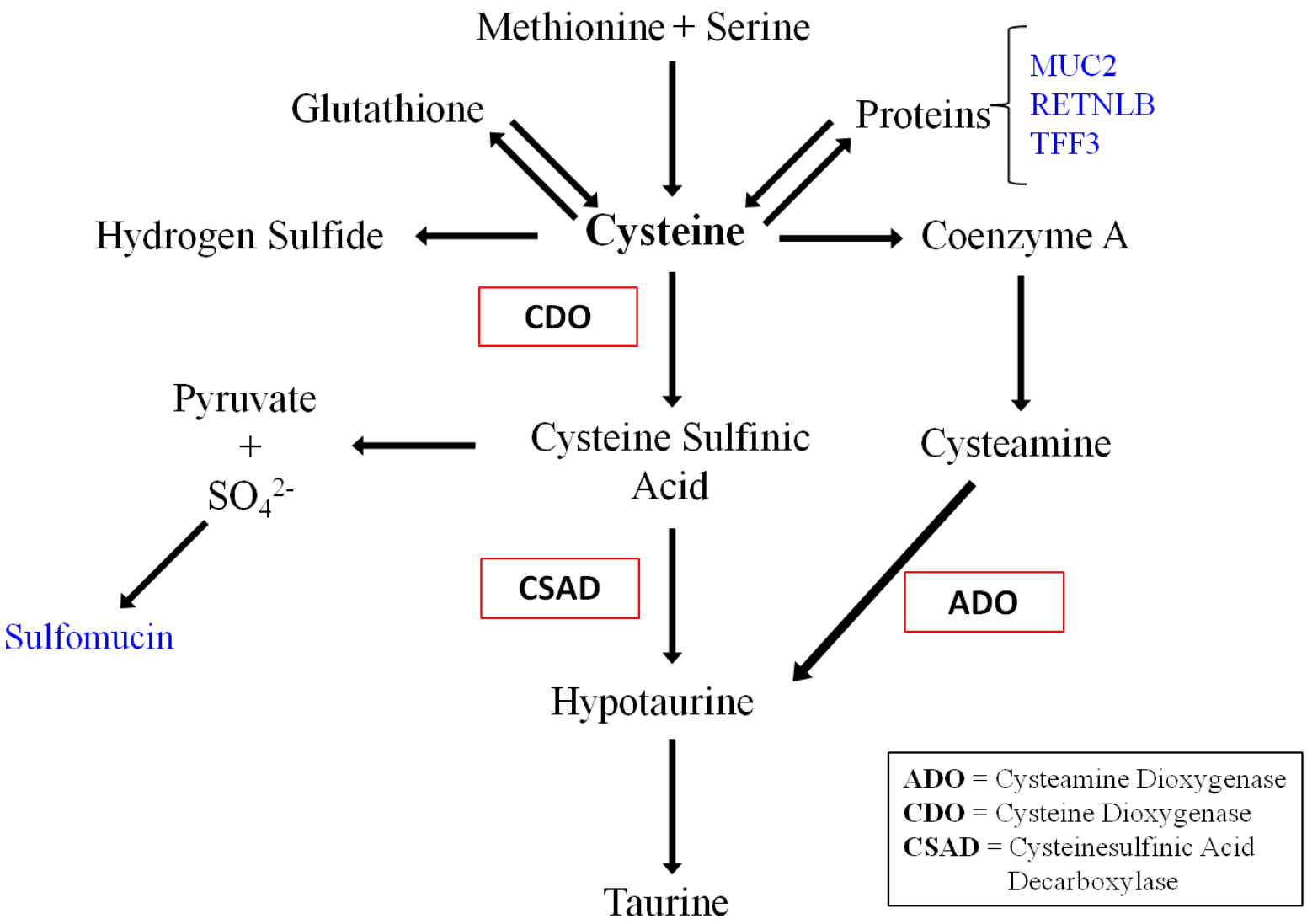

Figure 1.3: A metabolic flow chart illustrating the many products requiring cysteine, including goblet cell specific products (blue) as well as the enzymes involved in taurine biosynthesis from cysteine.

Table 1.1. Structural elements of mucin-type O-linked glycans.*

	Core structures
Tn antigen, sialyl Tn	GalNAcα1-Ser/Thr, NeuAcα6GalNAc
Core 1	Galβ1-3GalNAcα1-Ser/Thr (TF antigen when unsubstituted)
Core 2	Galβ1-3(GlcNAcβ1-6)GalNAcα1-Ser/Thr
Core 3	GlcNAcβ1-3GalNAcα1-Ser/Thr
Core 4	GlcNAcβ1-3(GlcNAcβ1-6)GalNAcα1-Ser/Thr
Core 5	GalNAcα1-3GalNAcα1-Ser/Thr
Core 6, 7, 8	GlcNAcβ1-6GalNAc-, GalNAcα1-6GalNAc-, GalNAcα1-6GalNAc-
	Backbone structures
Type 1	Galβ3GlcNAcβ-
Type 2	Galβ4GlcNAcβ-
Unbranched (i antigen)	GlcNACβ3Galβ-
Branched (I antigen)	GlcNAcβ3(GlcNAcβ6)Galβ-
	Peripheral structures
A, B, H blood group	GalNAcα3(Fucα2)Galβ-, Galα3(Fucα2)Galβ-, Fucα2Galβ-
Le^a, Le^b	Galβ3(Fucα4)Galβ-, Fucα2Galβ3(Fucα4)Galβ-
LeX, LeY	Galβ4(Fucα3)Galβ-, Fucα2Galβ4(Fucα3)Galβ-
Sialyl Lea, Sia LeX	NeuAcα3Galβ3(Fucα4)Galβ-, NeuAcα3Galβ4(Fucα3)Galβ-
Sulfate	HSO_3-3Galβ-, HSO_3-6GlcNAcβ-
Sd^a/Cad	GalNAcβ4[NeuAcα3]Galβ-

Standard abbreviations: Fuc, fucose; Gal, galactose; GalNAc, N-acetyl-galactosamine; GlcNAc, N-acetyl-glucosamine; NeuAc, N-acetyl-neuraminic acid; Ser, serine; Thr, threonine.

* With kind permission from Springer Science+Business Media: Cancer and Metastasis Reviews, Mucins and mucin binding proteins in colorectal cancer, 23, 2004, p. 77-99, J.C. Byrd and R.S. Bresalier, Table 2, Copyright 2004 Kluwer Academic Publishers.

Chapter 2

CHARACTERIZATION OF SULFOMUCIN AND SIALOMUCIN EXPRESSION AND THEIR RELATIONSHIP WITH SULFATE-REDUCING BACTERIA IN THE HEALTHY HUMAN COLON

ABSTRACT

Goblet cell mucins are important components of mucosal barrier function through their role in forming the mucus gel layer which serves as a medium for protection between the luminal contents and epithelial lining. Mucins show great structural heterogeneity, but can be broadly classified into neutral and acidic subtypes (chemotypes), which are classified further into sulfomucins or sialomucins based on the presence of terminal sulfate or sialic acid groups on the oligosaccharide chains. Mucin chemotypes vary regionally throughout the gastrointestinal tract, but normal colonic mucin tends to be highly sulfated. Quantitative data and a description of interindividual variation in sulfo- and sialomucin content in the human colon are lacking. It is important to understand both regional and interindividual variation in these two mucin chemotypes as differences in their expression has been observed in diseases such as inflammatory bowel disease and colorectal cancer. Furthermore, both regional and interindividual variation in sulfo- and sialomucins may influence microbial colonization. For example, sulfomucins may promote the colonization of sulfate reducing bacteria (SRB), which through sulfate respiration generate the genotoxic gas hydrogen sulfide. In this regard, a pilot study was conducted to better characterize sulfo- and sialomucins and their relationship to SRB diversity in the human colon. Paired biopsies from the right colon, left colon, and rectum were collected from 20 healthy subjects undergoing routine screening colonoscopies. Goblet cell

sulfo- and sialomucins were identified by high iron diamine and alcian blue, pH 2.5 (HID/AB) histochemistry, quantified, and scored in each biopsy. SRB diversity was examined with nested PCR-terminal restriction fragment length polymorphism (TRFLP) of the 16S rRNA gene of *Desulfovibrio* spp. and the functional gene, dissimilatory sulfite reductase (*dsrA*). Regional variation was observed in sulfomucins and sialomucins with the greatest abundance of each found in the rectum. Scoring along the crypt revealed this was likely due to an increase in sulfomucin in the lower crypt and an increase in sialomucin along the surface epithelium and upper crypt. Pairwise comparisons of mucin data revealed interindividual differences among regions with the right colon exhibiting the greatest extent of interindividual variation.Interindividual variation in SRB profiles was found to be greater than that in mucin profiles and was lowest in the right colon, indicating that interindividual variation in sulfo- and sialomucin chemotypes does not entirely account for interindividual variation in SRB profiles. Combined mucin and SRB data revealed no differences in interindividual variation among intestinal regions. Multivariate analysis of the mucin and SRB data revealed that samples clustered based on subject rather than location. Using principal component analysis it was found that specific terminal restriction fragments (microbial phylotypes) and sulfomucin abundance had the greatest influence on the formation of these clusters. These results highlight the importance of sampling from defined colonic regions and demonstrate that while both sulfo- and sialomucins differ by region, their relationship with SRB is not influenced by location in the colon, but rather by the host. Additional studies are necessary to further elucidate the factors that contribute to interindividual variation in mucin chemotypes and SRB.

INTRODUCTION

The colonic mucus layer is an important interface between the host epithelium and the luminal contents, including the mutualistic microbiota. Mucins, which are largely responsible for the viscous properties of the mucus layer, consist of a peptide backbone containing alternating glycosylated and non-glycosylated domains [1]. The oligosaccharide chains attached to the peptide backbone in the glycosylated domains show great structural heterogeneity [2, 3], which may determine the biological and physiological properties of the mucins as well as the bacteria able to colonize the mucus layer [4-6]. Mucins can be broadly classified into neutral and acidic subtypes (chemotypes), which are classified further into sulfomucins or sialomucins based on the presence of terminal sulfate or sialic acid groups on the oligosaccharide chain, respectively [7]. These mucin chemotypes can be identified using various histochemical stains. Of particular interest for this study is the high iron diamine and alcian blue (HID/AB) stain, which distinguishes sulfomucin and sialomucin [8]. Previous studies using the HID/AB stain to examine the distribution of sulfomucins and sialomucin report an overall predominance of sulfomucin in the human colon with distinct patterns of sulfomucin and sialomucin distribution both regionally and along the crypt [7, 9]. However, quantitative measurements of sulfomucin and sialomucin have not been reported and there has been little description of the extent of interindividual variation in acidomucin chemotypes in healthy individuals.

Alterations in sulfo- and sialomucin chemotypes have been observed in patients with inflammatory bowel disease and colorectal cancer [7, 10-13]. Specifically, a significant decrease in sulfomucins and an increase in sialomucins have been observed in ulcerative colitis and were found to correlate with disease severity [10, 12, 13]. In the case of colorectal cancer a similar change is seen in the transitional mucosa and in non-mucinous adenocarcinomas [3, 7]. The

cause and significance of these changes in mucin chemotypes in disease as well as the spatial variation observed in healthy individuals remain to be fully understood.

One possible consequence of the expression of particular mucin chemotypes is selection for specific microbiota. Carbohydrates and terminal groups on mucin oligosaccharide chains can serve as binding sites as well as a potential source of nutrients for microbes. A number of interactions between microbes and mucins have been demonstrated in the colon and other mucosal regions of the body [4, 6]. Particular focus is given here to the sulfate-reducing bacteria (SRB), members of the normal colonic microbiota, which through sulfate respiration generate the gas hydrogen sulfide (H_2S) [14]. Previously described commensal SRB include *Desulfotomaculum* sp., *Desulfobacter* sp., *Desulfomonas* sp., *Desulfobulbus* sp. and *Desulfovibrio* sp. [15-20], but *Desulfovibrio* spp. are believed to be the most predominant [16]. There is considerable evidence implicating SRB and their end product, H_2S, in the pathogenesis of UC, including the observation of increased numbers of SRB in feces of UC patients compared to controls and in UC patients with active disease compared to those in remission [21, 22]. In addition, H_2S has been shown to be a potent genotoxin [23, 24] and has been linked with chronic inflammatory disorders of the colon [25, 26]. Relatively little is known about the diversity and ecology of colonic SRB populations in the human colon, but in the mouse SRB populations were found to be most abundant in intestinal regions harboring the greatest density of sulfomucin-containing goblet cells [27]. Furthermore, mouse studies suggest that sulfate for sulfate reducers may be derived from sulfomucins rather than exogenous sulfate [28].

The aim of the present study was to better understand spatial and interindividual variation in sulfomucins and sialomucins and the relationship between acidomucin chemotypes and SRB in the human colon. To achieve this goal sulfomucins and sialomucins were quantified and

scored in human colon biopsies from right colon, left colon, and rectum. Molecular-based methods were used to examine the diversity of *Desulfovibrio* spp. 16S rRNA and the functional dissimilatory sulfite reductase (*dsrA*) gene from SRB in a matched set of biopsies. The combined data were subjected to multivariate analyses to elucidate possible relationships between acidomucin chemotypes and SRB.

MATERIALS AND METHODS

Sample Collection. All procedures were approved by the Carle Foundation Hospital and University of Illinois at Urbana-Champaign Institutional Review Boards. Twenty healthy subjects (12 women and 8 men) aged 47-64 years undergoing routine screening colonoscopy at Carle Foundation Hospital (Urbana, IL USA) were recruited for this study. Enrolled subjects had no known history of gastrointestinal disease and had not been on antibiotics for at least thirty days prior to sample collection. After obtaining informed consent, mucosal biopsies were collected during a routine screening colonoscopy from the right colon, left colon, and rectum for mucin histochemistry, histopathological analysis, and microbial analysis. Biopsies for microbial analysis were immediately frozen in liquid nitrogen and then stored at -80^{o}C. Biopsies for mucin histochemistry were fixed in Bouin's solution while biopsies for histopathological examination were fixed in 10% neutral buffered formalin. Fixed biopsies were sent to the Carle Clinic Pathology Services Laboratory (Urbana, IL USA) for processing, embedding, and sectioning. Demographic information including age, gender, height, weight, race, and smoking were collected from review of subjects' medical charts. Subject demographic information and endoscopic findings are summarized in **Table 2.1**.

Mucin Histochemistry and Histopathological Analysis. To identify sialomucins and sulfomucins, biopsy sections were stained with high iron diamine (HID) and alcian blue (AB), pH 2.5 as previously described [27] and counterstained with nuclear fast red for 2 minutes. For histopathological analysis, sections were stained with hematoxylin and eosin and then examined by a board certified pathologist.

Quantification of Sialomucin and Sulfomucin. Images of HID/AB stained sections were captured using a Zeiss Axiovert 200M Microscope and the Mosaix module in Axiovision 4.5 software. The Automeasure module in Axiovision 4.5 was then used to select and quantify the area of sialomucin and sulfomucin within goblet cells based on pixel color as shown for sulfomucin in **Figure 2.1**. For each biopsy, the area of sialomucin and sulfomucin within goblet cells was measured for the entire section with the exception of areas that were too damaged to distinguish goblet cells or the epithelium. The area of each mucin was normalized to the area of epithelium containing the quantified mucin.

Sialomucin and Sulfomucin Scoring. Positive staining for sialomucin and sulfomucin along the surface epithelium, upper crypt, and lower crypt was scored according to the system described in **Table 2.2**. Scoring was performed at two independent times for each image and the two scores were averaged.

SRB Analysis. The diversity of *Desulfovibrio* spp. (16S rRNA gene) and SRB (*dsrA* gene) were examined using a nested PCR-terminal restriction fragment length polymorphism (TRFLP) as

previously described [29]. For each microbial gene target, TRFLP analyses were performed using two independent restriction enzymes. HpyCh4IV and ScrfI endonucleases were used for the digestion of *Desulfovibrio* spp. 16S rRNA gene amplicons. For the analysis of *dsrA* genes, nested PCR amplicons were digested with Sau96I and BstUI endonucleases (NE Biolabs). Profiles obtained with two independent restriction analyses (endonucleases) were concatenated to form a collective data set, and the resulting output files were used in multivariate statistical analyses

Statistical Analysis. For comparison of regional and gender differences in sulfomucin and sialomucin areas, % sulfomucin (sulfomucin area/[sulfomucin area+sialomucin area]), and mucin scoring, an ANOVA and Fisher's Protected Least Significant Difference test (FLSD test) were used. Interindividual variation in sulfomucin and sialomucin was assessed by performing a pairwise comparison using the Morisita similarity index followed by an ANOVA and FLSD test to compare differences in similarities. Multivariate analyses were performed using matrix concatenation of mucin areas, mucin scores, and SRB profiles. First, non-metric multidimensional scaling (NMDS) analysis was performed to ordinate samples based on intestinal region (R, L, Re). Multivariate cluster analysis (MCA) was then carried out to group samples using a similarity index of 65%. NMDS ordinations were then performed to corroborate the MCA clusters. Principal component analysis (PCA) and factor analysis was used to identify major factors contributing to NMDS-clusters formation. Because PCA ordination confirmed NMDS analysis, PCA-factors were overlaid on NMDS plots. Finally, multivariate ANOVA (MANOVA) was used for an inferential statistical analysis for the quantitative assessment of SRB and mucin profiles among clusters. All multivariate statistical analyses were performed

with the PAST software package [30-33]. ANOVA and FLSD test were carried out using SAS software (Statview, Version 5.0.1; SAS Institute, Cary, NC). Differences were considered significant at $p < 0.05$.

RESULTS

Mucin Histochemistry. Both spatial and interindividual variation in sulfomucin and sialomucin content were evident in the HID/AB stained biopsies (**Figure 2.2**). In general, goblet cells in the right colon were predominantly sulfomucin positive with a few sialomucin positive goblet cells near the surface epithelium and occasionally in the lower crypt. Goblet cell mucins in the left colon were predominantly sulfated with variable numbers of sialomucin positive goblet cells found in the upper crypt and surface epithelium. In the rectum, an increase in the density of sialomucin in the surface epithelium and upper crypt was consistently found among individuals. The lower crypt in the rectum primarily contained sulfomucin positive goblet cells. Interindividual variation included differences in the abundance of sulfomucin and sialomucin and their spatial distribution.

Sulfomucin and Sialomucin Abundance. To better understand regional and interindividual differences in sialo- and sulfomucin abundance, the area of sialo- and sulfomucin staining within goblet cells was measured per area of epithelium analyzed. Data obtained from quantitative analysis of sulfomucin and sialomucin staining in all 60 biopsies as well as the percent of stained mucin that stained as sulfomucin (% sulfomucin = sulfomucin area/[sulfomucin area + sialomucin area]) are shown in **Table 2.3**. These data reveal that sulfomucin containing goblet cells are present in all biopsies collected and that sulfomucin abundance is greater than

sialomucin abundance in all biopsies with the exception of the right colon biopsy from subject 4 and the rectal biopsy from subject 8. Comparison of sulfomucin and sialomucin among the three colonic regions revealed both mucin chemotypes to be most abundant in the rectum, but not significantly different between right colon and rectum (**Figure 2.3A and B**). Analysis of the % sulfomucin revealed sulfomucins to be predominant in all three regions (**Figure 2.3C**), but less predominant in the rectum where the presence of sialomucins is increased. A comparison of sulfomucin and sialomucin abundance between male and female subjects revealed that female subjects harbored significantly more sialomucin in the rectum than male subjects (**Figure 2.4)**, although the abundance of the two acidomucin chemotypes was similar in male and female subjects for all other colonic regions.

Sulfomucin and Sialomucin Distribution along the Crypt. To define sulfomucin and sialomucin gradients along the crypt semi-quantitatively, sulfo- and sialomucin staining were scored along the surface epithelium, upper crypt, and lower crypt. These data are shown in **Table 2.4**. Score comparisons for each region are shown in **Figure 2.5**. For sulfomucin, scores were highest in the lower crypt of the left colon and rectum and lowest for the surface epithelium of the rectum. Thus, the greater abundance of sulfomucin in the rectum likely reflects more sulfomucin in the lower crypt. A trend towards decreasing sulfomucin on the surface epithelium in more distal regions of the colon was also observed. Sialomucin scores were highest in the surface epithelium and upper crypt of the rectum, indicating that the greater area of rectal sialomucin reflects increasing amounts in those regions of the crypt. Both surface and upper crypt sialomucin appeared to increase for more distal sections. Sialomucin score was lowest in the lower crypt of the left colon.

Interindividual Variation in Sulfomucin and Sialomucin. To assess interindividual variability in sulfomucin and sialomucin abundance and distribution along the crypt-surface epithelium within the three colonic regions, pairwise similarities between right colon, left colon and rectum were estimated using Morisita similarity indices (**Figure 2.6**). Statistical analysis revealed that for mucin abundance (**Figure 2.6A**), interindividual variation was greatest in the right colon (R vs R) and lowest in the left colon (L vs L) with rectum (Re vs Re) being intermediate. Furthermore, mucin abundance was most similar between the right colon and left colon (R vs L) and least similar between the right colon and rectum (R vs Re). Interindividual variation in mucin scores was also highest in the right colon, but was comparable between the left colon and rectum (**Figure 2.6B**). Mucin scores were most similar between right colon and left colon and left colon and rectum and least similar between right colon and rectum. Analysis of combined mucin area and mucin score data indicated that interindividual variation in overall mucin data was lowest in the rectum and equivalent between the right and left colon (**Figure 2.6C**). Similar to the score data alone, combined score and abundance data were most similar between right colon and left colon and between left colon and rectum and least similar between right colon and rectum.

SRB Analysis. Nested PCR for the *Desulfovibrio* spp. 16S rRNA gene demonstrated that all 20 subjects harbored mucosa-associated *Desulfovibrio* populations in at least one colonic region. Examination of SRB populations associated with the colonic mucosa via nested PCR analysis of a functional gene for sulfate reduction, dissimilatory sulfite reductase (*dsrA)* indicated that 19 out of 20 subjects harbored mucosa-associated SRB populations in at least one region of the colon. Neither the *Desulfovibrio* spp. 16S rRNA gene nor the *dsrA* gene was detected in the right colon of subject 6 and the left colon biopsy of subject 1. Consequently, these samples were excluded

from further analyses of interindividual variation and multivariate analyses involving SRB profiles. It should be noted that histopathological analysis of additional biopsies from left colon of subject 1 showed acute inflammation and minor abnormalities were observed in additional biopsies from right colon of subject 6. To measure diversity of mucosa associated SRB in the human colon, TRFLP analyses of the *Desulfovibrio* 16S rRNA gene and the *dsrA* functional gene were conducted. Multivariate analysis of the resulting SRB profiles for each biopsy revealed that SRB are highly diverse within healthy subjects, but the diversity of SRB is comparable across colonic regions. However, in a few samples, SRB profiles were found to be slightly more homogenous in the right colon than other regions. For additional details and figures see reference [29].

Interindividual Variation in SRB Profiles and Combined SRB and Mucin Profiles. Interindividual variation in SRB profiles was analyzed by performing pairwise comparisons among right colon, left colon and rectum using Morisita similarity indices (**Figure 2.7A**). Statistical analysis indicated that interindividual variation was greater in the rectum than the right colon, but neither differed significantly from the left colon, and left colon and rectum exhibited the greatest difference in SRB profiles. Furthermore, the much lower similarity indices for SRB profiles compared to mucin abundance and scores (**Figure 2.6**), indicate greater interindividual variation in SRB profiles than in mucin chemotypes. Interindividual variation was also examined in combined SRB profile and mucin data and found to be comparable in all three regions (**Figure 2.7B**). The low similarity indices demonstrate high interindividual variation in combined SRB and mucin data.

Multivariate Cluster Analysis of Mucin and SRB Data. Multivariate cluster analysis of sulfomucin and sialomucin areas demonstrated clustering by region and minimal clustering by subject (**Figure 2.8**). Rectal biopsies tended to cluster, while right colon and left colon biopsies were often found in a common cluster. Similar observations were made for cluster analysis of mucin scoring data (**Figure 2.9**) as well as cluster analysis of combined mucin areas and scoring data (**Figure 2.10**). Thus, for sulfo- and sialomucins there was generally more similarity among the same regions from different subjects than different regions from the same subject.

On the other hand, cluster analysis for SRB profiles showed clustering by subject with minimal clustering by region (**Figure 2.11**), indicating that microbial profiles tended to be more similar within the same individual than from the same region of different individuals. Due to the high interindividual variation, MCA of combined SRB and mucin profiles (**Figure 2.12**) was performed and a similarity index of 65% was used to select samples with comparable SRB-mucin profiles. This approach revealed the presence of four distinct SRB-mucin clusters, which encompassed all but five samples. Additionally, the SRB-mucin profiles clustered by subject rather than by colonic region. However, within some clusters of subjects, greater similarity indices could be found between samples from the same region. For example, all biopsies from subject 7 and 8 were contained in cluster III, but right colon from subject 7 (7R) was more similar to right colon of subject 8 (8R) than to the left colon of subject 7 (7L). Intriguingly, 3 of the 5 samples that did not fit within the four main clusters were identified as having minor abnormalities by routine histopathological analysis.

Non-Metric Multidimensional Scaling and Principal Component Analysis of SRB-Mucin Profiles. NMDS was performed for SRB-mucin profiles using the Morisita similarity index with

individual samples identified by region. As shown in **Figure 2.13**, the results of the NMDS analysis corroborated results from MCA in that samples did not cluster by location, but appeared to cluster by subject. A MANOVA was performed to compare SRB-mucin profiles among colonic regions and confirmed that SRB-mucin profiles were similar among right colon, left colon, and rectum. Because determination of clusters in the original NMDS plot appeared somewhat ambiguous, MCA was then carried out in order to group samples using a similarity index of 65% and then NMDS ordinations were performed to corroborate the MCA clusters. These analyses also revealed four distinct clusters (**Figure 2.14**). MANOVA confirmed SRB and mucin profiles diverge significantly among these four clusters. To identify major factors contributing to NMDS-clusters formation, PCA and factor analysis were performed. These analyses revealed 13 major factors contributing to the NMDS ordination. These factors were retrieved from the concatenated data matrix and included in a heat map. This figure shows the relative abundance of the terminal fragments identified as most contributory by PCA and all mucin data for each sample in the clusters and the cluster outliers to determine how these factors might influence formation of the different clusters (**Figure 2.15**). For certain terminal fragments, obvious differences in relative abundance among clusters (e.g. the relative abundance of terminal fragment 3 is higher in cluster I samples than all other samples) were evident, while the influence of specific terminal fragments and particular attributes of the mucin data was less obvious for other clusters.

DISCUSSION

In the present study a quantitative analysis of goblet cell sulfomucins and sialomucins in human colon biopsies was performed and compared with an analysis of SRB profiles from

matched biopsies collected from the same colonic regions among the individuals. Analysis of the two mucin chemotypes revealed both spatial and interindividual variation. Spatial variation in acidomucin profiles has been described previously, but had not been examined quantitatively. Quantification of the area of goblet cell mucin staining per area of epithelium (mucin abundance) revealed that sulfomucin and sialomucin were most abundant in the rectum. Sulfomucin was the predominant mucin chemotype in all three regions. The increase in sialomucins in the rectum compared to the right colon and an overall predominance of sulfomucin in the human colon is in accord with previously described observations [7]. Sulfomucin may offer additional protection from luminal insults by increasing mucus viscosity and resistance to bacterial degradation and microbe adhesion [5]. Thus, individuals who have either a lower predominance of sulfomucin or lower abundance of sulfomucin may be at greater risk to the effects of luminal substances with the potential to cause disease. Of interest, two out of the sixty biopsies did not show a predominance of sulfomucin. Additional studies should be conducted to determine whether individuals with lower sulfomucin predominance or overall sulfomucin abundance are at higher risk for developing gastrointestinal disease. Providing quantitative data for sulfomucin and sialomucin abundance should enhance the study of mucin chemotypes in disease by allowing definition of a normal range for each mucin chemotype. Furthermore, these data point out the importance of sampling from defined regions in experimental investigations of the human colon.

Intriguingly, a significant increase was observed for sialomucin abundance in the recturm of female subjects. Sulfomucin abundance, on the other hand, was similar in the three colonic regions between male and female subjects. The greater abundance of sialomucin in the female rectum could possibly reflect hormonal regulation of rectal sialomucin production as colonic sialomucin was previously found to increase during the late progesterone phase of the menstrual

cycle [34]. The observed gender difference in rectal sialomucin, however, should be examined further in a larger cohort of subjects to determine the consistency of this observation. A larger study would also be useful in determining whether other demographic factors such as smoking, age, race, or ethnicity affect mucin chemotypes, which could not be adequately assessed in this study due to the small sample size.

Scoring of each mucin chemotype along the surface epithelium, upper crypt, and lower crypt was performed to provide a semi-quantitative measurement of mucin variation along the crypt. Areas were not measured in this case due to the time consuming nature of the area analysis. Scoring confirmed previous descriptions of mucin chemotype distributions along the crypt, including a greater number of sialomucin containing goblet cells in the upper crypt of the rectum [7]. The scoring analysis also allowed us to determine that the increase in sulfomucin abundance measured in the rectum compared to right colon was due to increased sulfomucin in the lower crypt rather than in the upper crypt or surface epithelium. Such information is useful as it may be that mucins in surface and upper crypt goblet cells are more important in mediating host microbe interactions. On the other hand, disease related changes in mucin chemotypes may initially be observed in the lower crypt with less differentiated goblet cells and then be perpetuated as cells migrate up the crypt.

Interindividual variation in sulfo- and sialomucin abundance and distribution along the crypt among right colon, left colon, and rectum was measured quantitatively in the present study. Interindividual variation in *O*-acetylation of mucin sialic acid was previously reported in the colon [35], but to our knowledge other studies have not been reported that provide a detailed analysis of interindividual variation in sulfo- and sialomucins within specific colonic regions of healthy individuals. The greatest heterogeneity in both sialo- and sulfomucin abundance and

distribution along the crypt was found in the right colon, while left colon was most homogenous in terms of abundance, and rectum was most homogenous in terms of distribution along the crypt as well as overall mucin data. Thus, when comparing these mucin chemotypes between diseased and normal tissue, it may be easier to find differences in the rectum where there is less variation among normal individuals. This observation may also be relevant to reports of altered mucin sulfation and sialylation in ulcerative colitis, which shows ascending involvement of the colon from rectum, than in Crohn's disease which can involve any region of the gastrointestinal tract [36].

While quantitative analysis of sulfo- and sialomucin abundance and distribution along the crypt revealed spatial and interindividual variation in these two mucin chemotypes, the factors that contribute to this variation remain to be defined. It is likely that both environmental and genetic components are involved. Previously reported heterogeneity in *O*-acetylation of sialomucin is believed to reflect genetic differences in expression of an *O*-acetyltransferase [37]. Thus, there may be some differences in specific sulfo- and/or sialotransferases involved in determination of sulfo- and sialomucin expression. Animal studies indicate that the commensal microbiota and diet may also influence mucin composition [6, 38-42], but additional studies are needed to understand their contribution in humans.

Nested PCR for the *Desulfovibrio* spp. 16S rRNA gene demonstrated that all 20 subjects harbored mucosa-associated *Desulfovibrio* populations in at least one colonic region and, for *dsrA*, that 19 out of 20 subjects harbored mucosa-associated SRB populations in at least one region of the colon [29]. These results indicate that SRB populations are ubiquitously associated with the human colonic mucosa and concur with observations by Fite et al [43], in which the use of quantitative PCR also revealed that intestinal mucosa is persistently colonized by

Desulfovibrio spp. TRFLP analysis further indicated that mucosa-associated SRB populations are highly diverse in the human colon [29]. Additional analyses of microbial diversity revealed that the right colon, left colon and rectum harbor similar SRB populations [29]. In contrast to the mucin data, interindividual variation in SRB profiles showed increasing heterogeneity moving proximally to distally from the right colon to the rectum. Variability among subjects and regions was much greater for SRB profiles than mucin data, indicating that additional factors are contributing to SRB heterogeneity. However, combined SRB-mucin profiles showed similar variability across the colon.

Multivariate cluster analysis revealed that sulfo- and sialomucin abundance and distribution along the crypt was more similar among the same regions from different subjects than for different regions from the same subject, while SRB profiles were generally more similar within the same individual than from the same region of different individuals. Thus, the observed regional differences in sulfo- and sialomucins do not appear to significantly impact regional differences in SRB profiles.

Multivariate analyses of SRB-mucin profiles revealed the presence of four distinct profiles in this particular cohort of healthy human subjects. In addition, it demonstrated that the relationship between SRB diversity and sulfo- and sialomucins appeared to be influenced to a greater extent by undetermined host-specific attributes than colonic location. Specific terminal fragments and sulfomucin abundance were identified by PCA to be the major factors contributing to the formation of the four clusters. This indicates that in some healthy individuals, sulfomucin concentrations may influence the diversity of SRB. However, in other subjects sulfomucin abundance was not observed to significantly influence SRB profiles. Of note, 3 of the 5 samples that did fit into the four groups were sampled from regions that were identified as

having some abnormality by histopathological analysis. This suggests that abnormalities in colon tissue may lead to altered SRB-mucin profiles, which prevent these samples from clustering with one of the four "healthy" groups or perhaps results in the formation of a separate cluster. Examination of SRB-mucin profiles in additional colon biopsies from normal and diseased tissue will be needed to distinguish these possibilities.

In summary, this study provides the first quantitative assessment of regional and interindividual variation in sulfo- and sialomucins in healthy human subjects. In addition, it provides the first description of the relationship between SRB and specific acidomucin chemotypes. Four distinct mucin-SRB profiles were observed in the human colon for this particular cohort of healthy subjects. Furthermore, the mucin-SRB profiles were host-specific in healthy individuals. This outcome indicates that it may be possible to detect distinct SRB-acidomucin profiles in subjects susceptible to or exhibiting chronic colonic disease.

REFERENCES

1. Moncada, D. and K. Chadee., *Production, structure, and biologic relevance of gastrointestinal mucins,* in *Infections of the Gastrointestinal Tract*, S.P.D. Blaser M. J., Ravdin J. I., Greenberg H. B., Guerrant R. L., Editor. 2002. Lippincott Williams & Wilkins: Philadelphia. p. 57-79.

2. Robbe, C., et al., *Structural diversity and specific distribution of O-glycans in normal human mucins along the intestinal tract.* Biochem J, 2004. **384**(Pt 2): p. 307-16.

3. Byrd, J.C. and R.S. Bresalier, *Mucins and mucin binding proteins in colorectal cancer.* Cancer Metastasis Rev, 2004. **23**(1-2): p. 77-99.

4. Linden, S.K., et al., *Mucins in the mucosal barrier to infection.* Mucosal Immunol, 2008. **1**(3): p. 183-97.

5. Nieuw Amerongen, A.V., et al., *Sulfomucins in the human body.* Biol Chem, 1998. **379**(1): p. 1-18.

6. Deplancke, B. and H.R. Gaskins, *Microbial modulation of innate defense: goblet cells and the intestinal mucus layer.* Am J Clin Nutr, 2001. **73**(6): p. 1131S-1141S.

7. Filipe, M.I., *Mucins in the human gastrointestinal epithelium: a review.* Invest Cell Pathol, 1979. **2**(3): p. 195-216.

8. Spicer, S.S. and B.A. Schulte, *Diversity of cell glycoconjugates shown histochemically: a perspective.* J Histochem Cytochem, 1992. **40**(1): p. 1-38.

9. Matsuo, K., et al., *Histochemistry of the surface mucous gel layer of the human colon.* Gut, 1997. **40**(6): p. 782-9.

10. Shirazi, T., et al., *Mucins and inflammatory bowel disease.* Postgrad Med J, 2000. **76**(898): p. 473-8.

11. Tamai, O., et al., *Morphologic and mucin histochemical analysis of transitional zones in advanced ulcerated colorectal carcinomas: potential prognostic indicators.* J Surg Oncol, 1998. **67**(2): p. 85-9.

12. Corfield, A.P., et al., *Colonic mucins in ulcerative colitis: evidence for loss of sulfation.* Glycoconj J, 1996. **13**(5): p. 809-22.

13. Raouf, A.H., et al., *Sulphation of colonic and rectal mucin in inflammatory bowel disease: reduced sulphation of rectal mucus in ulcerative colitis.* Clin Sci (Lond), 1992. **83**(5): p. 623-6.

14. Muyzer, G. and A.J. Stams, *The ecology and biotechnology of sulphate-reducing bacteria.* Nat Rev Microbiol, 2008. **6**(6): p. 441-54.

15. Gibson, G.R., G.T. Macfarlane, and J.H. Cummings, *Occurrence of sulphate-reducing bacteria in human faeces and the relationship of dissimilatory sulphate reduction to methanogenesis in the large gut.* J Appl Bacteriol, 1988. **65**(2): p. 103-11.

16. Gibson, G.R., et al., *Alternative pathways for hydrogen disposal during fermentation in the human colon.* Gut, 1990. **31**(6): p. 679-83.

17. Gibson, G.R., *Metabolic interactions involving sulphate-reducing and methanogenic bacteria in the human large intestine.* FEMS Microbiology Ecology, 1993. **12**(2): p. 117-125.

18. Loubinoux, J., et al., *Sulfate-reducing bacteria in human feces and their association with inflammatory bowel diseases.* FEMS Microbiol Ecol, 2002. **40**(2): p. 107-12.

19. Pitcher, M.C., E.R. Beatty, and J.H. Cummings, *The contribution of sulphate reducing bacteria and 5-aminosalicylic acid to faecal sulphide in patients with ulcerative colitis.* Gut, 2000. **46**(1): p. 64-72.

20. Zinkevich, V.V. and I.B. Beech, *Screening of sulfate-reducing bacteria in colonoscopy samples from healthy and colitic human gut mucosa.* FEMS Microbiol Ecol, 2000. **34**(2): p. 147-155.

21. Gibson, G.R., *Growth and activities of sulphate-reducing bacteria in gut contents of healthy subjects and patients with ulcerative colitis.* FEMS Microbiology Ecology, 1991. **86**(2): p. 103-111.

22. Christl, S.U., W. Scheppach, and H. Kasper, *[Hydrogen metabolism in the large intestine--physiology and clinical implications]*. Z Gastroenterol, 1995. **33**(7): p. 408-13.

23. Attene-Ramos, M.S., et al., *Evidence that hydrogen sulfide is a genotoxic agent.* Mol Cancer Res, 2006. **4**(1): p. 9-14.

24. Attene-Ramos, M.S., et al., *Hydrogen sulfide induces direct radical-associated DNA damage.* Mol Cancer Res, 2007. **5**(5): p. 455-9.

25. Levine, J., et al., *Fecal hydrogen sulfide production in ulcerative colitis.* Am J Gastroenterol, 1998. **93**(1): p. 83-7.

26. Roediger, W.E., J. Moore, and W. Babidge, *Colonic sulfide in pathogenesis and treatment of ulcerative colitis.* Dig Dis Sci, 1997. **42**(8): p. 1571-9.

27. Deplancke, B., et al., *Molecular ecological analysis of the succession and diversity of sulfate-reducing bacteria in the mouse gastrointestinal tract.* Appl Environ Microbiol, 2000. **66**(5): p. 2166-74.

28. Deplancke, B., et al., *Gastrointestinal and microbial responses to sulfate-supplemented drinking water in mice.* Exp Biol Med (Maywood), 2003. **228**(4): p. 424-33.

29. Nava, G., *Toward an understanding of interindividual variation in hydrogenotrophic microbes in the human colon*, in *Nutritional Sciences*. 2009, University of Illinois: Urbana-Champaign.

30. Hammer, *Past: Paleontological statistics software package for education and data analysis.* Palaeonto Elec, 2001. **4**: p. e1-e9.

31. Scupham, A.J., *Campylobacter colonization of the Turkey intestine in the context of microbial community development.* Appl Environ Microbiol, 2009. **75**(11): p. 3564-71.

32. Rodriguez, C., et al., *Lettuce for human consumption collected in Costa Rica contains complex communities of culturable oxytetracycline- and gentamicin-resistant bacteria.* Appl Environ Microbiol, 2006. **72**(9): p. 5870-6.

33. Farzan, A., et al., *Molecular epidemiology and antimicrobial resistance of Salmonella typhimurium DTI04 on Ontario swine farms.* Can J Vet Res, 2008. **72**(2): p. 188-94.

34. Rameshkumar, K., *Mucin histochemistry of the colon in relation to the menstrual cycle and its significance in colonic carcinogenesis.* Indian J Cancer, 1997. **34**(3): p. 107-10.

35. Sugihara, K. and J.R. Jass, *Colorectal goblet cell sialomucin heterogeneity: its relation to malignant disease.* J Clin Pathol, 1986. **39**(10): p. 1088-95.

36. Baumgart, D.C. and W.J. Sandborn, *Inflammatory bowel disease: clinical aspects and established and evolving therapies.* Lancet, 2007. **369**(9573): p. 1641-57.

37. Corfield, A.P., et al., *Reduction of sialic acid O-acetylation in human colonic mucins in the adenoma-carcinoma sequence.* Glycoconj J, 1999. **16**(6): p. 307-17.

38. Conour, J.E., et al., *Acidomucin goblet cell expansion induced by parenteral nutrition in the small intestine of piglets.* Am J Physiol Gastrointest Liver Physiol, 2002. **283**(5): p. G1185-96.

39. More, J., et al., *Histochemical characterization of glycoproteins present in jejunal and colonic goblet cells of pigs on different diets. A biopsy study using chemical methods and peroxidase-labelled lectins.* Histochemistry, 1987. **87**(2): p. 189-94.

40. Sharma, R. and U. Schumacher, *The influence of diets and gut microflora on lectin binding patterns of intestinal mucins in rats.* Lab Invest, 1995. **73**(4): p. 558-64.

41. Sharma, R. and U. Schumacher, *Morphometric analysis of intestinal mucins under different dietary conditions and gut flora in rats.* Dig Dis Sci, 1995. **40**(12): p. 2532-9.

42. Yang, K., et al., *Cytokeratin, lectin, and acidic mucin modulation in differentiating colonic epithelial cells of mice after feeding Western-style diets.* Cancer Res, 1996. **56**(20): p. 4644-8.

43. Fite, A., et al., *Identification and quantitation of mucosal and faecal desulfovibrios using real time polymerase chain reaction.* Gut, 2004. **53**(4): p. 523-9.

FIGURES AND TABLES

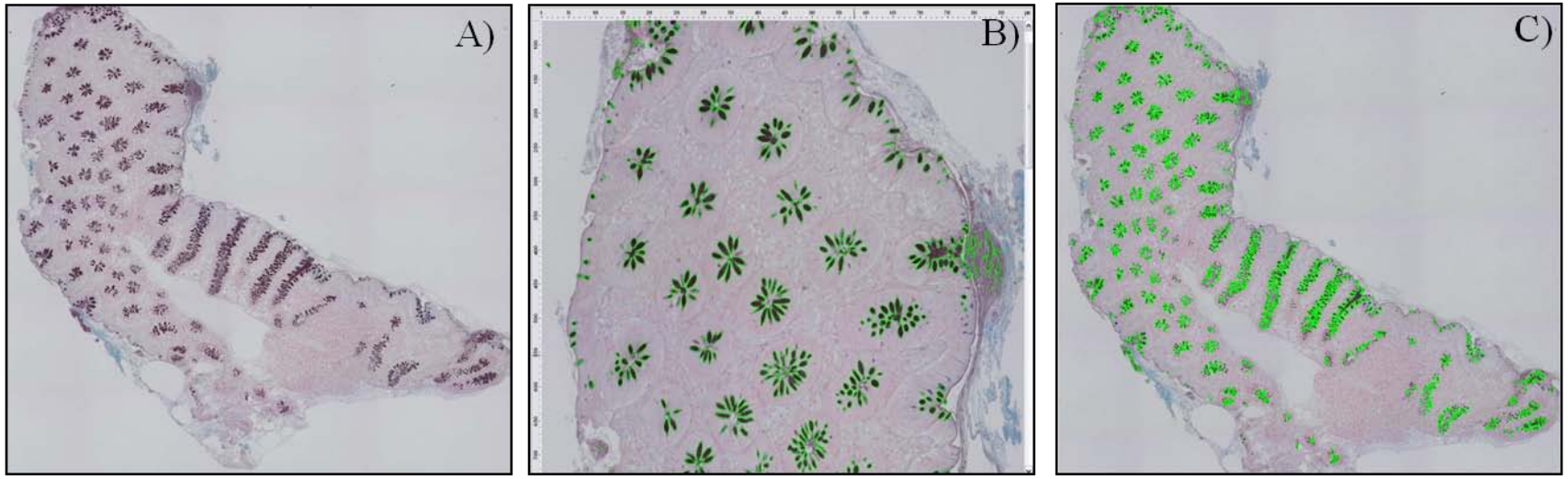

Figure 2.1: Image Analysis of mucin area. **A)** Images were captured at 200X magnification using a Zeiss Axiovert 200M Microscope and Axiovision 4.5 software. The MosaiX module was used to scan the entire area of the section at 200X magnification and generate a single image. **B)** The Automeasure module was used to select and quantify area of sulfomucin (outlined in green) based on parameters that were used to define a sulfomucin staining. **C)** Selection (in green) of all sulfomucin area by the computer in the entire section.

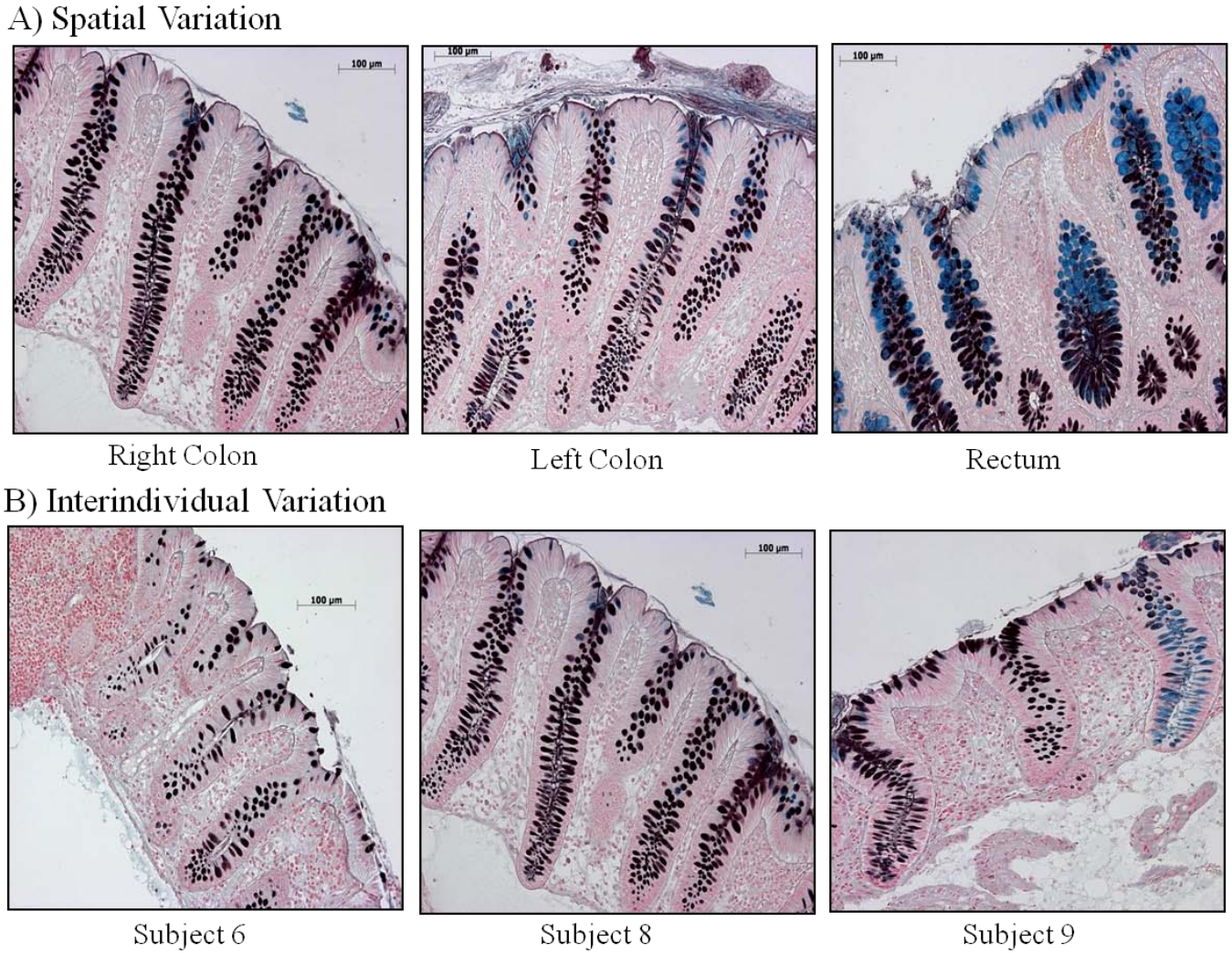

Figure 2.2: High iron diamine and alcian blue (pH 2.5) stained sections of human colon (magnification : X 200). Sulfomucin is stained black/brown and sialomucin is stained blue. **A)** Stained sections from different regions of colon from a single subject show patterns of spatial variation which are common among subjects. **B)** Sections of right colon from three subjects showing observed interindividual variation.

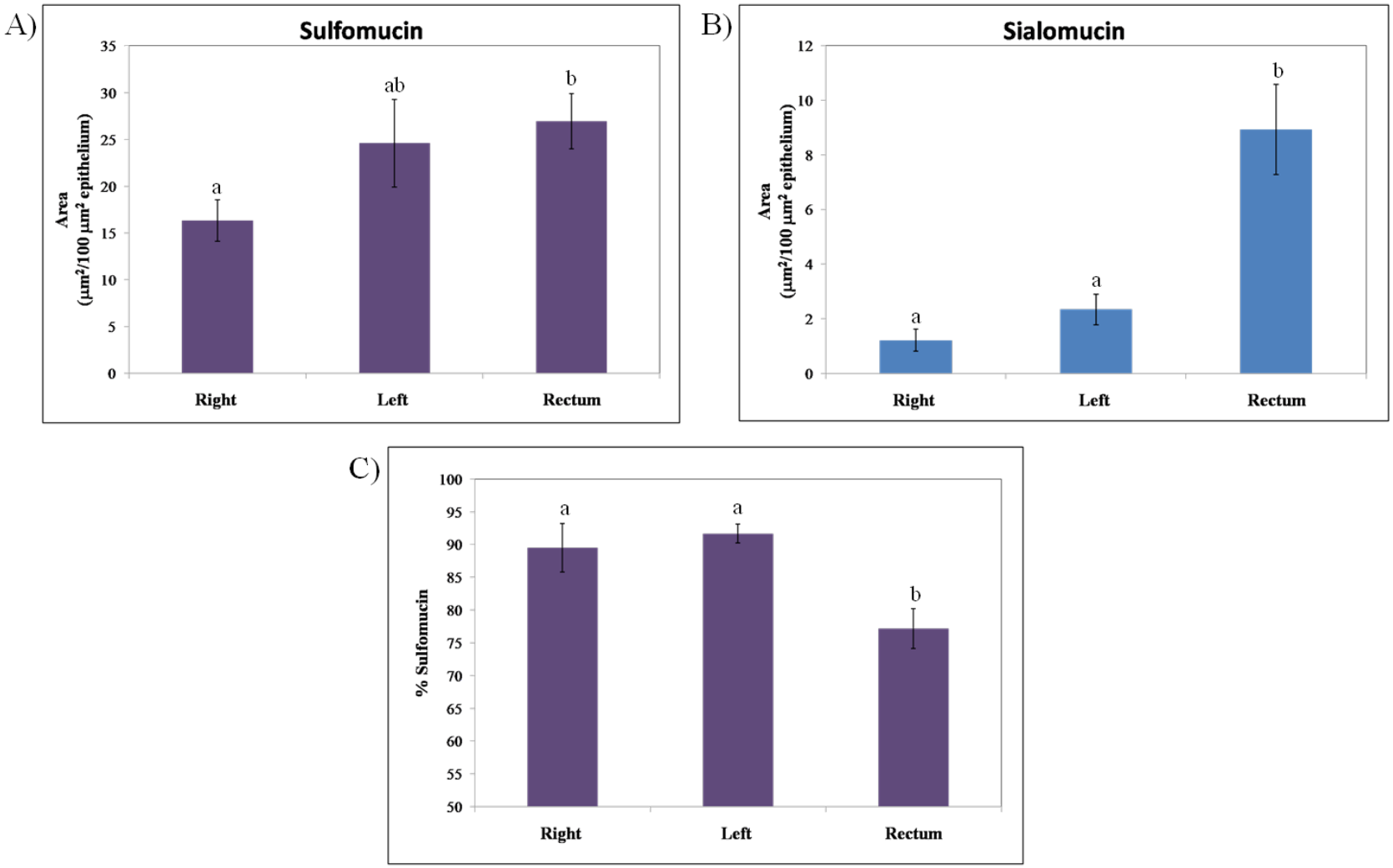

Figure 2.3: A) and **B)** area of sulfomucin and sialomucin staining per area of epithelium in right colon, left colon, and rectum biopsies from 20 healthy subjects. **C)** % Sulfomucin in right colon, left colon, and rectum biopsies from 20 healthy subjects. The data represent mean ± SEM (n=20); statistically significant differences are indicated by different letters ($p < 0.05$)

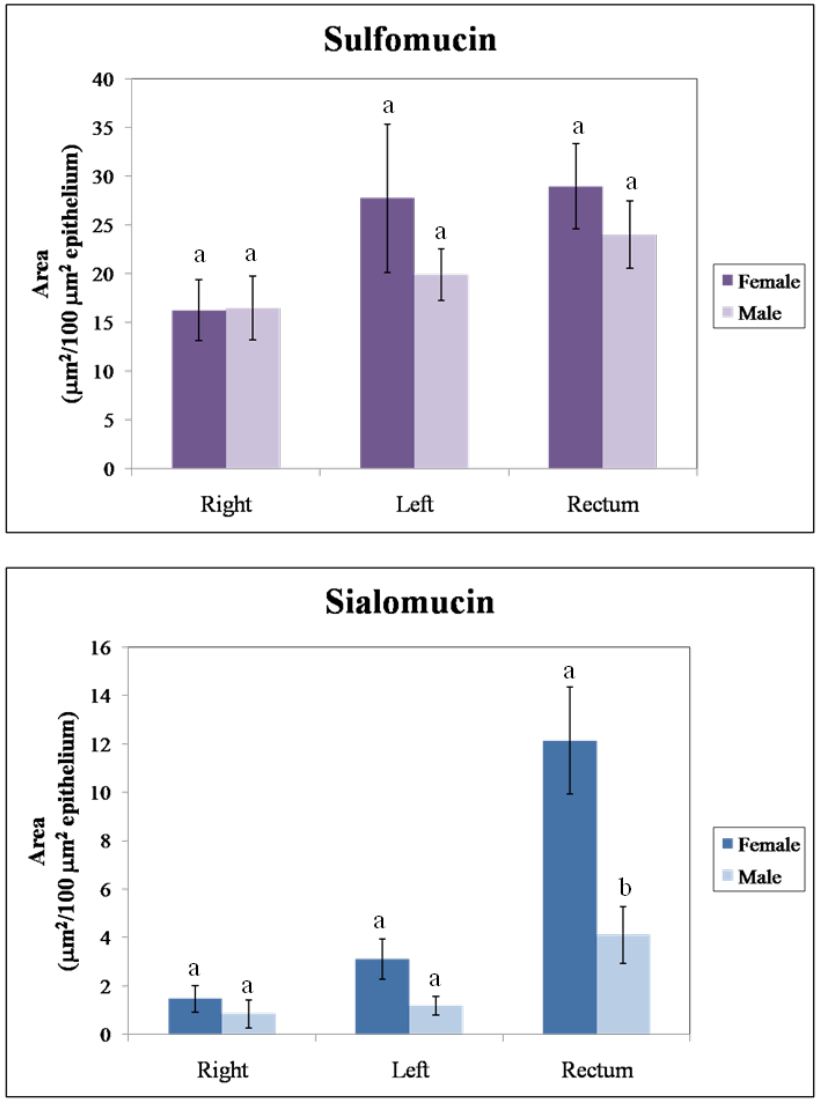

Figure 2.4: Comparison of area of sulfomucin and sialomucin staining in right colon, left colon, and rectum biopsies between female and male subjects. The data represent mean ± SEM (female n=12, male n=8); statistically significant differences are indicated by different letters ($p < 0.05$)

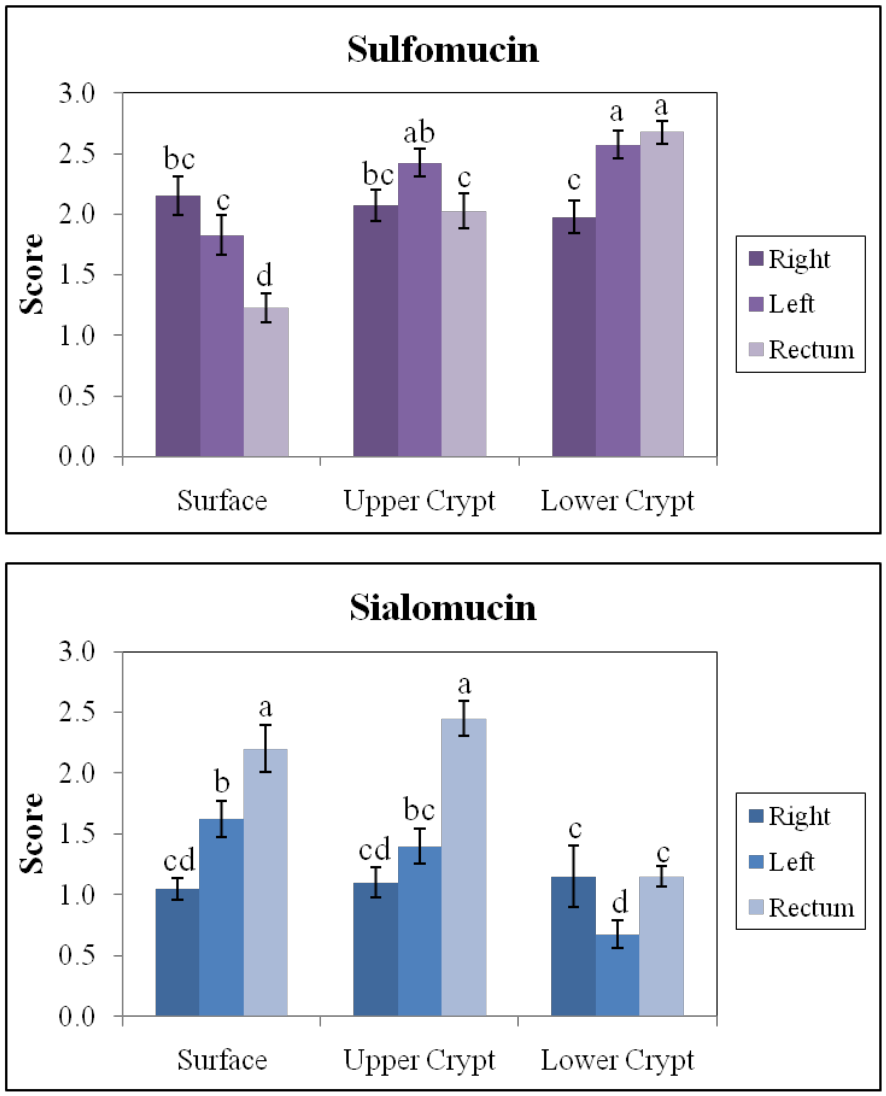

Figure 2.5: Sulfomucin and sialomucin scores for the surface epithelium, upper crypt, and lower crypt of the right colon, left colon, and rectum. The data represent mean ± SEM (n=20); statistically significant differences are indicated by different letters ($p < 0.05$)

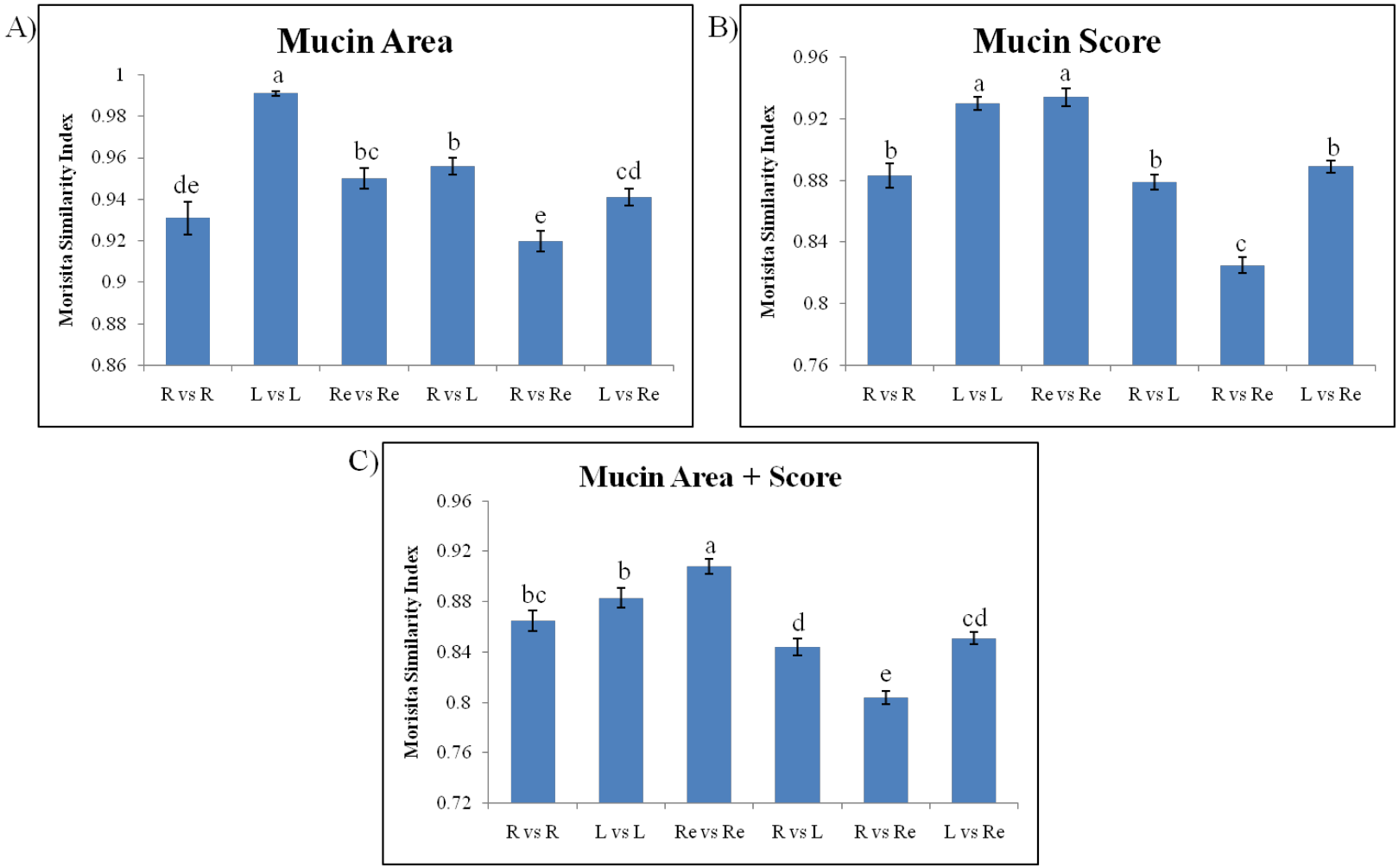

Figure 2.6: Interindividual variation in sulfomucin and sialomucin area (**A**), score (**B**), and combined area and score (**C**). Pairwise comparisons of Morisita similarity indices were calculated across the right colon (R vs R), left colon (L vs L), and rectum (Re vs Re) and between right colon and left colon (R vs L), right colon and rectum (R vs Re), and left colon and rectum (L vs Re). The data represent mean similarity indices ± SEM; statistically significant differences are indicated by different letters ($p < 0.05$)

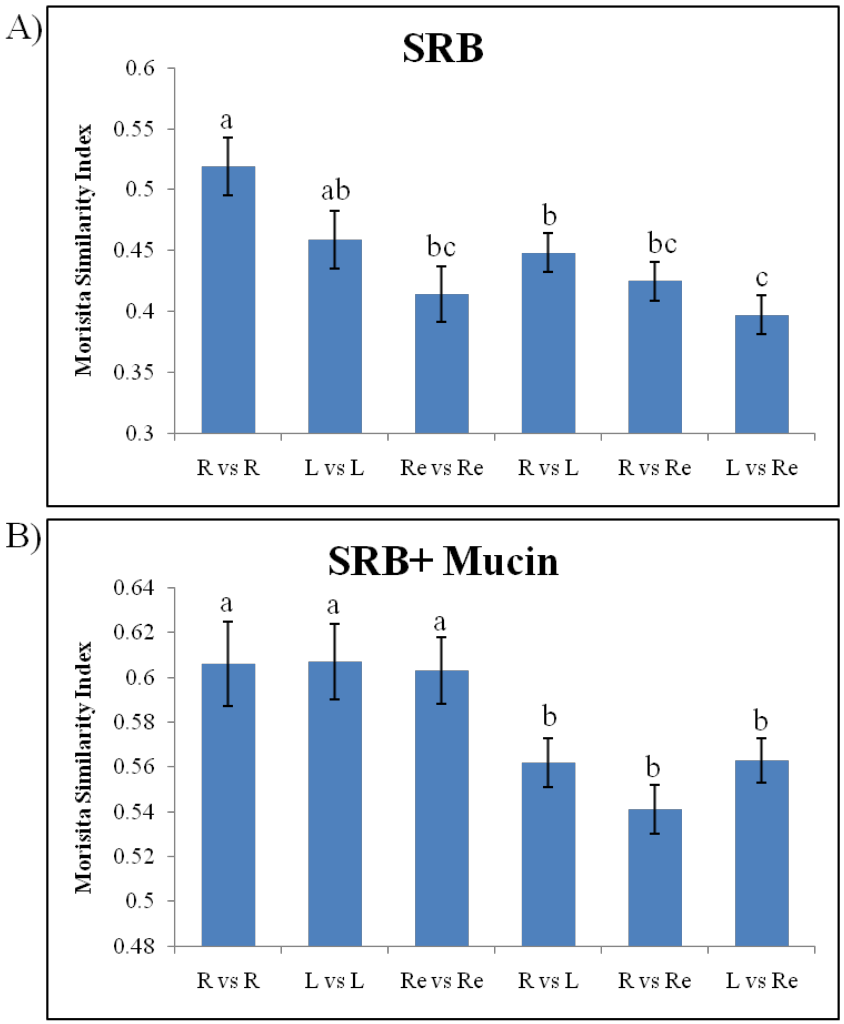

Figure 2.7: Interindividual variation in SRB profiles (**A**), and combined SRB profiles and mucin data(**B**). Pairwise comparisons of Morisita similarity indices were calculated across the right colon (R vs R), left colon (L vs L), and rectum (Re vs Re) and between right colon and left colon (R vs L), right colon and rectum (R vs Re), and left colon and rectum (L vs Re). The data represent mean similarity indices ± SEM**;** statistically significant differences are indicated by different letters ($p < 0.05$)

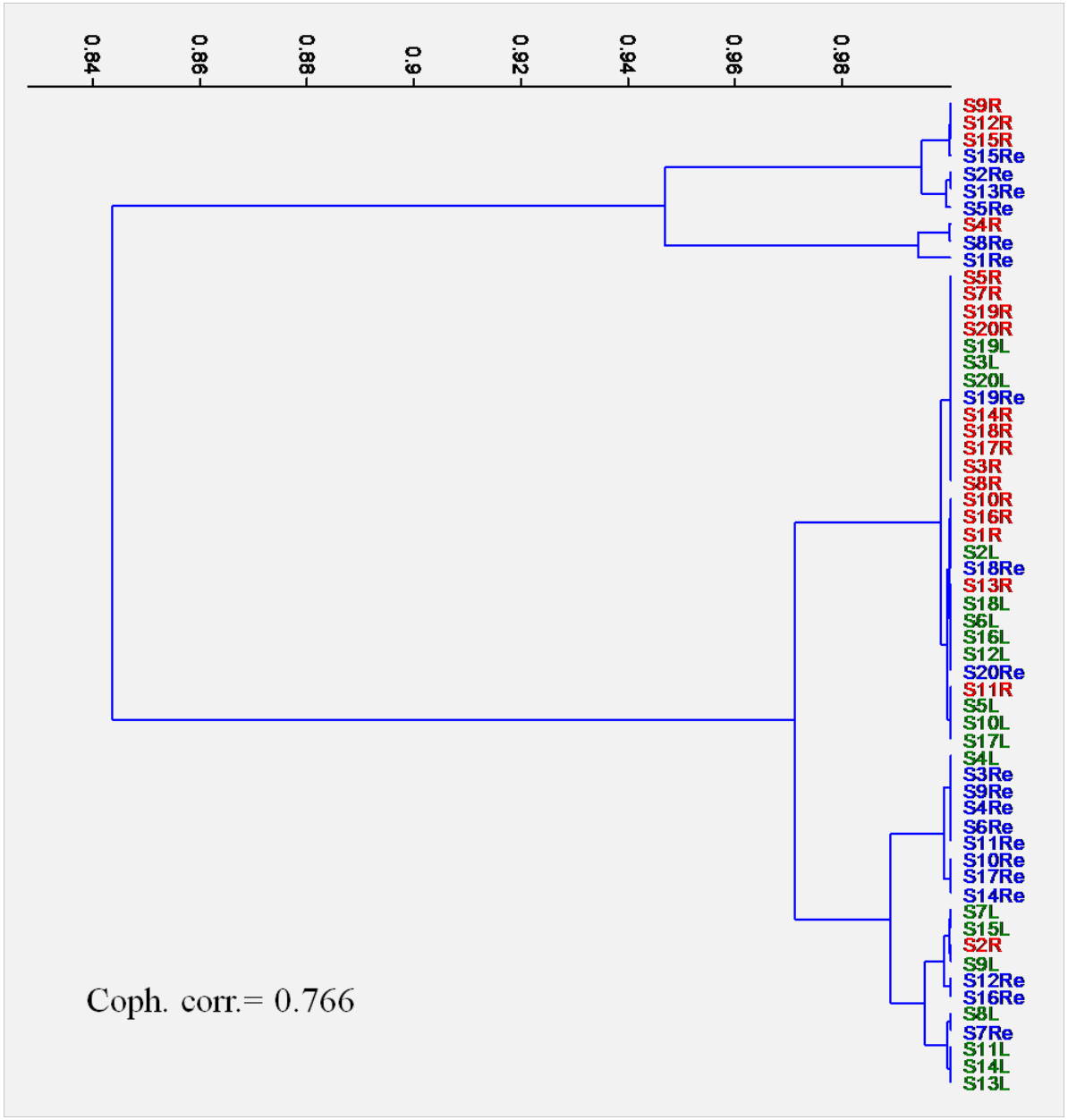

Figure 2.8: Multivariate cluster analysis using Morisita similarity index of sulfomucin and sialomucin areas in right colon (R), left colon (L), and rectum (Re) of all 20 subjects with the exception of right colon of subject 6 and the left colon biopsy of subject 1. Numbers correspond to subject number. Cophenetic correlation coefficient (Coph. Corr) value is shown.

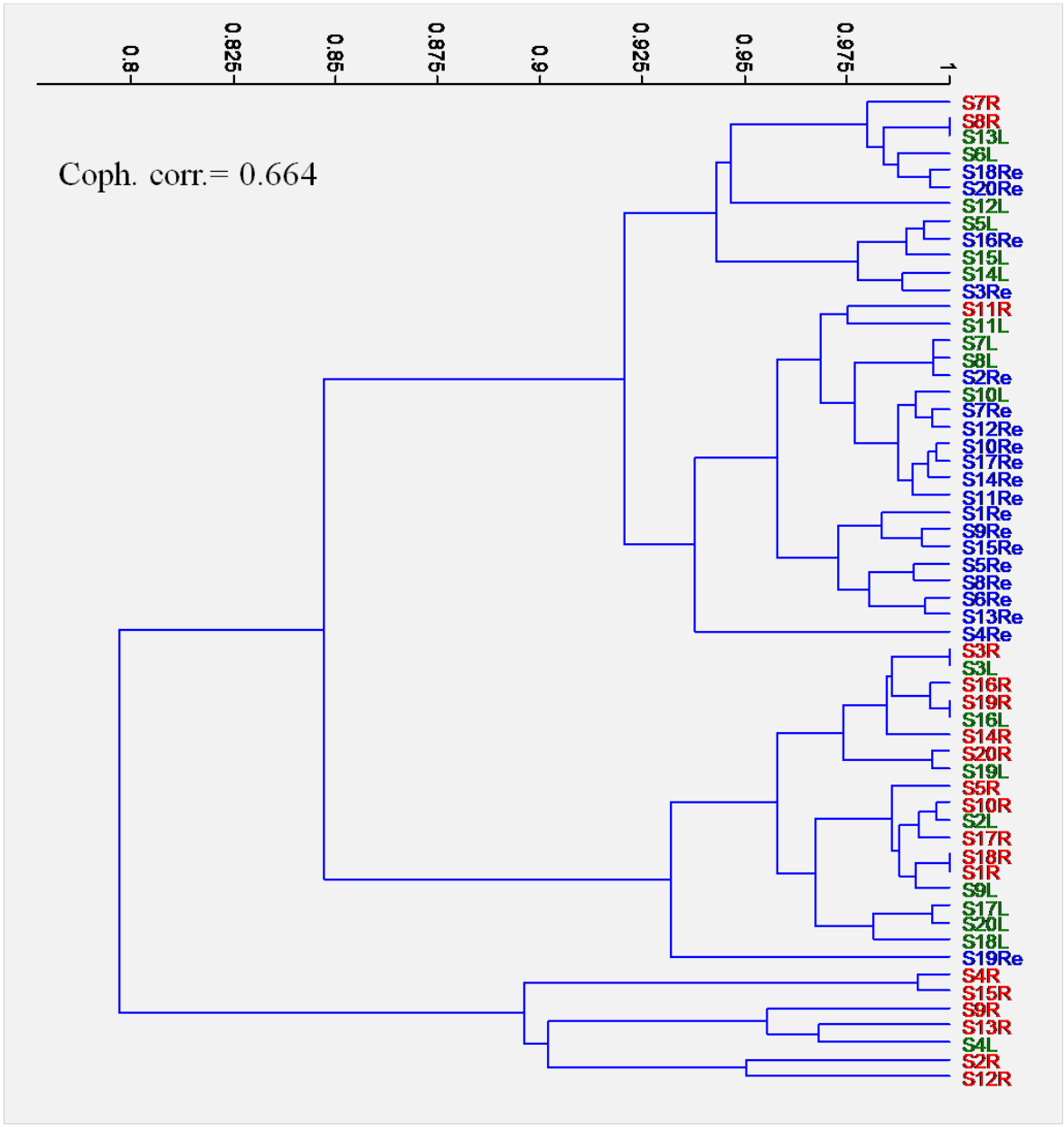

Figure 2.9: Multivariate cluster analysis using Morisita similarity index of sulfomucin and sialomucin scores in right colon (R), left colon (L), and rectum (Re) of all 20 subjects with the exception of right colon of subject 6 and the left colon biopsy of subject 1. Numbers correspond to subject number. Cophenetic correlation coefficient (Coph. Corr) value is shown.

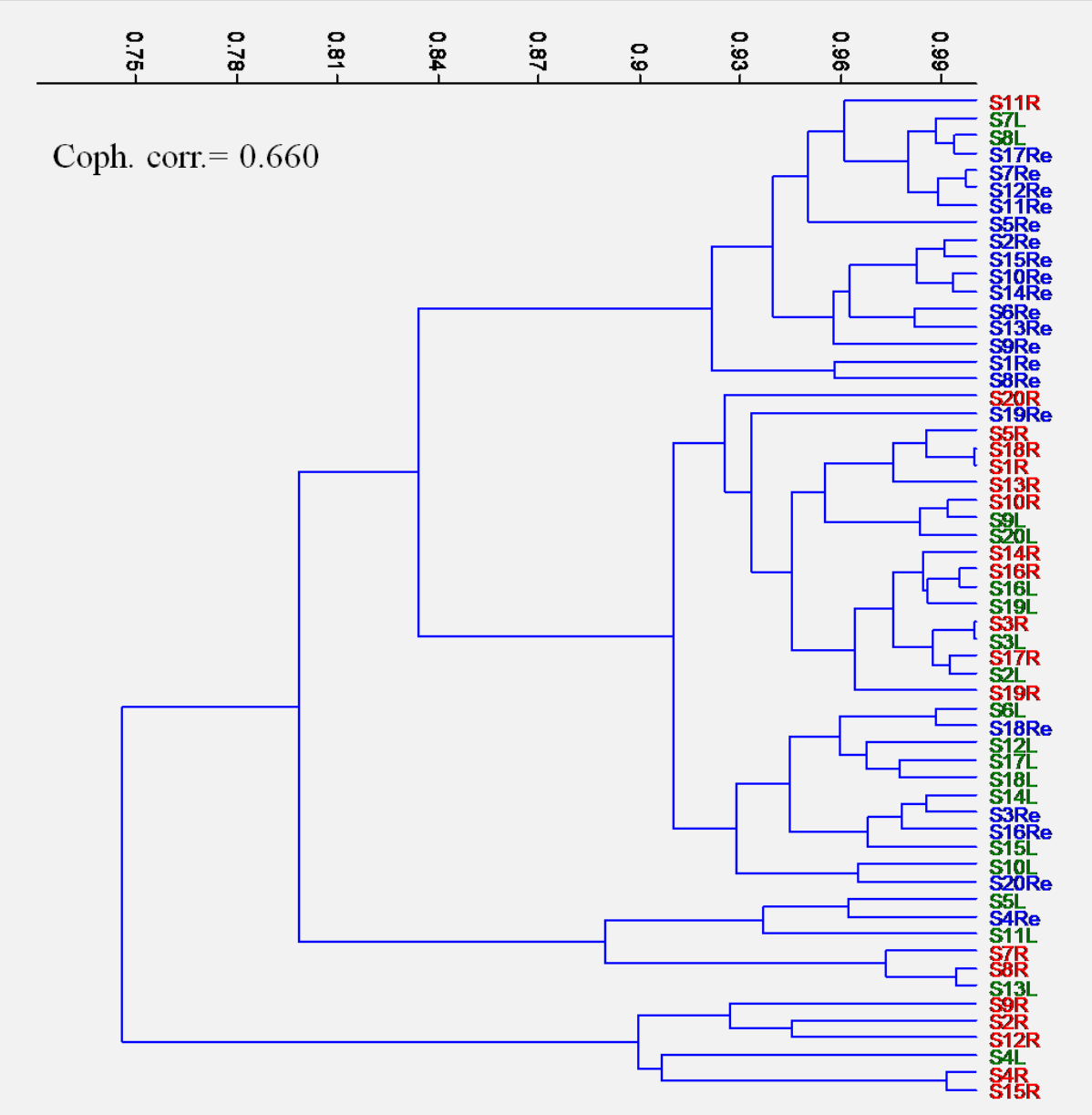

Figure 2.10: Multivariate cluster analysis using Morisita similarity index of combined sulfomucin and sialomucin area and scores in right colon (R), left colon (L), and rectum (Re) of all 20 subjects with the exception of right colon of subject 6 and the left colon biopsy of subject 1. Numbers correspond to subject number. Cophenetic correlation coefficient (Coph. Corr) value is shown.

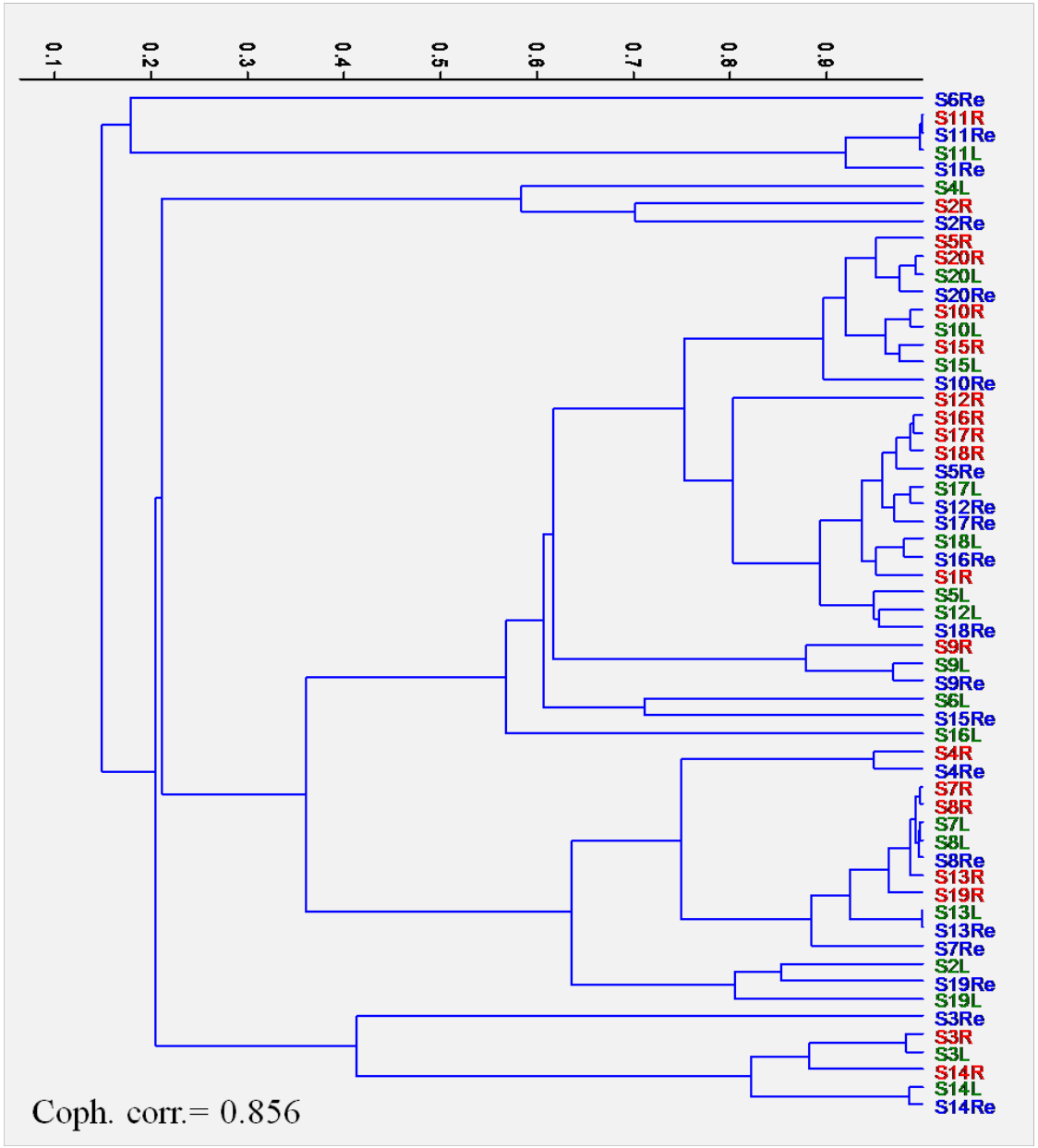

Figure 2.11: Multivariate cluster analysis using Morisita similarity index of SRB profiles in right colon (R), left colon (L), and rectum (Re) of all 20 subjects with the exception of right colon of subject 6 and the left colon biopsy of subject 1. Numbers correspond to subject number. Cophenetic correlation coefficient (Coph. Corr) value is shown.

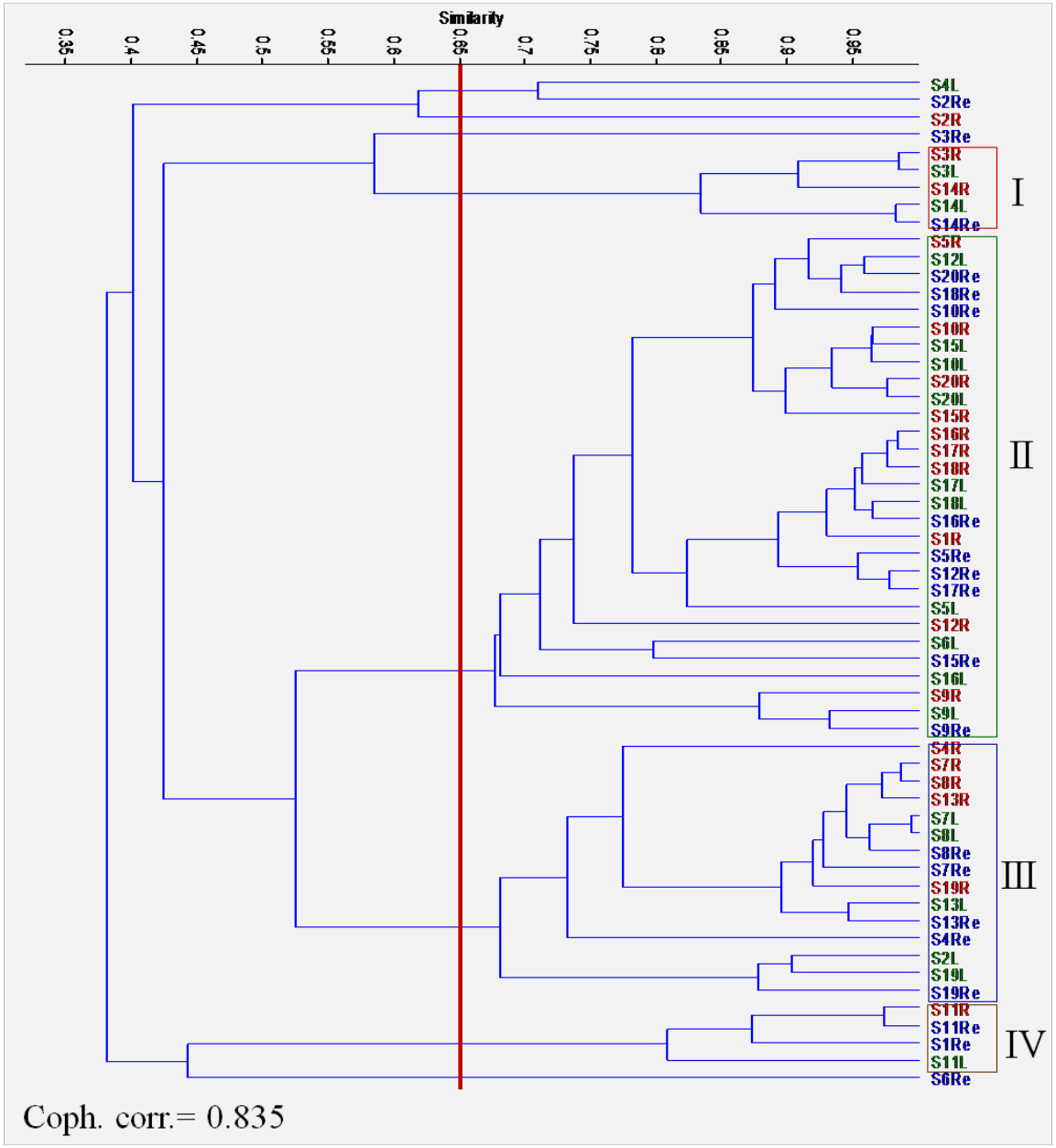

Figure 2.12: Multivariate cluster analysis using Morisita similarity index of combined mucin data and SRB profiles in right colon (R), left colon (L), and rectum (Re) of all 20 subjects with the exception of right colon of subject 6 and the left colon biopsy of subject 1. Numbers correspond to subject number. Cophenetic correlation coefficient (Coph. Corr) value is shown. A similarity value of 65% was used to identify clusters I-IV.

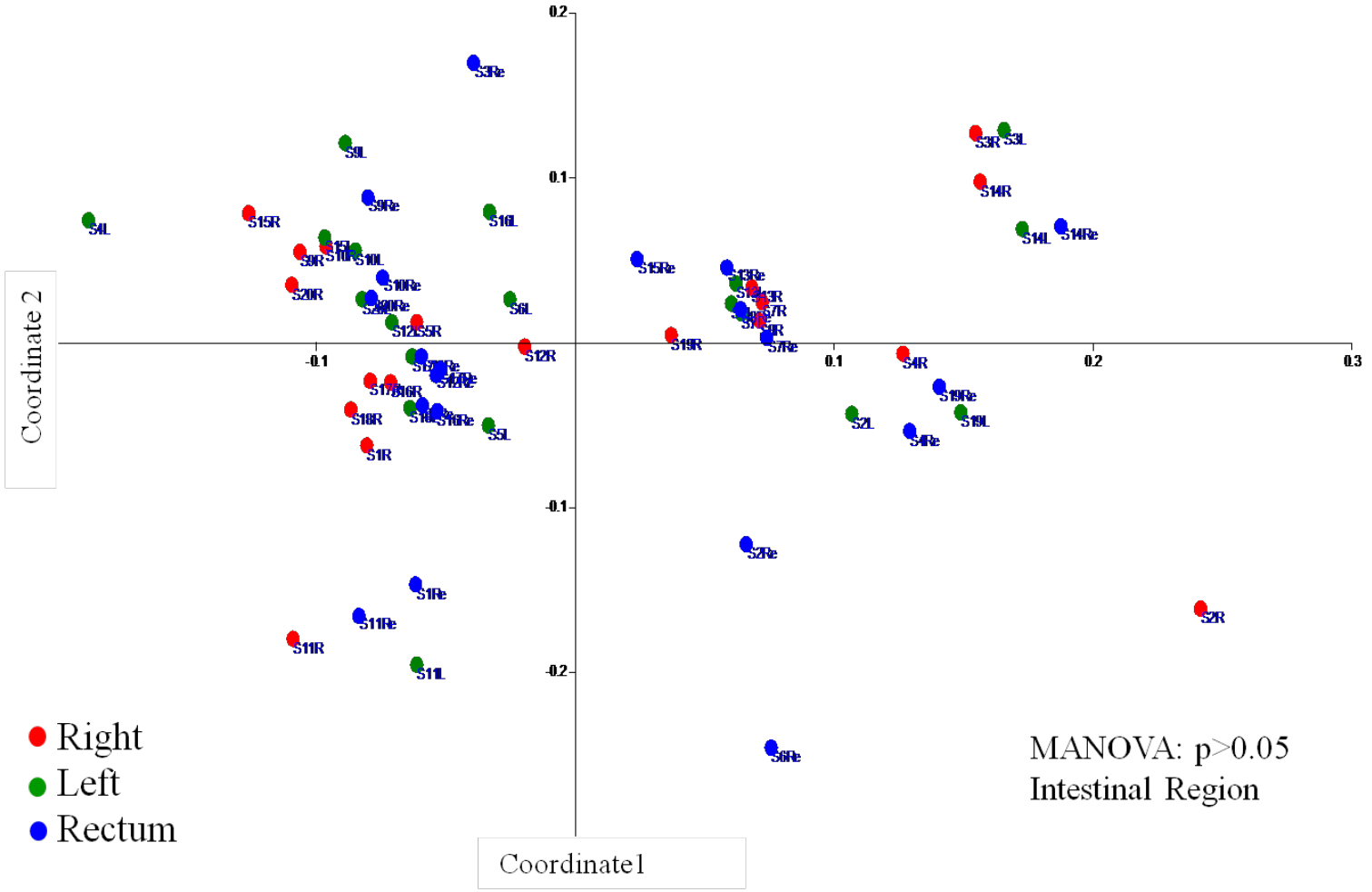

Figure 2.13: Non-metric multidimensional scaling (NMDS) analysis using Morisita similarity index of combined mucin and SRB profiles in the right colon (R), left colon (L), and rectum (Re) of all 20 subjects with the exception of right colon of subject 6 and the left colon biopsy of subject 1. Samples were identified by region. Numbers correspond to subject number. Intestinal regions were compared by MANOVA using the Morisita similarity index. Differences were considered significant if $p < 0.05$.

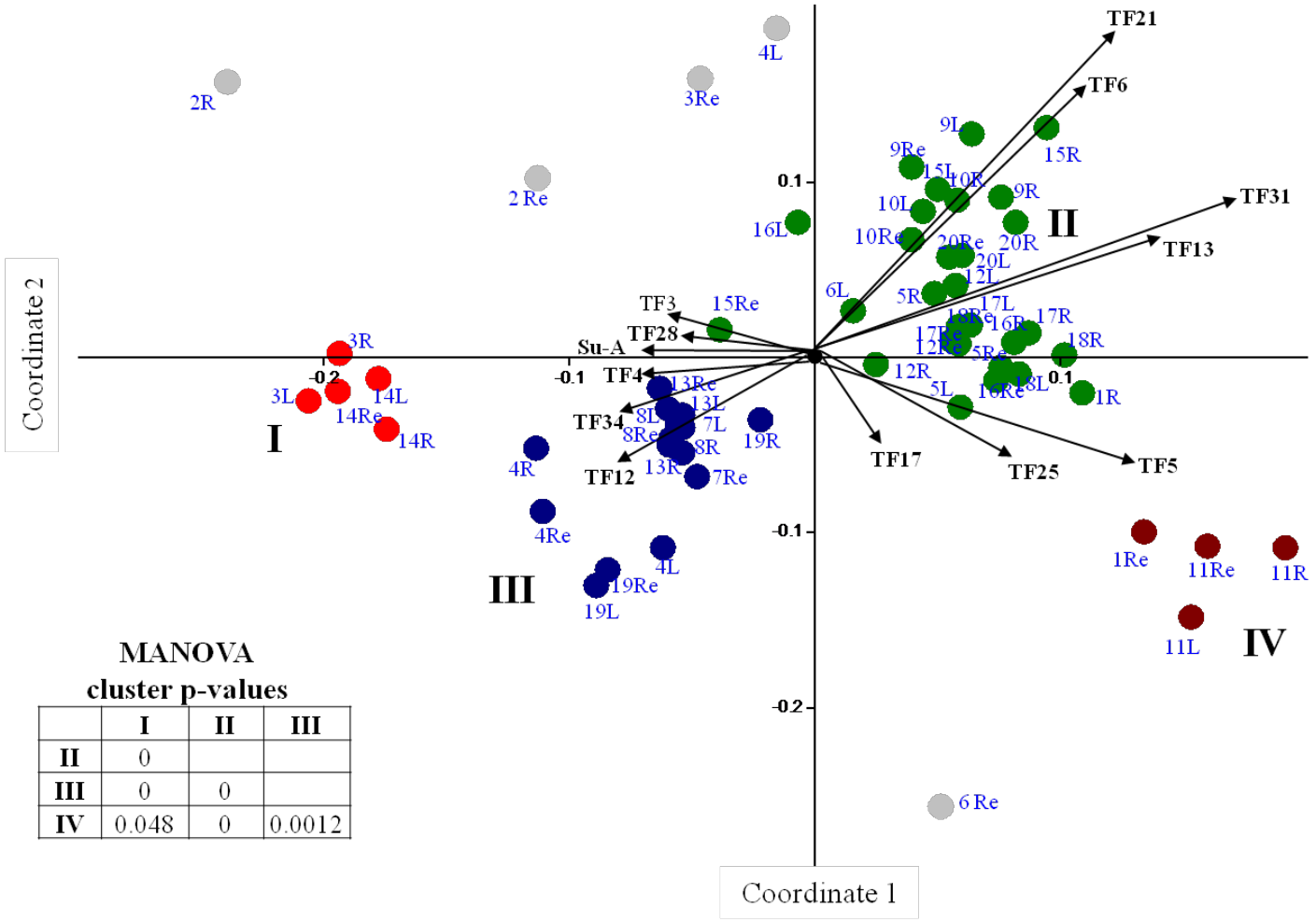

MANOVA
cluster p-values

	I	II	III
II	0		
III	0	0	
IV	0.048	0	0.0012

Figure 2.14: Non-metric multidimensional scaling (NMDS) analysis using Morisita similarity index of combined mucin and SRB profiles in the right colon (R), left colon (L), and rectum (Re) of all 20 subjects with the exception of right colon of subject 6 and the left colon biopsy of subject 1. Samples were identified by clusters based on 65% similarity in MCA. Numbers correspond to subject number. Clusters were compared by MANOVA using the Morisita similarity index. Differences were considered significant if $p < 0.05$. Principal component analysis was used to identify major contributing factors and overlaid (not drawn to scale) on the NMDS plot. TF= terminal fragment and Su-A = sulfomucin area.

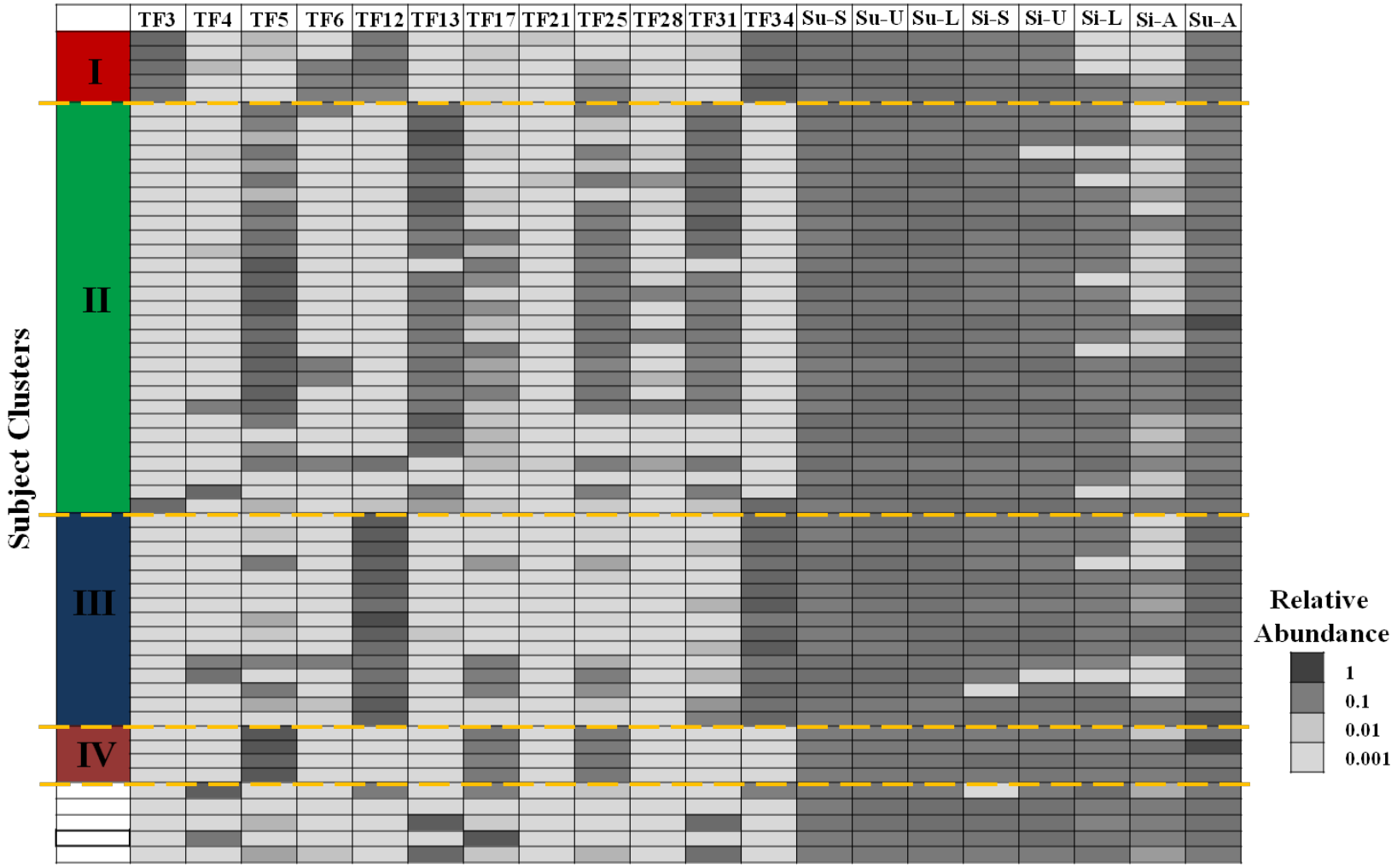

Figure 2.15: Heat map showing abundance of terminal fragments contributing the most to cluster formation and mucin data for each sample in the four clusters and cluster outliers. TF=terminal fragment, Su-S=sulfomucin score surface epithelium, Su-U=sulfomucin score upper crypt, Su-L=sulfomucin score lower crypt, Si-S=sialomucin score surface epithelium, Si-U=sialomucin score upper crypt, Si-L = sialomucin score lower crypt, Si-A =sialomucin area and Su-A = sulfomucin area.

Table 2.1 Subject Characteristics and Endoscopic Findings

Gender	Female (n=12)	Male (n=8)
Age (y)	55.4 (1.61) [50-63.5]	51.4 (1.10) [47-56]
Height (cm)	164.5 (1.50) [157-171]	176.8 (1.68) [171-183]
Body Weight (kg)	74.9 (3.76) [55-97.3]	97.0 (5.50) [73.6-118.2]
BMI (kg/m^2)	26.6 (1.02) [21.3-30.1]	29.1 (1.62) [24-33.2]
Race (n)		
African American	1	0
Caucasian	5	4
Unknown	6	4
Smoking (n)		
Non-smoker	10	6
Ex-smoker	1	1
Smoker	1	1
Endoscopic Findings (n)		
Polyp	1	2
Diverticulosis	0	1
Hemorrhoids	0	2

Values are mean (SEM) [range] or number of subjects (n). Height and BMI data unavailable for subjects 8 (female), 12 (male), and 19 (male).

Score	Description
0	No mucin staining in epithelium
1	1-10% mucin staining in epithelium
2	11-50% mucin staining in epithelium
3	>50% mucin staining in epithelium

Table 2.2: Scoring system for sulfomucin and sialomucin staining in goblet cells in the surface epithelium, upper crypt, and lower crypt

Table 2.3: Sulfomucin and sialomucin areas and % sulfomucin for each biopsy.

Subject #	Region	Sulfomucin Area ($\mu m^2/100\mu m^2$ epithelium)	Sialomucin Area ($\mu m^2/100\mu m^2$ epithelium)	% Sulfomucin
1	Right	12.56	0.46	96.50
1	Left	11.11	1.42	88.64
1	Rectum	17.88	16.41	52.14
2	Right	13.22	2.61	83.49
2	Left	16.39	0.51	96.98
2	Rectum	23.61	11.73	66.80
3	Right	16.17	0.25	98.46
3	Left	14.61	0.05	99.67
3	Rectum	26.01	7.60	77.39
4	Right	5.48	6.13	47.18
4	Left	11.79	3.61	76.55
4	Rectum	71.07	21.00	77.19
5	Right	23.23	0.03	99.85
5	Left	80.70	5.40	93.73
5	Rectum	39.74	17.52	69.41
6	Right	24.54	0.14	99.45
6	Left	18.67	1.00	94.91
6	Rectum	22.35	6.62	77.15
7	Right	26.31	0.03	99.87
7	Left	36.72	7.64	82.78
7	Rectum	33.57	4.61	87.93
8	Right	40.07	0.64	98.43
8	Left	29.13	3.67	88.81
8	Rectum	24.47	28.54	46.16
9	Right	3.70	2.23	62.37
9	Left	7.83	1.51	83.80
9	Rectum	10.75	3.13	77.43
10	Right	6.88	0.19	97.34
10	Left	10.08	0.67	93.76
10	Rectum	23.24	5.73	80.21
11	Right	16.68	1.15	93.57
11	Left	81.91	8.86	90.24
11	Rectum	30.39	8.56	78.03
12	Right	8.03	4.87	62.23
12	Left	17.16	0.83	95.41
12	Rectum	36.46	5.96	85.95
13	Right	15.29	0.65	95.90
13	Left	34.02	3.24	91.29

Tab1e 2.3 (cont.)

13	Rectum	15.10	7.33	67.32
14	Right	19.06	0.15	99.20
14	Left	22.40	2.40	90.33
14	Rectum	17.29	4.40	79.72
15	Right	6.10	3.74	61.98
15	Left	14.02	3.06	82.08
15	Rectum	24.37	14.10	63.35
16	Right	19.37	0.74	96.34
16	Left	16.87	0.88	95.06
16	Rectum	29.85	5.04	85.56
17	Right	15.27	0.18	98.82
17	Left	18.50	1.13	94.23
17	Rectum	36.03	8.72	80.52
18	Right	13.51	0.13	99.06
18	Left	20.19	0.92	95.63
18	Rectum	23.95	0.81	96.73
19	Right	35.96	0.00	100.00
19	Left	23.00	0.01	99.96
19	Rectum	23.67	0.12	99.51
20	Right	5.37	0.00	99.98
20	Left	7.20	0.03	99.64
20	Rectum	9.50	0.47	95.31

Table 2.4: Sulfomucin and sialomucin scores along the crypt and surface epithelium.

Subject #	Region	Sulfomucin Score			Sialomucin Score		
		Surface	Upper	Lower	Surface	Upper	Lower
1	Right	2	2	2	1	1	1
1	Left	2.5	2	2	2.5	2	0.5
1	Rectum	1	2	2	3	2.5	2
2	Right	2	2	1	0	1	3
2	Left	2.5	2.5	2.5	1.5	1	0.5
2	Rectum	1	2.5	3	3	2.5	1
3	Right	2.5	2	2	1	1	0
3	Left	2.5	2	2	1	1	0
3	Rectum	2	2.5	3	2.5	2.5	0.5
4	Right	2	1.5	1	2	2.5	3
4	Left	1	1.5	1.5	1	1	2
4	Rectum	1	1.5	2	3	1.5	1
5	Right	3	3	2.5	1	1	1
5	Left	2.5	3	3	3	2	1
5	Rectum	1	1	3	3	3	1
6	Right	1.5	2	2	1	1	0
6	Left	1	2	2.5	1	1.5	0.5
6	Rectum	1	1	2	2	3	1.5
7	Right	1	2.5	2	1	1	1
7	Left	1	2.5	2.5	2.5	2	1
7	Rectum	1	2	2.5	1.5	2.5	1
8	Right	1	2	2.5	1	1	1
8	Left	1	2.5	2.5	2.5	2.5	1
8	Rectum	1	1.5	2.5	3	3	1
9	Right	3	2.5	2	1	2	2.5
9	Left	2.5	2.5	3	1.5	1	1
9	Rectum	1.5	2	3	3	3	2
10	Right	2	2	2	1	1	0.5
10	Left	1.5	2	3	1.5	2.5	1
10	Rectum	1	2	3	2.5	3	1
11	Right	1	1	2	1	1.5	1
11	Left	1	1.5	1.5	1	1.5	1
11	Rectum	1	1.5	2	1.5	2	1
12	Right	3	1.5	1	1	1	3
12	Left	1	2	3	1.5	1	0
12	Rectum	1	2	3	1.5	3	1
13	Right	1.5	2	2	1	1	1.5
13	Left	1	2	2.5	1	1	1

Table 2.4 (cont.)

13	Rectum	1	1	2.5	2.5	3	1.5
14	Right	3	2.5	2	1	0.5	0
14	Left	2	3	3	2	2.5	1
14	Rectum	1	2	3	2	2.5	1
15	Right	2	1	1	2	2	3
15	Left	1.5	2.5	2	2.5	1.5	1
15	Rectum	1	2	3	3	3	1.5
16	Right	3	3	3	1	0.5	0
16	Left	3	3	3	1	1	0
16	Rectum	2	3	3	2.5	1.5	1
17	Right	2.5	2	2.5	1	1	0.5
17	Left	2	3	3	2	1	0.5
17	Rectum	1	2.5	3	2.5	3	1
18	Right	2	2	2	1	1	1
18	Left	2	3	3	1	1	0
18	Rectum	1	3	3	1	1.5	1
19	Right	3	3	3	1	1	0
19	Left	3	3	3	1	0	0
19	Rectum	3	2.5	2	0	1	1
20	Right	2	2	2	1	0	0
20	Left	2	3	3	1.5	1	0.5
20	Rectum	1	3	3	1	2	1

Chapter 3

THE EFFECT OF MICROBIAL AND HOST INFLAMMATORY SIGNALS ON MUCIN SULFATION

ABSTRACT

The signals that mediate goblet cell expression of specific mucin chemotypes are poorly defined. Both animal and *in vitro* studies show that mucin chemotype may be altered by changes in the normal microbiota and inflammation. To begin to identify factors that may elicit this response, human adenocarcinoma-derived LS174T cells, which have a goblet cell-like phenotype and produce both sulfo- and sialomucins, were used to examine the effects of selected host and microbial factors on mucin sulfation. Expression of genes encoding goblet cell secretory products mucin 2 (*MUC2*), resistin-like molecule β (*RETNLB*), and trefoil factor 3 (*TFF3*) and Golgi sulfotransfereases, carbohydrate (*N*-acetylglucosamine 6-*O*) sulfotransferase 5 (*CHST5*) and galactose-3-*O*-sulfotransferase 2 (*GAL3ST2*), were determined by quantitative RT-PCR following treatment with bacterial flagellin, TNFα, or the mucogenic cytokine IL-13. Expression of caudal type homeobox 2 (CDX2) and toll-like receptor 5 (TLR5) genes were also analyzed. Sulfomucin expression was examined via HID/AB staining and immunofluorescent staining for the Sulfo Le^a antigen, which is synthesized in part by GAL3ST2. Flagellin, IL-13, and TNFα were all found to significantly increase *GAL3ST2*, *MUC2*, *TFF3*, and *TLR5* expression, but only IL-13 and TNFα increased *CHST5* expression and decreased *RETNLB* expression. Only IL-13 increased *CDX2* expression. Mucin sulfation based on HID/AB staining was significantly increased in response to both flagellin and IL-13, but not TNFα. Only treatment with flagellin increased the expression of the Sulfo Le^a antigen. These results indicate that flagellin, IL-13, and

TNFα have differential effects on mucin sulfotransferases and sulfation as well as the goblet cell secretory product genes. IL-13 may increase sulfomucins primarily via increased expression of *CHST5*, while flagellin may increase sulfomucins by increasing expression of *GAL3ST2*. Although TNFα increased expression of both sulfotransferase genes, it did not increase sulfomucin content during the time period examined. Together these data indicate that both host and microbial factors influence mucin chemotypes.

INTRODUCTION

Inflammatory bowel disease (IBD) is a complex disorder characterized by poorly controlled chronic inflammation of the intestinal mucosa [1]. A number of changes in mucins and goblet cells have been reported in association with IBD. These include alterations in the thickness of the mucus gel layer, goblet cell number and intracellular mucin content, and mucin glycosylation [2-5]. Although decreased sulfation of mucins has been associated with active inflammation in human IBD, the underlying causes and the relationship to disease pathology remain undefined. There is a similar lack of understanding about the factors governing both regional and interindividual variation observed in sialo- and sulfomucin chemotypes in healthy individuals (described in Chapter 2).

Both animal and *in vitro* studies demonstrate that mucin chemotype may be altered by changes in the normal microbiota and inflammation [6-10]. The evidence for microbial modulation of mucin chemotypes comes from developmental studies and studies comparing conventionally raised and germfree rodents. In mice, for example, the temporal development of sialo- and sulfomucin chemotypes in the colon appears to parallel the establishment of microbial communities and is not observed in germfree mice, in which crypt mucins remain predominantly

sulfated [7, 11]. Specific microbial components or products may be responsible for the observed effects of microbiota on mucin chemotypes.

A number of bioactive microbial factors have been shown to induce mucin synthesis, secretion, and degradation, but few studies have examined the role of these in determining mucin composition [7]. There is, however, some evidence for the ability of certain microbial components to alter mucin chemotypes [7, 12, 13]. For example, administration of lipopolysaccharide (LPS) from a commensal strain of *E. coli* to germfree rats increased colonic neutral mucin [12]. In addition, LPS from *H. pylori* inhibited mucin glycosylation and sulfation when applied to rat gastric mucosal segments [13]. Whether the effects of the microbiota and specific microbial components on mucin chemotypes occur via direct recognition by intestinal goblet cells or by a microbe-induced inflammatory response to which goblet cells respond remains to be determined. In addition, because of distinct interspecies differences in mucin chemotype patterns [14], it is important to bear in mind that changes in sialo- and sulfomucin observed in animal models may not translate to humans.

Similar to microbial components, a number of host inflammatory signals alter mucin synthesis and secretion, but only a few studies have examined effects on mucin composition [7]. TNFα, IL-1β, and IL-6, which are all proinflammatory cytokines considered to be involved in the pathogenesis of CD [1], were found to induce the release of less glycosylated mucins with altered carbohydrate composition from the mucin-secreting intestinal cancer cell line LS180 [10]. In another study, TNFα increased the expression of α-2,3-sialyltransferase expression in HT29 cells [15], a finding that is consistent with the increased sialomucin seen in active IBD. Likewise, TNFα increased α-2,3-sialyltransferase expression and mucin sialylation in a human respiratory glandular cell line [16]. However, TNFα may also contribute to mucin sulfation as

evidenced by a mouse model of salmonellosis where TNFα was linked to an observed increase in sulfomucins in villus goblet cells [6]. A study using human bronchial mucosa indicated that IL-6 and IL-8 can increase expression of sialyltransferases and sulfotransferases, paralleling an increase in sialyl-Lewis^x and 6-sulfo-sialyl-Lewis^x epitopes on bronchial proteins, including MUC4 [8]. Thus, proinflammatory cytokines, especially TNFα, may have an important role in mucin glycosyation, sulfation, and sialylation that remains to be fully understood.

Increased sialomucins and sulfomucins, altered terminal sugar chains, and increased gene expression of sulfotransferases have been observed in rodent models of intestinal nematode infections [17-19]. While the Th2 cytokines, IL-4 and IL-13, are considered to be mucogenic and important mediators of a number of other goblet cell responses to intestinal nematode infections, little is known regarding the ability of these cytokines to alter mucin composition in the human colon [20, 21]. IL-4 treatment of the human goblet-cell like line, LS174T, resulted in enhanced gene expression of specific *N*–acetylgalactosaminyltransferases and stimulated the attachment of more *N*-acetylgalactosamine into a tandem repeat domain of the MUC2 [22]. In the rat intestinal epithelial cell line, IEC-6, both IL-4 and IL-13 increased gene expression of sialyltransferase 4C (ST3GalIV), considered to be the major sialyltransferase expressed in the intestine following nematode infection [23]. Therefore, there is some indication that IL-4 and IL-13 may alter mucin composition via effects on specific glycosyltransferases, sulfotransferases, and sialyltransferases involved in mucin biosynthesis.

Mucin sulfation occurs within the *trans*-Golgi as a late step in glycoprotein synthesis when specific sulfotransferases transfer sulfate from 3′-phosphoadenosine 5′-phosphosulfate (PAPS) to mucin *O*-glycans at the C-3 position of galactose residues or the C-6 position of *N*-acetylglucosamine [24, 25]. Of the known galactose 3-*O*-sulfotransferases and *N*-

acetylglucosamine-6-*O* sulfotransferases, galactose-3-*O*-sulfotransferase 2 (GAL3ST2) appears to be the sulfotransferase responsible for sulfate addition to the C-3 position of Gal in human colonic mucins and carbohydrate (*N*-acetylglucosamine 6-*O*) sulfotransferase 5 (CHST5) the most likely candidate for sulfation of the C-6 position of *N*-acetylglucosamine [26-28]. Evidence for the involvement of these two sulfotransferases in colonic sulfomucin synthesis includes the downregulation of GAL3ST2 expression in non-mucinous adenocarcinomas, corresponding to a decrease in sulfomucin expression [26], and the abundance and specificity of CHST5 for human small intestine and colon [27, 28]. In addition, CHST5 shows a preference for sulfating O-linked chains of the mucin-type [27], suggesting that it is involved in transfer of sulfate to the C-6 position of *N*- acetylglucosamine in sulfomucins.

The aim of this study was to better understand both host and microbial factors that contribute to intestinal goblet cell mucin sulfation by examining effects of bacterial flagellin, IL-13, and TNFα on sulfotransferases, *CHST5* and *GAL3ST2*, and sulfomucin production in intestinal goblet cells. The human colonic LS174T adenocarcinoma cell line, which has a goblet cell-like phenotype, was used for this purpose [29]. This cell line synthesizes and constitutively secretes mucins as well as other goblet cell products and is responsive to conventional mucin secretagogues [30, 31]. Furthermore, unlike many other mucin-producing cell lines, the LS174T cell line produces both sialo- and sulfomucin under normal growth conditions [7, 30].

MATERIALS AND METHODS

Reagents and Cell Culture. Recombinant human IL-13 and TNFα were purchased from PeproTech. Recombinant Flagellin from *S. typhimurium* was purchased from InvivoGen. The human LS174T colorectal cancer cell line was obtained from the American Type Culture

Collection (ATCC). LS174T cells were maintained in Minimum Essential Medium (MEM) supplemented with 10% Fetalplex (Gemini Biosciences), 1.5 g/L of Na_2CO_3, 50 units/mL penicillin G and 50 mg/mL streptomycin sulfate at 37°C in 5% CO_2.

Treatments for Gene Expression and IL-8 Secretion. Cells were seeded into 24-well plates at a density of 2 x 10^5 cells/well and allowed to grow for 48 h. Cells were then washed twice with 1X HBSS and fresh antibiotic-free media containing different concentrations of flagellin, IL-13, or TNFα were added to the cells. After 24 h, conditioned media were collected for measurement of IL-8 secretion, and cells were harvested for RNA isolation.

RNA Isolation and Reverse Transcription. Total RNA was isolated from cells using the RNeasy Plus Kit (Qiagen) according to the manufacturer's instructions for animal cells. The quality and quantity of RNA isolates were determined by Nanodrop (Thermo Fisher Scientific). RNA isolates were reverse transcribed using the High Capacity cDNA Reverse Transcription Kit (Applied Biosystems) or Superscript III First Strand Synthesis system (Invitrogen).

TLR Expression. Gene expression for human TLRs 1-10 was examined in LS174T cells using conventional RT-PCR as previously described [32], except 400 ng of LS174T cell cDNA or equivalent of no reverse transcription control was used in each 25 uL PCR reaction, and cycles were extended to 40.

Gene Expression. Quantitative real-time PCR was performed using SYBR Green PCR Master Mix (Applied Biosystems) and the primers described in **Table 3.1**. Reactions were run in

triplicate in a 384-well plate using an Applied Biosystems 7900HT Fast Real-Time PCR System. Final quantifications were performed using the standard curve method with the geometric mean of *GAPDH* and *RPLP0* used for normalization. No reverse transcription reactions were performed to confirm the specificity of the reactions for RNA.

IL-8 Secretion. Secretion of IL-8 from LS174T cells was measured in conditioned media using a Human CXCL8/IL-8 Quantikine ELISA Kit (R & D Systems) according to the manufacturer's instructions.

Sulfomucin Analysis via High Iron Diamine and Alcian Blue (HID/AB) Staining. LS174T cells were seeded in μ-chamber 12-well slides (IBIDI) at a density of 4 x 10^4 cells/well and allowed to grow for 48 h. Cells were then washed twice with 1X HBSS, and fresh antibiotic-free media containing different concentrations of flagellin, IL-13, or TNFα were added to the cells. After 48 h, cells were washed once with 1X PBS and fixed in Carnoy's solution for 10 minutes. Cells were subsequently washed with 100% ethanol, 95% ethanol, and 70% ethanol for 10 minutes each and maintained in 70% ethanol until staining was initiated. For staining, cells were first rehydrated in nanopure water for 3 minutes and then stained in high iron diamine (HID) for 16 h [33]. Following HID staining, cells were washed for 5 minutes in tap H_2O, stained with alcian blue (pH 2.5) for 5 minutes, and washed for 3 minutes in tap H_2O. Cells were then counterstained with nuclear fast red for 1 minute and rinsed 5 minutes in tap H_2O. Stained cells were dehydrated in increasing concentrations of ethanol and cleared in xylene. Glass coverslips were mounted onto slides with Permount (Fisher). Slides were scanned at 40X using the Nanozoomer Digital Pathology System (Hamamatsu). Twenty images were selected from each

well at 20X resolution for analysis. Images were imported into Axiovision 4.7 software (Zeiss) and the area of sulfomucin staining was selected and measured in μm^2 in each image using the Automeasure module. The total area of cells in the image was measured in μm^2 and used to normalize the area of sulfomucin staining.

Analysis of Sulfo Le^{a}Antigen Expression via Immunofluorescent Staining. LS174T cells were seeded in 8-well μ-slides (IBIDI) at a density of 6 x 10^4 cells/well and allowed to grow for 48 h. Cells were then washed twice with 1X HBSS (without phenol red), and fresh antibiotic-free media (without phenol red) containing flagellin, IL-13, or TNFα were added to the cells. After 48 h, cells were washed 3X in 1X PBS and fixed with 4% paraformaldehyde (Electron Microscopy Sciences) for 20 minutes. Following fixation, cells were washed 3X in 1X PBS for 5 minutes each, incubated in 0.1% Triton X-100 for 15 minutes to permeabilize cells, and rinsed 3X in 1X PBS. Blocking was performed for 30 minutes in 5% normal goat serum (Vector Laboratories) and 5% IgG-Free BSA (Jackson ImmunoResearch Laboratories) in 1X PBS. Cells were rinsed once in 1X PBS, incubated for 2 h at room temperature with a mouse monoclonal [F2] antibody to Sulfo Le^a (Abcam) diluted 1:60 in 10% blocking solution, and washed 3X in 1XPBS for 5 minutes each. Incubation with Alexa Fluor 647 Goat Anti-Mouse IgM (H+L) (Invitrogen) diluted 1:200 in 10% blocking solution was performed for 2 h at room temperature and followed by 3 washes with 1X PBS for 5 minutes each. Cells were counterstained with 10 μg/mL of DAPI (Invitrogen) for 15 minutes, rinsed 3X in 1X PBS, and covered with Prolong Gold Antifade Reagent (Invitrogen). After allowing Prolong Gold to cure for 24 h in the dark at room temperature, stained cells were stored in the dark at 4^{o}C prior to imaging. Stained cells were imaged with a Zeiss LSM 710 confocal microscope using the 40X water objective and Zen

2008 software (Zeiss). Nine 2 x 2 tiled z-stacked images were collected from each well. Images were imported into Imaris (Bitplane) for reconstruction into 3-D isosurfaces. Volume of Sulfo Le^a staining was measured in each image in μm^3 and normalized to volume of stained nuclei in each image in μm^3.

Statistical Analysis. ANOVA and Fisher's protected least significant difference (FLSD) test were used to compare differences. These analyses were carried out using SAS software (Statview, Version 5.0.1; SAS Institute, Cary, NC). Differences were considered significant at $p < 0.05$.

RESULTS

TLR Expression in LS174T Cells. The expression of TLRs 1-10 at the mRNA level was examined in LS174T cells using conventional RT-PCR. As shown in **Figure 3.1**, all TLRs were detected in LS174T cells. There was some genomic DNA contamination in reactions for *TLR3* and *-6*, but amplicons using cDNA were still distinguishable. Multiple bands were observed for *TLR9*, including an amplicon of expected size. Expression of *TLR3* and *TLR5* was greatest while expression for *TLR4* and *TLR10* was the weakest.

IL-8 Secretion from LS174T Cells. IL-8 secretion was measured in conditioned media following treatment with flagellin, IL-13, and TNFα for 24 h. This was done to determine whether cells were responding to the flagellin and TNFα treatments. As indicated in **Figure 3.2**, treatments with flagellin at 500 ng/mL and 1000 ng/mL resulted in a significant increase in IL-8 secretion from LS174T cells. Treatment with TNFα from 10 ng/mL to 1000 ng/mL also significantly increased IL-8 secretion from LS174T cells. These results indicate that cells were indeed

responding to both flagellin and TNFα. IL-13, on the other hand, produced a decrease in IL-8 secretion at the two highest concentrations examined.

Validation of Primers for Gene Expression Studies in LS174T Cells. All primers used for quantitative RT-PCR were shown to produce a single amplicon (**Figures 3.3A** and **3.4A**) of expected size (**Table 3.1**) by conventional RT-PCR and a single peak upon dissociation curve analysis following quantitative RT-PCR (**Figures 3.3B** and **3.4B**). Data are not shown for housekeeping genes, *RPLP0* and *GAPDH*, but primers were equivalently validated.

Expression of Sulfotransferases CHST5 and GAL3ST2 in Duodeum, Rectum, and Liver. Conventional RT-PCR was performed using human RNA from duodenum, rectum, and liver purchased from Stratagene. As shown in **Figure 3.4C**, *CHST5* is expressed in duodenum, rectum, and liver while *GAL3ST2* is only expressed in the rectum. The level of *CHST5* expression in liver appeared to be less than that in duodenum and rectum.

Expression of Goblet Cell Secretory Product Genes in Response to Flagellin, IL-13, and *TNFα.* Gene expression for *MUC2, RETNLB,* and *TFF3* was examined in LS174T cells following treatment with flagellin, IL-13, or TNFα for 24 h (**Figure 3.5**). *MUC2* was increased by all three treatments with flagellin and IL-13 producing up to a 4-fold increase in gene expression, and TNFα producing up to a 5.5-fold increase in gene expression. *RETNLB* expression was decreased approximately 2-fold by the three lowest concentrations of IL-13 and approximately 1.5 to 3-fold with increasing concentrations of TNFα. Flagellin did not significantly alter *RETNLB* expression. All concentrations of *TNFα* examined and 1000 ng/mL of flagellin lead to

a 1.5-fold increase in *TFF3* expression. *TFF3* was also increased 1.5 to 1.7 fold by all but the highest concentration of IL-13.

Expression of Golgi Sulfotransferases, CHST5 and GAL3ST2, in Response to Flagellin, IL-13, and *TNFα.* Gene expression for *CHST5* and *GAL3ST2* was measured in LS174T cells following treatment with flagellin, IL-13, or TNFα for 24 h (**Figure 3.6**). IL-13 increased *CHST5* expression in a dose dependent manner up to 7.5-fold for the highest concentration. Flagellin did not significantly affect *CHST5* expression, and treatment with TNFα resulted in only a 1.4-fold increase in *CHST5* expression at the two lowest concentrations. *GAL3ST2* expression was significantly increased by the two highest concentrations of IL-13 (2 to 3-fold) and flagellin (2 to 2.5-fold). *GAL3ST2* expression was also increased approximately 3-fold by treatment with 10 ng/mL to 1000 ng/mL of TNFα.

Expression of CDX2 and TLR5 in Response to Flagellin, IL-13, and *TNFα.* Gene expression for *CDX2* and *TLR5* was analyzed in LS174T cells following treatment with flagellin, IL-13, or TNFα for 24 h (**Figure 3.7**). Expression of *CDX2* was only increased by treatment with 100 ng/mL of IL-13 (1.6-fold) and 10 ng/mL of TNFα (1.1-fold). *TLR5* expression was increased approximately 2-fold by treatment with 500 and 1000 ng/mL of flagellin. Treatment with 5, 10, and 100 ng/mL of IL-13 also significantly increased *TLR5* expression up to 2-fold. Treatment with TNFα increased *TLR5* expression at concentrations of 10, 100, and 1000 ng/mL and produced up to a 3.7-fold increase in *TLR5* expression.

Sulfomucin Expression in LS174T cells in Response to Flagellin, IL-13, and *TNFα.* Sulfomucin was identified by HID/AB staining of LS174T cells as shown in **Figure 3.8** following treatment with various concentrations of flagellin, IL-13, and TNFα for 48 h. The area of sulfomucin staining in each image was measured and normalized to the area of cells in the image. Comparison between treated and control cells revealed a significant increase in sulfomucin expression in cells treated with 5 and 100 ng/mL of IL-13 and 1000 ng/mL of flagellin (**Figure 3.9**). Measurable increases in sulfomucin expression were not observed in LS174T cells treated with any of the TNFα concentrations examined.

Sulfo Le^{a}Antigen Expression in LS174T cells in Response to Flagellin, IL-13, and *TNFα.* To examine effects of flagellin, IL-13, and TNFα on Sulfo Le^a antigen expression, LS174T cells were treated with 500 ng/mL of flagellin, 100 ng/mL of IL-13, or 100 ng/mL of TNFα for 48 h. These concentrations were selected based on the lowest concentrations of flagellin, IL-13, and TNFα that produced the maximal increase in *GAL3ST2* expression at 24 h (**See Figure 3.6**). A representative z-stacked, tiled image of the immunofluorescent staining is shown in **Figure 3.10A** and a 3-D isosurface generated from that data is shown in **Figure 3.10B**. Comparison of the volume of Sulfo Le^a staining per volume of nuclear staining between treatments revealed an increase in Sulfo Le^a expression in LS174T cells treated with 500 ng/mL of flagellin for 48 h, while treatment with IL-13 or TNFα did not significantly alter the level of Sulfo Le^a expression (**Figure 3.10C**).

Summary of Results. A summary of the results of measured end points is provided in **Table 3.2**.

DISCUSSION

The factors contributing to expression of specific mucin chemotypes are poorly understood, but there is evidence for the involvement of both host and microbial factors. In this study, we focused on the role of bacterial flagellin, IL-13, and TNFα in mucin sulfation. Gene expression for human TLRs 1-10 was analyzed in LS174T cells to aid in the selection of a microbial factor and revealed the expression of all ten human TLR genes by this cell line. This finding may reflect the importance of goblet cells in mediating host-microbe interactions in the intestinal epithelium. Expression of certain TLRs appeared to be greater than others, with TLR5 being among the most abundantly expressed. For this reason, flagellin, a known agonist of TLR5 [34], was selected as the microbial factor for this study.

LS174T cells constitutively secrete mucin, which may make them more resistant to certain treatments. Previous studies have shown TNFα to induce IL-8 secretion from LS174T cells and bacterial flagellin to be a strong inducer of IL-8 secretion from intestinal epithelial cells, but flagellin had not been previously tested in this cell line [34, 35]. Therefore, to confirm that LS174T cells were responding to flagellin and TNFα, IL-8 secretion was measured in conditioned media following stimulus with flagellin and TNFα for 24 h. The increased secretion of IL-8 indicated that the LS174T cell line was indeed responsive to both flagellin and TNFα. On the other hand, IL-13 treatment decreased IL-8 secretion at higher concentrations. These results are consistent with a previous report that IL-13 reduced IL-8 secretion by human intestinal epithelial cells [36].

Flagellin, IL-13, and TNFα all upregulated expression of *MUC2*, indicating that increased mucin production is a common response to these stimuli. The increase in *MUC2* expression in response to IL-13 and TNFα is consistent with published work in the LS174T cell

line showing IL-13 and TNFα increase *MUC2* expression via a mitogen-activated protein (MAP) kinase pathway [37]. To our knowledge, this is the first study to report an increase in *MUC2* expression by an intestinal epithelial cell line in response to flagellin from *S. typhimurium*. Flagellin isolated from *P. aeruginosa* was, however, previously found to activate *MUC2* transcription via downstream signaling following binding to the surface glycolipid receptor, Asialo-GM1, and requiring intact functioning of TLR5 [38, 39].

To determine whether there was a general increase in the expression of goblet cell secretory product genes, expression of *RETNLB* and *TFF3* were also examined. Similar to results with *MUC2*, flagellin, IL-13 and TNFα all upregulated expression of *TFF3*, but the response was much less than that observed with *MUC2*. The enhanced expression of *TFF3* as a result of IL-13 treatment is in accord with work done in HT29 CL.16E cells, which develop a goblet-cell like phenotype after reaching confluence [20]. However, our results with TNFα are in contrast to another study showing a dramatic reduction in *TFF3* expression in the HT-29 cell line in response to this proinflammatory cytokine [40]. The use of a different cell line is one possible explanation for the contrasting results. Both IL-13 and TNFα caused a downregulation in *RETNLB* expression while flagellin did not alter expression levels significantly from the control. The results for IL-13 and TNFα are surprising considering that previous studies demonstrated increased *RETNLB* expression in LS174T cells treated with IL-13 or TNFα [21, 41, 42]. Analysis of *RETNLB* expression after shorter and longer treatment times with IL-13 and TNFα might help to clarify the conflicting results. The effects of bacterial flagellin on *RETNLB* expression had not been previously examined, but LPS was shown in an earlier study to upregulate expression of *RETNLB* indicating that other microbial components may have a greater influence on *RETNLB* expression [41]. Overall, our results demonstrate the increase in *MUC2*

expression elicited by flagellin, IL-13, and TNFα was not due to a common upregulation of goblet cell secretory product genes. Furthermore, *TFF3* expression was similarly unregulated, but to a lesser extent, while expression of *RETNLB* did not follow this trend and was instead decreased or unaltered in response to the treatments.

The expression of sulfotransferases, *CHST5* and *GAL3ST2*, was examined in RNA isolated from human duodenum, rectum, and liver. *CHST5* was expressed in all three tissues while *GAL3ST2* was only expressed in the rectum. The presence of *CHST5* in the small intestine and rectum is consistent with a previous study [28], but this finding indicates that *GAL3ST2* is likely the more important sulfotransferase for biosynthesis of sulfomucin seen in the colon, since, based on histochemical staining, human small intestine does not typically express sulfomucin [43].

Enhancement of *GAL3ST2* expression was observed in LS174T cells following treatment with flagellin, IL-13, and TNFα for 24 h indicating that increased mucin sulfation at the C-3 position of Gal might be a common response to inflammatory stimuli. Analysis of *CHST5* expression revealed IL-13 to be a strong inducer of expression in a dose dependent manner, flagellin to not significantly alter expression, and TNFα to minimally increase expression at low concentrations. This observation is consistent with the possibility that mucin sulfation at the C-6 position of *N*-acetylglucosamine is augmented in response to IL-13. To determine whether increased expression of these sulfotransferases corresponded to an increase in mucin sulfation, sulfomucin associated with the cells (identified by HID/AB staining) and expression of the Sulfo Le^a antigen, which is synthesized in part by *GAL3ST2* [44], were measured in cells after 48 h of treatment with selected concentrations of flagellin, IL-13, and TNFα. Overall sulfomucin was increased by flagellin and IL-13 but remained unchanged by TNFα. Only exposure to flagellin

increased the expression of the Sulfo Le^a antigen. Together, these results indicate that IL-13 may increase sulfomucins primarily via increased expression of *CHST5*, while flagellin may increase sulfomucins, including those with the Sulfo Le^a antigen, by enhancing expression of *GAL3ST2*. Although TNFα increased expression of both sulfotransferase genes, it did not increase sulfomucin content during the time period examined. It is possible that the increased expression of *GAL3ST2* seen with IL-13 and TNFα treatment would have resulted in increased Sulfo Le^a antigen with extended treatment or that Sulfo Le^a antigen was increased by both of these, but that mucin containing the Sulfo Le^a antigen was secreted into the media. Both IL-13 and TNFα have been shown to induce mucin secretion from LS174T cells [37]. Thus additional studies, measuring secreted sulfomucin, are needed to fully examine the effects of flagellin, IL-13 and TNFα on sulfomucins.

The upregulation of *MUC2* and *GAL3ST2* in response to flagellin, IL-13, and TNFα suggests that intestinal goblet cells attempt to upregulate sulfomucin biosynthesis in response to microbial and inflammatory stimuli, perhaps in an attempt to increase host protection. This is in accord with the idea that sulfomucins are protective because they increase mucus viscosity and resistance to bacterial degradation and microbe adhesion [45]. The results with TNFα are of particular interest because of its association with IBD and the reduced mucin sulfation seen with active IBD. Consistent with the idea that individuals with IBD mount an inappropriate immune response [46], it may be that those with IBD do not respond appropriately to TNFα and thus do not increase sulfomucin. The same may also be true of their response to microbial-derived factors, such as flagellin. One study reported that sulfomucins are preferentially secreted by individuals with ulcerative colitis while sulfate incorporation into mucins is reduced [47]. Thus, it may be that TNFα, either as a normal or abnormal response, also elicits a preferential secretion

of sulfated mucins so that sulfomucins are eventually depleted within goblet cells. Alternatively, since we use a transformed cell line for this study, it could be that the responses we observed with LS174T cell exposure to flagellin, IL-13, and TNFα, are not what typically occur in normal healthy colon. Further studies should be conducted to determine whether responses are consistent *in situ* or in non-transformed cells.

Additional studies are also needed to better understand the mechanisms by which flagellin, IL-13, and TNFα enhance expression of specific sulfotransferases and sulfomucin production. Previous studies have identified pathways governing goblet cell secretory product gene expression in response to TNFα and IL-13 [37, 48-50]. These pathways may be similarly involved in regulation of *CHST5* and *GAL3ST2* transcription. We did examine gene expression of the transcription factor *CDX2*, which has been shown to transactivate the promoters of *MUC2*, *RETNLB*, and *TFF3* [51-53]. We found *CDX2* to be upregulated in response to IL-13 exposure. It is possible that CDX2 may also transactivate *CHST5* or even *GAL3ST2*, and it would be beneficial to establish whether there are CDX2 binding sites within their promoter regions. The mechanisms of flagellin's effects on goblet cell secretory products and the sulfotransferases, especially need to be further studied to determine whether changes are a direct response involving TLR signaling in intestinal goblet cells or whether IL-8 or other inflammatory cues might be triggering the goblet cell response to flagellin. We observed an upregulation of *TLR5* expression with the concentrations of flagellin that induced IL-8 secretion and *MUC2* and *GAL3ST2* expression. However, a similar upregulation of *TLR5* expression was also seen with IL-13 and TNFα, so the significance of this finding is uncertain.

In summary, our results indicate that flagellin, IL-13, and TNFα have differential effects on mucin sulfotransferases and sulfation as well as the goblet cell secretory product genes. All

three stimuli significantly increase *MUC2* expression. IL-13 increases sulfomucin most likely via increased expression of *CHST5*, while flagellin increases sulfomucin possibly by increasing expression of *GAL3ST2*. Although TNFα increased expression of both sulfotransferase genes, it did not increase sulfomucin content during the time period examined. Together these data indicate that both host and microbial factors influence mucin chemotypes. Additional studies are needed to understand the mechanisms underlying these results and their role in the reduced mucin sulfation observed in IBD.

REFERENCES

1. Baumgart, D.C. and W.J. Sandborn, *Inflammatory bowel disease: clinical aspects and established and evolving therapies.* Lancet, 2007. **369**(9573): p. 1641-57.

2. Campbell, B.J., L.G. Yu, and J.M. Rhodes, *Altered glycosylation in inflammatory bowel disease: a possible role in cancer development.* Glycoconj J, 2001. **18**(11-12): p. 851-8.

3. Shirazi, T., et al., *Mucins and inflammatory bowel disease.* Postgrad Med J, 2000. **76**(898): p. 473-8.

4. Strugala, V., P.W. Dettmar, and J.P. Pearson, *Thickness and continuity of the adherent colonic mucus barrier in active and quiescent ulcerative colitis and Crohn's disease.* Int J Clin Pract, 2008. **62**(5): p. 762-9.

5. Swidsinski, A., et al., *Comparative study of the intestinal mucus barrier in normal and inflamed colon.* Gut, 2007. **56**(3): p. 343-50.

6. Arnold, J.W., G.R. Klimpel, and D.W. Niesel, *Tumor necrosis factor (TNF alpha) regulates intestinal mucus production during salmonellosis.* Cell Immunol, 1993. **151**(2): p. 336-44.

7. Deplancke, B. and H.R. Gaskins, *Microbial modulation of innate defense: goblet cells and the intestinal mucus layer.* Am J Clin Nutr, 2001. **73**(6): p. 1131S-1141S.

8. Groux-Degroote, S., et al., *IL-6 and IL-8 increase the expression of glycosyltransferases and sulfotransferases involved in the biosynthesis of sialylated and/or sulfated Lewisx epitopes in the human bronchial mucosa.* Biochem J, 2008. **410**(1): p. 213-23.

9. Conour, J.E., et al., *Acidomucin goblet cell expansion induced by parenteral nutrition in the small intestine of piglets.* Am J Physiol Gastrointest Liver Physiol, 2002. **283**(5): p. G1185-96.

10. Enss, M.L., et al., *Proinflammatory cytokines trigger MUC gene expression and mucin release in the intestinal cancer cell line LS180.* Inflamm Res, 2000. **49**(4): p. 162-9.

11. Hill, R.R., H.M. Cowley, and A. Andremont, *Influence of colonizing micro-flora on the mucin histochemistry of the neonatal mouse colon.* Histochem J, 1990. **22**(2): p. 102-5.

12. Enss, M.L., et al., *Effects of perorally applied endotoxin on colonic mucins of germfree rats.* Scand J Gastroenterol, 1996. **31**(9): p. 868-74.

13. Liau, Y.H., et al., *Helicobacter pylori lipopolysaccharide effect on the synthesis and secretion of gastric sulfomucin.* Biochem Biophys Res Commun, 1992. **184**(3): p. 1411-7.

14. Sheahan, D.G. and H.R. Jervis, *Comparative histochemistry of gastrointestinal mucosubstances.* Am J Anat, 1976. **146**(2): p. 103-31.

15. Majuri, M.L., et al., *Expression and function of alpha 2,3-sialyl- and alpha 1,3/1,4-fucosyltransferases in colon adenocarcinoma cell lines: role in synthesis of E-selectin counter-receptors.* Int J Cancer, 1995. **63**(4): p. 551-9.

16. Delmotte, P., et al., *Influence of TNFalpha on the sialylation of mucins produced by a transformed cell line MM-39 derived from human tracheal gland cells.* Glycoconj J, 2001. **18**(6): p. 487-97.

17. Karlsson, N.G., et al., *Identification of transient glycosylation alterations of sialylated mucin oligosaccharides during infection by the rat intestinal parasite Nippostrongylus brasiliensis.* Biochem J, 2000. **350 Pt 3**: p. 805-14.

18. Ishikawa, N., Y. Horii, and Y. Nawa, *Immune-mediated alteration of the terminal sugars of goblet cell mucins in the small intestine of Nippostrongylus brasiliensis-infected rats.* Immunology, 1993. **78**(2): p. 303-7.

19. Soga, K., et al., *Alteration of the expression profiles of acidic mucin, sialytransferase, and sulfotransferases in the intestinal epithelium of rats infected with the nematode Nippostrongylus brasiliensis.* Parasitol Res, 2008. **103**(6): p. 1427-34.

20. Blanchard, C., et al., *IL-4 and IL-13 up-regulate intestinal trefoil factor expression: requirement for STAT6 and de novo protein synthesis.* J Immunol, 2004. **172**(6): p. 3775-83.

21. Artis, D., et al., *RELMbeta/FIZZ2 is a goblet cell-specific immune-effector molecule in the gastrointestinal tract.* Proc Natl Acad Sci U S A, 2004. **101**(37): p. 13596-600.

22. Kanoh, A., et al., *Interleukin-4 induces specific pp-GalNAc-T expression and alterations in mucin O-glycosylation in colonic epithelial cells.* Biochim Biophys Acta, 2008. **1780**(3): p. 577-84.

23. Takeda, K., et al., *Direct effects of IL-4/IL-13 and the nematode Nippostrongylus brasiliensis on intestinal epithelial cells in vitro.* Parasite Immunol. **32**(6): p. 420-9.

24. Brockhausen, I., *Pathways of O-glycan biosynthesis in cancer cells.* Biochim Biophys Acta, 1999. **1473**(1): p. 67-95.

25. Robbe, C., et al., *Structural diversity and specific distribution of O-glycans in normal human mucins along the intestinal tract.* Biochem J, 2004. **384**(Pt 2): p. 307-16.

26. Seko, A., et al., *Down-regulation of Gal 3-O-sulfotransferase-2 (Gal3ST-2) expression in human colonic non-mucinous adenocarcinoma.* Jpn J Cancer Res, 2002. **93**(5): p. 507-15.

27. Lee, J.K., et al., *Activities and expression pattern of the carbohydrate sulfotransferase GlcNAc6ST-3 (I-GlcNAc6ST): functional implications.* Glycobiology, 2003. **13**(4): p. 245-54.

28. Nishimura, M. and S. Naito, *Tissue-specific mRNA expression profiles of human carbohydrate sulfotransferase and tyrosylprotein sulfotransferase.* Biol Pharm Bull, 2007. **30**(4): p. 821-5.

29. Tom, B.H., et al., *Human colonic adenocarcinoma cells. I. Establishment and description of a new line.* In Vitro, 1976. **12**(3): p. 180-91.

30. Gottke, M.U., et al., *Functional heterogeneity of colonic adenocarcinoma mucins for inhibition of Entamoeba histolytica adherence to target cells.* J Eukaryot Microbiol, 1998. **45**(2): p. 17S-23S.

31. Sands, B.E., et al., *Molecular cloning of the rat intestinal trefoil factor gene. Characterization of an intestinal goblet cell-associated promoter.* J Biol Chem, 1995. **270**(16): p. 9353-61.

32. Omueti, K.O., et al., *Domain exchange between human toll-like receptors 1 and 6 reveals a region required for lipopeptide discrimination.* J Biol Chem, 2005. **280**(44): p. 36616-25.

33. Spicer, S.S., *Diamine Methods for Differentialing Mucosubstances Histochemically.* J Histochem Cytochem, 1965. **13**: p. 211-34.

34. Gewirtz, A.T., et al., *Salmonella typhimurium translocates flagellin across intestinal epithelia, inducing a proinflammatory response.* J Clin Invest, 2001. **107**(1): p. 99-109.

35. Barshishat, M., et al., *TNFalpha and IL-8 regulate the expression and function of CD44 variant proteins in human colon carcinoma cells.* Clin Exp Metastasis, 2002. **19**(4): p. 327-37.

36. Lugering, N., et al., *Interleukin (IL)-13 and IL-4 are potent inhibitors of IL-8 secretion by human intestinal epithelial cells.* Dig Dis Sci, 1999. **44**(3): p. 649-55.

37. Iwashita, J., et al., *mRNA of MUC2 is stimulated by IL-4, IL-13 or TNF-alpha through a mitogen-activated protein kinase pathway in human colon cancer cells.* Immunol Cell Biol, 2003. **81**(4): p. 275-82.

38. McNamara, N., et al., *AsialoGM1 and TLR5 cooperate in flagellin-induced nucleotide signaling to activate Erk1/2.* Am J Respir Cell Mol Biol, 2006. **34**(6): p. 653-60.

39. Dharmani, P., et al., *Role of intestinal mucins in innate host defense mechanisms against pathogens.* J Innate Immun, 2009. **1**(2): p. 123-35.

40. Loncar, M.B., et al., *Tumour necrosis factor alpha and nuclear factor kappaB inhibit transcription of human TFF3 encoding a gastrointestinal healing peptide.* Gut, 2003. **52**(9): p. 1297-303.

41. He, W., et al., *Bacterial colonization leads to the colonic secretion of RELMbeta/FIZZ2, a novel goblet cell-specific protein.* Gastroenterology, 2003. **125**(5): p. 1388-97.

42. Fujio, J., et al., *Regulation of gut-derived resistin-like molecule beta expression by nutrients.* Diabetes Res Clin Pract, 2008. **79**(1): p. 2-10.

43. Filipe, M.I., *Mucins in the human gastrointestinal epithelium: a review.* Invest Cell Pathol, 1979. **2**(3): p. 195-216.

44. Loveless, R.W., et al., *Monoclonal antibody 91.9H raised against sulfated mucins is specific for the 3'-sulfated Lewisa tetrasaccharide sequence.* Glycobiology, 1998. **8**(12): p. 1237-42.

45. Nieuw Amerongen, A.V., et al., *Sulfomucins in the human body.* Biol Chem, 1998. **379**(1): p. 1-18.

46. Strober, W., I. Fuss, and P. Mannon, *The fundamental basis of inflammatory bowel disease.* J Clin Invest, 2007. **117**(3): p. 514-21.

47. Van Klinken, B.J., et al., *Sulphation and secretion of the predominant secretory human colonic mucin MUC2 in ulcerative colitis.* Gut, 1999. **44**(3): p. 387-93.

48. Ahn, D.H., et al., *TNF-alpha activates MUC2 transcription via NF-kappaB but inhibits via JNK activation.* Cell Physiol Biochem, 2005. **15**(1-4): p. 29-40.

49. Stutz, A.M., et al., *The Th2 cell cytokines IL-4 and IL-13 regulate found in inflammatory zone 1/resistin-like molecule alpha gene expression by a STAT6 and CCAAT/enhancer-binding protein-dependent mechanism.* J Immunol, 2003. **170**(4): p. 1789-96.

50. Wang, M.L., et al., *Immune-mediated signaling in intestinal goblet cells via PI3-kinase- and AKT-dependent pathways.* Am J Physiol Gastrointest Liver Physiol, 2008. **295**(5): p. G1122-30.

51. Silberg, D.G., et al., *Cdx1 and cdx2 expression during intestinal development.* Gastroenterology, 2000. **119**(4): p. 961-71.

52. Wang, M.L., et al., *Regulation of RELM/FIZZ isoform expression by Cdx2 in response to innate and adaptive immune stimulation in the intestine.* Am J Physiol Gastrointest Liver Physiol, 2005. **288**(5): p. G1074-83.

53. Yamamoto, H., Y.Q. Bai, and Y. Yuasa, *Homeodomain protein CDX2 regulates goblet-specific MUC2 gene expression.* Biochem Biophys Res Commun, 2003. **300**(4): p. 813-8.

54. Johnson, C.M. and R.I. Tapping, *Microbial products stimulate human Toll-like receptor 2 expression through histone modification surrounding a proximal NF-kappaB-binding site.* J Biol Chem, 2007. **282**(43): p. 31197-205.

55. Rozen, S. and H. J. Skaletsky. *Primer3 on the WWW for general users and for biologist programmers*. In: *Bioinformatics Methods and Protocols: Methods in Molecular Biology.* Krawetz S, Misener S., Eds., 2000. Humana Press, Totowa, NJ, p. 365-386. Source code available at http://fokker.wi.mit.edu/primer3/.

56. Dydensborg, A.B., et al., *Normalizing genes for quantitative RT-PCR in differentiating human intestinal epithelial cells and adenocarcinomas of the colon.* Am J Physiol Gastrointest Liver Physiol, 2006. **290**(5): p. G1067-74.

FIGURES AND TABLES

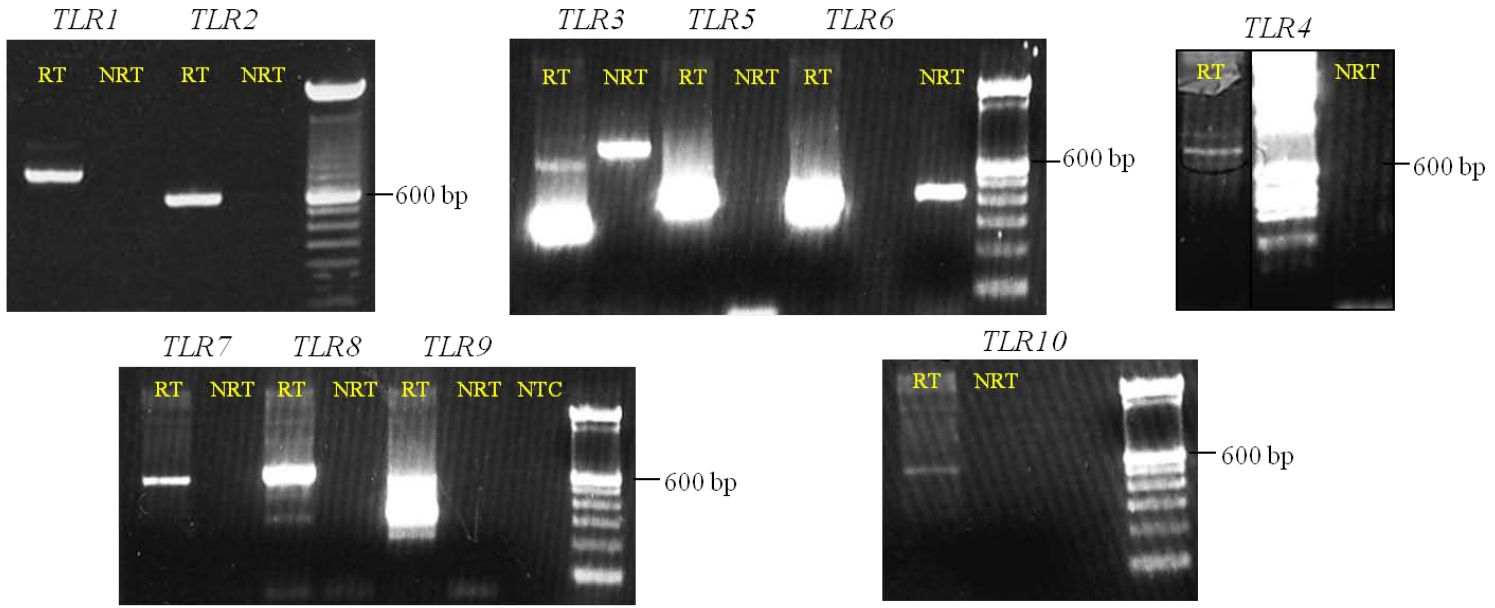

Product	Size (bp)	Product	Size (bp)
TLR 1	889	TLR 6	411
TLR 2	676	TLR 7	591
TLR 3	319	TLR 8	636
TLR 4	622	TLR 9	331
TLR 5	445	TLR 10	540

Figure 3.1: TLR expression in LS174T cells. RT-PCR for human TLRs 1-10 using cDNA from LS174T cells. Total RNA was isolated from the cells and cDNA was prepared with and without reverse transcriptase (RT). Wells containing the reverse transcribed LS174T RNA are labeled with RT and wells containing LS174T RNA that was not reverse transcribed are labeled NRT. The expected amplicon sizes are included.

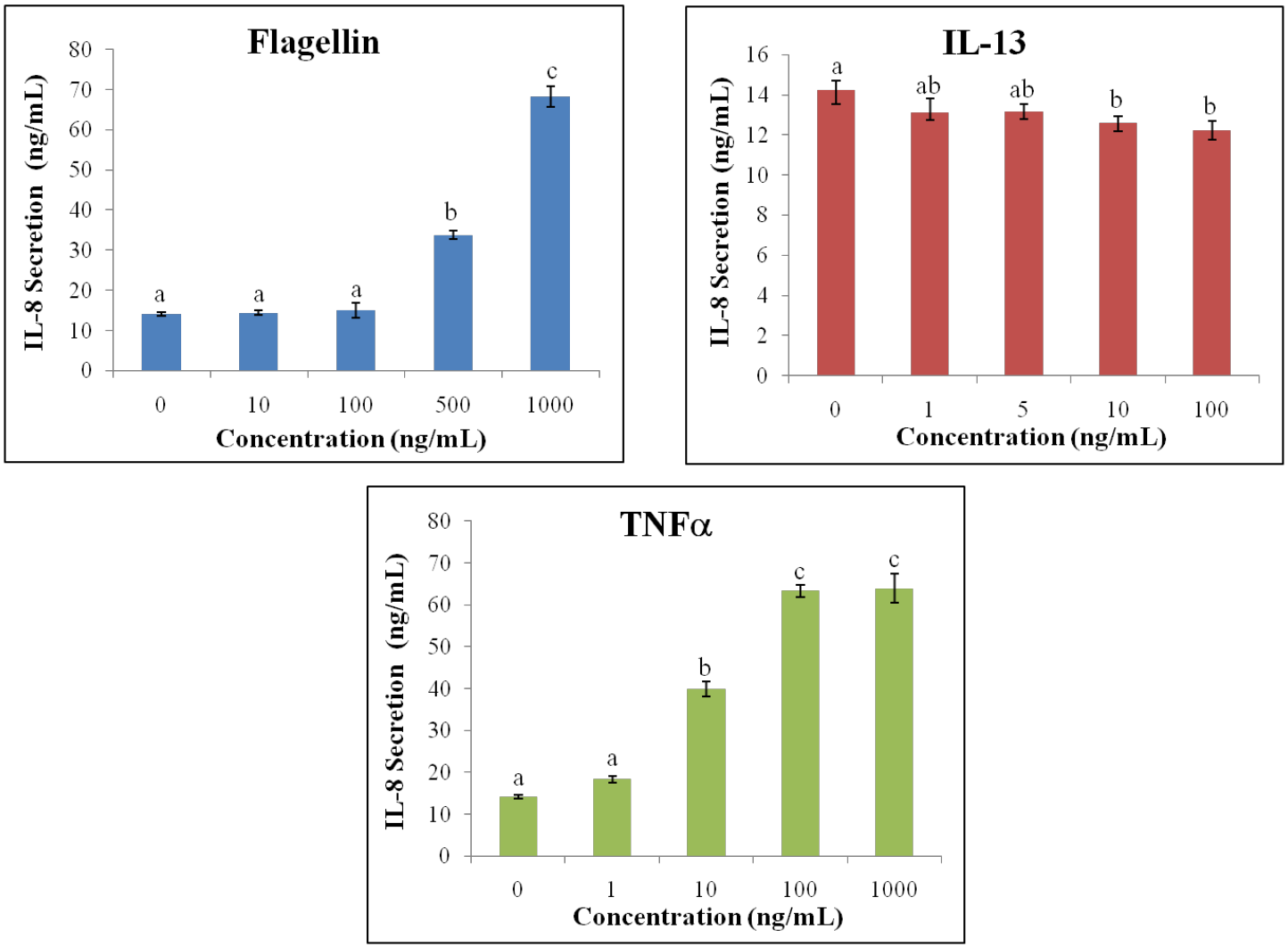

Figure 3.2: IL-8 secretion from LS174T cells incubated for 24 h with the indicated treatments. The data represent means ± SEM (n=4). Statistical differences are indicated by different letters ($p < 0.05$).

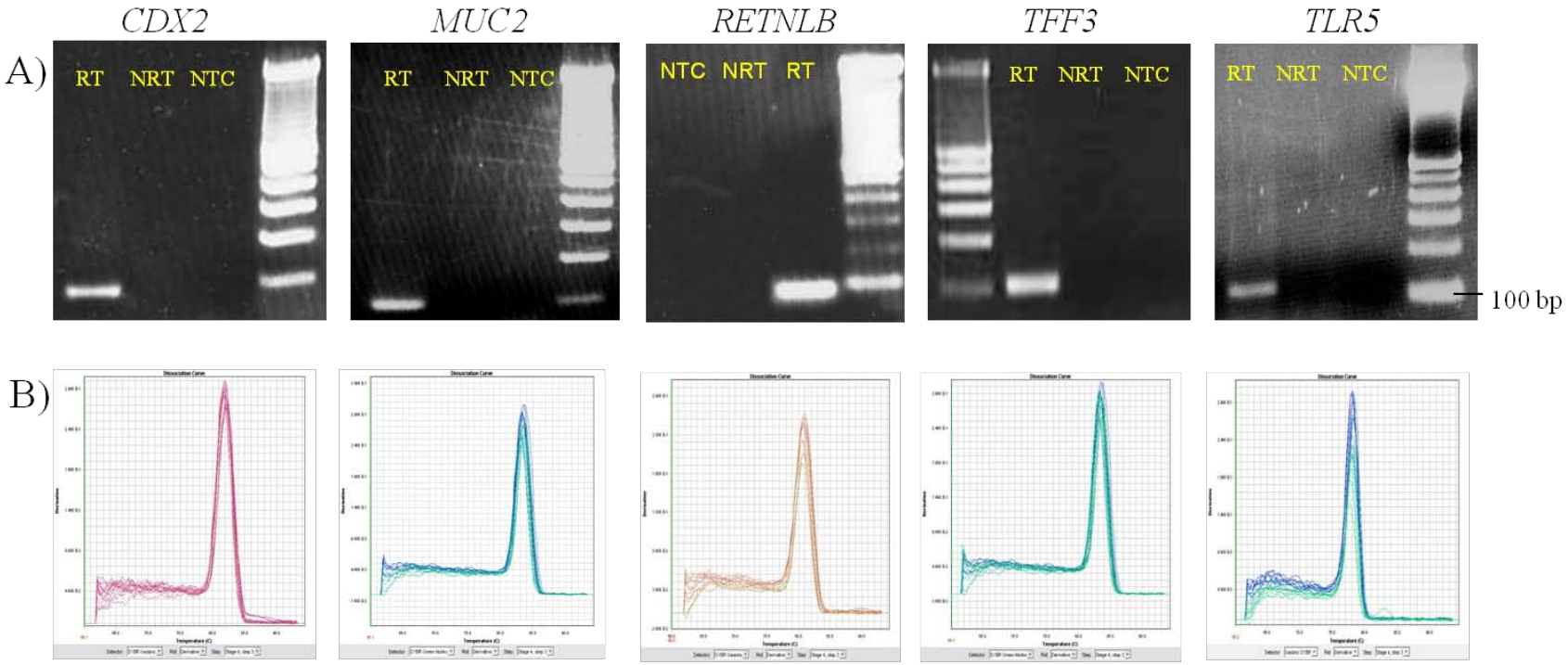

Figure 3.3: Validation of *CDX2, MUC2, RETNLB, TFF3,* and *TLR5* primers. **A)** RT-PCR products for *CDX2, MUC2, RETNLB, TFF3*, and *TLR5* using cDNA from LS174T cells. Total RNA was isolated from the cells and cDNA was prepared with and without reverse transcriptase (RT). Wells containing the reverse transcribed LS174T RNA are labeled with RT and wells containing LS174T RNA that was not reverse transcribed are labeled NRT. NTC = No template control. **B)** Dissociation curve analysis following SYBR Green quantitative RT-PCR for each gene.

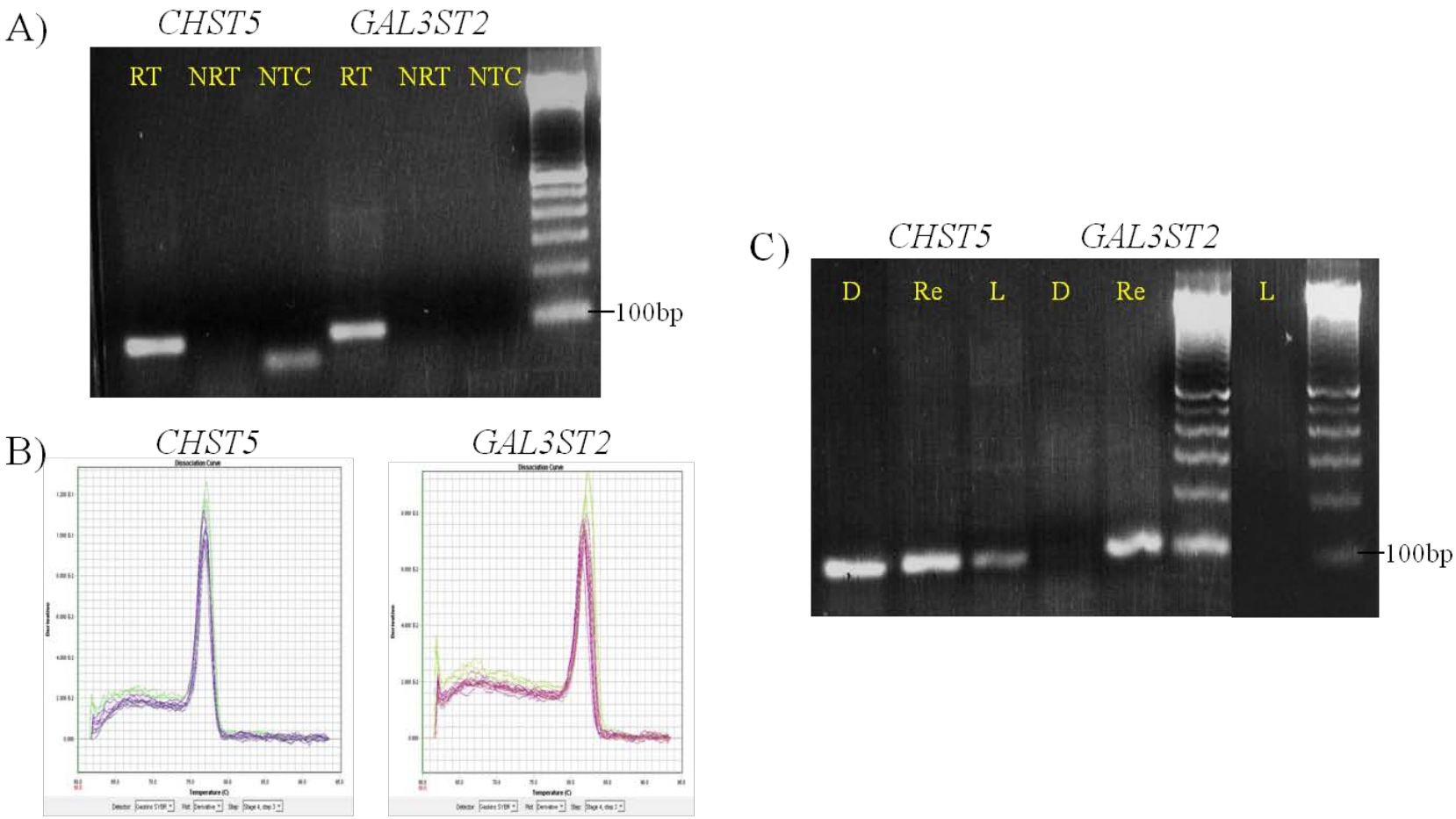

Figure 3.4: Validation of *CHST5* and *GAL3ST2* primers and expression in human duodenum, rectum, and liver. A) RT-PCR products for *CHST5* and *GAL3ST2* using cDNA from LS174T cells. Total RNA was isolated from the cells and cDNA was prepared with and without reverse transcriptase (RT). Wells containing the reverse transcribed LS174T RNA are labeled with RT and wells containing LS174T RNA that was not reverse transcribed are labeled NRT. NTC = No template control. B) Dissociation curve analysis following SYBR Green quantitative RT-PCR for each gene. C) RT-PCR using RNA from human duodenum (D), rectum (Re), liver (L)

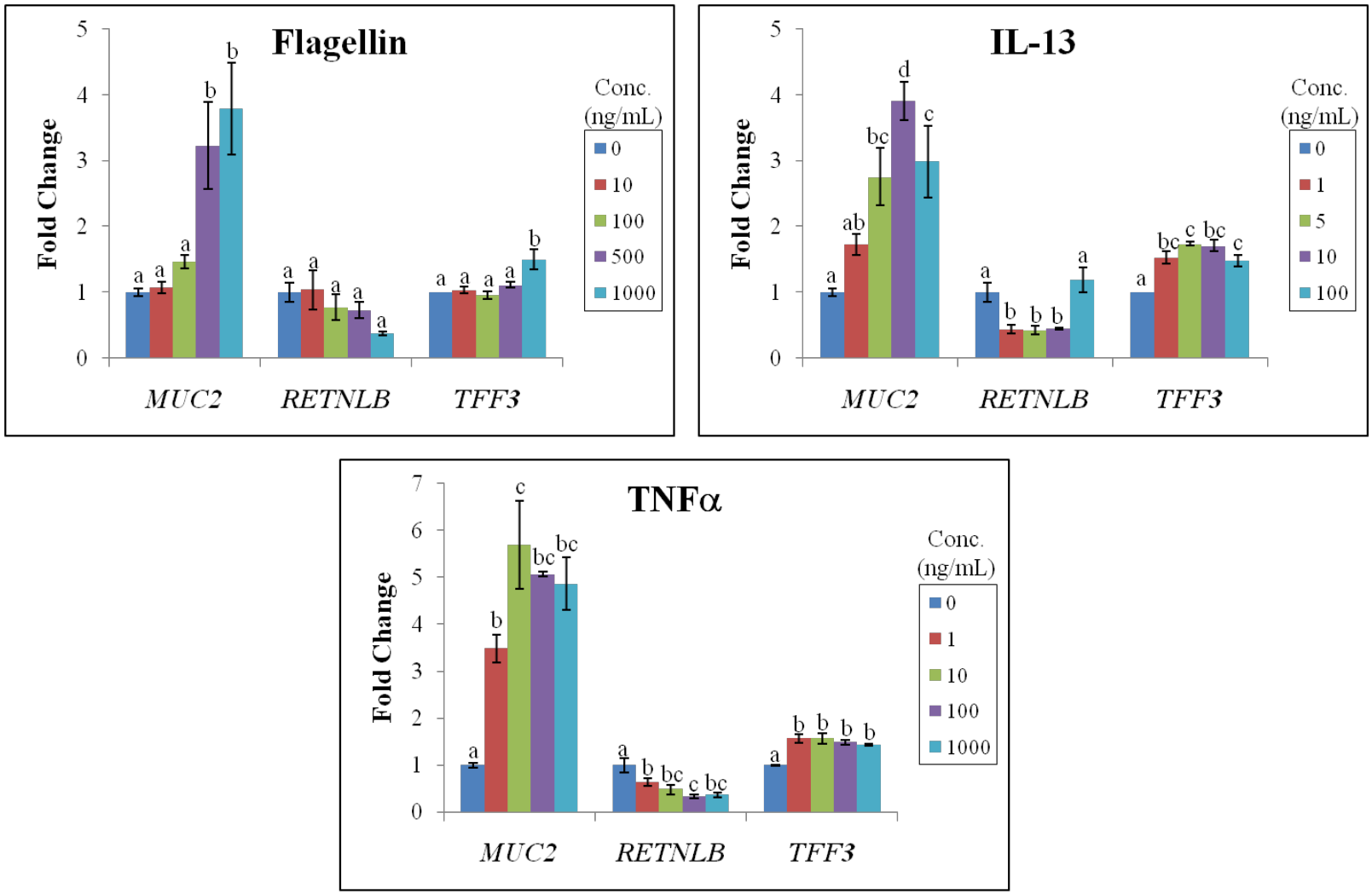

Figure 3.5: Relative expression (setting controls as 1) of goblet cell secretory product genes *MUC2, RETNLB,* and *TFF3* in response to treatment with flagellin, IL-13, or TNFα for 24 h. The data represent mean ± SEM (n=4); statistical differences are indicated by different letters ($p < 0.05$).

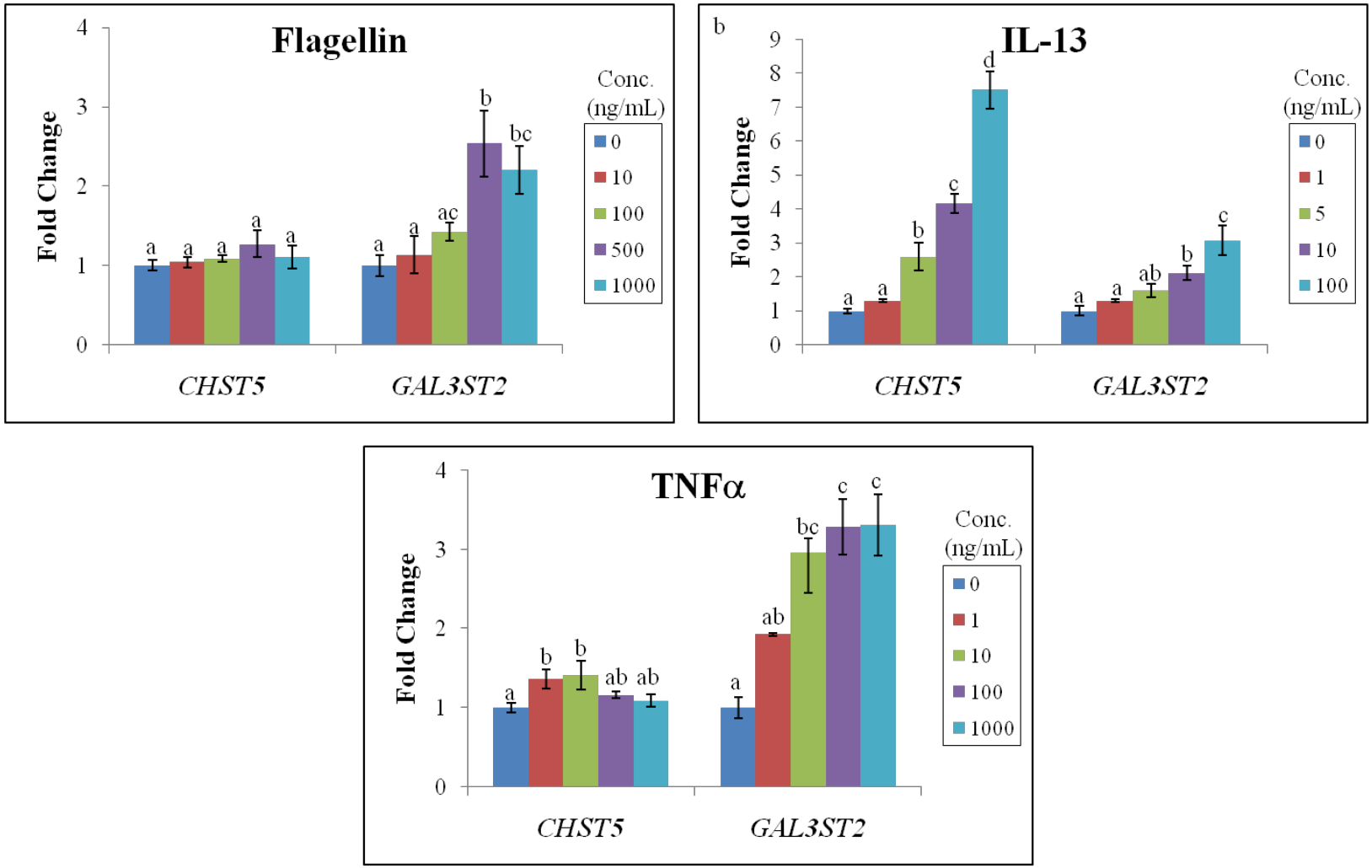

Figure 3.6: Relative expression (setting controls as 1) of sulfotransferase genes *CHST5* and *GAL3ST2* in response to treatment with flagellin, IL-13, or TNFα for 24 h. The data represent mean ± SEM (n=4); statistical differences are indicated by different letters ($p < 0.05$).

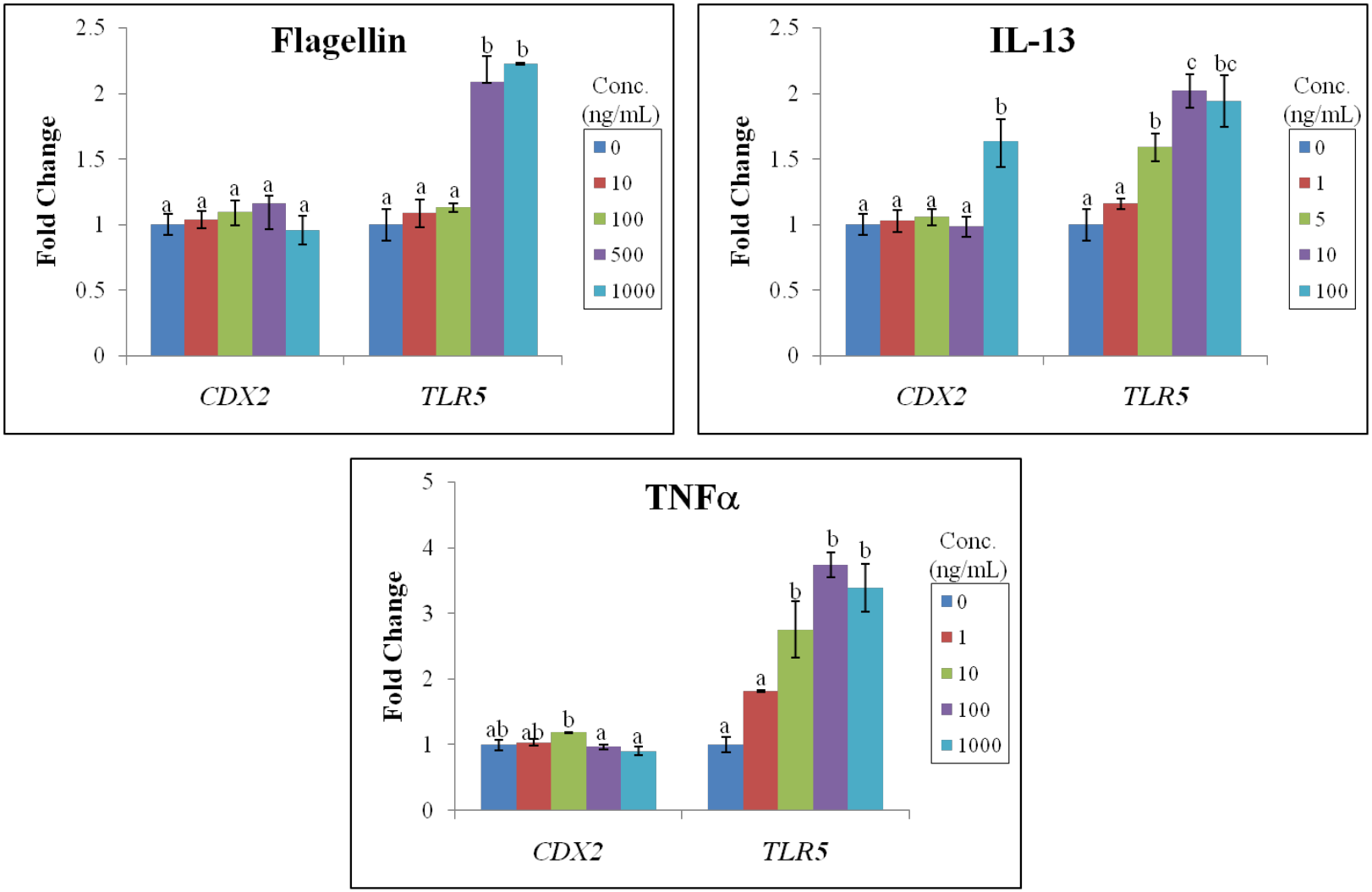

Figure 3.7: Relative expression (setting controls as 1) of *CDX2* and *TLR5* in response to treatment with flagellin, IL-13, or TNFα for 24 h. The data represent mean ± SEM (n=4); statistical differences are indicated by different letters ($p < 0.05$).

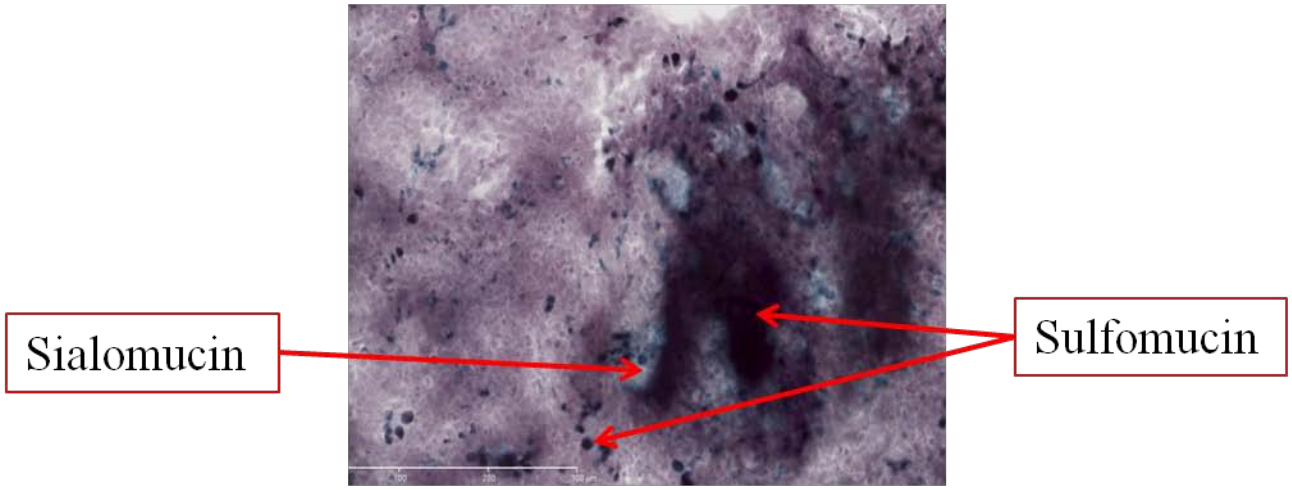

Figure 3.8: Sulfomucin (purple/black) and sialomucin (blue) identification in LS174T cells by HID/AB staining (20X magnification).

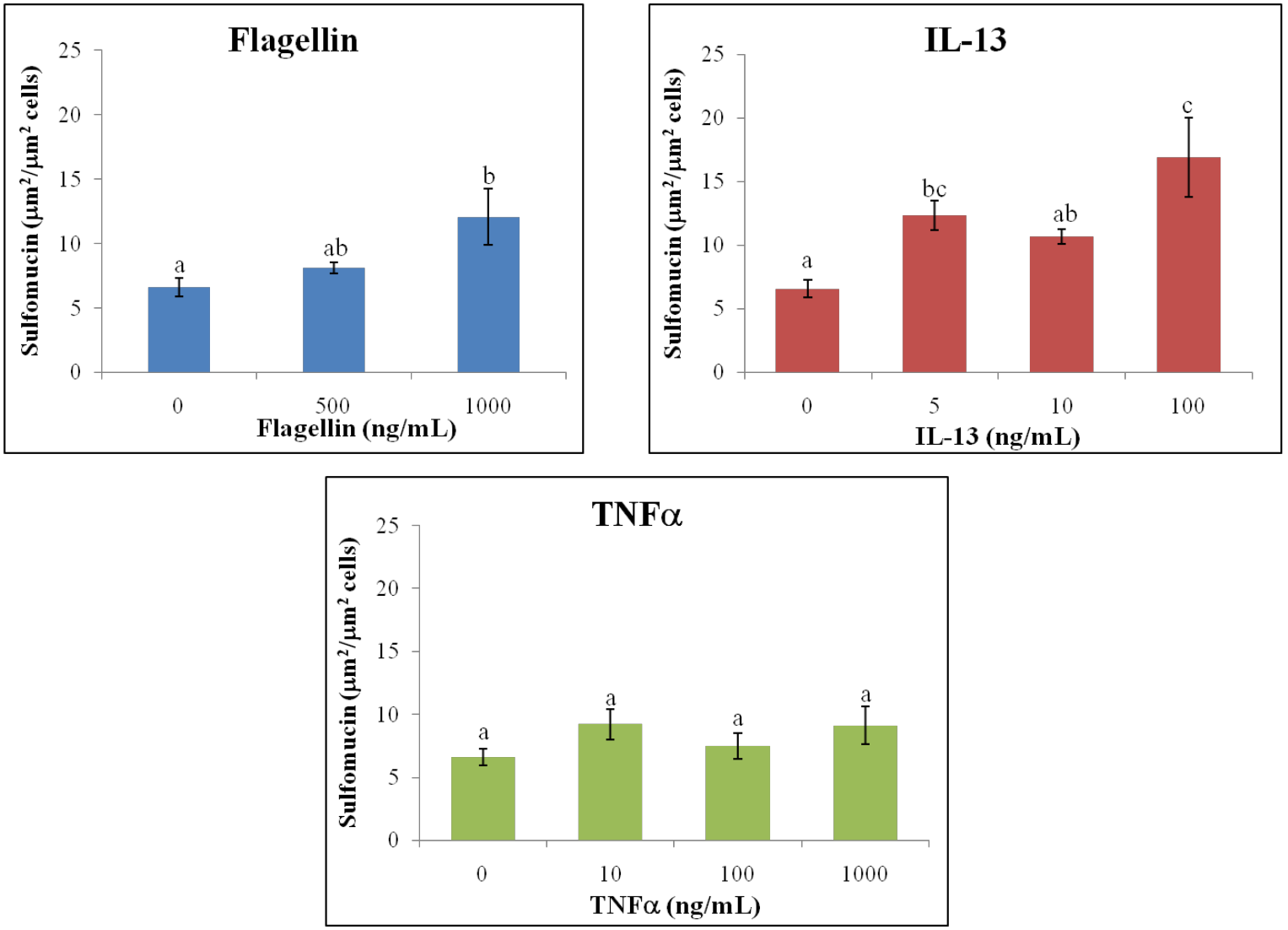

Figure 3.9: Sulfomucin expression measured by HID/AB staining of LS174T cells incubated for 48 h with the indicated treatments. The data represent means ± SEM (n=3-4). Statistical differences are indicated by different letters ($p < 0.05$).

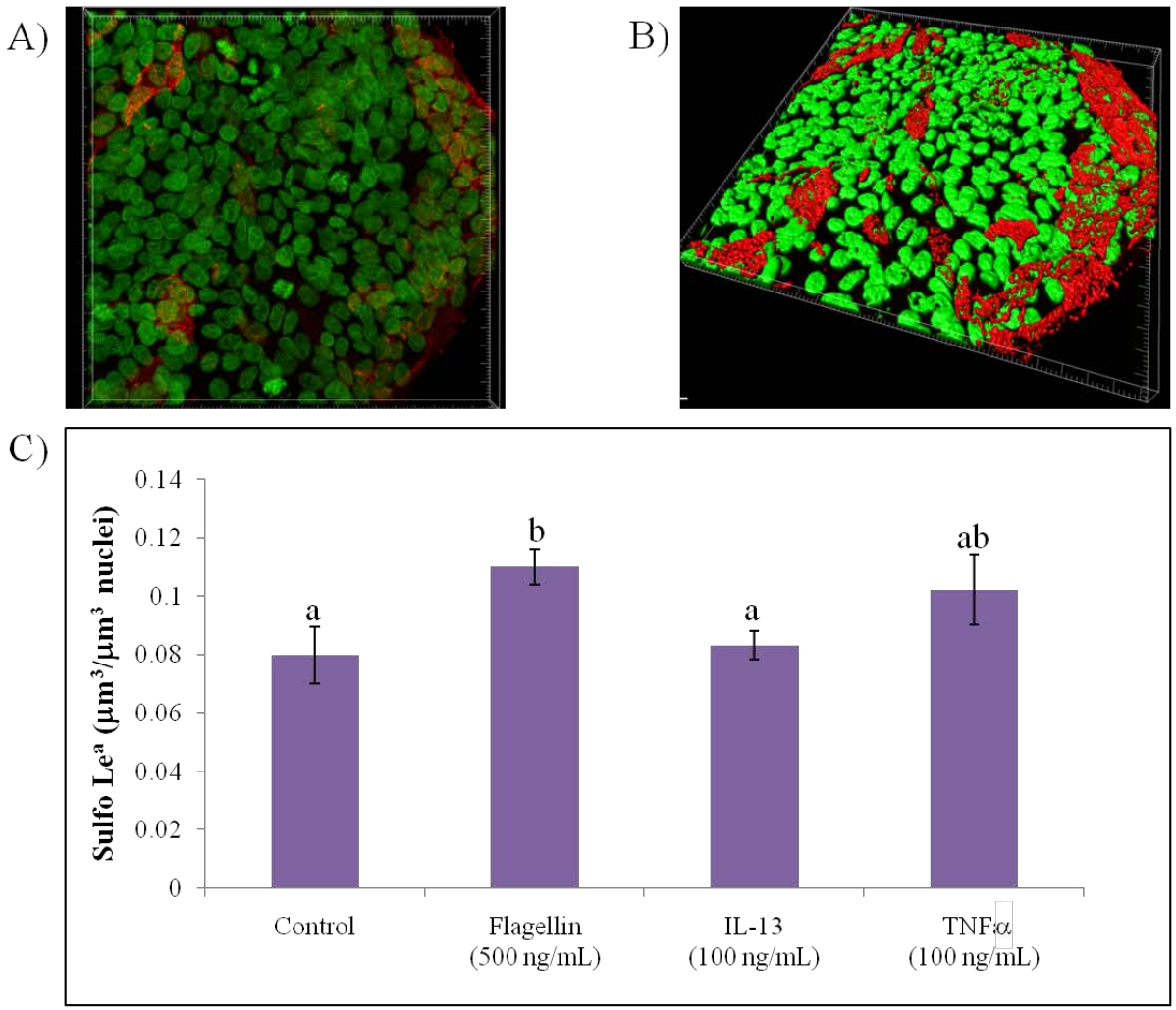

Figure 3.10: Sulfo Le^a antigen expression . **A)** Immunofluorescent staining of the Sulfo Le^a antigen (red) in LS174T cells. Nuclear staining with DAPI (green) **B)** 3-D isosurface generated from z-stacked image. **C**) Sulfo Le^a antigen expression in LS174T cells in response to incubation for 48 h with the indicated treatments. The data represent means ± SEM (n=3-4). Statistical differences are indicated by different letters ($p < 0.05$).

Table 3.1: Primers used in this study for quantitative RT-PCR

Gene Symbol	Fwd Primer Sequence	Rev Primer Sequence	Product Size (bp)	Source
CDX2	5'-CAA AGA CTG CAG AAC CCC CA-3'	5'-CCC CTC ATA CCA CAC CCT GT-3'	101	Designed using Primer Express*
CHST5	5'-CCC AGT GAG GAA CTG GTC TTC-3'	5'-ATC TGT GTT CCA GGA AAG CC-3'	91	Designed using Primer Express*
GAL3ST2	5'-TGG GCG GCT TGC AGA GAT A-3'	5'-GCT CTA AGT CCG AGT GCA GGA-3'	96	Designed using Primer Express*
GAPDH	5'-AAG ATC ATC AGC AAT GCC TCC TGC-3'	5'-ATG GAC TGT GGT CAT GAG TCC TTC-3'	105	See reference [54]
MUC2	5'-AAC ACA GTC CTG GTG GAA GG-3'	5'-CAT TGT CAG GTC CCA CAC AG-3'	106	Designed using Primer3 [55]
RETNLB	5'-CAC CCA GGA GCT CAG AGA TCT AA-3'	5'-ACG GCC CCA TCC TGT ACA-3'	82	See reference [41]
RPLP0	5'-GCA ATG TTG CCA GTG TCT G-3'	5'-GCC TTG ACC TTT TCA GCA A-3'	142	See reference [56]
TFF3	5'-CAT GTC ACC CCC AAG GAG TG-3'	5'-AGG TGC ATT CTG CTT CCT GC-3'	103	Designed using Primer Express*
TLR5	5'-GAC CCT CTG CCC CTA GAA TAA-3'	5'-GCC ATG AGC ACC ACT CCT A-3'	105	Quantitative PCR primer database**

*Software available from Applied Biosystems
**Available at http://web.ncifcrf.gov/rtp/gel/primerdb/default.asp

Table 3.2: Summary of results for Chapter 3

	IL-8 Secretion	***MUC2***	***RETNLB***	***TFF3***	***CHST5***	***GAL3ST2***	***CDX2***	***TLR5***	**Sulfomucin (HID/AB)**	**Sulfo Le^a Antigen**
Flagellin	↑↑↑	↑↑↑	NC	↑	NC	↑↑	NC	↑↑	↑	↑
IL-13	↓	↑↑↑	↓↓	↑	↑↑↑	↑↑↑	↑	↑↑	↑↑	NC
TNFα	↑↑↑	↑↑↑	↓↓↓	↑	↑	↑↑↑	NC	↑↑↑	NC	NC

NC= No change at any concentration examined, ↑= increased < 2-fold, ↑↑ = increased 2 to 3-fold, ↑↑↑ = increased >3-fold, ↓=decreased < 2-fold, ↓↓ =decreased 2 to 3-fold, ↓↓↓ =decreased >3-fold based on concentration producing the greatest response and statistically significant differences ($p<0.05$).

Chapter 4

CYSTEINE DIOXYGENASE EXPRESSION IN THE INTESTINAL EPITHELIUM

ABSTRACT

Cysteine dioxygenase (CDO) catalyzes the oxidation of cysteine to cysteine sulphinic acid, which is the first and rate limiting step for cysteine utilization. Mammals regulate cysteine metabolism through CDO to maintain sufficient cysteine for protein synthesis and production of other essential molecules such as glutathione, taurine, pyruvate and inorganic sulfate, but below the threshold for cytotoxicity. While CDO is known to be highly expressed in liver, its expression in the intestine remains uncharacterized. Here, CDO expression and localization in mouse small and large intestine is examined using immunohistochemical and immunofluorescence staining techniques. Adult mouse duodenum, jejunum, ileum, and proximal and distal colon were stained with an anti-CDO antibody and analyzed microscopically. Additional sections were stained using two-color immunofluorescence for CDO and matrix metalloproteinase 7 (MMP-7), a marker of Paneth cells, or chromagranin A (ChrA), a marker of enteroendocrine cells. Immunohistochemical analysis of mouse intestine revealed positive CDO staining in goblet cells, Paneth cells (small intestine only), and enteroendocrine cells while CDO staining was notably absent in absorptive epithelium. Dual immunofluorescent staining for CDO and ChrA or MMP-7 confirmed CDO expression in mouse enteroendocrine cells and Paneth cells, respectively. These results demonstrate that CDO expression in mouse small and large intestine is restricted to cells of the secretory lineage. This striking difference in CDO expression between the absorptive and secretory cell lineages is likely due to higher cysteine catabolism requirements in goblet, Paneth, and enteroendocrine cells relative to absorptive epithelial cells

either to synthesize additional taurine and sulfate or to metabolize excess cysteine when cells are not actively synthesizing cysteine-rich secretory products.

INTRODUCTION

Cysteine dioxygenase (CDO, EC 1.13.11.20) catalyzes the first and rate-limiting step of cysteine catabolism, which is the oxidation of cysteine (Cys) to cysteinesulfinate (**Figure 4.1**) [1, 2]. Cysteinesulfinate is further metabolized to yield a number of important products, including hypotaurine/taurine, pyruvate and sulfate (**Figure 4.1**). Mammals regulate cysteine metabolism through CDO to maintain cysteine levels within a limited range. Cysteine concentrations must be maintained at an adequate level to meet requirements for the synthesis of proteins and other essential molecules such as glutathione, coenzyme A, taurine, and inorganic sulfur while being kept below the threshold of cytotoxicity [1, 3, 4]. The toxicity of cysteine has been demonstrated in multiple animal models [5-7], and chronically elevated levels of cysteine have been associated with neurodegenerative and autoimmune diseases, including Parkinson's Disease [8], Alzheimer's disease [8], rheumatoid arthritis [9], and systemic lupus erythematosus [10]. Thus, CDO may have important implications in disease. In fact, a decline in CDO activity has been associated with the neurological disorder pantothenate kinase-associated neurodegeneration (PKAN) formerly known as Hallervorden-Spatz disease and characterized by degeneration of principal movement centers in the brain [11, 12].

Rodent and human CDO gene expression has been reported in a number of tissues [13-17], indicating the importance of CDO in whole body cysteine homeostasis. However, highest mRNA levels of CDO were present in the liver in rats, mice, and humans. Regarding intestinal tissue, CDO mRNA was detected in whole tissue homogenates of mouse small intestine but

found to be quite low and did not appear to be detected at the protein level [13]. A recently published paper, though, demonstrated low, but detectable CDO expression at the protein level in both mouse duodenum and colon [18]. Published studies examining CDO expression in rat or human small intestine or colon at the mRNA level could not be found, although an earlier study reported that rat enterocytes could metabolize cysteine to cysteinesulfinate via CDO [19]. However, a recent report described the localization of CDO specifically to goblet cells in the rat small intestine [20]. Published descriptions of CDO localization in the colon were also not found.

The aim of this study was to characterize the cell types that express CDO in mouse small intestinal and colonic epithelium. The epithelium in the small intestine and colon consists of absorptive and secretory cells, which derive from a common precursor cell [21]. The secretory lineage consists of goblet cells and enteroendocrine cells in both the small intestine and colon and includes Paneth cells in the small intestine. Since CDO was reported to be expressed in rat goblet cells, we sought to determine whether this was also true in mouse intestine and whether CDO expression was common among cells of the secretory lineage.

MATERIALS AND METHODS

Collection of Mouse Tissues. Procedures were approved by the University of Illinois Institutional Animal Care and Use Committee. Small intestine, colon, and cecum were harvested from adult male B6EiC3Sn a/A-Otc^{+} mice and fixed in Carnoy's solution for two hours. Fixed tissues were subsequently processed, embedded in paraffin, and sectioned onto glass slides.

CDO Immunohistochemistry. After deparaffinization, endogenous peroxidases were blocked by immersion in 0.5% hydrogen peroxide in methanol for 10 minutes. Sections were then blocked with 10% goat serum (Vector Laboratories) in 2X casein (Vector Laboratories) for 20 minutes prior to incubation with a 1:50 dilution in 1X casein of an affinity-purified rabbit anti-rat CDO antibody [16] for 2 hours at 37^{o}C. After washing, sections were sequentially incubated with biotinylated goat anti-rabbit IgG antibody (1:200 dilution in 1X casein) for 20 min at room termperature, peroxidase-labeled avidin-biotin complex for 30 min at room temperature, and DAB substrate (Vector Laboratories) for approximately 5 min color development. Sections were counterstained with Mayer's hematoxylin (Sigma), washed in tap H_2O, dehydrated, cleared in xylene, and mounted with Permount (Fisher). Biotinylated goat anti-rabbit IgG antibody and peroxidase-labeled avidin-biotin complex were part of a Rabbit IgG VECTSTAIN Elite ABC Kit (Vector Laboratories). Slides were imaged using a Zeiss Axiovert 200M microscope and Axiovision 4.7 software.

Immunofluorescence. Deparaffinized sections were blocked with 5% donkey serum (Jackson ImmunoResearch Laboratories) and 5% IgG-Free BSA (Jackson ImmunoResearch Laboratories) for 30 minutes followed by incubation with a 1:50 dilution of rabbit anti-rat CDO antibody and either a 1:50 dilution of goat anti-mouse ChrA antibody (Santa Cruz Biotechnology) or goat anti-mouse MMP-7 (R & D Systems) antibody for 2 hours at room temperature. Sections were washed 3X with 1X PBS for 5 min each and then sequentially incubated with a 1:200 dilution of Alexa Fluor 647 donkey anti-rabbit IgG (H+L) antibody (Invitrogen) for 1 hour, a 1:200 dilution of Alexa Fluor 546 donkey anti-goat IgG (H+L) antibody (Invitrogen) for 1 hour, and 10 μg/mL of DAPI (Invitrogen) for 15 min. Sections were washed 3X with 1X PBS for 5 min after

incubation with each antibody. Following counterstaining with DAPI, tissues were rinsed 3X in 1X PBS and mounted with Prolong Gold Antifade Reagent (Invitrogen). After allowing Prolong Gold to cure for 24 hours in the dark at room temperature, stained cells were stored in the dark at 4^{o}C prior to imaging. Slides were imaged using a Zeiss Axiovert 200M microscope and Axiovision 4.7 software.

RESULTS

CDO Immunohistochemistry: Immunohistochemical staining revealed positive CDO staining in goblet cells but not enterocytes in mouse duodenum, jejunum, ileum, cecum, proximal colon, and distal colon (**Figure 4.2**). In the small intestine, positive CDO staining was also observed at the base of the crypts, which suggested staining of Paneth cells. In addition, positive CDO staining appeared to be present in fewer cells in the distal colon compared to the proximal colon. Preliminary studies in human right colon, left colon, and rectum have also indicated that CDO is expressed in secretory goblet cells but not absorptive cells (data not shown). Initially, we used a secondary antibody-only negative control, which revealed no positive staining. Rabbit IgG (Vector Laboratories) was later tested as a negative control at the same IgG concentration as the CDO antibody. The rabbit IgG control produced some staining of goblet cells in small intestinal and colon tissue sections, but positive staining was absent from the small intestinal crypt base and was weaker and in fewer cells compared to staining with the anti-CDO antibody. Furthermore, CDO and rabbit IgG staining performed using another set of mouse small intestinal and colon tissues fixed in formalin and a modified protocol resulted in the same pattern of positive staining with the CDO antibody as with the Carnoy's fixed tissues but no positive staining with the rabbit IgG control.

CDO Localization in Paneth Cells. To confirm that CDO was also expressed in Paneth cells, small intestinal tissue sections were simultaneously stained for CDO and MMP-7, a marker for Paneth cells [22]. As shown in **Figure 4.3A**, when images of CDO (red) and MMP-7 (green) staining in small intestine were merged, colocalization (yellow) of the two stains was observed at the base of the crypt. This observation along with the IHC images confirms that there is positive CDO staining within Paneth cells. However, from the high magnification image in **Figure 4.3B**, it appears that CDO and MMP-7 are not localized in exactly the same area within Paneth cells and there may also be some staining for CDO in between and adjacent to Paneth cells where populations of intestinal stem cells are located [23].

CDO Localization in Enteroendocrine Cells. To determine whether the remaining member of the secretory lineage, the enteroendocrine cell, expressed CDO, small intestine, colon, and cecum were simultaneously stained for CDO and ChrA, a marker for enteroendocine cells [24]. Merged images of CDO (red) and ChrA (green) staining in small intestine, colon, and cecum demonstrate colocalization (yellow) of CDO in apparently all ChrA expressing cells (**Figure 4.4A**). Hence, CDO is also expressed in enteroendocrine cells. The high magnification image (**Figure 4.4B**) shows the CDO and ChrA are in a similar region of the enteroendocrine cell.

DISCUSSION

CDO is an important enzyme in regulating cysteine levels in the liver and possibly other tissues in the body. The enzyme had previously been detected in mouse small intestine and colon at the protein level [18], but information regarding its localization in the intestinal epithelium remained to be fully characterized. In this study, immunohistochemical staining for CDO

revealed localization of CDO to goblet cells in mouse colon and cecum and to Paneth and goblet cells in mouse small intestine. The localization of CDO to goblet cells was in accord with an earlier report describing CDO localization in rat small intestine [20]. Localization of CDO to Paneth cells as well as enteroendocrine cells was confirmed by dual immunofluorescent staining for CDO and markers for these two secretory cell types. Enteroendocrine cells in small intestine, colon, and cecum all expressed CDO. Overall, these results demonstrate that CDO expression in mouse small intestine, colon, and cecum is restricted to cells of the secretory lineage. There was some indication that CDO might also be expressed within intestinal stem cells, which would suggest that the secretory lineage may acquire CDO before differentiating into individual cell types. However, additional colocalization studies are needed to confirm the presence of CDO in intestinal stem cells.

A major question to address is why cells of the secretory lineage would have a higher requirement for CDO than absorptive cells. One possible reason is a higher cysteine requirement in goblet, Paneth, and enteroendocrine cells relative to absorptive epithelial cells because of a greater requirement for cysteine for synthesizing secretory products. Goblet cells, in particular, synthesize and secrete multiple cysteine-rich products, including mucin 2 [25], resistin-like molecule beta [26], and trefoil factor 3 [27, 28]. Likewise, Paneth cells are known to secrete cysteine-rich α-defensins [29]. In liver, CDO is known to be highly regulated by cysteine availability [1]. Thus, CDO may provide secretory cells with a means for regulating cysteine levels to ensure ample cysteine for synthesis of secretory products while preventing cysteine levels from becoming cytotoxic. Comparison of cysteine metabolism in specific intestinal epithelial cell types and CDO expression in response to differing cysteine concentrations would provide more evidence for this hypothesis.

Alternatively, the secretory lineage could have a high requirement for end products of cysteine catabolism, which include sulfate and taurine. Goblet cells, for example, synthesize and secrete sulfomucins, and CDO catabolism of cysteine may be necessary to provide sufficient sulfate for sulfomucin biosynthesis. In adult mice, small intestinal and cecal goblet cells predominantly produce sulfated mucins, while proximal colon goblet cells primarily produce non-sulfated sialomucins, and distal colon goblet cells produce both sialo- and sulfomucins depending on their location along the crypt [30]. Since we observed abundant CDO expression in the proximal colon, it appears that CDO expression is not restricted to sulfomucin containing goblet cells. Thus, CDO may be expressed in goblet cells in order to catabolize cysteine to form sulfate for biosynthesis of sulfomucins, but this does not fully explain CDO localization to intestinal goblet cells or its localization in Paneth or enteroendocrine cells.

Taurine can be synthesized from cysteine via oxidation by CDO to cysteine sulfinate, which is converted to hypotaurine by cysteinesulfinic acid decarboxylase (CSAD), and followed by hypotaurine oxidation to taurine via an unknown mechanism [31]. Consistent with CDO localization to goblet cells, taurine was reported to localize within the mucus granules of mouse intestinal goblet cells [32]. There was no mention of whether taurine was also present in other cells of the secretory lineage. Taurine has a number of cytoprotective properties, including antioxidant, anti-inflammatory, and osmoregulatory effects, which would make its production beneficial to secretory cells [33]. The osmoregulatory function of taurine might be especially important for secretory cells undergoing cell volume changes with release of secretory products. It should be noted, though, that taurine can be synthesized from cysteine via a CDO independent pathway as well, which involves cysteine conversion to Coenzyme A (CoA) followed by the degradation of CoA to cysteamine, which is then oxidized to hypotaurine/taurine via cysteamine

dioxygenase (ADO) [34]. Thus, future studies should be done to see whether the CDO/CSAD and/or ADO pathways for taurine biosynthesis are intact and functional in secretory cells and whether they are responsive to inflammatory triggers, oxidative stress, or osmotic changes. Experiments described in Chapter 5 indicate that the ADO pathway, and possibly the CDO/CSAD pathway, are intact and responsive to certain inflammatory stimuli in the human goblet cell-like LS174T cells.

In summary, we observed that CDO expression in the small intestine and colon is restricted to secretory cells and not expressed by absorptive enterocytes. Additional studies are necessary to determine the functional significance of this finding and whether CDO expression is present in intestinal stem cell populations.

REFERENCES

1. Stipanuk, M.H., et al., *Mammalian cysteine metabolism: new insights into regulation of cysteine metabolism.* J Nutr, 2006. **136**(6 Suppl): p. 1652S-1659S.

2. Joseph, C.A. and M.J. Maroney, *Cysteine dioxygenase: structure and mechanism.* Chem Commun (Camb), 2007(32): p. 3338-49.

3. Lee, J.I., et al., *Regulation of cysteine dioxygenase and gamma-glutamylcysteine synthetase is associated with hepatic cysteine level.* J Nutr Biochem, 2004. **15**(2): p. 112-22.

4. Sandberg, M., *L-Cysteine toxicity: effects on non-sulfur amino acids, sulfur-containing excitatory amino acids and gamma-glutamyl peptides in the immature brain.* J. Neurochem., 1991. **57**.

5. Andine, P., et al., *Extracellular acidic sulfur-containing amino acids and gamma-glutamyl peptides in global ischemia: postischemic recovery of neuronal activity is*

paralleled by a tetrodotoxin-sensitive increase in cysteine sulfinate in the CA1 of the rat hippocampus. J Neurochem, 1991. **57**(1): p. 230-6.

6. Lehmann, A., *Alterations in hippocampal extracellular amino acids and purine catabolites during limbic seizures induced by folate injections into the rabbit amygdala.* Neuroscience, 1987. **22**(2): p. 573-8.

7. Lehmann, A., et al., *Cysteine sulphinate and cysteate: mediators of cysteine toxicity in the neonatal rat brain?* Eur J Neurosci, 1993. **5**(10): p. 1398-412.

8. Heafield, M.T., et al., *Plasma cysteine and sulphate levels in patients with motor neurone, Parkinson's and Alzheimer's disease.* Neurosci Lett, 1990. **110**(1-2): p. 216-20.

9. Bradley, H., et al., *Sulfate metabolism is abnormal in patients with rheumatoid arthritis. Confirmation by in vivo biochemical findings.* J Rheumatol, 1994. **21**(7): p. 1192-6.

10. Gordon, C., et al., *Abnormal sulphur oxidation in systemic lupus erythematosus.* Lancet, 1992. **339**(8784): p. 25-6.

11. Perry, T.L., et al., *Hallervorden-Spatz disease: cysteine accumulation and cysteine dioxygenase deficiency in the globus pallidus.* Ann Neurol, 1985. **18**(4): p. 482-9.

12. Gordon, N., *Pantothenate kinase-associated neurodegeneration (Hallervorden-Spatz syndrome).* Eur J Paediatr Neurol, 2002. **6**(5): p. 243-7.

13. Hirschberger, L.L., et al., *Murine cysteine dioxygenase gene: structural organization, tissue-specific expression and promoter identification.* Gene, 2001. **277**(1-2): p. 153-61.

14. Tsuboyama, N., et al., *Structural organization and tissue-specific expression of the gene encoding rat cysteine dioxygenase.* Gene, 1996. **181**(1-2): p. 161-5.

15. Tsuboyama-Kasaoka, N., et al., *Human cysteine dioxygenase gene: structural organization, tissue-specific expression and downregulation by phorbol 12-myristate 13-acetate.* Biosci Biotechnol Biochem, 1999. **63**(6): p. 1017-24.

16. Ueki, I. and M.H. Stipanuk, *Enzymes of the taurine biosynthetic pathway are expressed in rat mammary gland.* J Nutr, 2007. **137**(8): p. 1887-94.

17. Shimada, M., et al., *Expression and localization of cysteine dioxygenase mRNA in the liver, lung, and kidney of the rat.* Amino Acids, 1998. **15**(1-2): p. 143-50.

18. Stipanuk, M.H. and I. Ueki, *Dealing with methionine/homocysteine sulfur: cysteine metabolism to taurine and inorganic sulfur.* J Inherit Metab Dis.

19. Coloso, R.M. and M.H. Stipanuk, *Metabolism of cyst(e)ine in rat enterocytes.* J Nutr, 1989. **119**(12): p. 1914-24.

20. Stipanuk, M.H., et al., *Cysteine dioxygenase: a robust system for regulation of cellular cysteine levels.* Amino Acids, 2009. **37**(1): p. 55-63.

21. van der Flier, L.G. and H. Clevers, *Stem cells, self-renewal, and differentiation in the intestinal epithelium.* Annu Rev Physiol, 2009. **71**: p. 241-60.

22. Wilson, C.L., et al., *The metalloproteinase matrilysin is preferentially expressed by epithelial cells in a tissue-restricted pattern in the mouse.* Mol Biol Cell, 1995. **6**(7): p. 851-69.

23. Barker, N., M. van de Wetering, and H. Clevers, *The intestinal stem cell.* Genes Dev, 2008. **22**(14): p. 1856-64.

24. O'Connor, D.T., D. Burton, and L.J. Deftos, *Chromogranin A: immunohistology reveals its universal occurrence in normal polypeptide hormone producing endocrine glands.* Life Sci, 1983. **33**(17): p. 1657-63.

25. Gum, J.R., Jr., et al., *The human MUC2 intestinal mucin has cysteine-rich subdomains located both upstream and downstream of its central repetitive region.* J Biol Chem, 1992. **267**(30): p. 21375-83.

26. Banerjee, R.R. and M.A. Lazar, *Dimerization of resistin and resistin-like molecules is determined by a single cysteine.* J Biol Chem, 2001. **276**(28): p. 25970-3.

27. Podolsky, D.K., et al., *Identification of human intestinal trefoil factor. Goblet cell-specific expression of a peptide targeted for apical secretion.* J Biol Chem, 1993. **268**(16): p. 12230.

28. Hauser, F., et al., *hP1.B, a human P-domain peptide homologous with rat intestinal trefoil factor, is expressed also in the ulcer-associated cell lineage and the uterus.* Proc Natl Acad Sci U S A, 1993. **90**(15): p. 6961-5.

29. Patil, A., A.L. Hughes, and G. Zhang, *Rapid evolution and diversification of mammalian alpha-defensins as revealed by comparative analysis of rodent and primate genes.* Physiol Genomics, 2004. **20**(1): p. 1-11.

30. Deplancke, B., et al., *Molecular ecological analysis of the succession and diversity of sulfate-reducing bacteria in the mouse gastrointestinal tract.* Appl Environ Microbiol, 2000. **66**(5): p. 2166-74.

31. Stipanuk, M.H., *Sulfur amino acid metabolism: pathways for production and removal of homocysteine and cysteine.* Annu Rev Nutr, 2004. **24**: p. 539-77.

32. Terauchi, A., et al., *Immunohistochemical localization of taurine in various tissues of the mouse.* Amino Acids, 1998. **15**(1-2): p. 151-60.

33. Bouckenooghe, T., C. Remacle, and B. Reusens, *Is taurine a functional nutrient?* Curr Opin Clin Nutr Metab Care, 2006. **9**(6): p. 728-33.

34. Coloso, R.M., et al., *Cysteamine dioxygenase: evidence for the physiological conversion of cysteamine to hypotaurine in rat and mouse tissues.* Adv Exp Med Biol, 2006. **583**: p. 25-36.

FIGURES AND TABLES

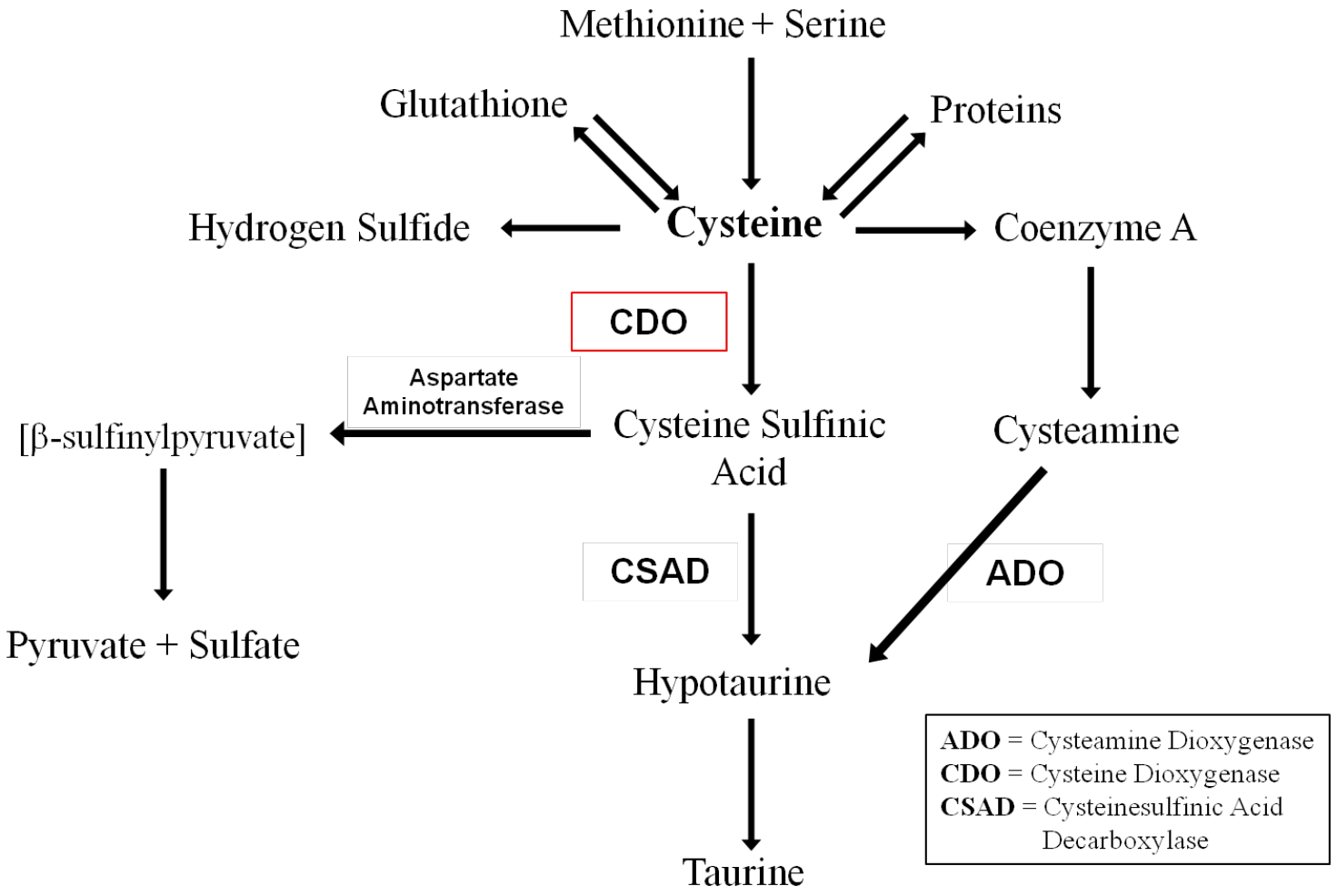

Figure 4.1: Role of CDO in cysteine metabolism and products of cysteine catabolism. Adapted from [1] .

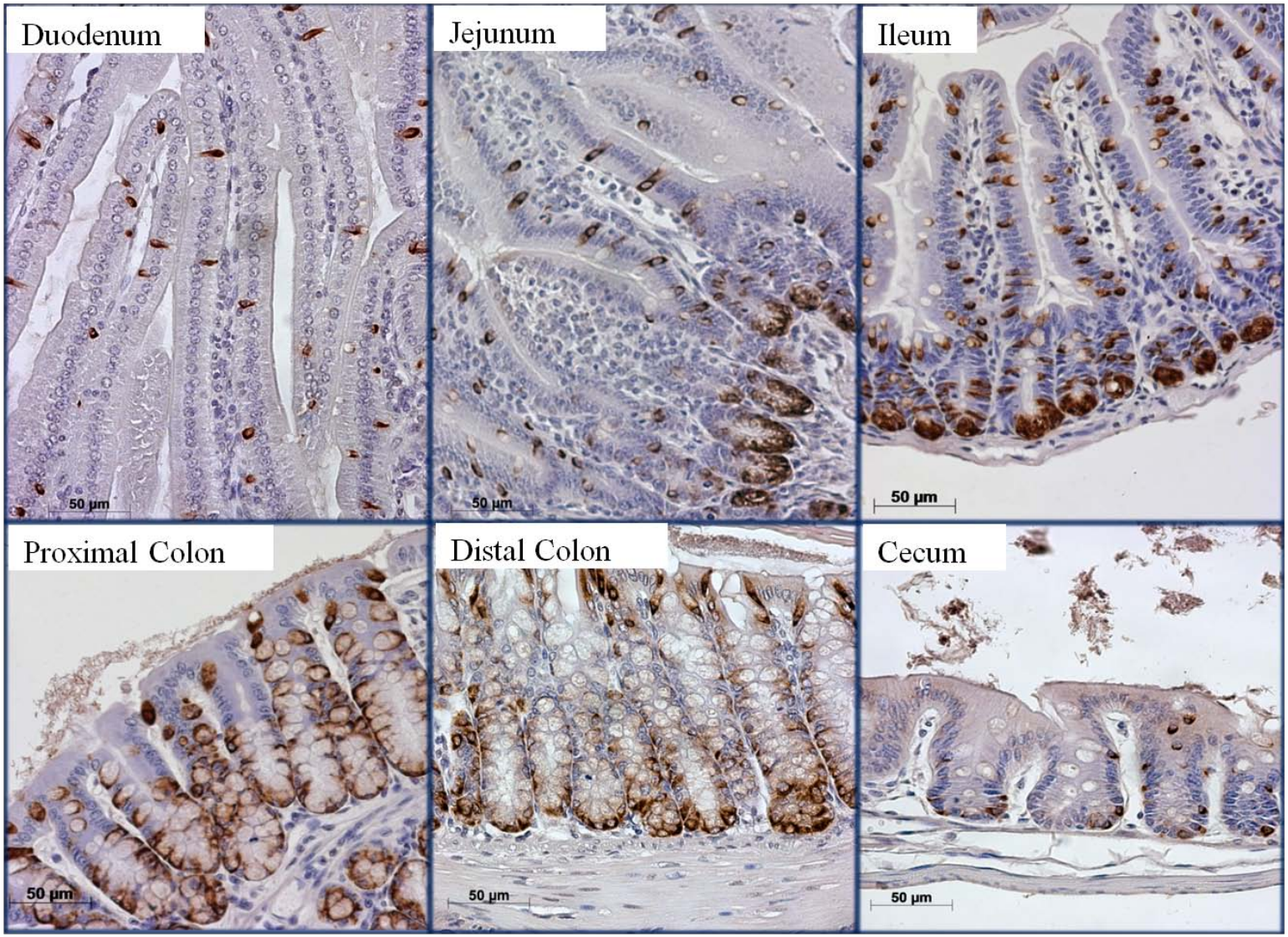

Figure 4.2: CDO immunohistochemical staining in mouse small intestine, colon, and cecum showing positive staining for CDO (brown) in goblet cells and Paneth cells (400X magnification).

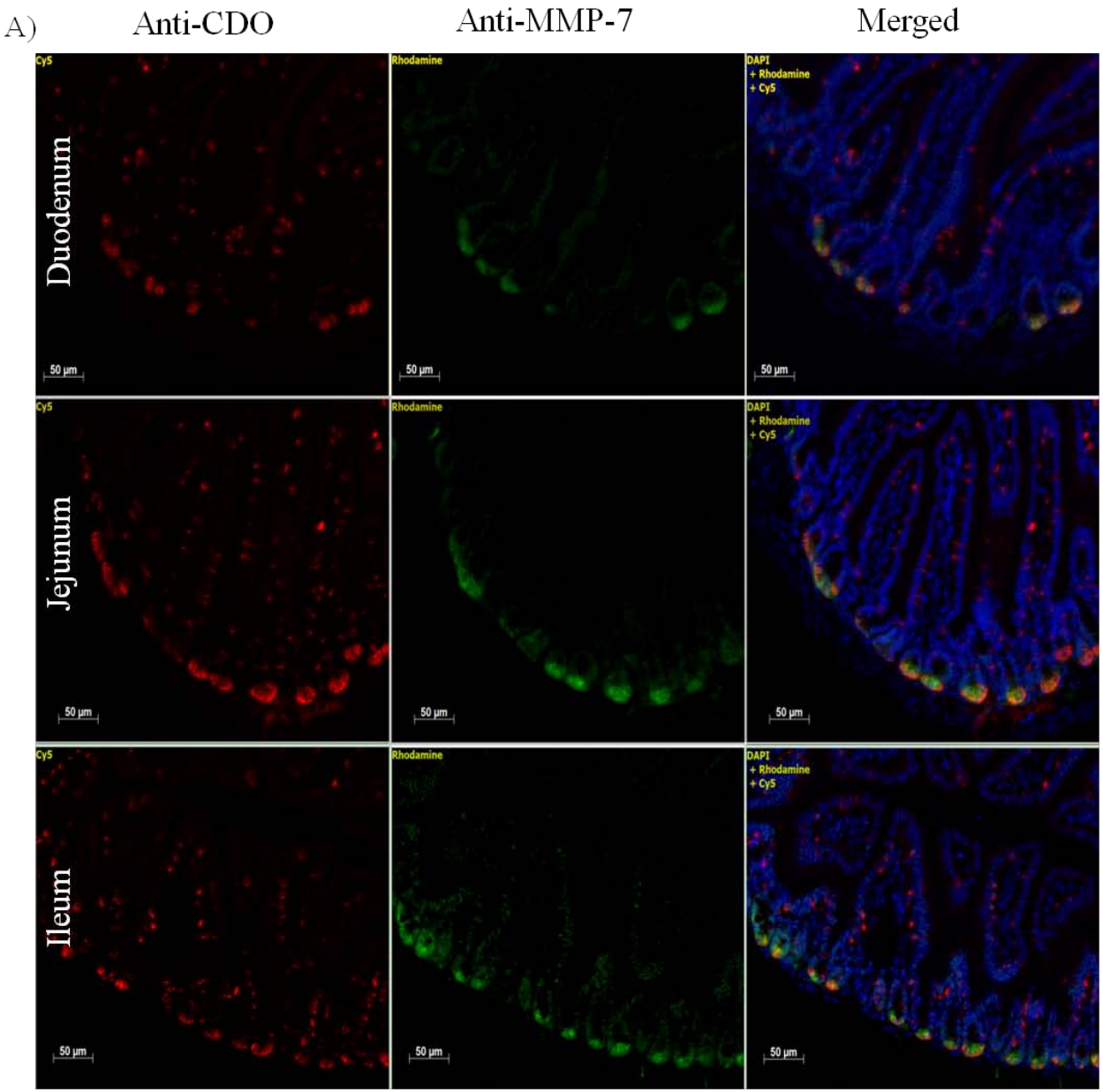

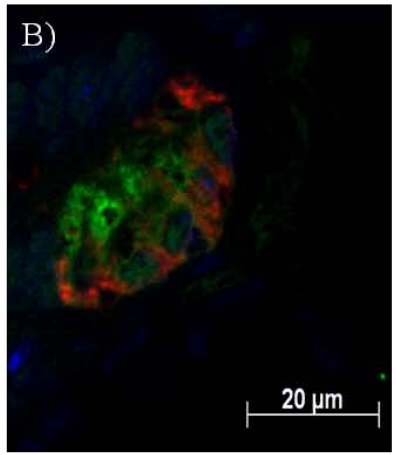

Figure 4.3: CDO (red) and Paneth cell marker MMP-7 (green) immunoreactivity in mouse small intestine. (A) Merged images (20X magnification) show colocalization (yellow) at the crypt base confirming CDO expression in mouse Paneth cells. (B) High magnification (630X) image of CDO and MMP-7 in Paneth cells.

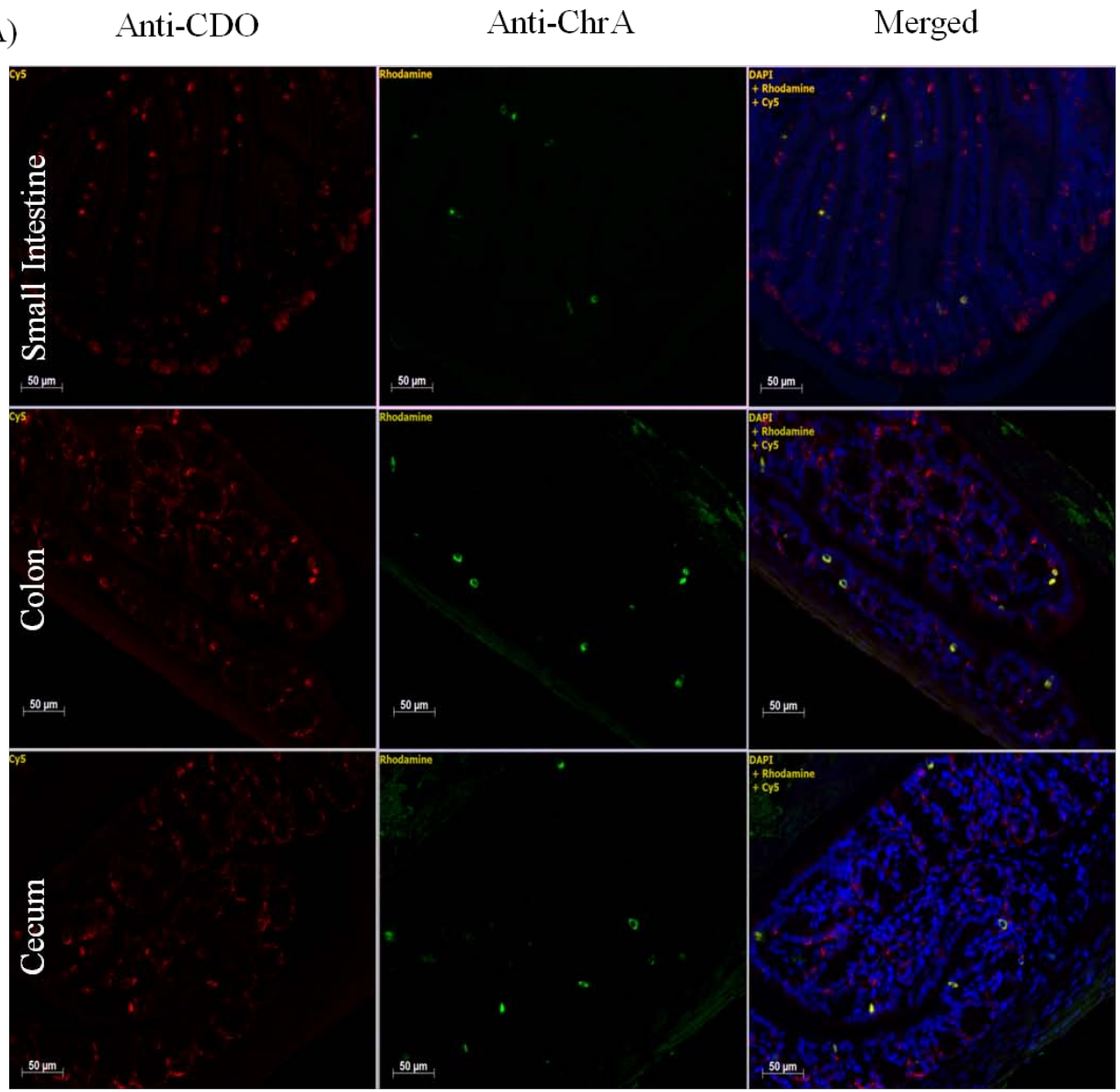

Figure 4.4: CDO (red) and enteroendocrine cell marker ChrA (green) immunoreactivity in mouse small intestine (jejunum), colon (proximal), and cecum. (A) Merged images (20X magnification) show colocalization (yellow) confirming CDO expression in mouse enteroendocrine cells. (B) High magnification (630X) image of CDO and ChrA in an enteroendocrine cell.

Chapter 5

TAURINE BIOSYNTHESIS IN INTESTINAL GOBLET CELLS BY THE CYSTEINE DIOXYGENASE/CYSTEINESULFINATE DECARBOXYLASE AND CYSTEAMINE DIOXYGENASE PATHWAYS

ABSTRACT

Taurine, one of the most abundant amino acids in the body, has a number of important physiological functions, including antioxidant, anti-inflammatory, and osmoregulatory properties. It can be synthesized in mammals by 2 pathways. One pathway involves the oxidation of cysteine via cysteine dioxygenase (CDO) to cysteinesulfinate, which is decarboxylated by cysteinesulfinic acid decarboxylase (CSAD) to hypotaurine. The other pathway involves the conversion of cysteine to Coenzyme A, which releases cysteamine during degradation. Cysteamine is then oxidized to hypotaurine via cysteamine dioxygenase (ADO). In both pathways, hypotaurine is subsequently oxidized to taurine. Taurine has been shown to be beneficial to intestinal function; however, little is known regarding taurine biosynthesis in the intestine. Recent studies have localized the expression of CDO in rodent intestine to goblet cells, suggesting they may be able to synthesize taurine. To determine whether the pathways for taurine biosynthesis are present in intestinal goblet cells, we measured ADO, CDO, and CSAD mRNA as well as hypotaurine and taurine levels in LS174T cells in response to cysteine and cysteamine. In addition, we examined the same end points in response to different inflammatory triggers, namely bacterial flagellin, IL-13, and TNFα to determine whether they might induce taurine biosynthesis. ADO, CDO, and CSAD were all detected at the mRNA level in the LS174T cell line, suggesting that these cells could have the capacity to synthesize taurine via both

pathways. Increased intra- and extracellular hypotaurine and intracellular taurine levels were observed in response to cysteamine treatment, indicating that LS174T cells can synthesize hypotaurine/taurine from cysteamine via the ADO pathway. This was not associated with an increase in ADO mRNA levels. Intracellular taurine was increased in response to cysteine, which suggested taurine synthesis via the CDO/CSAD pathway but needs to be confirmed by additional studies. Flagellin, IL-13, and TNFα treatments differentially upregulated gene expression of taurine biosynthetic enzymes. IL-13 increased intracellular taurine levels but did not increase taurine export at the times and concentrations examined. TNFα appeared to increase hypotaurine and taurine synthesis and export, while flagellin primarily increased taurine and hypotaurine export. Overall, these results demonstrate that LS174T cells synthesize taurine and that taurine synthesis and transport is modulated by certain inflammatory signals.

INTRODUCTION

Taurine (2-aminoethanesulfonate) is one of the most abundant free amino acids present in the body [1, 2]. It can be obtained exogenously from the diet or be synthesized in the body from cysteine [1, 2]. Taurine has a number of cytoprotective properties, including antioxidant, anti-inflammatory, osmoregulatory, and membrane stabilizing effects [1, 2]. Taurine's precursor, hypotaurine, can also serve as an antioxidant [2].

Recent studies have revealed taurine supplementation to be beneficial in rodent models of inflammatory bowel disease due to its anti-inflammatory and antioxidant properties. Taurine supplementation was demonstrated to ameliorate inflammatory parameters in trinitrobenzene sulfonic acid (TNBS)-induced inflammatory bowel disease in rats possibly by decreasing inflammatory reactions, oxidative damage, and apoptosis [3, 4]. Furthermore, use of 5-

aminosalicyltaurine as a colon-specific pro-drug of 5-aminosalicylic acid (5-ASA), which is cleaved into taurine and 5-ASA in cecal contents [5], showed enhanced anti-inflammatory effects compared to 5-ASA alone in TNBS-induced colitis in rats [6], again suggesting an anti-inflammatory role for taurine in the colon. Likewise, taurine supplementation diminished disease severity and inflammatory response in dextran sulfate sodium (DSS)-induced colitis in mice [7, 8]. In vitro studies using human intestinal epithelial Caco-2 cells showed that taurine could inhibit TNFα induced IL-8 secretion and mRNA expression [8]. Taurine is absorbed across the apical membrane in the intestine by two transporters, TauT and PAT1 [9]. TNFα was found to increase taurine uptake by Caco-2 cells, which was associated with an increase in TauT mRNA levels and affinity [10]. Thus, current evidence suggests that taurine is beneficial against inflammation and that intestinal epithelial cells increase taurine uptake in response to inflammatory signals. However, the ability of intestinal epithelial cells to synthesize taurine under normal conditions and in response to inflammation remains unknown.

In mammals, there are two pathways for taurine synthesis (**Figure 5.1**). One is via oxidation of cysteine to cysteinesulfinate (CSA) by cysteine dioxygenase (CDO; EC1.13.11.20), followed by decarboxylation of CSA to hypotaurine by cysteinesulfinic acid decarboxylase (CSAD; EC4.1.1.29), and finally the oxidation of hypotaurine to taurine by a poorly understood mechanism [11]. The other pathway begins with the incorporation of cysteine into Coenzyme A (CoA), followed by the release of cysteamine during CoA degradation, the oxidation of cysteamine to hypotaurine and finally the oxidation of hypotaurine to taurine [12]. CDO is expressed in both a tissue- and cell-specific manner and is especially abundant in the liver, while ADO is expressed more ubiquitously [12-15]. CSAD expression tends to be high in tissues expressing high levels of CDO [14]. There have been no published descriptions of ADO

expression within the small intestine or colon. However, CDO was previously demonstrated to be expressed in mouse small intestine and colon at the protein level and appeared to localize to goblet cells in rat small intestine [14, 16]. In Chapter 4, we showed that CDO localized to goblet cells in mouse small intestine, colon, and cecum, as well as the other two cell types of the secretory lineage, enteroendocrine and Paneth cells. One possible reason for CDO localization to intestinal goblet cells is to allow for taurine biosynthesis. In fact, taurine was demonstrated to localize to mucus granules in goblet cells in mouse intestine [17]. CSAD was also shown to be expressed in mouse colon at the protein level, but was not detected in mouse duodenum [14]. The inability to detect CSAD in mouse duodenum, however, might have been due to the use of whole tissue homogenates of which the secretory lineage would comprise a limited portion in the small intestine.

To understand more about taurine biosynthesis in intestinal goblet cells we examined ADO, CDO, and CSAD mRNA and taurine and hypotaurine levels in response to cysteine and cysteamine in LS174T cells, a human adenocarcinoma cell line which expresses a goblet cell like phenotype. Because of the potential anti-inflammatory role of taurine in the intestine, we also sought to determine whether intestinal goblet cells would be induced to produce more taurine in response to different inflammatory triggers, namely bacterial flagellin, IL-13, and TNFα.

MATERIALS AND METHODS

Reagents. Bathocuproine disulfonic acid (BCS), cysteamine hydrochloride, hypotaurine, glutathione ethyl ester (GSHee), taurine, and 2-aminoethyl hydrogen sulfate (2-AEHS) were purchased from Sigma. L-cysteine free base was purchased from MP Biomedicals. Recombinant

human IL-13 and TNFα were purchased from PeproTech. Recombinant Flagellin from *S. typhimurium* was purchased from InvivoGen.

Cell Culture. The human LS174T colorectal cancer cell line was obtained from the American Type Culture Collection (ATCC). LS174T cells were maintained in Minimum Essential Medium (MEM) supplemented with 10% Fetalplex (Gemini Biosciences), 1.5g/L of Na_2CO_3, 50 units/mL penicillin G and 50 mg/mL streptomycin sulfate at 37°C in 5% CO_2. To examine the effects of cysteine and cysteamine, cells were seeded into 12-well plates at a density of 4 x 10^5 cells/well. After approximately 48 h, cells were washed twice with 1X HBSS and fresh maintenance media containing 40 μM bathocuproine disulfonic acid + 1 mM cysteine or 1 mM cysteamine was added. After 48 h, conditioned media were collected and cells were harvested for RNA isolation. For experiments examining effects of flagellin, IL-13, and TNFα, cells were seeded into 24-well plates at a density of 2 x 10^5 cells/well. After approximately 48 h, cells were washed twice with 1X HBSS and fresh antibiotic-free maintenance media containing different concentrations of flagellin, IL-13, or TNFα were added to the cells. After 24 h, conditioned media were collected and cells were harvested for RNA isolation.

Quantitative RT-PCR. Total RNA was isolated from cells using the RNeasy Plus Kit (Qiagen) according to the manufacturer's instructions for animal cells. The quality and quantity of RNA isolates were determined by Nanodrop (Thermo Fisher Scientific). RNA isolates were reverse transcribed using the High Capacity cDNA Reverse Transcription Kit (Applied Biosystems) according to the manufacturer's instructions. Quantitative real-time PCR was performed using SYBR Green PCR Master Mix (Applied Biosystems) and the primers described in **Table 5.1** and

Table 3.1. Reactions were run in triplicate in a 384-well plate using an Applied Biosystems 7900HT Fast Real-Time PCR System. Final quantifications were performed using the standard curve method with the geometric mean of GAPDH and RPLP0 used for normalization. No reverse transcription reactions were performed to confirm the specificity of the reactions for RNA.

LC/MS/MS Measurement of Cysteine, Cystine, Hypotaurine, and Taurine in Cysteine- and Cysteamine-treated samples. Cysteine, cystine, hypotaurine, and taurine were measured in conditioned media (extracellular) and cellular lysates (intracellular) using LC/MS/MS. Conditioned media was collected mixed with internal standards glutathione ethyl ester (GSHee) and 2-aminoethyl hydrogen sulfate (2-AEHS) and diluted into 5 mM iodoacetic acid (IAA) in 5 mM ammonium bicarbonate. After collection of conditioned media, cells were washed once in 1X HBSS, harvested using 1X trypsin/EDTA, and washed in 1X PBS. Cells were resuspended in 10 mM IAA in 10 mM ammonium bicarbonate and were lysed by 3 cycles of freezing and-thawing. Lysates were centrifuged at 13,000 rpm for 2 min. The supernatant fraction was collected, mixed with internal standards GSHee and 2-AEHS, and diluted for a final IAA concentration of 5 mM. Reactions with IAA were allowed to proceed for 15 minutes at room temperature. Samples were stored at -80^{o}C until analyzed using an ABI 5500 QTrap MS with Agilent 1200 LC. Values for cysteine, cystine, hypotaurine, and taurine were calculated using external calibration. The total protein content of the cellular lysates was measured using the Reducing Agent Compatible BCA Protein Assay kit (Pierce). Intracellular values for cysteine, cystine, hypotaurine, and taurine were normalized to lysate protein concentration.

LC/MS/MS Measurement of Hypotaurine and Taurine in Flagellin-, IL-13-, and TNFα–treated samples. Hypotaurine, and taurine were measured in conditioned media (extracellular) and cellular lysates (intracellular) using LC/MS/MS. Conditioned media were collected, mixed with internal standard 2-AEHS and diluted into nanopure water. After collection of conditioned media, cells were washed once in 1X HBSS, harvested using 1X trypsin/EDTA, and washed in 1X PBS. Cells were resuspended in nanopure water and were lysed by 3 cycles of freezing and-thawing. Lysates were centrifuged at 13,000 rpm for 2 min. The supernatant fraction was collected, mixed with 2-AEHS, and diluted with nanopure water to match volumes of hypotaurine and taurine standards and conditioned media samples. Samples were stored at -80^{o}C until analyzed using an ABI 5500 QTrap MS with Agilent 1200 LC. Values for hypotaurine and taurine were calculated using external calibration. The total protein content of the cellular lysates was measured using the Reducing Agent Compatible BCA Protein Assay kit (Pierce). Intracellular values for hypotaurine and taurine were normalized to lysate protein concentration.

Statistical Analysis. ANOVA and Fisher's protected least significant difference test (FLSD test) were used to compare differences. These analyses were carried out using SAS software (Statview, Version 5.0.1; SAS Institute, Cary, NC). Differences were considered significant at $p < 0.05$.

RESULTS

Expression of ADO, CDO, and CSAD in LS174T Cells and Validation of Primers for Quantitative RT-PCR. Primers for *ADO, CDO,* and *CSAD* produced a single amplicon (**Figure 5.2A**) of expected size (**Table 5.1**) by conventional RT-PCR and a single peak upon dissociation

curve analysis following quantitative RT-PCR (**Figures 5.2B**). These results confirmed the expression of ADO, CDO and CSAD at the mRNA level in LS174T cells. Quantitative RT-PCR also revealed *CDO* expression to be much lower in LS174T cells than in human liver RNA (data not shown). Primers for *CSAD* were found to produce multiple bands when used with human liver RNA (data not shown).

ADO, CDO, and CSAD Expression in Response to Cysteine and Cysteamine. Changes in ADO, CDO, and CSAD were examined at the mRNA level using quantitative RT-PCR to determine whether there were any transcriptional changes in response to cysteine or cysteamine treatment. Expression of *ADO* was found to be slightly decreased by cysteamine, but unaltered by cysteine (**Figure 5.3**). *CSAD* gene expression remained unchanged by cysteamine or cysteine, and *CDO* expression was only minimally downregulated by cysteine.

MUC2, RETNLB, and TFF3 Expression in Response to Cysteine and Cysteamine. Quantitative RT-PCR for *MUC2, RETNLB,* and *TFF3* was performed to determine whether treatment of LS174T with cysteine and cysteamine affected transcription of the cysteine-rich goblet cell secretory products. As shown in **Figure 5.4**, there was no change in *MUC2* or *TFF3* expression in response to cysteine or cysteamine, but *RETNLB* expression was increased approximately 2-fold in response to cysteamine.

Hypotaurine/Taurine Biosynthesis in LS174T Cells from Cysteamine and Cysteine. Hypotaurine is formed as a product of cysteine catabolism by CDO plus CSAD or as a product of cysteamine catabolism by ADO. Hypotaurine is further oxidized to taurine by a still unknown mechanism.

Hypotaurine and taurine can be transported out of cells, so to assess the ability of LS174T cells to synthesize hypotaurine and taurine from cysteamine and cysteine, we measured both intracellular and extracellular levels using LC/MS/MS. We also measured intracellular cysteine and cystine. Two independent experiments were performed. However, in the case of cysteine, levels were found to be nearly 5X higher in the second experiment compared to the first experiment (**Figure 5.5A** and **B**). Consequently, the two experiments were analyzed separately and it was observed in each that intracellular cysteine concentrations were increased in cells grown in media with 1 mmol/L cysteine added. Values for intracellular cystine were relatively similar between experiments and, when analyzed together, cystine was observed to be more than 5 times greater in cells grown with added cysteine (**Figure 5.5C**). Both intracellular and extracellular hypotaurine levels were significantly increased in response to addition of cysteamine to the media, but remained unchanged with cysteine (**Figure 5.6**). A moderate increase in intracellular taurine levels occurred in response to both cysteamine and cysteine, but extracelluar taurine was unaltered by cysteamine and somewhat decreased by cysteine.

Hypotaurine/Taurine Biosynthesis in Response to Flagellin, IL-13, and TNFα. To determine whether inflammatory signals might stimulate goblet cells to increase taurine biosynthesis, changes in ADO, CDO, and CSAD expression at the mRNA level and intra- and extracellular hypotaurine and taurine were measured in response to treatment with flagellin, IL-13, and *TNFα* for 24 h. Exposure to flagellin led to a slight increase in *ADO* expression at 500 ng/mL and about a 3.5-fold increase in *CSAD* expression at 1000 ng/mL (**Figure 5.7**). Expression of *CDO* was not significantly changed by treatment with flagellin. Intra- and extracellular hypotaurine and taurine levels were only examined in response to 500 ng/mL and 1000 ng/mL concentrations of flagellin

since only those concentrations seemed to modulate gene expression and had been previously shown to induce IL-8 secretion from LS174T cells (see Chapter 3). Intracellular hypotaurine and taurine were decreased in response to 1000 ng/mL of flagellin (**Figures 5.8A and 5.9A**), but extracellular levels of hypotaurine and taurine were elevated (**Figures 5.8B and 5.9B**). The increases in extracellular hypotaurine and taurine following exposure to 1000 ng/mL of flagellin for 24 h are consistent with a previous experiment (data not shown). IL-13 enhanced expression of *ADO*, *CSAD*, and *CDO*, with *CSAD* expression being the most affected of the three in terms of relative fold change (**Figure 5.7**). Because 5 ng/mL and 10 ng/mL of IL-13 seemed to have the greatest influence on *CSAD* and *CDO* expression, these concentrations were used to analyze hypotaurine and taurine biosynthesis in response to IL-13. Intracellular taurine concentrations were higher with 5 ng/mL of IL-13, but intracellular hypotaurine was unchanged with either concentration (**Figures 5.8A and 5.9A**). Both extracellular hypotaurine and taurine appeared to be slightly elevated in response to IL-13, but this did not reach statistical significance (**Figures 5.8B and 5.9B**). However, in a previous study, IL-13 treatment at concentrations of 5 ng/mL and 10 ng/mL resulted in statistically significant increases in extracellular hypotaurine and taurine. TNFα produced a less than 2-fold increase in *ADO* expression and a 2 to 2.5-fold increase in *CDO* expression (**Figure 5.7**). Of the three taurine biosynthetic enzymes, expression of *CSAD* was most affected by TNFα being increased more than 3-fold. Intracellular hypotaurine and taurine were not changed by TNFα (**Figures 5.8A and 5.9A**), while extracellular hypotaurine and taurine were both increased with 10-1000 ng/mL of TNFα (**Figures 5.8B and 5.9B**). Increased extracellular hypotaurine with 1000 ng/mL of TNFα and taurine with 100-1000 ng/mL of TNFα were also observed in previous experiment (data not shown).

DISCUSSION

Recent *in vivo* and *in vitro* studies indicate taurine can help attenuate inflammation associated with inflammatory bowel disease [3, 4, 6-8, 10]. These studies have focused on exogenous provision of taurine, but our recent finding that CDO is expressed in the secretory lineage of mouse small intestine and colon suggests that intestinal epithelial cells may have the capacity to synthesize taurine. In this study we focused on intestinal goblet cells, using the human adenocarcinoma LS174T cell line, which expresses a goblet cell-like phenotype. We observed that this cell line expresses ADO, CDO, and CSAD at the mRNA level, indicating that these cells may be able to synthesize taurine via both the CDO/CSAD and the ADO pathway. The increase in intra- and extracellular hypotaurine and intracellular taurine in response to cysteamine confirmed that LS174T cells are capable of synthesizing hypotaurine/taurine via the ADO pathway. This was not associated with an increase in ADO mRNA levels, consistent with studies conducted in adipocytes where ADO mRNA and protein levels were also unchanged in response to cysteamine [18]. Thus, the increased hypotaurine production was likely due to increased substrate for ADO. The incomplete oxidation of hypotaurine to taurine may indicate that the cells have limited capacity to oxidize hypotaurine to taurine.

Intracellular taurine was increased in response to cysteine, but intra- and extracellular hypotaurine were unaltered and extracellular taurine was decreased. The increase in intracellular taurine could have resulted from increased synthesis via the CDO/CSAD pathway. The increased intraceullar taurine in response to cysteine was not associated with an increase in ADO, CDO, or CSAD mRNA expression. The unresponsiveness of ADO and CSAD to cysteine at the mRNA level was expected based on previous studies [12, 18, 19]. CDO is not typically regulated in response to cysteine at the mRNA level or protein level in non-hepatic tissues, with the apparent

exception of adipose tissue [18, 19]. In liver, CDO is also not regulated at the mRNA level, but protein abundance increases in response to cysteine. Thus, additional studies should be done to determine whether CDO protein abundance is increased in LS174T cells in response to cysteine. This additional data plus confirmation of CSAD expression at the protein level would help validate that cysteine is increasing intracellular taurine via the CDO/CSAD pathway. Alternatively, since extracellular taurine levels were decreased in response to cysteine, intracellular taurine levels may have been elevated due to taurine transport into the cells rather than additional synthesis. Perhaps the elevated intracellular cysteine and cystine levels observed with addition of 1 mmol/L of cysteine altered the intracellular redox potential, stimulating cells to take up extracellular taurine in order to maintain redox homeostasis.

Because of taurine's reported anti-inflammatory effects, we examined whether selected inflammatory stimuli, namely flagellin, IL-13, and TNFα, could induce taurine biosynthesis in LS174T cells and alter ADO, CDO, and CSAD abundance at the mRNA level. Flagellin upregulated *CSAD* expression, indicating possible stimulation of taurine biosynthesis via the CDO/CSAD pathway. However, the decreased intracellular hypotaurine and taurine levels and increased extracellular levels of hypotaurine and taurine following treatment with flagellin, suggest that hypotaurine and taurine are exported from cells in response to flagellin before or faster than additional hypotaurine and taurine can be synthesized. The upregulation of *ADO*, *CDO*, and *CSAD* expression and increase in intracellular taurine by IL-13 treatments indicates that cells may increase taurine biosynthesis via both taurine biosynthetic pathways. TNFα similarly increased *ADO*, *CDO*, and *CSAD* expression, but since a greater fold change was observed with *CDO* and *CSAD* than *ADO*, the *CSAD*/*CDO* pathway may play a more significant role in taurine biosynthesis in response to TNFα. Thus, TNFα likely induces cells to synthesize

and export hypotaurine/taurine. Contrary to our findings, another study examined the effects of TNFα and TGFβ on CDO expression in human neuronal and hepatic cell lines and observed a decrease in CDO expression [20]. This could indicate that responses of taurine biosynthetic enzymes to cytokines are cell type-specific.

Overall our results indicate that IL-13 and TNFα increase hypotaurine/taurine biosynthesis in part by increased gene expression of taurine biosynthetic enzymes and that both flagellin and TNFα stimulate cells to export hypotaurine/taurine extracellularly. Additional studies should be conducted to determine whether extended treatment with IL-13 also results in export of hypotaurine and taurine and whether extended treatments with flagellin and TNFα eventually lead to increased intracellular hypotaurine and taurine. Since CDO is primarily regulated at the protein level in liver, it would be interesting to determine whether the inflammatory stimuli found to increase *CDO* gene expression in this study also increase CDO protein abundance.

It is interesting that the LS174T cell line appears to export taurine in response to two inflammatory stimuli, flagellin and TNFα, rather than taking up taurine as had been observed in Caco-2 cells in response to TNFα and IL-1β [10]. The phenotype of Caco-2 cells is more similar to that of an enterocyte while the phenotype of LS174T cells is more similar to that of a goblet cell. Thus, the observed difference in taurine transport between these cell lines may reflect differences in taurine handling between enterocytes and goblet cells. This would be consistent with our observation of CDO being expressed in goblet cells but not enterocytes. Since Paneth cells and enteroendocrine cells were also observed to express CDO in mouse, it would be interesting to see whether these two secretory cell types respond similarly to goblet cells when treated with inflammatory stimuli.

Taurine synthesized and exported from intestinal goblet cell in response to inflammation may provide an endogenous source of taurine for enterocytes to use to counteract inflammation as well as a source of taurine to react with hypochlorous acid, which is produced by myeloperoxidase in activated leukocytes, and forms taurine chloramines [21]. Taurine chloramine exhibits strong anti-inflammatory activity by downregulating nuclear factor-κb (NF-κB) activity and proinflammatory products including prostaglandins, nitric oxide, and cytokines [22, 23]. This is considered to be the major mechanism by which taurine potentiates the effect of 5-ASA in TNBS-induced colitis [24]. Further studies should be conducted to determine whether goblet cells provide taurine for use by other cells in situ.

In summary, we demonstrated that the LS174T cell line expresses ADO, CDO, and CSAD at the mRNA level. LS174T cells were able to synthesize hypotaurine/taurine via the ADO pathway starting with cysteamine and possibly the CDO/CSAD pathway starting with cysteine. However, additional studies are required to confirm the use of the CDO/CSAD pathway. Flagellin, IL-13, and TNFα can induce taurine biosynthesis and/or export from LS174T cells, and increased taurine biosynthesis appears to involve enhanced expression of genes encoding taurine biosynthetic enzymes in response to these inflammatory stimuli.

REFERENCES

1. Sturman, J.A., *Taurine in development.* Physiol Rev, 1993. **73**(1): p. 119-47.

2. Huxtable, R.J., *Physiological actions of taurine.* Physiol Rev, 1992. **72**(1): p. 101-63.

3. Son, M.W., et al., *Protective effect of taurine on TNBS-induced inflammatory bowel disease in rats.* Arch Pharm Res, 1998. **21**(5): p. 531-6.

4. Giris, M., et al., *Effect of taurine on oxidative stress and apoptosis-related protein expression in trinitrobenzene sulphonic acid-induced colitis.* Clin Exp Immunol, 2008. **152**(1): p. 102-10.

5. Jung, Y.J., et al., *Synthesis and properties of 5-aminosalicyl-taurine as a colon-specific prodrug of 5-aminosalicylic acid.* Arch Pharm Res, 2003. **26**(4): p. 264-9.

6. Jung, Y., et al., *Evaluation of 5-aminosalicyltaurine as a colon-specific prodrug of 5-aminosalicylic acid for treatment of experimental colitis.* Eur J Pharm Sci, 2006. **28**(1-2): p. 26-33.

7. Shimizu, M., et al., *Dietary taurine attenuates dextran sulfate sodium (DSS)-induced experimental colitis in mice.* Adv Exp Med Biol, 2009. **643**: p. 265-71.

8. Zhao, Z., et al., *Attenuation by dietary taurine of dextran sulfate sodium-induced colitis in mice and of THP-1-induced damage to intestinal Caco-2 cell monolayers.* Amino Acids, 2008. **35**(1): p. 217-24.

9. Anderson, C.M., et al., *Taurine uptake across the human intestinal brush-border membrane is via two transporters: H+-coupled PAT1 (SLC36A1) and Na+- and Cl(-)-dependent TauT (SLC6A6).* J Physiol, 2009. **587**(Pt 4): p. 731-44.

10. Mochizuki, T., H. Satsu, and M. Shimizu, *Tumor necrosis factor alpha stimulates taurine uptake and transporter gene expression in human intestinal Caco-2 cells.* FEBS Lett, 2002. **517**(1-3): p. 92-6.

11. Stipanuk, M.H., *Sulfur amino acid metabolism: pathways for production and removal of homocysteine and cysteine.* Annu Rev Nutr, 2004. **24**: p. 539-77.

12. Coloso, R.M., et al., *Cysteamine dioxygenase: evidence for the physiological conversion of cysteamine to hypotaurine in rat and mouse tissues.* Adv Exp Med Biol, 2006. **583**: p. 25-36.

13. Dominy, J.E., Jr., et al., *Discovery and characterization of a second mammalian thiol dioxygenase, cysteamine dioxygenase.* J Biol Chem, 2007. **282**(35): p. 25189-98.

14. Stipanuk, M.H. and I. Ueki, *Dealing with methionine/homocysteine sulfur: cysteine metabolism to taurine and inorganic sulfur.* J Inherit Metab Dis.

15. Hirschberger, L.L., et al., *Murine cysteine dioxygenase gene: structural organization, tissue-specific expression and promoter identification.* Gene, 2001. **277**(1-2): p. 153-61.

16. Stipanuk, M.H., et al., *Cysteine dioxygenase: a robust system for regulation of cellular cysteine levels.* Amino Acids, 2009. **37**(1): p. 55-63.

17. Terauchi, A., et al., *Immunohistochemical localization of taurine in various tissues of the mouse.* Amino Acids, 1998. **15**(1-2): p. 151-60.

18. Ueki, I. and M.H. Stipanuk, *3T3-L1 adipocytes and rat adipose tissue have a high capacity for taurine synthesis by the cysteine dioxygenase/cysteinesulfinate decarboxylase and cysteamine dioxygenase pathways.* J Nutr, 2009. **139**(2): p. 207-14.

19. Stipanuk, M.H., et al., *Enzymes and metabolites of cysteine metabolism in nonhepatic tissues of rats show little response to changes in dietary protein or sulfur amino acid levels.* J Nutr, 2002. **132**(11): p. 3369-78.

20. Wilkinson, L.J. and R.H. Waring, *Cysteine dioxygenase: modulation of expression in human cell lines by cytokines and control of sulphate production.* Toxicol In Vitro, 2002. **16**(4): p. 481-3.

21. Schuller-Levis, G., et al., *Taurine protects against oxidant-induced lung injury: possible mechanism(s) of action.* Adv Exp Med Biol, 1994. **359**: p. 31-9.

22. Barua, M., Y. Liu, and M.R. Quinn, *Taurine chloramine inhibits inducible nitric oxide synthase and TNF-alpha gene expression in activated alveolar macrophages: decreased NF-kappaB activation and IkappaB kinase activity.* J Immunol, 2001. **167**(4): p. 2275-81.

23. Schuller-Levis, G.B. and E. Park, *Taurine and its chloramine: modulators of immunity.* Neurochem Res, 2004. **29**(1): p. 117-26.

24. Kim, H., et al., *A molecular mechanism for the anti-inflammatory effect of taurine-conjugated 5-aminosalicylic acid in inflamed colon.* Mol Pharmacol, 2006. **69**(4): p. 1405-12.

25. Dominy, J.E., Jr., et al., *Regulation of cysteine dioxygenase degradation is mediated by intracellular cysteine levels and the ubiquitin-26 S proteasome system in the living rat.* Biochem J, 2006. **394**(Pt 1): p. 267-73.

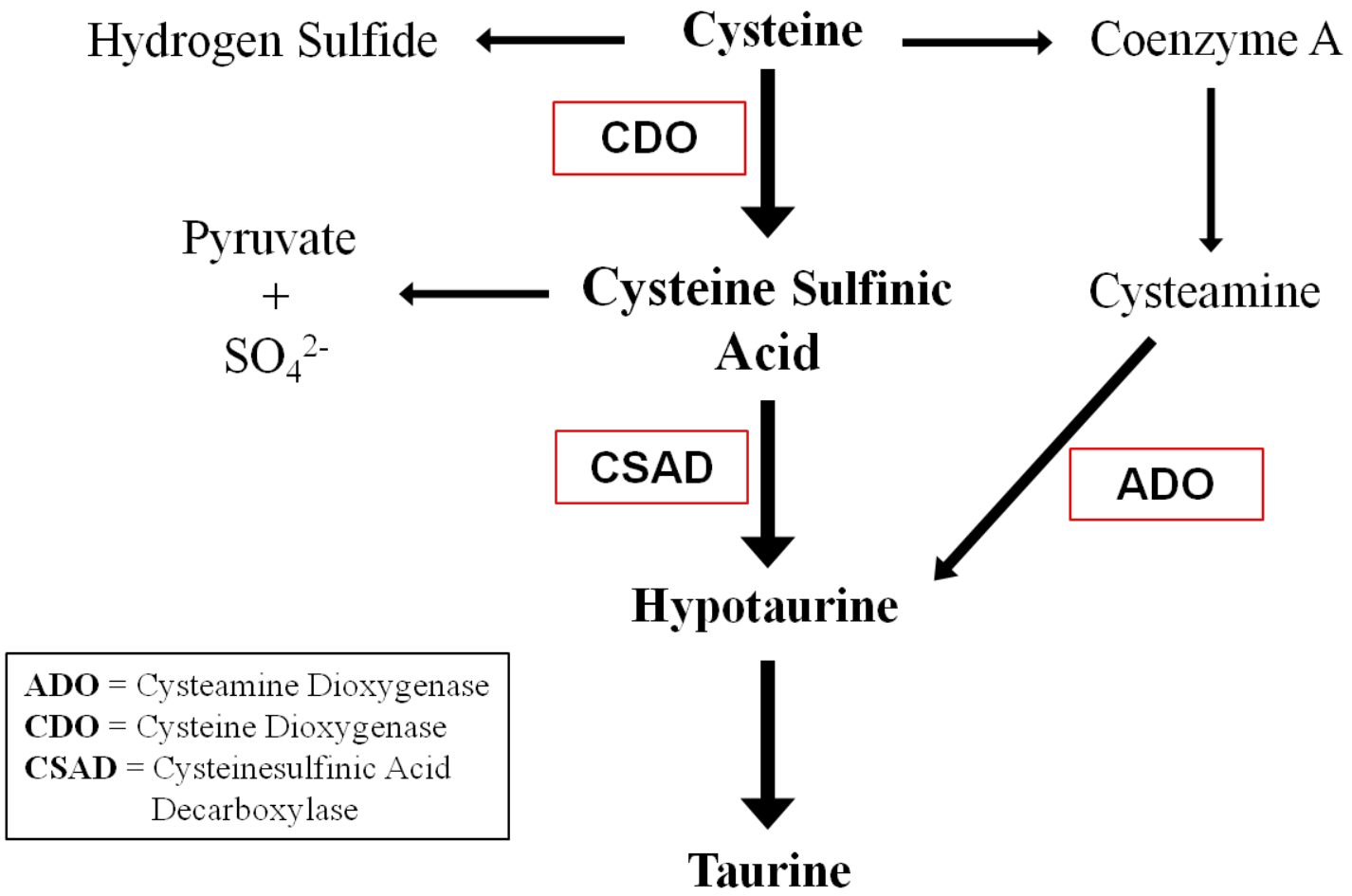

Figure 5.1: Taurine biosynthetic pathways and important enzymes. There are two pathways in mammals that can be used for taurine biosynthesis starting from cysteine: (1) Taurine can be synthesized using the CDO/CSAD pathway or (2) via the ADO pathway. Figure adapted from [25].

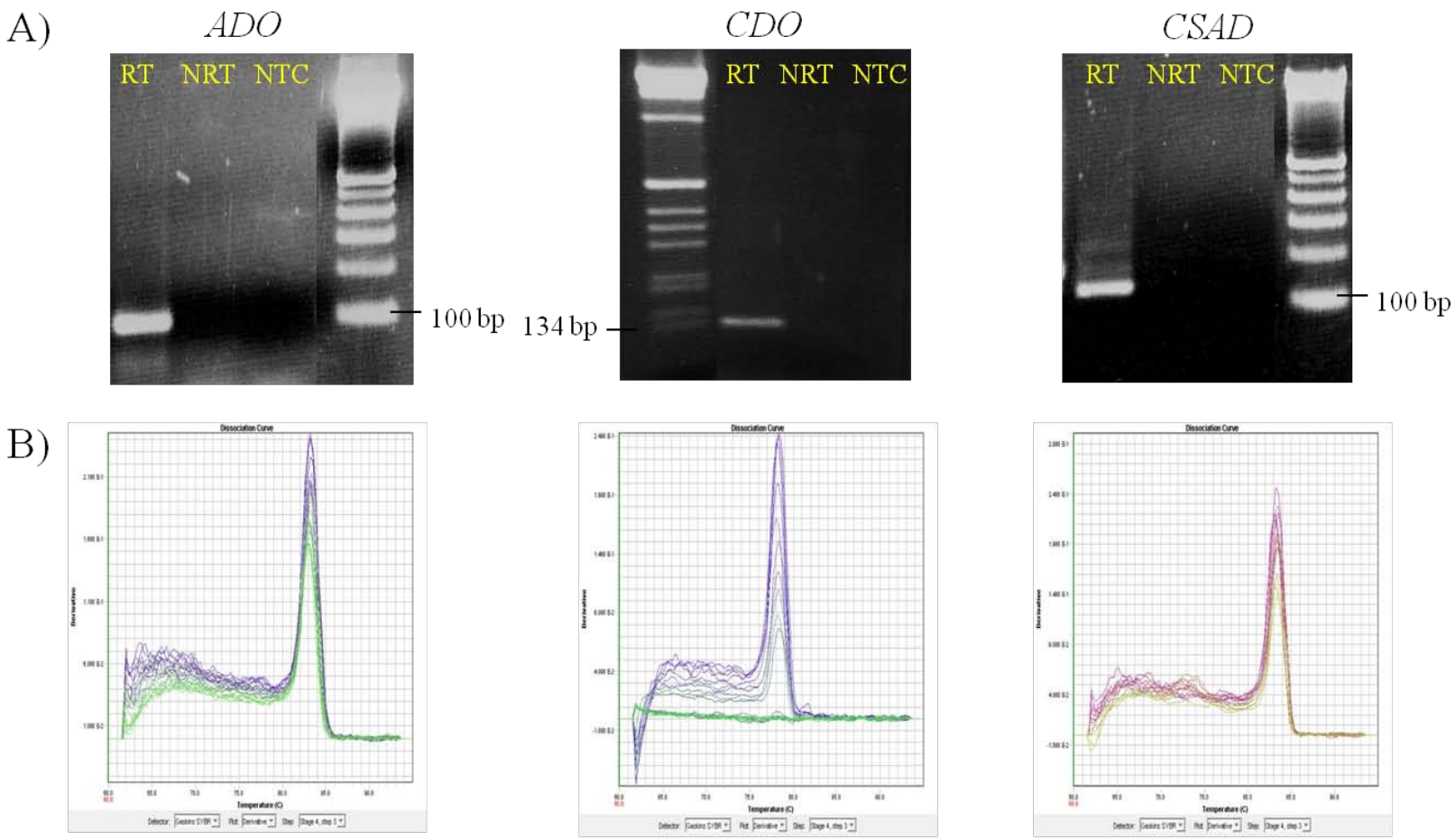

Figure 5.2: Validation of *ADO CDO,* and *CSAD* primers. **A)** RT-PCR products for *ADO, CDO,* and CSAD using cDNA from LS174T cells. Total RNA was isolated from the cells and cDNA was prepared with and without reverse transcriptase (RT). Wells containing the reverse transcribed LS174T RNA are labeled with RT and wells containing LS174T RNA that was not reverse transcribed are labeled NRT. NTC = No template control. **B)** Dissociation curve analysis following SYBR Green quantitative RT-PCR for each gene.

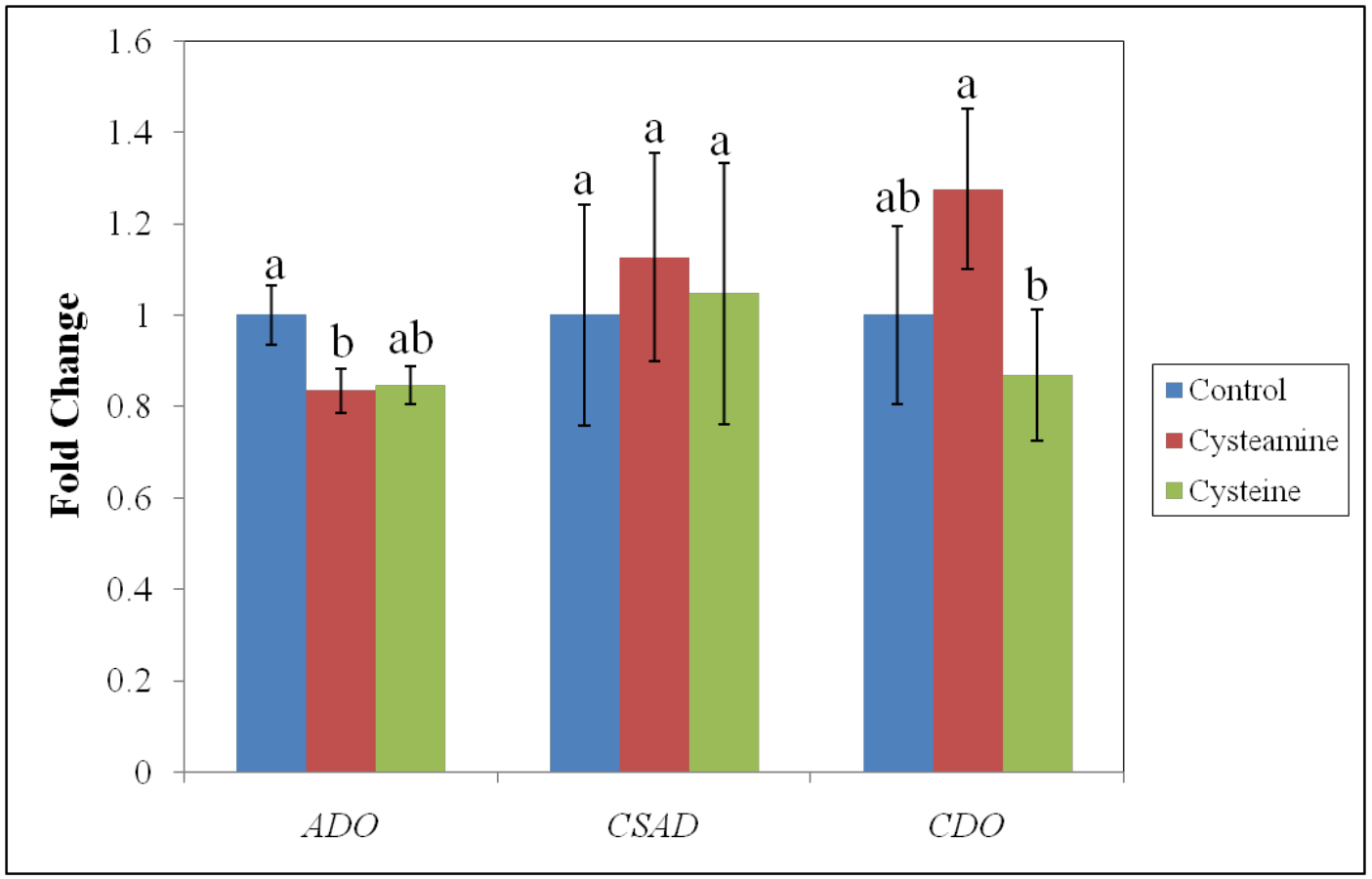

Figure 5.3: Relative expression (setting controls as 1) of taurine biosynthetic enzyme genes *ADO, CSAD,* and *CDO* in LS174T cells treated for 48 h with cysteamine or cysteine. The data represent means ± SEM (n=4); statistical differences are indicated by different letters ($p < 0.05$).

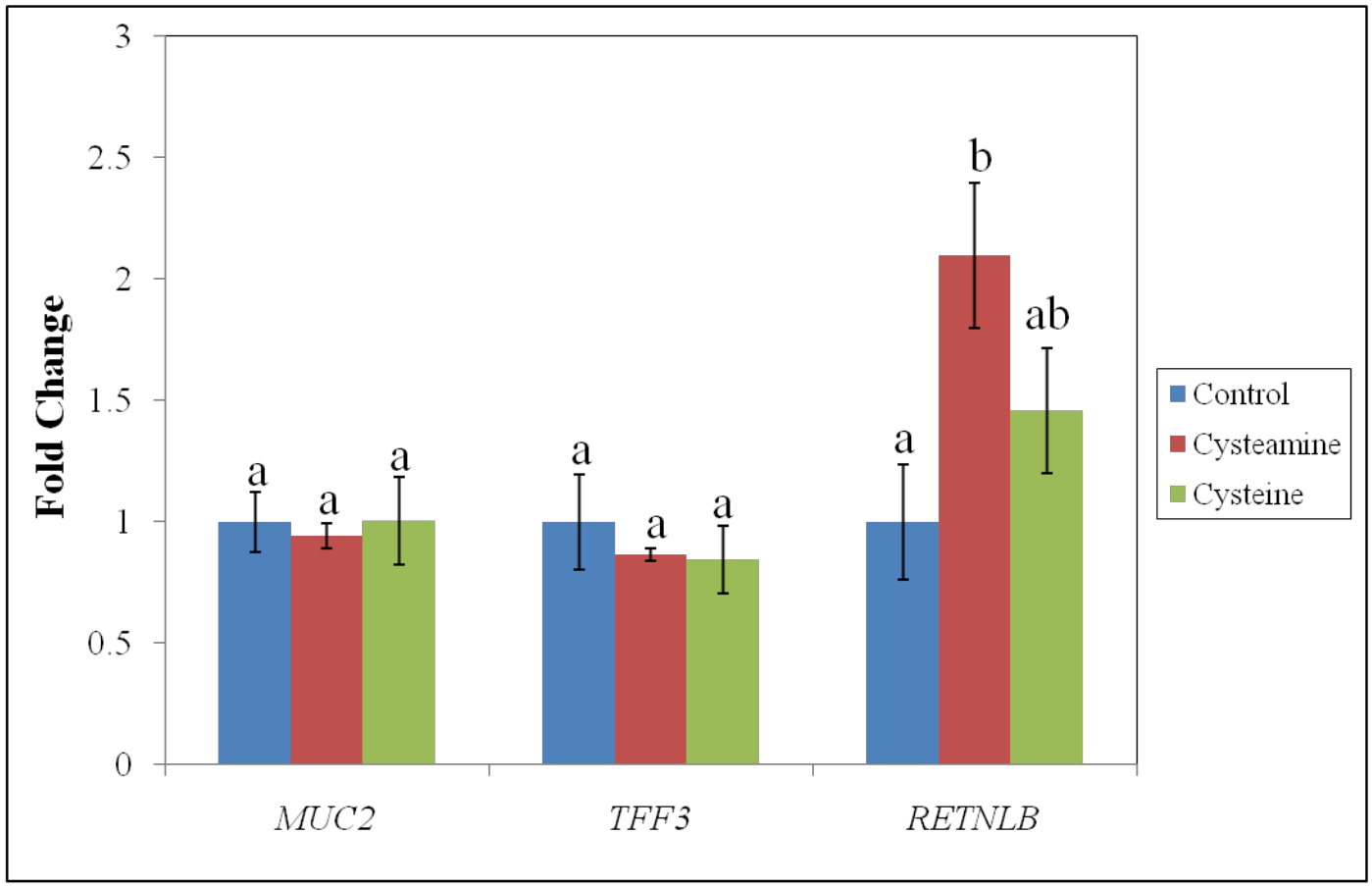

Figure 5.4: Relative expression (setting controls as 1) of goblet cell secretory product genes *MUC2, TFF3,* and *RETNLB* in LS174T cells treated for 48 h with cysteamine or cysteine. The data represent means ± SEM (n=4); statistical differences are indicated by different letters ($p < 0.05$).

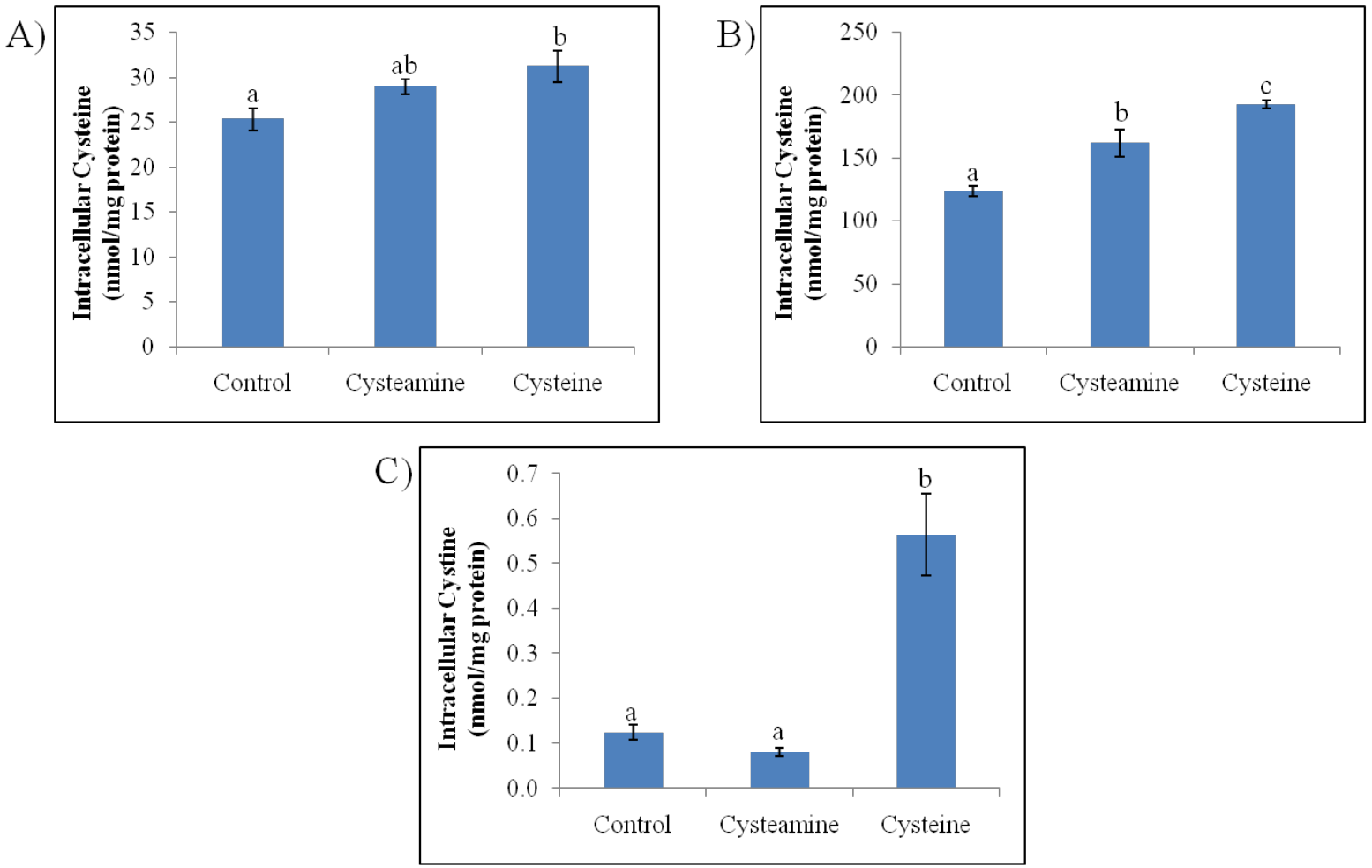

Figure 5.5: Intracellular cysteine and cystine levels in LS174T cells treated for 48 h with 1 mmol/L cysteamine, 1 mmol/L cysteine, or maintained in basal media (control). Two independent experiments were performed. Intracellular cysteine values for the first experiment are presented in **A**. Intracellular cysteine values for the second experiment are presented in **B**. Intracellular cystine values from the combined experiments are presented in **C**. The data represent means ± SEM (n=4 for cysteine and n=8 for cystine); statistical differences are indicated by different letters ($p < 0.05$).

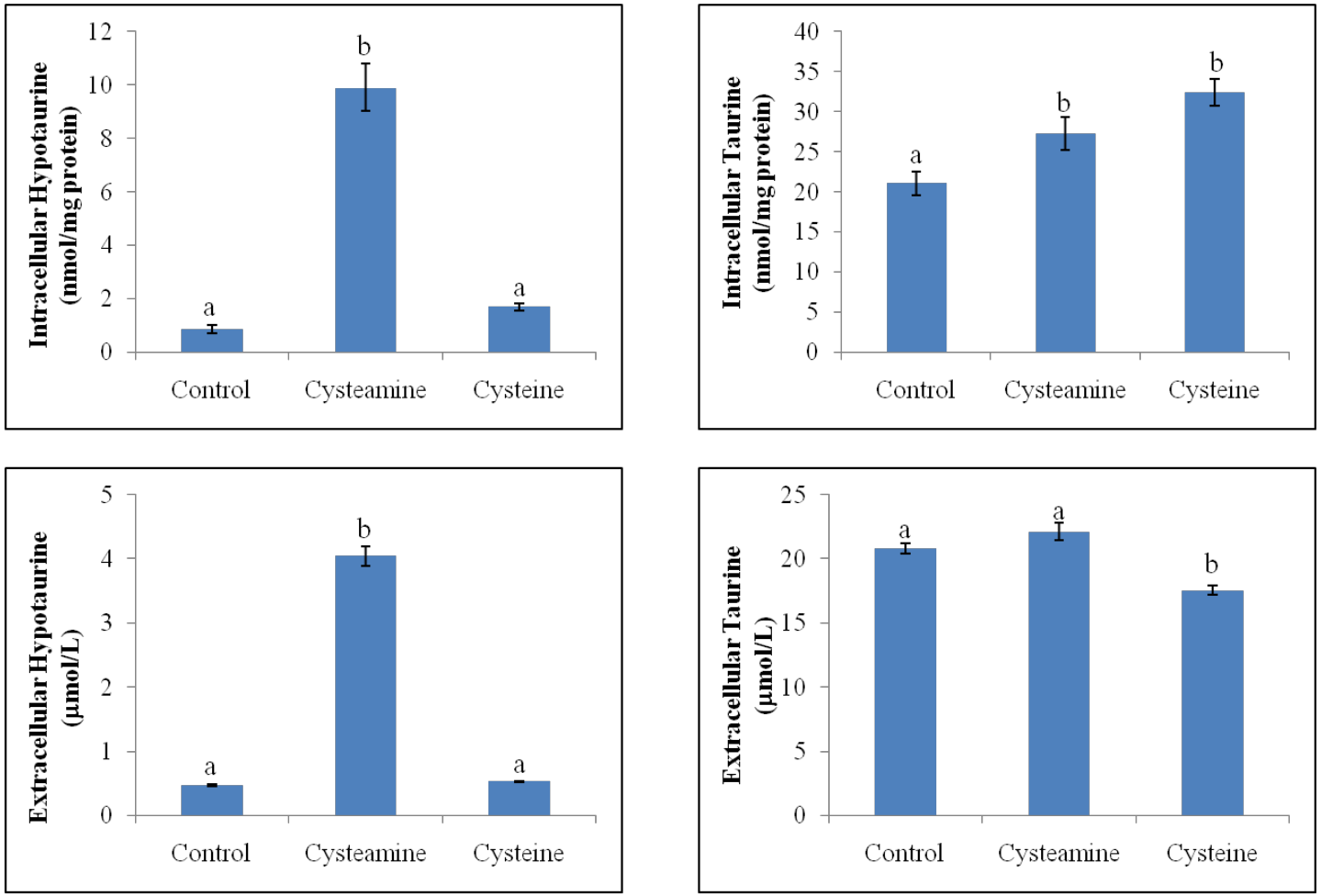

Figure 5.6: Intracellular and extracellular hypotaurine and taurine levels in LS174T cells treated for 48 h with 1 mmol/L cysteamine, 1 mmol/L cysteine, or maintained in basal media (control). Two independent experiments were performed with 4 replicates each. The data represent means ± SEM (n=8); statistical differences are indicated by different letters ($p < 0.05$).

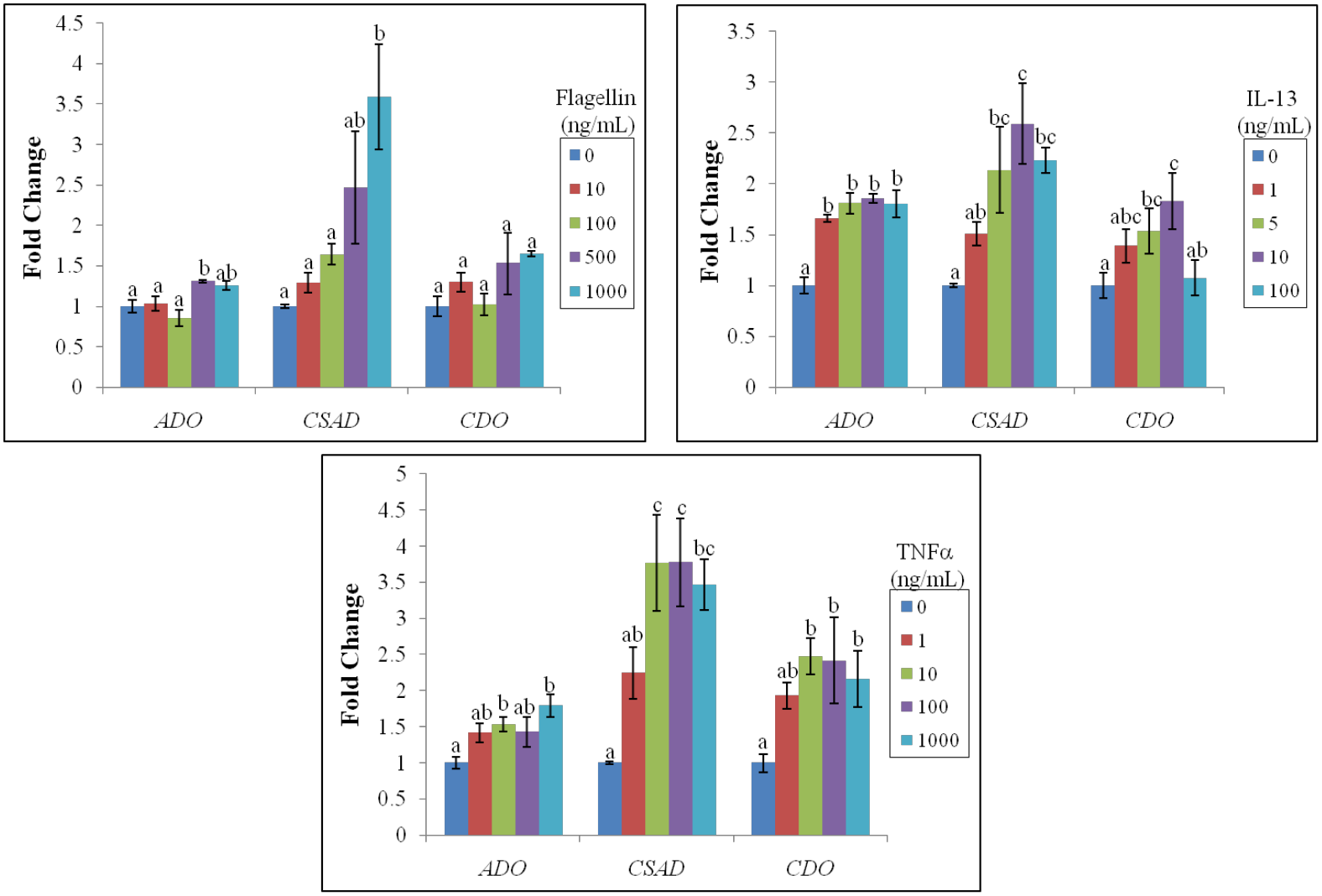

Figure 5.7: Relative expression (setting controls as 1) of taurine biosynthetic enzyme genes *ADO, CSAD,* and *CDO* in response to treatment with flagellin, IL-13, and TNFα for 24 h. The data represent mean ± SEM (n=4); statistical differences are indicated by different letters ($p < 0.05$).

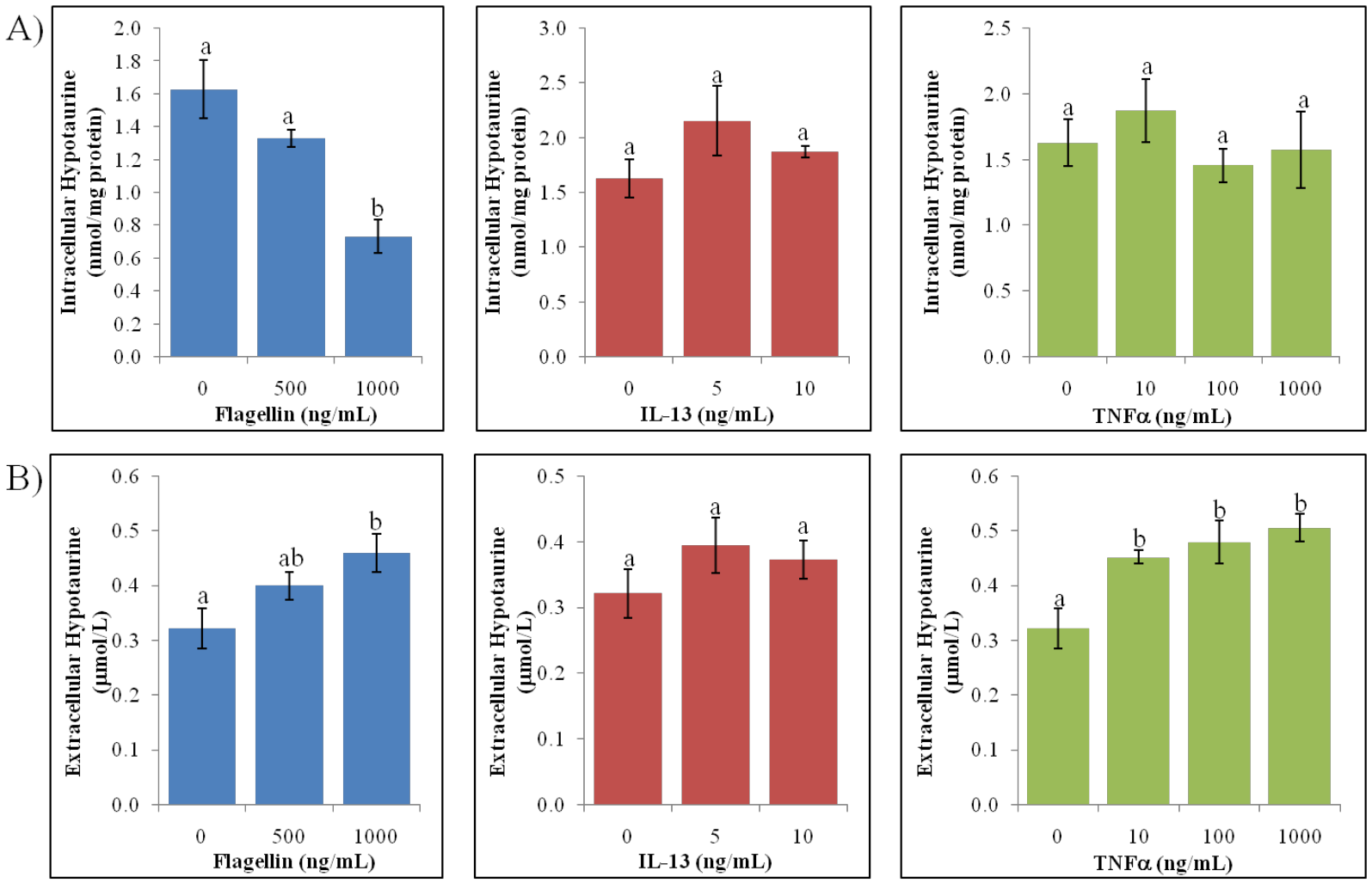

Figure 5.8: Intracellular (**A**) and extracellular (**B**) hypotaurine in LS174T cells treated for 24 h with the indicated concentrations of flagellin, IL-13, or TNFα The data represent means ± SEM (n=4); statistical differences are indicated by different letters ($p < 0.05$).

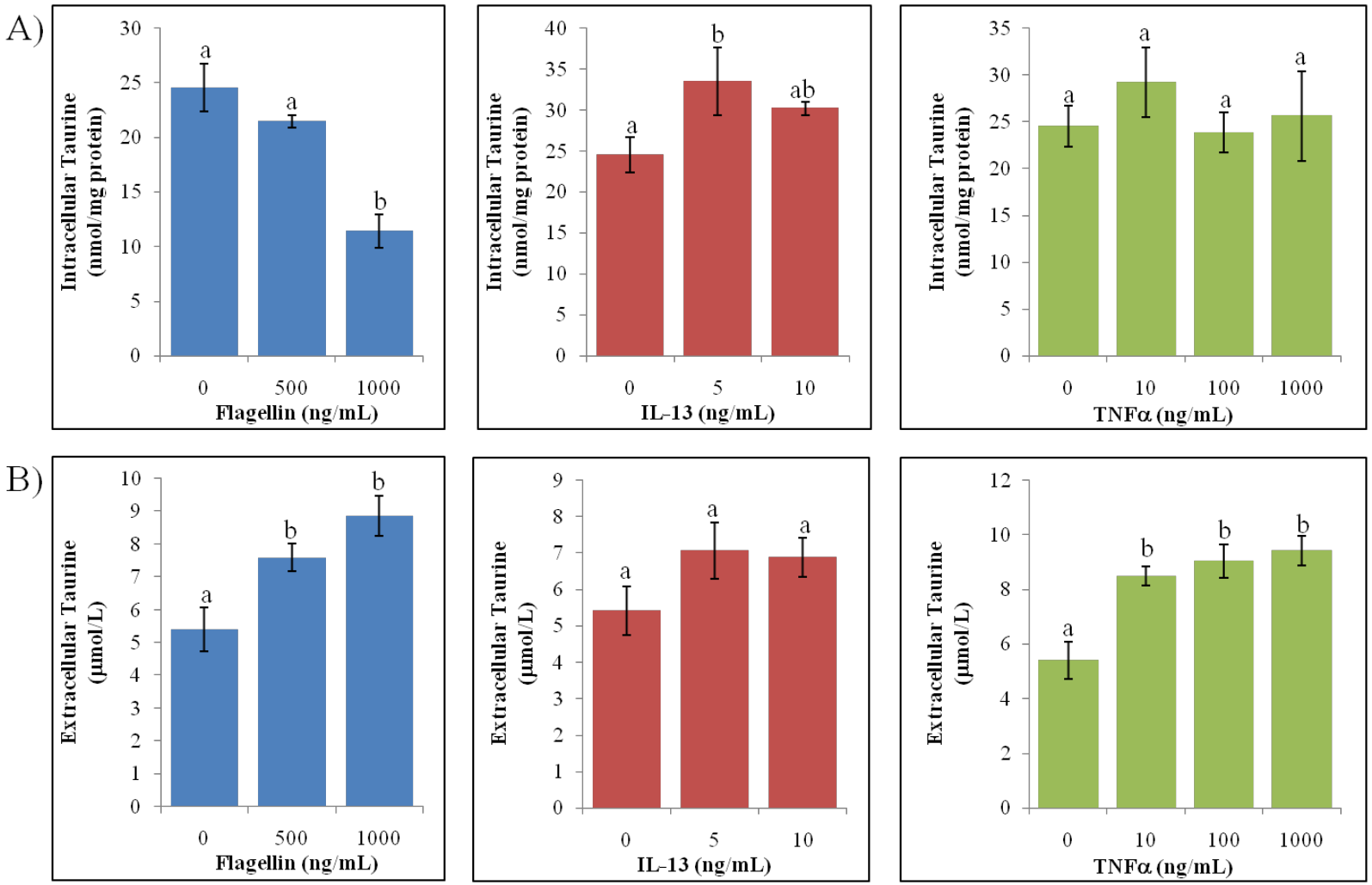

Figure 5.9: Intracellular (**A**) and extracellular (**B**) taurine in LS174T cells treated for 24 h with the indicated concentrations of flagellin, IL-13, or TNFα The data represent means ± SEM (n=4); statistical differences are indicated by different letters ($p < 0.05$).

Table 5.1: Primers used in this study for quantitative RT-PCR

Gene Symbol	Fwd Primer Sequence	Rev Primer Sequence	Product Size (bp)	Source
ADO	5'-GAG GGA GAA CCC TAT CCA GG-3'	5'-AGA GAC ACA GCC CTT GTG GT-3'	105	Quantitative PCR primer database**
CDO	5'-CCA AAT GCA ACT TCG GGC T-3'	5'-GCC TTT TTG TCC AAG GCA AAC-3'	100	Designed using Primer Express*
CSAD	5'-GAC AGT GTC CGA GTG GTC AA-3'	5'-CAA AGG CCC CTA GCA CAG T-3'	145	Quantitative PCR primer database**

*Software available from Applied Biosystems
**Available at http://web.ncifcrf.gov/rtp/gel/primerdb/default.asp

Chapter 6

FUTURE DIRECTIONS

In Chapter 2, interindividual and regional differences in sulfomucins and sialomucins were quantified in the right colon, left colon, and rectum of healthy individuals. While the approach used for quantitative analysis yielded important information regarding sulfo- and sialomucin abundance in the human colon, the method was found to be time consuming and somewhat subjective due to issues with the selection of the pixel color in the Automeasure module. There are also some inherent issues with the high iron diamine and alcian blue (HID/AB) stain that was used to distinguish sulfomucins and sialomucins, including masking of the presence of sialomucin by the HID stain and the potential for the HID stain to react non-specifically with other anionic groups [1]. Furthermore, the HID/AB staining cannot provide detailed information about which sugar groups are sulfated or sialylated or how many sulfate or sialic acid groups are present. To eliminate some of these issues, current work is in progress to develop a Fourier Transform Infrared (FTIR) spectroscopy imaging based approach to analyze sulfomucins and sialomucins in human intestinal biopsies. FTIR spectroscopic imaging combines the molecular selectivity of spectroscopy with the spatial specificity of optical microscopy [2]. Once algorithms are developed to classify sulfomucins and sialomucins, FTIR imaging will allow us to quantify these mucin chemotypes in unstained biopsy sections based on their chemical composition. Since the process is fully automated and eliminates the need for staining, it is much less time consuming than the image analysis technique used for mucin quantification in Chapter 2. FTIR imaging is also a much more objective way to analyze tissues since it eliminates the need for interpretation of staining. With the development of this technique

it may also be possible to analyze mucin composition in much more detail than can be performed with current staining protocols. Having this detail would be very useful in providing a deeper understanding of mucin-microbe associations.

It was reported in Chapter 2 that female subjects in our study on average exhibited greater sialomucin abundance in the rectum than male subjects and noted that additional studies should be completed to determine whether this finding would hold true for a larger number of subjects. More information is also needed regarding the influence of other demographic variables on mucin chemotypes, because normal values may vary between different groups of individuals depending on race, ethnicity, age, etc., and this information may help identify why certain populations are more susceptible to gastrointestinal disease than others. Associations between mucin chemotypes and diet in humans could also provide useful information. Animal models have demonstrated that mucin composition can be altered by diet [3-8]. By distinguishing individuals by diet and examining both mucin chemotypes and microbes, the high interindividual variation observed in SRB profiles might be reduced within dietary groups, and thereby enable the identification of associations between mucin chemotypes and SRB.

Changes in sulfo- and sialomucin have been previously described in association with ulcerative colitis (UC) and colorectal adenocarcinomas, but have been examined to a much lesser extent in Crohn's disease (CD). Furthermore, whether changes in mucin chemotype are associated with altered microbiota in human gastrointestinal disease has not been fully examined. A study is currently in progress to study sulfo- and sialomucins and microbial profiles in ileal and colonic biopsies collected from healthy subjects and inflamed and adjacent normal tissue in patients with CD and UC. As shown in **Figure 6.1**, we have already observed an increase in sialomucins associated with inflamed regions in a subject with CD. Once we have finished

analyzing mucins and microbial profiles in these subjects, we can use multivariate analysis as was done in Chapter 2 to determine the extent to which subjects cluster based on disease severity or whether only samples from actively inflamed regions cluster together.

In Chapter 3, an *in vitro* model of human colonic goblet cells was used to determine factors that might contribute to differences in sulfomucin abundance and the loss of mucin sulfation previously described in both inflammatory bowel disease and colonic adenocarcinomas. We determined that both host and microbial factors could enhance sulfomucin production possibly via upregulation of mucin sulfotransferases. A major component missing from this study, however, was analysis of secreted sulfomucin. This is important as treatments could be inducing additional sulfomucin to be secreted from the cells, which could make it appear that sulfomucin synthesis has not been altered. Several treatment time points should also be examined to better understand the dynamics of how long it takes for an increase in sulfotransferase expression to result in increased sulfomucin synthesis and secretion. Additional studies are also needed to determine the mechanisms by which microbial and host factors modulate expression of sulfotransferases. For example, it needs to be determined whether flagellin induces mucin sulfotransferases via interaction with TLR5 and downstream signaling or via another mechanism. The findings from Chapter 3 should also be examined in non-transformed cells to ascertain whether they are specific to the LS174T cell line or are reflective of the normal response of intestinal goblet cells. Finally, if protocols could be developed to examine mucin sulfation in goblet cells using primary cell culture, one could explore whether goblet cells from subjects with active IBD exhibit the same mucin sulfation responses as in normal subjects.

As described in Chapter 4, expression of cysteine dioxygenase (CDO), an important enzyme in cysteine catabolism, was demonstrated to be restricted to cells of the secretory but not

the absorptive lineage in the small intestine, colon, and cecum. CDO may also be expressed by intestinal stem cells. Studies are underway to determine whether CDO colocalizes with intestinal stem cell markers, leucine-rich repeat-containing G-protein-coupled receptor (LGR5), a marker for rapidly cycling intestinal stem cells, and doublecortin and CaM kinase-like-1 (DCAMKL-1), a marker for quiescent intestinal stem cells [9]. Additional studies are also needed to determine whether the cell type-specific expression of CDO in the intestine is consistent among species. Finally, recent staining for CDO performed in CDO knockout mice revealed positive CDO staining (see Appendix B), so whether the CDO antibody is actually staining CDO or cross-reacting with another protein needs to be resolved.

Taurine is one possible end product of cysteine catabolism by CDO. Consequently, as described in Chapter 5, we examined taurine biosynthesis in LS174T cells, a human goblet-cell like line via the two pathways of taurine biosynthesis. It was demonstrated that LS174T cells synthesize taurine via the ADO pathway but that synthesis of taurine via the CDO/CSAD pathway was equivocal. The first issue that should be addressed in this regard is whether CDO and CSAD are expressed at the protein level in LS174T cells. Then, it should be determined if CDO and/or CSAD protein abundance and activity are increased in response to cysteine. In 3T3-L1 cells, CDO, CSAD, and ADO protein levels increased during adipogenic differentiation and this was accompanied by changes in hypotaurine and taurine production [10]. Additional experiments could be performed using the HT29-Cl.16E cell line, which differentiates into goblet cells, to examine whether the differentiation state affects taurine biosynthesis and expression of taurine biosynthetic enzymes. We also observed that flagellin, IL-13, and TNFα modulated gene expression of taurine biosynthetic enzymes as well as taurine biosynthesis and/or taurine export from the cells. Further studies should be completed to determine whether

protein abundance of taurine biosynthetic enzymes is increased in response to flagellin, IL-13, and TNFα and whether longer treatment times result in higher hypotaurine and taurine levels. Since cysteine is involved in the synthesis of other products that could offer protection during inflammation, such as glutathione, goblet cell secretory products, and sulfate [11], which, in turn, could be used for sulfomucin synthesis, it would be interesting to measure these products in addition to taurine to determine whether cysteine might be preferentially used to synthesize certain products over others both under normal conditions and in response to inflammation. One could also examine whether provision of additional cysteine or cysteamine would allow cells to enhance synthesis of any of these products and thereby offer additional protection against inflammation. Such experiments would contribute to a much needed understanding of cysteine metabolism in intestinal goblet cells. Finally, the results of these studies should be examined in an animal model or using primary cell culture to determine whether these findings are applicable to normal intestinal goblet cells or specific to the LS174T cell line.

REFERENCES

1. Reid, P.E., et al., *The histochemical specificity of high iron diamine-alcian blue.* Histochem J, 1989. **21**(8): p. 501-7.

2. Levin, I.W. and R. Bhargava, *Fourier transform infrared vibrational spectroscopic imaging: integrating microscopy and molecular recognition.* Annu Rev Phys Chem, 2005. **56**: p. 429-74.

3. Deplancke, B. and H.R. Gaskins, *Microbial modulation of innate defense: goblet cells and the intestinal mucus layer.* Am J Clin Nutr, 2001. **73**(6): p. 1131S-1141S.

4. More, J., et al., *Histochemical characterization of glycoproteins present in jejunal and colonic goblet cells of pigs on different diets. A biopsy study using chemical methods and peroxidase-labelled lectins.* Histochemistry, 1987. **87**(2): p. 189-94.

5. Sharma, R. and U. Schumacher, *Morphometric analysis of intestinal mucins under different dietary conditions and gut flora in rats.* Dig Dis Sci, 1995. **40**(12): p. 2532-9.

6. Sharma, R. and U. Schumacher, *The influence of diets and gut microflora on lectin binding patterns of intestinal mucins in rats.* Lab Invest, 1995. **73**(4): p. 558-64.

7. Yang, K., et al., *Cytokeratin, lectin, and acidic mucin modulation in differentiating colonic epithelial cells of mice after feeding Western-style diets.* Cancer Res, 1996. **56**(20): p. 4644-8.

8. Ganessunker, D., et al., *Total parenteral nutrition alters molecular and cellular indices of intestinal inflammation in neonatal piglets.* JPEN J Parenter Enteral Nutr, 1999. **23**(6): p. 337-44.

9. May, R., et al., *Doublecortin and CaM kinase-like-1 and leucine-rich-repeat-containing G-protein-coupled receptor mark quiescent and cycling intestinal stem cells, respectively.* Stem Cells, 2009. **27**(10): p. 2571-9.

10. Ueki, I. and M.H. Stipanuk, *3T3-L1 adipocytes and rat adipose tissue have a high capacity for taurine synthesis by the cysteine dioxygenase/cysteinesulfinate decarboxylase and cysteamine dioxygenase pathways.* J Nutr, 2009. **139**(2): p. 207-14.

11. Stipanuk, M.H., et al., *Mammalian cysteine metabolism: new insights into regulation of cysteine metabolism.* J Nutr, 2006. **136**(6 Suppl): p. 1652S-1659S.

FIGURES

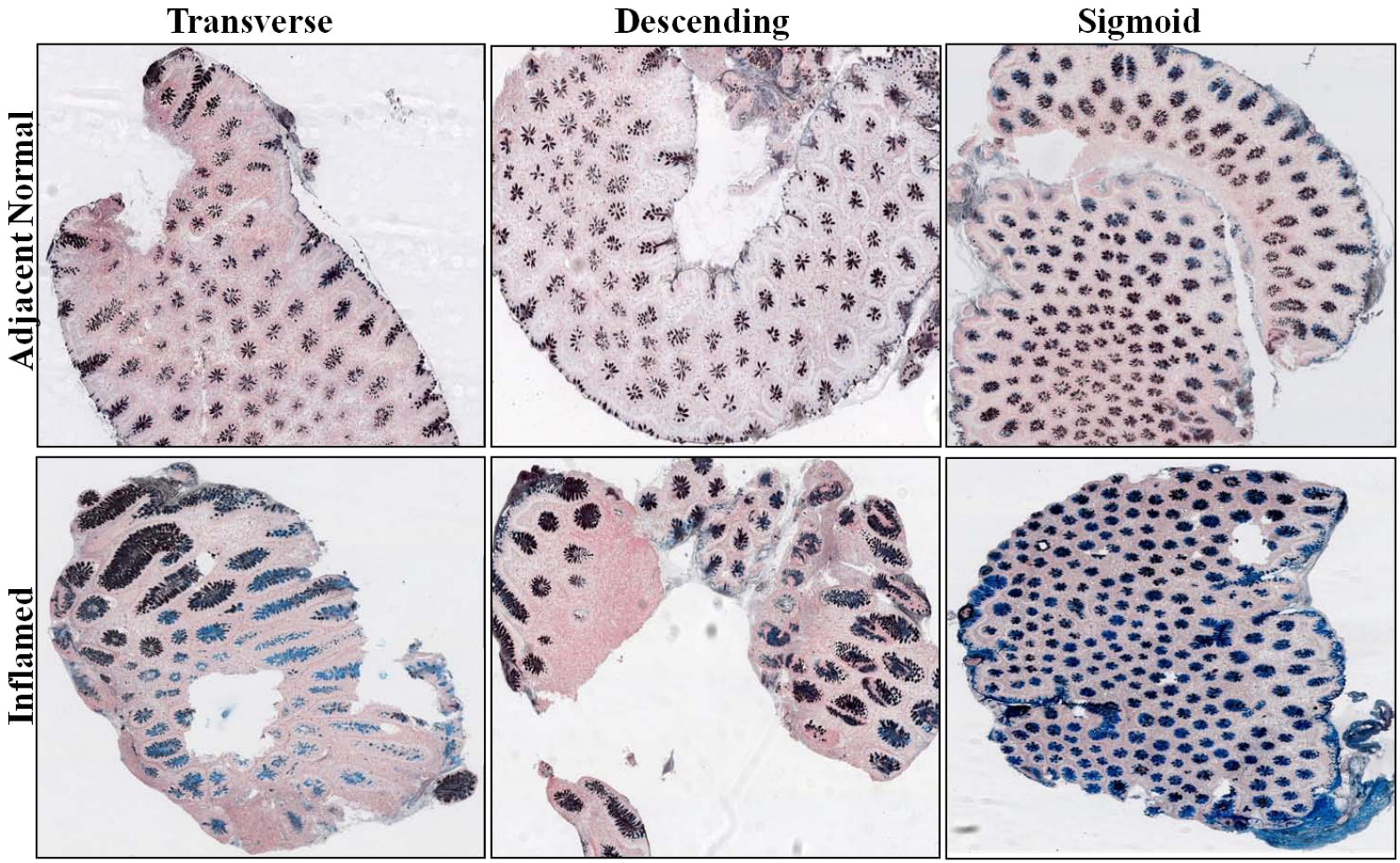

Figure 6.1: High iron diamine and alcian blue (pH 2.5) stained colon biopsies (200X magnification) collected from regions of inflamed and adjacent normal tissue from a patient with CD. Sulfomucin is stained black/brown and sialomucin is stained blue. Increased staining for sialomucin compared to adjacent normal tissue is present in all three regions of active inflammation.

APPENDIX A

ADDITIONAL EXPERIMENTS EXAMINING EFFECTS OF MICROBIAL COMPONENTS, IL-13, and HYDROGEN SULFIDE ON GOBLET CELLS

A.1 Lipopolysaccharide (LPS) and Pam3CSK4

The responsiveness of goblet cells to known TLR4 agonist LPS, and synthetic TLR 1/2 agonist (Pam3CSK4) was examined in the LS174T cell line. LPS from *E. coli* O111:B5 was provided by Dr. Richard Tapping and Pam3CSK4 was purchased from Invivogen. LS174T cells were cultured for 6 h and 24 h in medium containing different concentrations of Pam3CSK4 or LPS, after which the conditioned media and cells were collected. RNA was isolated from the cells, and *CDX2*, *MUC2*, *RETNLB*, and *TFF3* expression was examined using quantitative RT-PCR. The data were normalized to *GAPDH* and *RPLP0* expression. IL-8 secretion was also measured using an ELISA (R & D Systems) to determine whether the cells were responding to the treatments. Comparisons were performed using SAS software (Statview, Version 5.0.1; SAS Institute, Cary, NC). ANOVA and Fisher's protected least significant difference test were used to compare differences with an assigned p-value of < 0.05.

As shown in **Figure A.1**, significant changes were not observed upon treatment with LPS for 6 h, and only about a 25% decrease in *MUC2* and 30% decrease *TFF3* expression occurred after 24 h of treatment with the highest concentration of LPS. Secretion of IL-8 was measured in the conditioned media of cells treated for 24 h. A statistically significant decrease in IL-8 secretion occurred with the 1 μg/mL LPS treatment (**Figure A.2**). However, because it was only a 7% decrease compared to the untreated secretion of IL-8 with a p-value of 0.045, it is possible that this result is not a biologically significant difference. Thus, both the gene expression data

and IL-8 secretion data indicate that, overall, the cells were unresponsive to LPS. The limited response to LPS might be the result of insufficient expression of TLR4 by the cells.

Treatment with 10 ng/mL of Pam3CSK4 for 6 h resulted in a statistically significant, but small, increase in *MUC2* (1.3-fold) and *RETNLB* (1.5-fold) expression and decrease in *TFF3* (1.2-fold) expression (**Figure A.3**). At 24 h, a decrease in *RETNLB* (1.4-fold) was observed with 1 μg/mL of Pam3CSK4 and *MUC2* (1.3-fold) with all concentrations of Pam3CSK4. Expression of *CDX2* and *TFF3* was unaltered for all concentrations examined for 24 h. Since the goblet cell secretory product genes seemed to be somewhat responsive to Pam3CSK4, we proceeded to determine whether expression of the mucin sulfotransferase genes, *CHST5* and *GAL3ST2*, was altered by treatment with Pam3CSK4. At 6 h, an increase in both *CHST5* (1.4-fold) and *GAL3ST* (1.8-fold) was observed with 10 ng/mL of Pam3CSK4 (**Figure A.4**). After 24 h of treatment with Pam3CSK4, *GAL3ST2* expression did not differ significantly from the control, and *CHST5* was downregulated about 1.6-fold with 1 μg/mL of Pam3CSK4. IL-8 secretion was also measured from cells treated with Pam3CSK4. As shown in **Figure A.2**, a statistically significant decrease in IL-8 secretion occurred with the 1 μg/mL Pam3CSK4 treatment for 24 h. However, this only amounted to a 1.1-fold decrease with a p-value of 0.048, and when the treatment was repeated (**Figure A.5**) a significant difference was not observed. One possible explanation for the lack of IL-8 secretion by the cells in response to Pam3CSK4 is the chosen treatment times and concentrations. Other studies reported increased IL-8 secretion from the T84 intestinal epithelial cell line using 50 μg/mL of Pam3CSK 4 [1, 2], so we tested whether the LS174T cell line would secrete IL-8 in response to this higher concentration of Pam3CSK4. Treatments with TNFα and flagellin (*S. tymphimurium*) were performed as controls. Cells were incubated for 24 h with the treatments indicated in **Figure A.5**. Cells and conditioned media were collected for analysis of

gene expression and IL-8 secretion, respectively. Treatment with TNFα resulted in a 5-fold increase in IL-8 secretion and 500 ng/mL of flagellin produced a 3.5-fold increase, but none of the other treatments significantly altered secretion of IL-8. Podolsky et al. described an increase in TFF3 mRNA in LS174T cells after 30 minutes of treatment with 20 μg/mL of Pam3CSK4 and an increase in TFF3 secretion after 24 h of treatment with 20 μg/mL of Pam3CSK4 [3]. They did not mention whether IL-8 secretion was examined. Thus, it may be that Pam3CSK4 is able to initiate TFF3 transcription and secretion without inducing IL-8 secretion. Furthermore, early time points may need to be examined to detect changes in *TFF3* expression in response to certain stimuli.

A.2 IL-13 effects on pre- and post-confluent HT29CL.16E cells

The ability of IL-13 to modulate sulfated and sialylated mucins and the sulfotransferase genes, *CHST5* and *GAL3ST2*, at different stages of goblet cell differentiation was examined using HT29CL.16E cells, which differentiate to have a goblet cell-like phenotype in early post-confluence, at pre-confluen and 5 days post-confluence. re-confluent cells and 5 days post-confluent cells were treated with 1 ng/mL IL-13 (purchased from Sigma) for 24 h. Gene expression was evaluated using quantitative RT-PCR. Sialylated and sulfated mucin content was assessed by staining with HID/AB. Similar to results reported with the LS174T cell line in Chapter 3, *CHST5* expression increased in HT29CL.16E cells treated with IL-13 (**Figure A.6**). However, in this cell line the less differentiated pre-confluent cells were more responsive to IL-13, in terms of *CHST5* upregulation, than the more differentiated post-confluent cells. There was no detectable expression of *GAL3ST2* in IL-13 treated or untreated HT29CL.16E cells at either stage of differentiation. This corroborates previous data showing that certain oligosaccharides

isolated from HT29CL.16E cells contain a sulfate residue linked in position C-6 of a galactose residue [4]. Staining of pre- and post-confluent HT29Cl.16E cells revealed what appeared to be an increase in HID staining, and thus sulfomucin production (**Figures A.7** and **A.8**). However, additional analyses of mucins should be done to confirm this finding. Overall, it appears that IL-13 can induce mucin sulfation, possibly via the sulfotransferase CHST5 in the HT29Cl.16E cell line, which is in accord with the results reported with the LS174T cell line in Chapter 3. Furthermore, goblet cells that are more differentiated may be less responsive to IL-13 modulation. Thus, relative position along the crypt could affect how goblet cells respond to inflammatory stimuli.

A.4 Sulfide

The effects of sulfide on *CHST5* and *GAL3ST2* gene expression were investigated using the LS174T cell line. Cells were treated with sodium sulfide for 6 h and 24 h and then harvested for RNA isolation. Gene expression for *CHST5* and *GAL3ST2* was evaluated using quantitative RT-PCR and normalized to expression of *RPLP0*. As shown in **Figure A.9**, sulfide did not significantly alter expression of either sulfotransferase after 6 h of treatment. However, after 24 h of treatment with sulfide, *CHST5* expression was increased more than 4-fold and *GAL3ST2* expression was increased approximately two-fold. Thus, sulfide may stimulate goblet cells to produce more sulfomucins.

REFERENCES

1. Mueller, T., et al., *Th2 cytokines down-regulate TLR expression and function in human intestinal epithelial cells.* J Immunol, 2006. **176**(10): p. 5805-14.

2. Weng, M., W.A. Walker, and I.R. Sanderson, *Butyrate regulates the expression of pathogen-triggered IL-8 in intestinal epithelia.* Pediatr Res, 2007. **62**(5): p. 542-6.

3. Podolsky, D.K., et al., *Colitis-associated variant of TLR2 causes impaired mucosal repair because of TFF3 deficiency.* Gastroenterology, 2009. **137**(1): p. 209-20.

4. Capon, C., et al., *Oligosaccharide structures of mucins secreted by the human colonic cancer cell line CL.16E.* J Biol Chem, 1992. **267**(27): p. 19248-57.

FIGURES

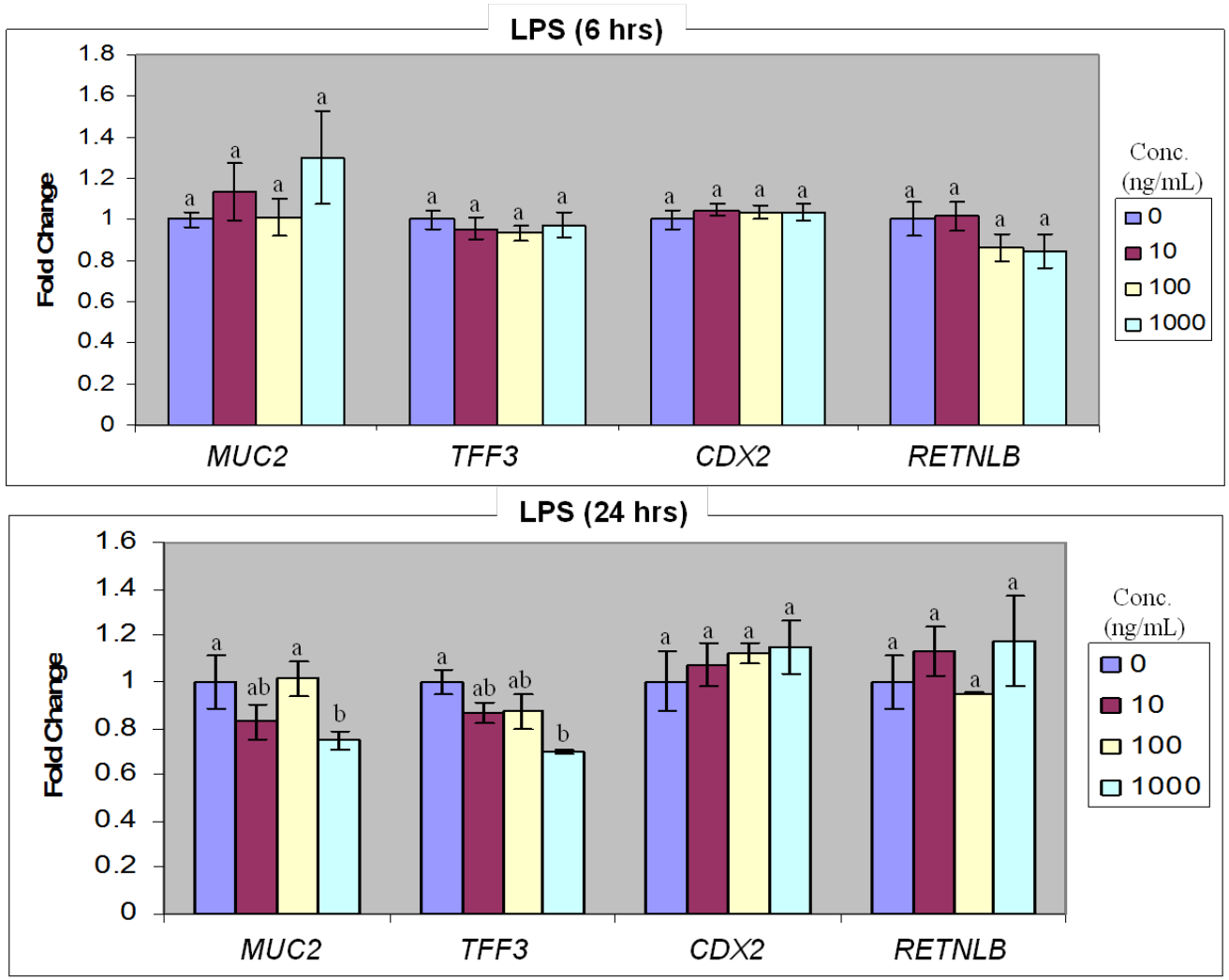

Figure A.1: Relative fold change (setting controls as 1) of *CDX2, MUC2, TFF3,* and *RETNLB* expression in response to treatment with LPS for 6h and 24h. The data represent means ± SEM (n=4)**;** ; statistical differences are indicated by different letters ($p < 0.05$).

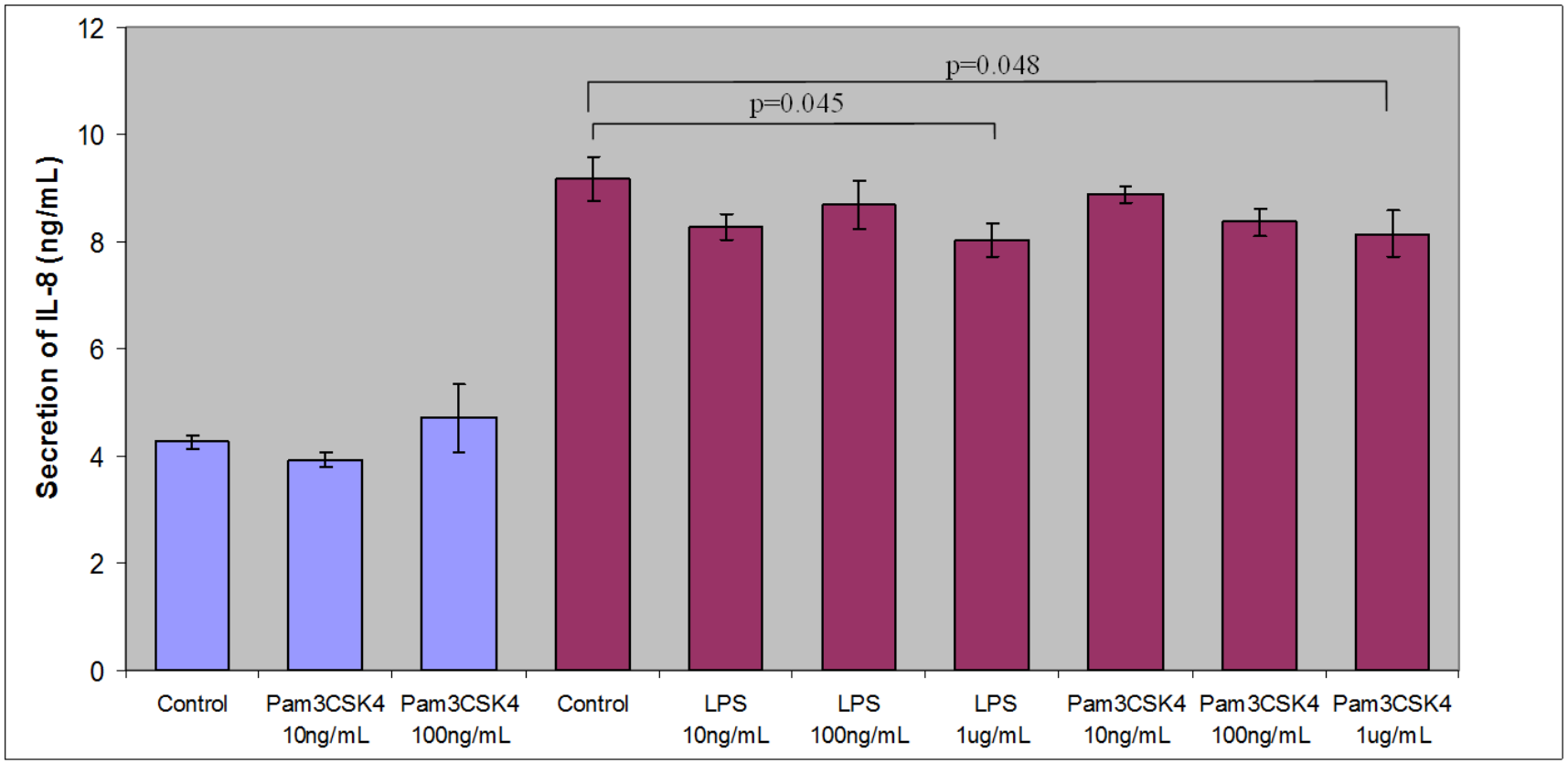

Figure A.2: IL-8 secretion from LS174T cells treated for 6h or 24h with LPS or Pam3CSK4. The data represent means ± SEM (n=4).

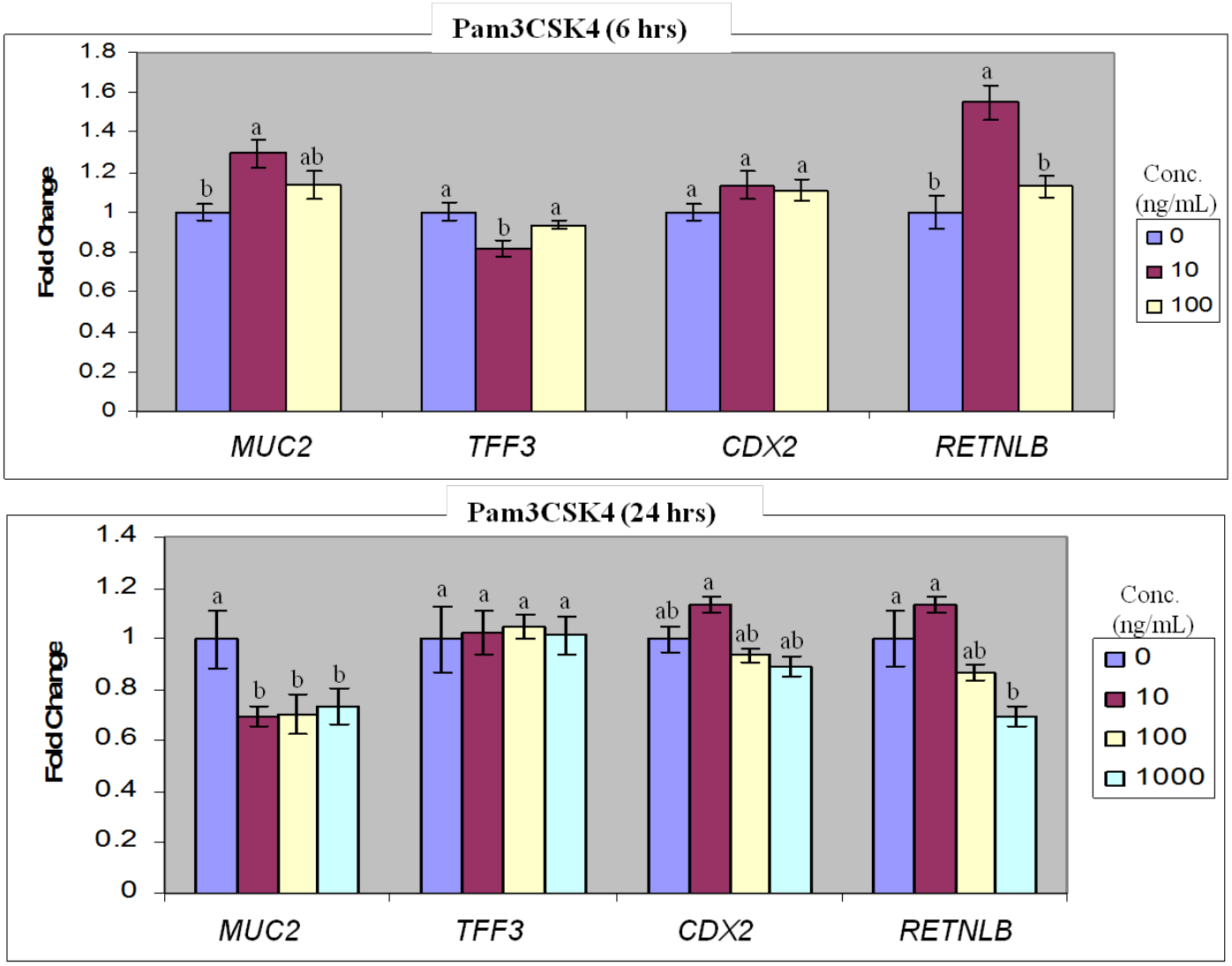

Figure A.3: Relative fold change (setting controls as 1) of *CDX2, MUC2, TFF3*, and *RETNLB* expression in LS174T cells in response to treatment with Pam3CSK4 for 6h and 24h. The data represent means ± SEM (n=4); statistical differences are indicated by different letters ($p < 0.05$).

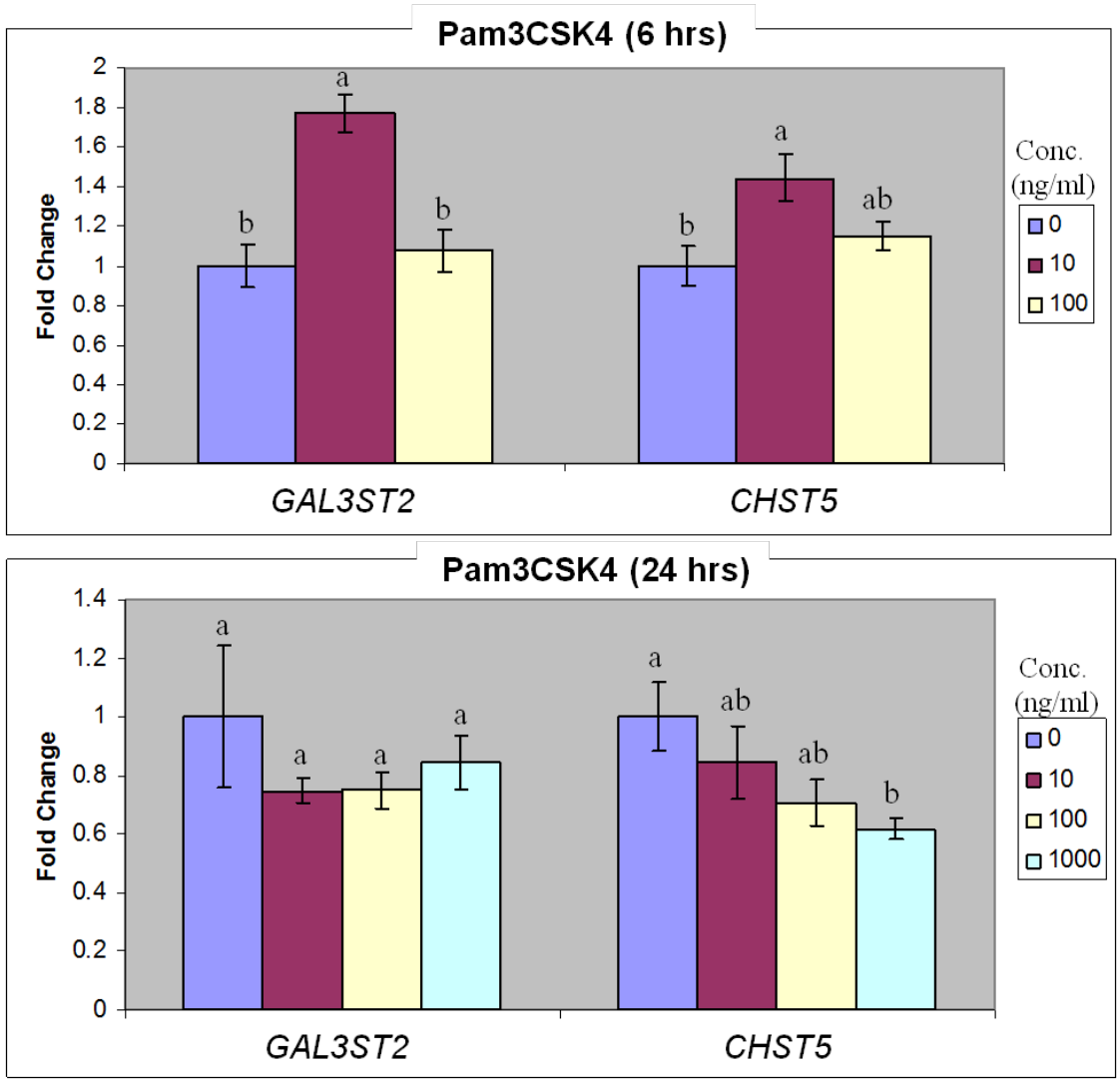

Figure A.4: Relative fold change (setting controls as 1) of expression of the sulfotransferase genes, *CHST5* and *GAL3ST2*, in response to treatment with Pam3CSK4 for 6h and 24h. The data represent mean ± SEM (n=4); statistical differences are indicated by different letters ($p < 0.05$).

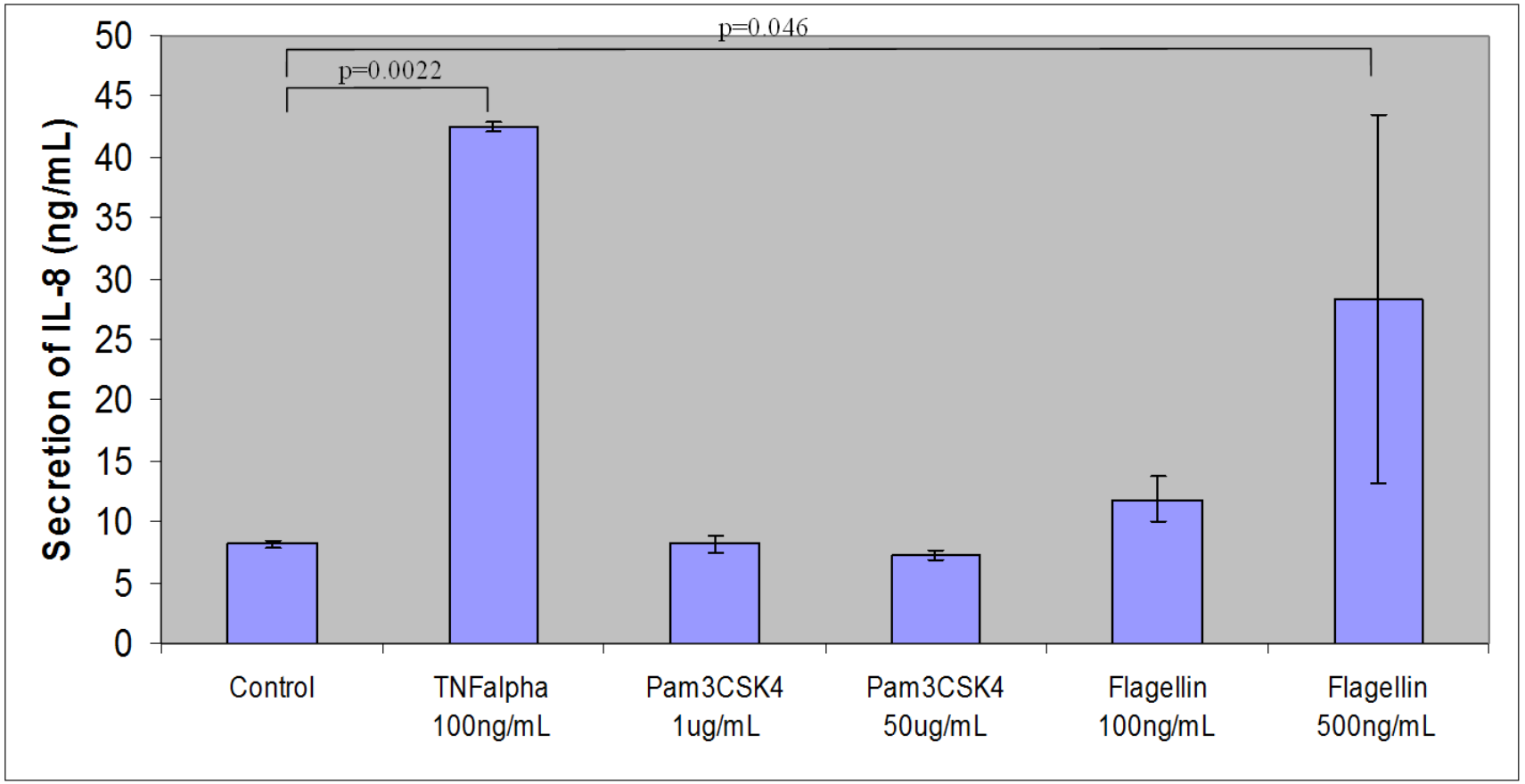

Figure A.5: IL-8 secretion from LS174T cells incubated for 24h with the indicated treatments. The data represent mean ± SEM (n=3).

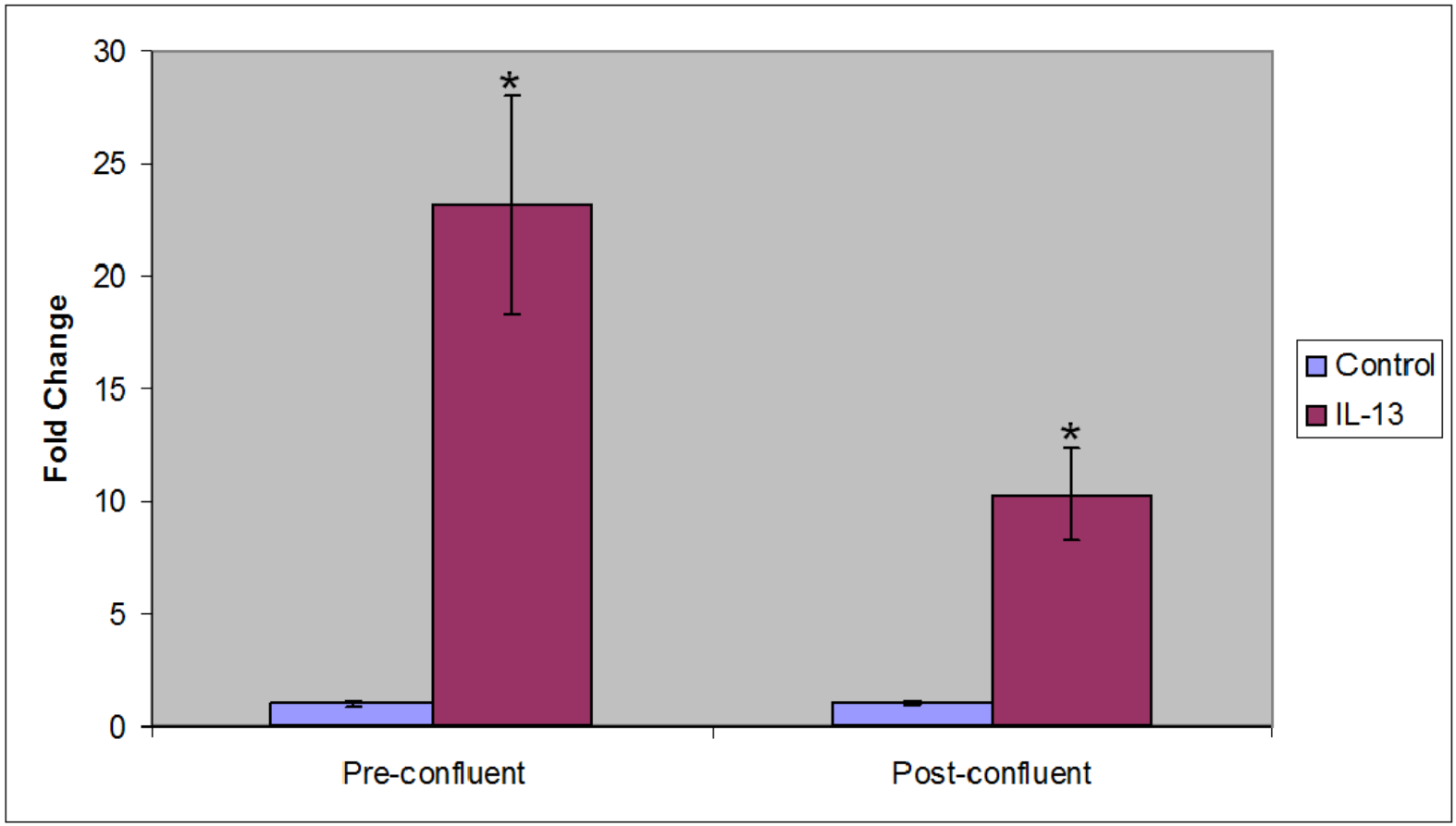

Figure A.6: Relative fold change (setting controls as 1) of expression of *CHST5* in HT29CL.16E cells in response to treatment with 1ng/mL of IL-13 for 24 h. The data represent means ± SEM (n=3); values statistically different ($p < 0.05$) from controls are indicated by an asterisk (*).

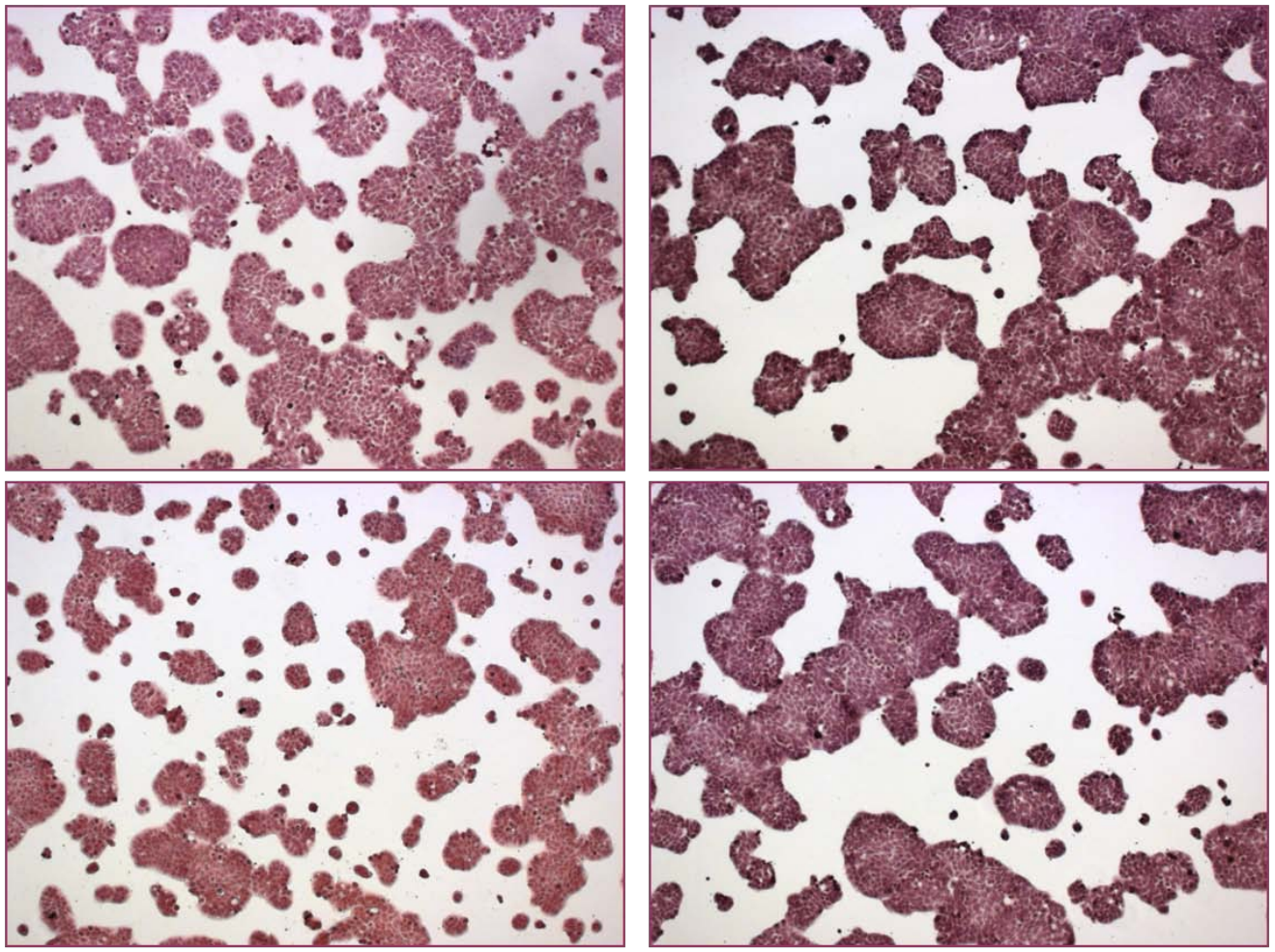

Figure A.7: Control and IL-13 treated pre-confluent HT29CL.16E cells stained with HID/AB (50X magnification). Cells were treated for 24h with 1ng/mL of IL-13 prior to reaching confluence. IL-13 treated cells show increased brown staining for sulfated mucins. These photomicrographs are representative of three replicate coverslips

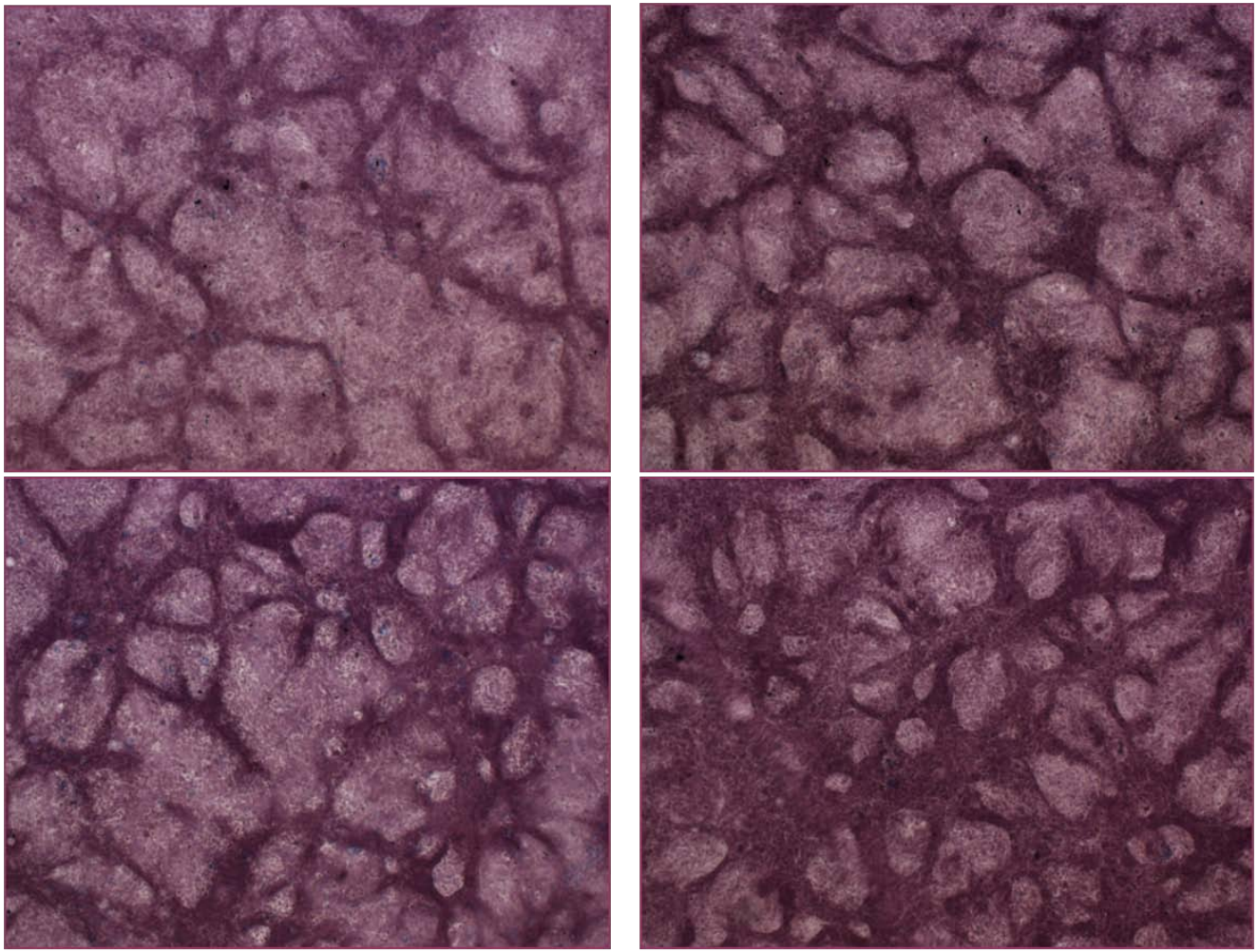

Figure A.8: Control and IL-13 treated post-confluent HT29CL.16E cells stained with HID/AB (50X magnification). Cells were treated with 1ng/mL of IL-13 for 24h 5 days after cells reached confluence. IL-13 treated cells show increased brown staining for sulfated mucins. These photomicrographs are representative of three replicate coverslips

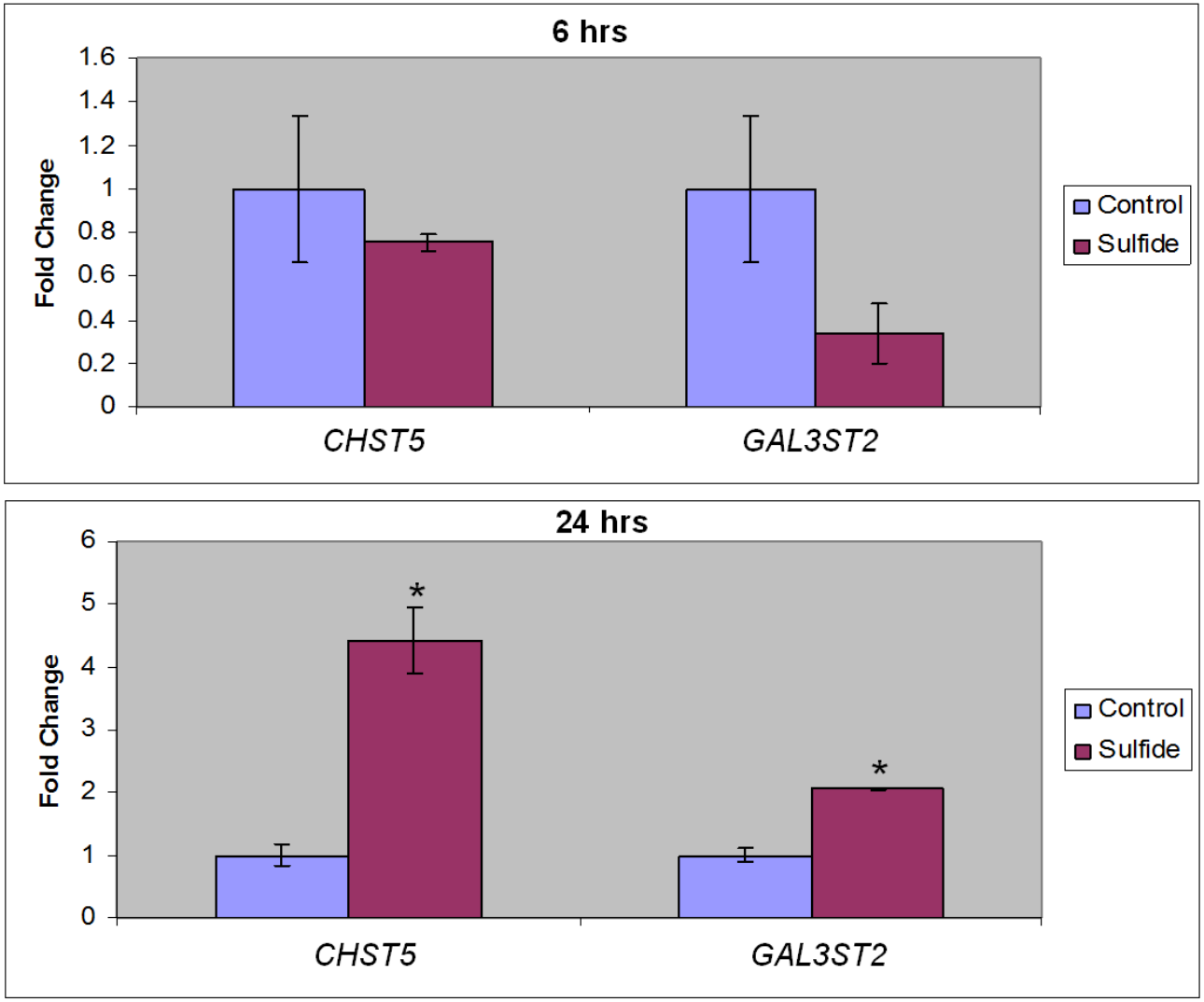

Figure A.9: Relative fold change (setting controls as 1) of expression of *CHST5* and *GAL3ST2* in response to treatment with sulfide 24 h. The data represent means ± SEM (n=3); values statistically different ($p < 0.05$) from controls are indicated by an asterisk (*).

APPENDIX B

CDO KNOCKOUT MICE

INTRODUCTION

The aim of this study was to better understand the functional significance of CDO in the intestine and the effects of dietary sulfur amino acids (SAA) on CDO expression in the intestine. This was done by examining small intestine and colon from CDO knockout (KO) and wild type (WT) mice on low and high sulfur amino acid diets.

MATERIALS AND METHODS

*Mouse Stud*y. All experimental procedures were conducted by the Stipanuk lab with the approval of the Cornell University Institutional Animal Care and Use Committee. Genotypes of pups were determined by PCR on genomic DNA samples obtained from tail snips. Twelve WT (+/+) and twelve male KO (CDO $^{-/-}$) mice (6 females and 6 males for each) were fed a basal semi-purified diet, containing adequate SAA from birth. At 7 weeks, they were placed on either a sulfur diet slightly low in SAA or a diet with excess SAA above the requirement level and fed this diet ad libitum for 1 week. Mice were killed at the end of the 1 week feeding trial at ~ 8 weeks of age. Three female and three male mice from WT and KO mice were placed on each diet.

CDO Immunohistochemistry. Small intestine and colon from two male and two female mice from each group (SAA deficient WT, SAA deficient KO, High SAA WT, High SAA KO) were isolated and fixed in 4% buffered paraformaldehyde for 48 hours prior to dehydration. Tissues

were embedded, sectioned and stained for CDO. Staining was performed by the University of Illinois Veterinary Biosciences Histology Laboratory. Sections were deparaffinized and brought to water. Antigen retrieval was performed for one hour in a steamer using Rodent Decloaker (Biocare). Following a rinse in deionized water, endogenous peroxidases were blocked by incubation in 3% hydrogen peroxide in water with agitation for 15 minutes. Sections were then rinsed with wash buffer, blocked with Biocare Rodent block M for 30 minutes, and rinsed briefly in deionized water. Sections were incubated in rabbit anti-rat CDO antibody (1:100 dilution) or an equivalent concentration of rabbit IgG (IgG control) for 30 minutes followed by 3 washes in Tris-Tween for 5 minutes each. Secondary detection was performed using Rabbit on Rodent HRP-Polymer (Biocare Medical) for 30 minutes, followed by three washes in Tris-Tween for 5 minutes each, DAB chromagen (Innovex Biosciences) for 5 minutes, and 1% copper sulfate for 1 minute. Sections were rinsed in tap water, counterstained with hematoxylin, dehydrated, cleared, and mounted. Stained slides were scanned at 40X using the Nanozoomer Digital Pathology System (Hamamatsu).

RESULTS

CDO Immunohistochemistry. As shown in **Figures B.1** and **B.2**, positive staining was observed in both WT and KO mice fed a low or high SAA diet. The distribution of the staining appeared to be the same in all mice; in addition, both goblet and Paneth cells stained positive. Thus, there was no apparent difference in CDO staining between WT or KO mice or between low and high SAA diets. Rabbit IgG controls (**Figures B.3** and **B.4**) did not show positive staining for CDO. Similar findings were observed in the duodenum and jejunum (data not shown).

DISCUSSION

The results of the CDO immunohistochemistry indicate that the observed positive CDO staining in the intestine may be the result of the antibody cross-reacting with another protein. Additional studies will be performed to determine whether this is the case or if there is some issue with the KO mice that is leading to positive CDO staining.

FIGURES

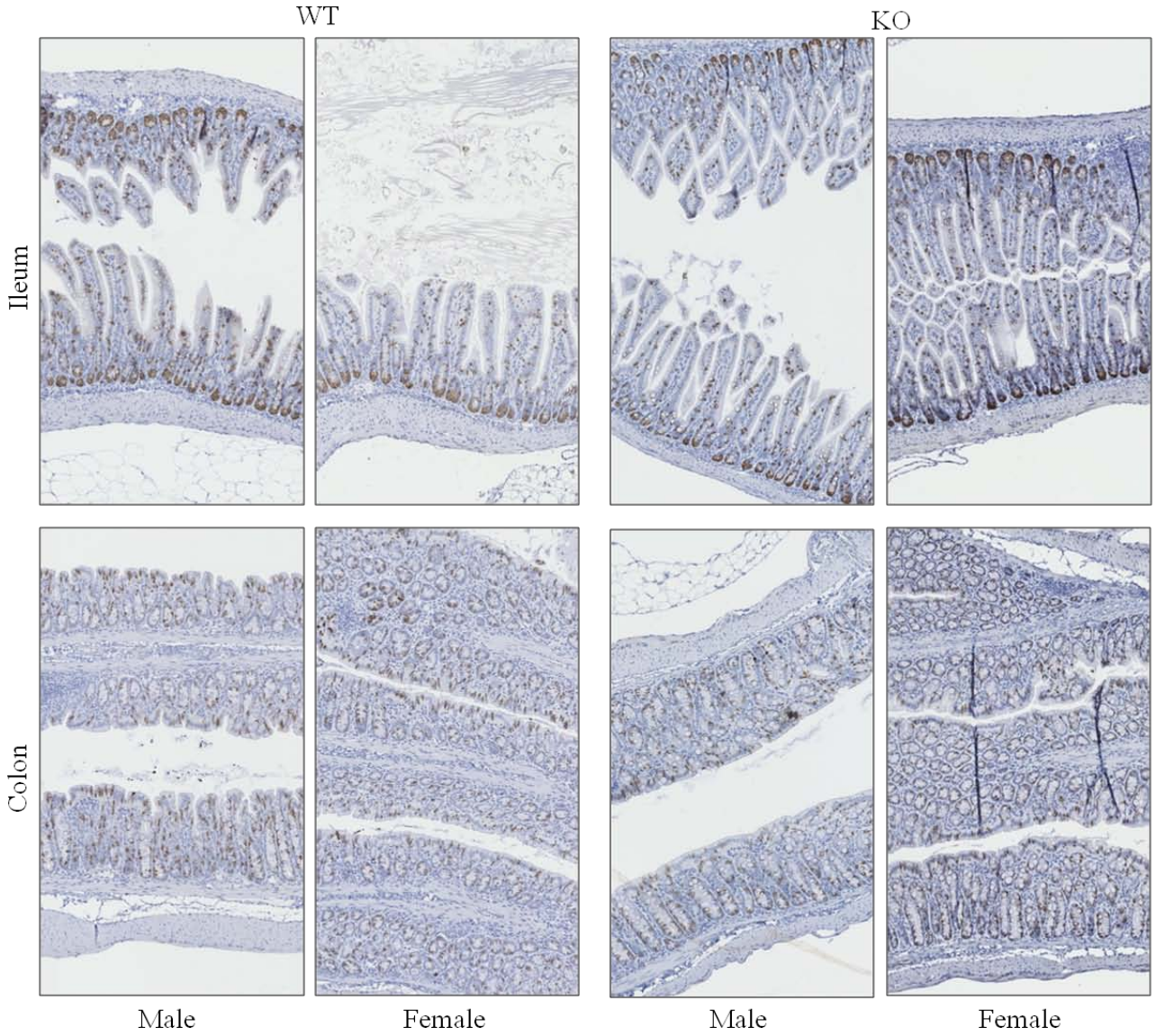

Figure B.1. Representative images of immunohistochemical staining for CDO in the ileum and colon of wild-type (WT) and CDO -/- mice (KO) fed a diet low in sulfur amino acids.

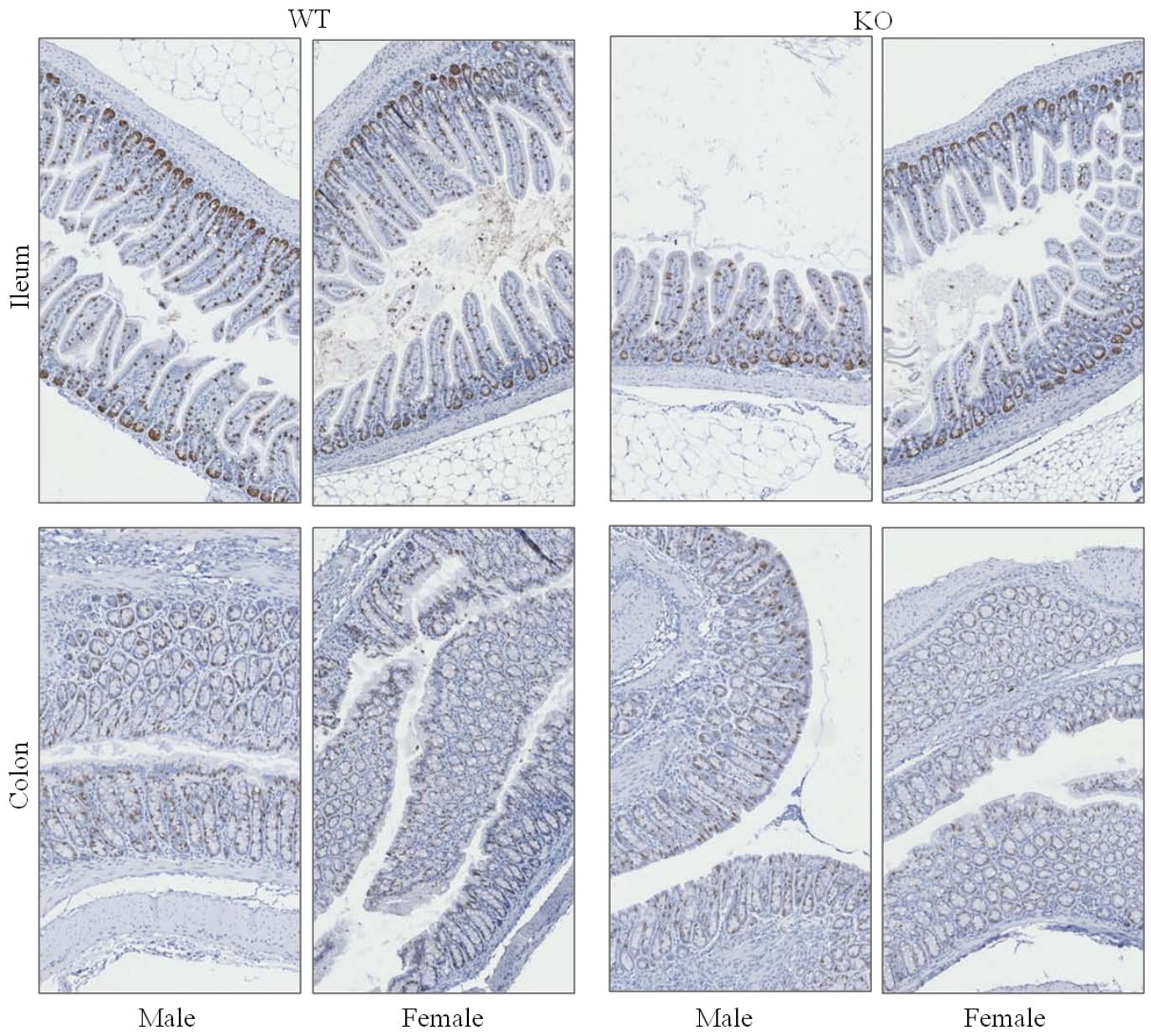

Figure B.2. Representative images of immunohistochemical staining for CDO in the ileum and colon of wild-type (WT) and CDO -/- mice (KO) fed a high sulfur amino acids diet.

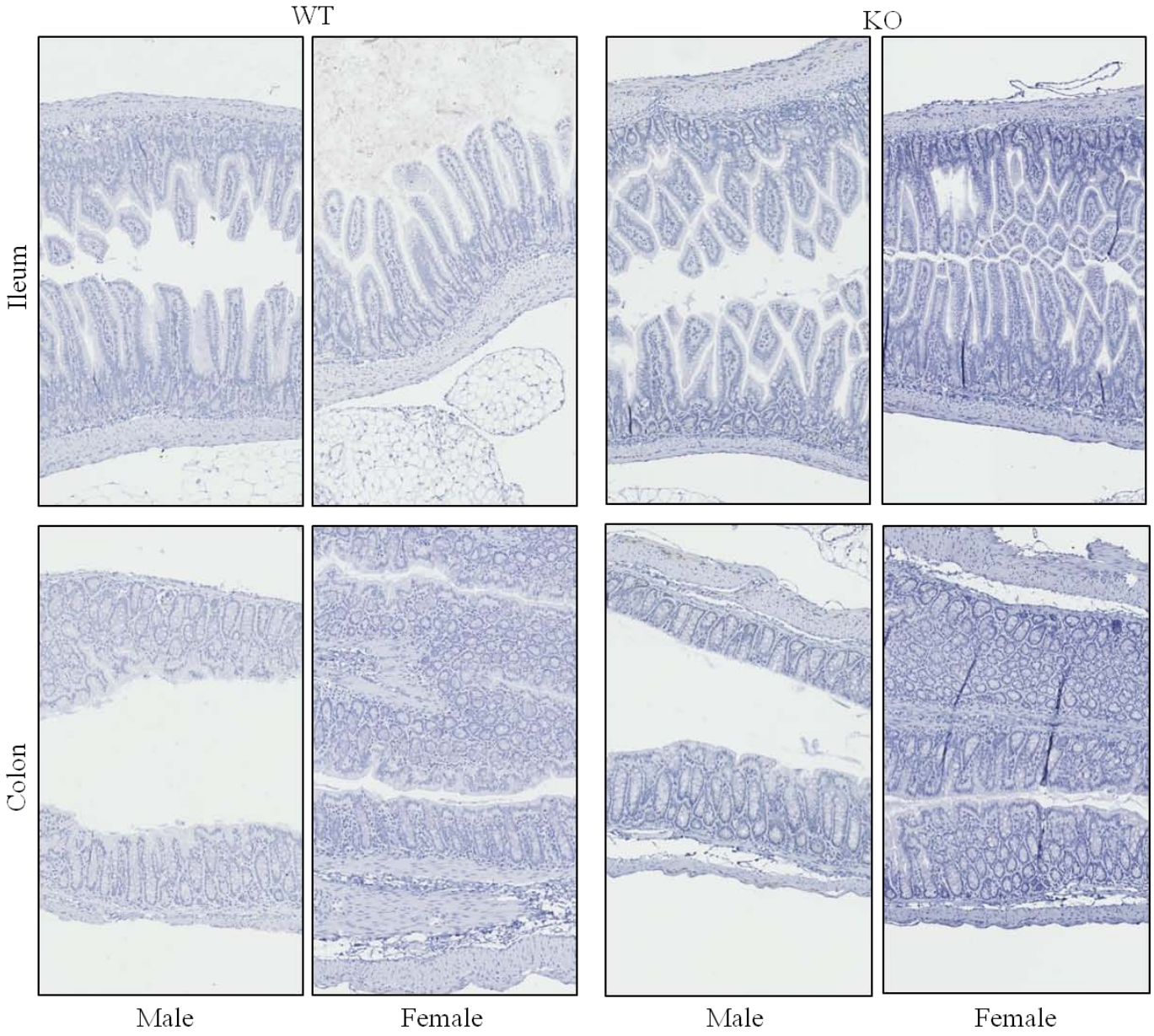

Figure B.3. Representative images of rabbit IgG control in the ileum and colon of wild-type (WT) and CDO -/- mice (KO) fed a diet low in sulfur amino acids.

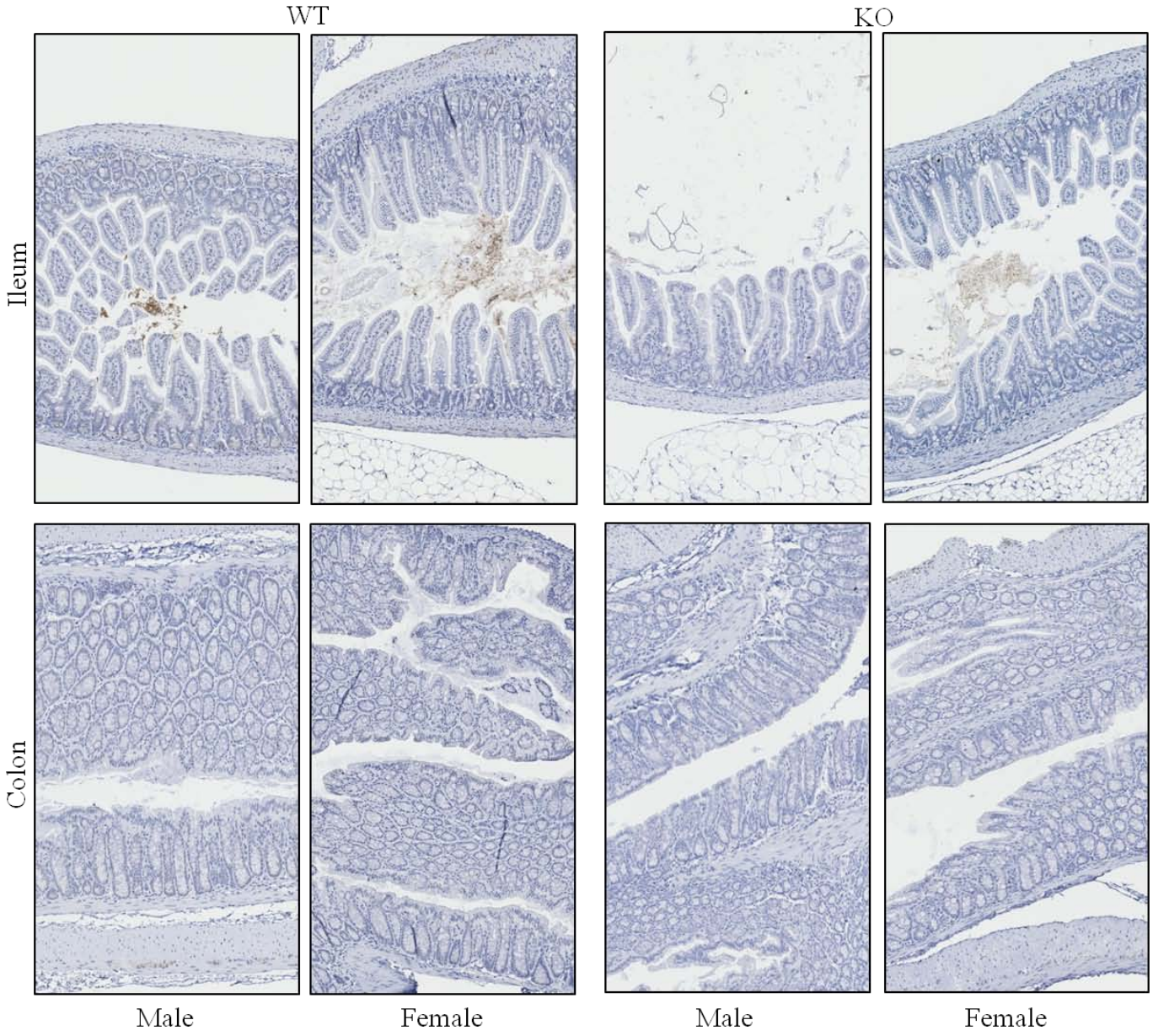

Figure B.4. Representative images of rabbit IgG control in the ileum and colon of wild-type (WT) and CDO -/- mice (KO) fed a high sulfur amino acids diet.

AUTHOR'S BIOGRAPHY

Jennifer Croix was born and raised in Champaign-Urbana, IL. Encouraged by her mother, who is a microbiologist, Jennifer enjoyed science from a young age. She began her college education at Parkland College and later transferred to the University of Illinois at Urbana-Champaign as a junior in the Chemistry Department. As an undergraduate at the University of Illinois, she conducted research under the guidance of Nobel Laureate, Dr. Paul Lauterbur. She received the Marvel Research Award for her undergraduate thesis research. In 2003, Jennifer graduated *summa cum laude* from the University of Illinois with a B.S. in chemistry. Following in the footsteps of her grandmother and uncle, she made the Bronze Tablet. After graduation, Jennifer worked for a year at the University of Illinois Veterinary Diagnostic Microbiology Laboratory.

In 2004, Jennifer joined the University of Illinois MD/PhD program in Nutritional Sciences. She conducted her dissertation research in the area of intestinal goblet cells in the lab of Dr. H. Rex Gaskins. She was selected as a recipient for an NIH Training Grant Fellowship and a University Fellowship. She also received a poster of distinction award for work presented at Digestive Disease Week 2009. From fall 2009 to spring 2010, she served as a teaching assistant for the medical anatomy course for which she made the list of teachers ranked as excellent by their students. Jennifer completed her PhD in December 2010 and is currently in her 3rd year of medical school. She plans to complete her MD in May 2012.

Jennifer married her wonderful husband, Alex Jerez, in 2005. Together they have adopted and cared for many pets from the Champaign County Humane Society.